

# System Analysis for Improved Energy Recovery on Prasa's Electrical Traction Network

by

Luca Lategan



*Thesis presented in partial fulfilment of the requirements for the  
degree of Master in Electrical Engineering in the Faculty of  
Engineering at Stellenbosch University*

Supervisors: Dr. P.J. Randewijk  
Prof. H.J. Vermeulen

March 2017

# Declaration

By submitting this thesis electronically, I declare that the entirety of the work contained therein is my own, original work, that I am the sole author thereof (save to the extent explicitly otherwise stated), that reproduction and publication thereof by Stellenbosch University will not infringe any third party rights and that I have not previously in its entirety or in part submitted it for obtaining any qualification.

Date: ..... March 2017 .....

Copyright © 2017 Stellenbosch University  
All rights reserved.

# Abstract

## System Analysis for Improved Energy Recovery on Prasa's Electrical Traction Network

L. Lategan

*Department of Electrical and Electronic Engineering,  
University of Stellenbosch,  
Private Bag X1, Matieland 7602, South Africa.*

Thesis: MEng (Elec)

December 2016

In the very competitive transport market, operators are constantly looking for ways to drive down operational expenses and act on social sentiment to promote their service. Energy recovery through regenerative braking provides an answer to both these issues by reducing energy expenditure and acting on the call for “greenness” by reducing the carbon-footprint of the operation.

This thesis investigates the possible energy savings that can be realised through harnessing the regenerative braking capabilities of new Alstom train sets ordered by the Passenger Rail Agency of South Africa (Prasa). A dynamic load-flow analysis of the 3 kV DC and 33 kV AC electrical network of Metrorail Western Cape will be done to analyse the current capacity of, and future demand on the electrical network. The feasibility of introducing, as well as the ideal placement of, energy recovery equipment will be investigated. This will be done to maximise the potential energy savings and return on investment that can be realised through the regenerative braking capabilities of the new train sets.

DIgSILENT PowerFactory, was chosen as simulation package to build a virtual model of the electrical traction network and conduct dynamic simulations. In order to validate the accuracy of the predicated future network state, with the

future rolling stock, the simulation results of the existing rolling stock and electrical network were benchmarked against real measured data. Due to the good correlation between the simulation results and the measured data, the simulation results of the network with other rolling stock models should also prove to be equally accurate. The simulation model was adapted with the dynamic load model of the future train sets to simulate the projected future state of the electrical traction network. This offered insight into the predicted supply versus demand, over and under voltages as well as the effect of regenerative braking on the power flow. More ideal feeding and sectioning philosophies were also investigated.

The new rolling stock's installed power of 11,2 MW is significantly higher than the 3,52 MW of the current rolling stock. The simulation results of the future network state indicate that the new trains will not be able to operate at their intended performance levels. The proposed feeding and sectioning alterations will increase efficiency, but the installed capacity will have to be increased and a number of substations have been identified in this regard. To better utilise the new rolling stock's regenerative capabilities, various options was investigated and the ideal location for the installation of energy recovery equipment was identified.

# Uittreksel

## Stelselanalise vir die nuttige aanwending van terugvoerremenergie in Prasa se trekkragnet

*(“System Analysis for Improved Energy Recovery on Prasa’s Electrical Traction Network”)*

L. Lategan

*Departement Elektriese en Elektroniese Ingenieurswese,  
Universiteit van Stellenbosch,  
Privaatsak X1, Matieland 7602, Suid Afrika.*

Tesis: MIng (Elek)

Desember 2016

In die hoogmededingende vervoerindustrie is operateurs aanhoudend op soek na wyses waarmee bedryfsuitgawes verlaag kan word asook om op maatskaplike gevoelens ag te slaan om hul diens te bevorder. Energieherwinning deur middel van terugvoerremming bied ’n antwoord vir beide van hierdie kwessies aangesien dit die kragrekening verlaag én die vraag na meer omgewingsvriendelikheid sus deur die koolstofvoetspoor van die bedryf te verlaag.

Hierdie tesis ondersoek die moontlike energiebesparing wat bereik kan word deur die terugvoerremfunksionaliteit van die nuwe Alstom treinstelle te benut. Dit is deur die Passasierspooragentskap van Suid-Afrika (Prasa) bestel. ’n Dinamiese energievloeianalise van Metrospoor Wes-Kaap se 3 kV GS en 33 kV WS elektriese netwerk sal aangepak word om die huidige vermoë en toekomstige belasting van die netwerk te ontleed. Die lewensvatbaarheid en ideale ligging van energieherwinningstoerusting sal ondersoek word. Dit sal gedoen word om die moontlike energiebesparing en beleggingsopbrengs, wat deur die nuwe treine se terugvoerremming moontlik gemaak word, te maksimeer.

DIgSILENT se PowerFactory is gekies as die simulasiepakket om 'n nabootsing van die elektriese trekkragnetwerk mee te bou en dinamiese simulaties te doen. Om die akkuraatheid van die voorspelde toekomstige netwerktoestand, met die toekomstige rolmat, te bevestig is simulasiuitslae van die huidige rolmat en elektriese netwerk vergelyk met gemete data. Danksy die goeie korrelasie tussen die simulasiuitslag en metings behoort die data wat verkry word deur die netwerk te simuleer met ander rolmatmodelle óók redelik akkuraat te wees. Die nabootsing is aangepas met die dinamiese model van die nuwe treinstelle om die toekomstige toestand van die trekkragnet te voorspel. Dit het insig verskaf oor die voorspelde toekomstige aanbod teenoor aanvraag, oor- en onderspanning asook die invloed van terugvoerremming op die energievloei. Meer gepaste voer- en seksie-indelingsstrategieë is ook ondersoek.

Die nuwe rolmat se kenvermoë van 11,2 MW is aansienlik hoër as die 3,52 MW van die huidige vloot. Die simulasiuitslae van die toekomstige netwerktoestand dui daarop dat die nuwe treine nie teen hul beoogde werkverrigtingsvlak sal kan loop nie. Die voorgestelde voer- en seksie-indeling-aanpassings sal die doeltreffendheid verhoog, maar die geïnstalleerde netkapasiteit sal verhoog móét word. 'n Aantal voorstelle is in hierdie verband gemaak. Om die nuwe rolmat se terugvoerremmingsvermoë beter te benut is 'n substasie geïdentifiseer waar energieherwinningstoerusting moontlik geïnstalleer kan word.

# Acknowledgements

I would like to express my sincere gratitude to the following people and organisations that assisted during the study

- My familie en vriende. Sonder julle onbaatsugtige ondersteuning sou ek hierdie tesis nóóit kon voltooi nie.
- Alstom: Bruno Gajan, François Maurin, Nikola Nuvut
- Gibb: André van der Walt, Mario Batt, Sinclair Harcus
- Gibela: Mike Scrooby
- Metrorail: Angilene Niewenhuizen, Daphne Kayster, Ernestus Fourie, Henning Pretorius, Jacques Carstens, Johan Kriel, Johan van Wyk, Kenny Baard, Larry Vockerodt, Louis Beukes, Oom Hanniball, Peet van der Merwe, Pieter Celliers, Riana Jacobs, Robert Venter, Sam Erlank, Shaun Dirks, Wilhelm “Bles” Vorsotz, Zweli Vanqa
- Metrorail drivers: Abrahams, Andrew, Benjamin, Bornman, Burger, Cloete, Dawid, De Souza, Elmba, Geldenhuys, Jaxa, Jordaan, Joubert, Landman, Lucas, Lukas, Marotye, Mfutwana, Murrie, Nieuwoudt, Ntozini, Palvie, Paterson, Pieters, Plaatjies, Roberts, Rodgers, Schoeman, Spence, Thomson, Tybosh, Van Eck, Van Niekerk, Van Papendorp, Van Rensburg, Wapi, Wolfaardt, Young
- Nationale Maatschappij der Belgische Spoorwegen: Bart van der Spiegel, Hendrik Bonne
- Société des Transports Intercommunaux de Bruxelles: François-Olivier Devaux, Ricardo Barrero
- Nederlandse Spoorwegen: Frans Slats

*ACKNOWLEDGEMENTS*

vii

- Semikron: Thinus Niemand, Willie van den Berg
- Stellenbosch University: Johan Vermeulen, Jonathan Nye, Neels Fourie, Peter-Jan Randewijk, Pieter Conradie, SP le Roux
- Transnet: Damba Xolile, Willie Coetzee
- Transurb: Koen De Gussemé



# Dedications

*Hierdie tesis word opgedra aan my Hemelse Vader vir die intellegensie wat hy aan my toevertrou het asook ook die dames en here wat elke dag hul lewens waag om die honderde duisende treinpendelaars van Suid-Afrika te vervoer en sodoende ons ekonomie aan die gang hou.*

# Contents

Declaration	i
Abstract	ii
Uittreksel	iv
Acknowledgements	vi
Dedications	viii
Contents	ix
List of Figures	xiii
List of Tables	xix
Glossary	xxii
Acronyms	xxvi
<b>1 Introduction</b>	<b>1</b>
1.1 Project Background . . . . .	1
1.2 General Background . . . . .	1
1.3 Background of the Network . . . . .	2
1.4 Outline of Report . . . . .	2
<b>2 Literature study</b>	<b>4</b>
2.1 Introduction . . . . .	4
2.2 Economic Driving . . . . .	4
2.2.1 Nederlandse Spoorwegen UZI . . . . .	4

## CONTENTS

x

2.2.2	Driver Advisory System . . . . .	7
2.2.3	Toshiba Greener Driving System . . . . .	8
2.3	Energy Regeneration . . . . .	9
2.3.1	Receptivity and Regeneration . . . . .	12
2.3.2	Increased Service Frequency . . . . .	13
2.3.3	Eliminate Islanding . . . . .	13
2.3.4	Paralleling . . . . .	14
2.3.5	Energy Storage Systems . . . . .	15
2.3.6	Reversible Substations . . . . .	17
2.3.7	Reversible Substation Hardware . . . . .	23
2.4	Load-flow Simulation Software . . . . .	27
2.4.1	Simulation from First Principles . . . . .	28
2.4.2	DIgSILENT PowerFactory . . . . .	29
2.4.3	Infrabel Load-flow Simulation . . . . .	31
2.4.4	Ingeteam . . . . .	33
2.4.5	Siemens Sitras <sup>®</sup> Sidytrac . . . . .	33
2.5	Historical South African Perspective . . . . .	33
2.5.1	Mainline Use . . . . .	34
2.5.2	Suburban Usage . . . . .	35
2.5.3	Economic Driving . . . . .	36
2.5.4	Reversible Substation Research . . . . .	36
2.6	Conclusion . . . . .	37
<b>3</b>	<b>Modelling moving trains</b>	<b>39</b>
3.1	Introduction . . . . .	39
3.2	Capacity of an Electrical Traction Network . . . . .	39
3.3	Simulating Trains as Moving Loads . . . . .	40
3.3.1	Present Rolling Stock . . . . .	42
3.3.2	Future Rolling stock . . . . .	43
3.4	Simulating Moving Loads . . . . .	51
3.4.1	Moving Train on an Open Section . . . . .	52
3.4.2	Moving Train on an Interrupted Section . . . . .	64
3.4.3	Defining the Relative Displacement Function . . . . .	86
3.5	Implementation of Model . . . . .	90
3.5.1	Converting the Timetable . . . . .	90

<i>CONTENTS</i>	<b>xi</b>
3.5.2 Present Rolling Stock . . . . .	94
3.5.3 Future Rolling Stock . . . . .	98
3.6 Conclusion . . . . .	103
<b>4 PowerFactory model</b>	<b>104</b>
4.1 Introduction . . . . .	104
4.2 AC grid . . . . .	105
4.2.1 Supply Points . . . . .	105
4.2.2 Ring-network . . . . .	108
4.2.3 Substations . . . . .	110
4.3 DC grid . . . . .	131
4.3.1 Overhead lines . . . . .	131
4.3.2 Train Representation . . . . .	132
4.3.3 Substations and Ties . . . . .	134
4.4 Load Flow Calculation Parameters . . . . .	134
4.5 Conclusion . . . . .	136
<b>5 Results</b>	<b>137</b>
5.1 Introduction . . . . .	137
5.2 Benchmarking the Model . . . . .	137
5.3 Results from Further Simulation . . . . .	141
5.3.1 Scenarios Investigated . . . . .	141
5.3.2 Comparison of Statistics . . . . .	144
5.4 Conclusion . . . . .	151
<b>6 Conclusion</b>	<b>152</b>
6.1 Synopsis . . . . .	152
6.2 Future Work and Recommendations . . . . .	153
<b>Appendices</b>	<b>155</b>
<b>A Network Diagram</b>	<b>156</b>
<b>B Diagram of Present Rolling Stock</b>	<b>158</b>
<b>C Diagram of New Rolling Stock</b>	<b>161</b>
<b>D Determination and Validation of Acceleration Parameters</b>	<b>163</b>

<i>CONTENTS</i>	<b>xii</b>
<b>E Python Processing Algorithm</b>	<b>167</b>
<b>F Train Running Times</b>	<b>168</b>
<b>G Removed Workings</b>	<b>181</b>
G.1 Diesel Hauled Trains . . . . .	181
G.2 Friday Only Empties . . . . .	181
G.3 Yard Movements . . . . .	181
G.4 Non-withdrawn trains . . . . .	182
<b>H Workings Highlighted During Processing of WTB</b>	<b>183</b>
H.1 Cape Flats Line . . . . .	183
H.2 Northern Lines . . . . .	183
H.3 Central Lines . . . . .	183
<b>I Comparison of Traction Energy Consumption</b>	<b>187</b>
<b>J Simulated DC Network Model</b>	<b>190</b>
<b>K Detailed Results</b>	<b>192</b>
K.1 Old . . . . .	192
K.2 New <sup>(m)</sup> . . . . .	196
<b>Bibliography</b>	<b>210</b>

# List of Figures

2.1	Speed-distance comparison between an “average ride” and a trip driven according to the eco-driving principle . . . . .	6
2.2	Simple eco-driving tool for train driver . . . . .	6
2.3	DAS process flow . . . . .	7
2.4	Routelint interface and device . . . . .	8
2.5	The consumption and regeneration in a metropolitan train running between two passenger stations . . . . .	10
2.6	Typical V–I characteristics of a traction energy network . . . . .	11
2.7	A Sankey diagram of the typical energy flow in a DC electrified railway system . . . . .	12
2.8	Voltage drops for different scenarios of section feeding . . . . .	14
2.9	Typical V-I characteristics for reversible substation control . . . . .	18
2.10	System behaviour in terms of inverter threshold voltage . . . . .	19
2.11	Annual energy savings as a function of the number of inverters and their power rating . . . . .	20
2.12	Line voltage along the overhead line when a regenerating train is providing in the full power requirement of a powering train that is far away . . . . .	20
2.13	Line voltage along the overhead line when an inverter is used and trains are far . . . . .	21
2.14	Line voltage along the overhead line when a regenerating train is providing in the full power requirement of a nearby powering train . . . . .	22
2.15	Line voltage along the overhead line when an inverter is used and trains are close . . . . .	22
2.16	Line voltage along the overhead line when the regenerated power is too little for the power requirement of a nearby powering train . . . . .	23

2.17	Screenshot of DIgSILENT PowerFactory showing the GUI with geographical representation, database manager and output graph . . . . .	29
2.18	Graph showing the simulated versus measured power of Enghien substation for 24 hours . . . . .	32
2.19	Map showing the prevalence of low line voltage during the simulation period . . . . .	32
3.1	Traction current at 3 kV pantograph voltage for a single motor coach	43
3.2	Maximum line current (traction + auxiliary) drawn by a single module during traction for different values of line voltage . . . . .	44
3.3	Maximum power demand (traction + auxiliary) of a single module during traction for different values of line voltage . . . . .	44
3.4	Current (black) and speed (blue) for a single module during traction with a pantograph voltage of 3 kV . . . . .	46
3.5	Maximum braking current (traction only) injected by a single module during regenerative braking for different values of pantograph voltage	47
3.6	Maximum regenerative braking power (no auxiliary) injected by a single module for different values of pantograph voltage . . . . .	48
3.7	Current (black) and speed (blue) for a single module during braking with a pantograph voltage of 3,75 kV . . . . .	49
3.8	Line current drawn from overhead line by a single M2 loaded module to maintain a constant speed at a pantograph voltage of 3,3 kV . . . . .	51
3.9	Diagram of a train moving between two points, supplied by two substations . . . . .	52
3.10	Typical form of the displacement function $m(t)$ . . . . .	53
3.11	Circuit of a single, moving load fed by two substations . . . . .	53
3.12	Circuit of two stationary dynamic loads fed by two substations . . . . .	55
3.13	Power dissipated by load along short open section for different load representations — Future rolling stock . . . . .	59
3.14	Power dissipated by load along short open section for different load representations — Present rolling stock . . . . .	60
3.15	Power dissipated by load along short open section for different load representations — Constant current 500 A . . . . .	60
3.16	Power dissipated by load along long open section for different load representations — Future rolling stock . . . . .	61

*LIST OF FIGURES*

xv

3.17	Power dissipated by load along long open section for different load representations — Present rolling stock . . . . .	63
3.18	Power dissipated by load along long open section for different load representations — Constant current 500 A . . . . .	63
3.19	Diagram of a train moving between two points, supplied by three substations . . . . .	64
3.20	Circuit of a single, moving load located between substations 1 and 2, but supplied by three substations . . . . .	65
3.21	Circuit of a single, moving load fed by three substations, located between substation 2 and 3 . . . . .	67
3.22	Circuit of two stationary dynamic loads fed by three substations . . . . .	70
3.23	Power dissipated by load along short interrupted section for different load representations — Future rolling stock . . . . .	73
3.24	Current contribution of substation 1 for different load representations — Future rolling stock . . . . .	74
3.25	Power dissipated by load along short interrupted section for different load representations — Present rolling stock . . . . .	75
3.26	Current contribution of substation 1 for different load representations — Present rolling stock . . . . .	76
3.27	Power dissipated by load along short interrupted section for different load representations — Constant current 500 A . . . . .	76
3.28	Current contribution of substation 1 for different load representations — Constant current 500 A . . . . .	77
3.29	Power dissipated by load along longer interrupted section for different load representations — Future rolling stock . . . . .	78
3.30	Current contribution of substation 1 for different load representations — Future rolling stock . . . . .	78
3.31	Power dissipated by load along longer interrupted section for different load representations — Present rolling stock . . . . .	80
3.32	Current contribution of substation 1 for different load representations — Present rolling stock . . . . .	80
3.33	Power dissipated by load along longer interrupted section for different load representations — Constant current 500 A . . . . .	81
3.34	Current contribution of substation 1 for different load representations — Constant current 500 A . . . . .	81



3.35	Power dissipated by load along long interrupted section for different load representations — Future rolling stock . . . . .	82
3.36	Current contribution of substation 1 for different load representations — Future rolling stock . . . . .	83
3.37	Power dissipated by load along long interrupted section for different load representations — Present rolling stock . . . . .	84
3.38	Current contribution of substation 1 for different load representations — Present rolling stock . . . . .	85
3.39	Power dissipated by load along long interrupted section for different load representations — Constant current 500 A . . . . .	85
3.40	Current contribution of substation 1 for different load representations — Constant current 500 A . . . . .	86
3.41	Idealised acceleration, speed and displacement curve of a single station-to-station journey . . . . .	88
3.42	Traction current at 3 kV pantograph voltage for a single motor coach	97
3.43	Current demand of a station-to-station journey . . . . .	98
3.44	Total line current for a single module accelerating with an M3 load from standstill to 120 km/h and a pantograph voltage of 3 kV . . . . .	100
3.45	Regenerative braking current for a single module decelerating with an M3 load from 120 km/h to standstill and a pantograph voltage of 3,75 kV	100
3.46	Current demand of a station-to-station journey . . . . .	102
4.1	Flowdiagram of the simulation process . . . . .	104
4.2	AC network, as modelled in PowerFactory . . . . .	106
4.3	Proposed routes for a new 33 kV transmission line from Modderdam to Bellville substation . . . . .	109
4.4	Soutrivier substation, as modelled in PowerFactory . . . . .	111
4.5	PowerFactory symbols of the two rectifier elements . . . . .	112
4.6	Detailed circuit of PowerFactory rectifier element (ElmRec) with commutation reactance and DC reactance (not part of the model) . . . . .	113
4.7	Equivalent rectifier element circuit with commutation reactance $R_{cr}$ . . . . .	114
4.8	Commutation reactance investigation test circuit . . . . .	115
4.9	Three-phase half-wave rectifier . . . . .	118
4.10	Three-phase half-wave rectifier equivalent circuit for one voltage pulse period . . . . .	119
4.11	Three-phase full-wave rectifier . . . . .	120

4.12	Three-phase full-wave rectifier equivalent circuit for one voltage pulse period . . . . .	120
4.13	Two three-phase half-wave rectifiers in series . . . . .	121
4.14	Two three-phase half-wave rectifiers in parallel . . . . .	122
4.15	Two three-phase full-wave rectifiers in series . . . . .	124
4.16	Two three-phase full-wave rectifiers in parallel . . . . .	125
4.17	Two three-phase full-wave rectifiers in parallel test circuit . . . . .	126
4.18	Nolungile substation, with inverting unit, as modelled in PowerFactory	130
4.19	Model of a single node . . . . .	132
4.20	Equivalent Circuit of the PWM Converter . . . . .	133
4.21	Model of a single node on a single line section . . . . .	134
4.22	Model of substation and tie busbars . . . . .	135
5.1	Averaged Power measured and simulated for the two feeds into Traction Main . . . . .	138
5.2	Averaged Power measured and simulated for Modderdam feed (SATS) and the total feed into Traction Main (TM) . . . . .	139
5.3	Comparison between the total amount energy consumed during the simulation and what was implied by the input . . . . .	144
5.4	Total energy delivered to system expressed as a percentage of the 711 232 kWh that is delivered for New <sup>(m)</sup> . . . . .	145
5.5	Total seconds that node voltages were below 2,7 kV, in blue, and 3 kV, in orange, relative to the 75 414 s and 721 610 s respectively counted for New <sup>(m)</sup> . . . . .	146
5.6	Total 3 kV transmission-line losses relative to the 40 638 kWh lost during the New <sup>(m)</sup> simulation . . . . .	146
5.7	Total 33 kV transmission-line losses relative to the 2852 kWh lost during the New <sup>(m)</sup> scenario . . . . .	147
5.8	Median dissipation in onboard rheostats whilst a train is dissipating .	148
5.9	Percentage of regenerated energy dissipated in onboard rheostats . . .	148
5.10	Total energy consumption by trains as a percentage of the total energy infeed . . . . .	149
D.1	Comparison of measured and calculated values of the relative displacement function for old rolling stock: Cape Town to Vishoek . . . . .	164

*LIST OF FIGURES***xviii**

D.2	Comparison of measured and calculated values of the relative displacement function for old rolling stock: Cape Town to Du Toit . . . . .	166
I.1	Comparison of traction energy consumption for different classes of commuter rolling stock and load levels . . . . .	189

# List of Tables

2.1	Comparison of different ESS technologies . . . . .	17
3.1	Comparison of the maximum power (traction + auxiliary) drawn from the overhead line for different values of pantograph voltage and speed . . . . .	45
3.2	Comparison of the maximum power (traction only) injected into the overhead line for different values of pantograph voltage and speed . .	48
3.3	Parameters used in calculation . . . . .	59
3.4	Load representation comparison — Future loading, short open section	59
3.5	Load representation comparison — Present loading, short open section	60
3.6	Load representation comparison — Constant current on short open section . . . . .	61
3.7	Parameters used in calculation . . . . .	62
3.8	Load representation comparison — Future loading, long open section	62
3.9	Load representation comparison — Present loading, long open section	62
3.10	Load representation comparison — Constant current on long open section . . . . .	63
3.11	Parameters used in calculation . . . . .	74
3.12	Load representation comparison — Future loading, short interrupted section . . . . .	75
3.13	Load representation comparison — Present loading, short interrupted section . . . . .	75
3.14	Load representation comparison — Constant current on short interrupted section . . . . .	77
3.15	Parameters used in calculation . . . . .	79
3.16	Load representation comparison — Future loading, longer interrupted section . . . . .	79

## LIST OF TABLES

xx

3.17	Load representation comparison — Present loading, longer interrupted section . . . . .	80
3.18	Load representation comparison — Constant current on longer interrupted section . . . . .	82
3.19	Parameters used in calculation . . . . .	83
3.20	Load representation comparison — Future loading, long interrupted section . . . . .	84
3.21	Load representation comparison — Present loading, long interrupted section . . . . .	84
3.22	Load representation comparison — Constant current on long interrupted section . . . . .	86
3.23	Extract of the official timetable for the network under review . . . . .	92
3.24	Example of a cleaned-up timetable . . . . .	95
3.25	Loading factors used for different train number prefixes . . . . .	97
3.26	Loading factors (amount of modules) used for different train number prefixes . . . . .	101
4.1	High voltage AC supply point parameters . . . . .	107
4.2	33 kV AC conductor parameters . . . . .	110
4.3	Known and calculated commutation reactance values . . . . .	115
4.4	Commutation reactance investigation results . . . . .	117
4.5	Auxiliary AC load parameters . . . . .	128
4.6	Scaling of auxiliary AC loads . . . . .	128
4.7	Wire combinations used for DC network . . . . .	132
5.1	Comparison of measured and simulated values of maximum current and transformer loading . . . . .	140
5.2	Summary of results for the various scenarios . . . . .	150
F.1	Official Metrorail running times for Southern Lines . . . . .	169
F.2	Official Metrorail running times for Northern Lines (1 of 2) . . . . .	170
F.3	Official Metrorail running times for Northern Lines (2 of 2) . . . . .	171
F.4	Official Metrorail running times for Central Lines . . . . .	172
F.5	Official SARCC version of running times for Southern Lines . . . . .	173
F.6	Official SARCC version of running times for Northern Lines (1 of 2) . . . . .	174
F.7	Official SARCC version of running times for Northern Lines (2 of 2) . . . . .	175

*LIST OF TABLES***xxi**

F.8	Official SARCC version of running times for Central Lines . . . . .	176
F.9	Running times from 1973 and amended version of Metrorail running times for Southern Lines . . . . .	177
F.10	Running times from 1973 and amended version of Metrorail running times for Northern Lines (1 of 2) . . . . .	178
F.11	Running times from 1973 and amended version of Metrorail running times for Northern Lines (2 of 2) . . . . .	179
F.12	Running times from 1973 and amended version of Metrorail running times for Central Lines . . . . .	180
H.1	Empty coach running times . . . . .	184

# Glossary

**antiparallel** is two electric components connected in parallel, but with their polarities reversed. 18, 19, 26, 34, 36

**coast** is continued movement without adding energy, but rather utilising acquired momentum. 5, 7, 22, 36, 87, 96, 97

**copper loss** is  $I^2R$  losses resulting from Joule heating, also called conductor or transmission losses. 11, 13, 15, 18, 19, 22, 143, 145, 147, 150

**cruise** is continued movement at a constant speed. Energy is used to overcome aerodynamic drag, rolling resistance and gravitational impact of an uphill. Gravitational potential energy assist on downhills and excess energy can be recovered using regenerative braking. 10, 22, 43, 50, 87

**electrical distance** is the distance that current has to flow from from one electrical component to the other. If two objects are in close electrical proximity the electrical distance is short. 12, 14

**electrical proximity** is the nearness of two electrical components in terms of the distance that current has to flow from one to the other. In an electrical network two objects may be in close physical proximity, but in the absence of a direct conductor the current may have to follow a much longer route. xxii, 12, 13, 48, 147

**Eskom** is the state owned national electricity supply company in South Africa. 107, 138, 142

**friction brake** is a type of brake used by trains. It works by dissipating the kinetic energy of the moving train by converting the energy into heat. The heat

arises from friction between the brake block and wheel tyre or brake pad and brake disc during braking. 9, 11, 12

**load case** refers to the weight designation of the rolling stock, typically expressed as M0 to M3 or AW0 to AW3 (Added Weight). Passengers are assumed to weigh an average of 75 kg. The four cases are defined as follow:

M0 = Tare: tare weight of rolling stock

M1 = Empty: tare weight including the (negligible) weight of train personnel, in the case of Passenger Rail Agency of South Africa (Prasa) a driver and guard, each weighing 80 kg

M2 = Full: tare plus all seats filled and 6 passengers per m<sup>2</sup> standing room

M3 = Crush: tare plus all seats filled and 9 passengers per m<sup>2</sup> standing room. 35, 42, 46, 49–51, 99–101, 187, 188

**ohmic drop** is the voltage drop measured between two points of an electrical conductor due to the current flowing through it. Using Ohm's law, this voltage is equal to the product of the current flowing through the conductor and the resistance of the conductor between the two points. 11, 12, 14, 19, 21, 44, 144

**overhead line** is overhead track-equipment, sometimes referred to as catenary, that delivers electric energy to an electric train. It consists of a contact wire that the pantograph press against, catenary that is used to suspend the contact wire at a constant height using droppers (vertical, non current carrying wires) and sometimes also a feeder cable of aluminium to reduce the effective resistance of the line. Also referred to as 3 kV line. xxiii–xxv, 2, 9, 11–16, 18, 20–24, 28, 31, 33, 34, 40–42, 44–52, 64, 111, 131, 132, 136, 142–145, 147, 150, 190

**pantograph** is a structure fitted to the roof of a rail vehicle to collect current from the overhead conductor by means of physical contact. xxiii, 40, 45, 49, 98, 102

**pantograph voltage** is the potential difference between the overhead line and return conductor (rail), as measured by the train's onboard control system. 11, 13, 19, 21, 22, 40, 41, 43–51, 58, 73, 97, 100, 143, 145, 150



**power factor** is the ratio of the real power flowing to the load to the apparent power in the circuit. 25, 26, 133

**quasi-dynamic simulation** is a series of simulation calculations that is performed to determine the effect of varying operating conditions. The network's dependence on time is modelled, because most operational parameters have an underlying dependence on time. The input parameters are defined for each time step. "Quasi" refers to the fact that each time step is regarded as a different, static (steady state) simulation. 30, 39, 105

**receptivity** is the capacity of the traction network to absorb regenerated braking energy. 12, 13, 15, 18, 25, 27, 34, 47, 50, 143

**regenerating** the act of braking using regenerative braking. 13, 20, 21, 23, 31, 144

**regenerative braking** is a type of electric braking where the rolling stock's traction motors is used to brake the train. The energy that is thus recovered, called the regenerated energy, is returned to the overhead line for use by other trains or the AC grid. Also referred to in the text as regeneration. xxiv, 1, 3, 9, 10, 12, 13, 15, 26, 32–38, 47–50, 58, 72, 100, 132, 133, 142–144, 147, 150

**reversible substation** is a railway substation that allows surplus energy to flow from the DC bus to the medium voltage AC grid using an inverter. 1, 4, 13, 15, 17, 18, 20–23, 129, 143, 147, 150

**rheostat** is an adjustable resistor so constructed that its resistance may be changed. In this document rheostat refers to an installation that is used to dissipate a variable amount of braking energy. It can be implemented as a resistor bank where resistors is switched in different configurations to vary the resistance or a single resistor that can be switched with an insulated-gate bipolar transistor (IGBT) or similar semiconductor to vary the effective resistance. Rheostats can be installed on track-side as well as on board rolling stock. xxiv, 9, 12, 18–20, 22, 35, 47, 129, 147, 150

**rheostatic braking** is a type of electric braking where the rolling stock's traction motors is used to brake the train. The braking energy is dissipated in onboard rheostats. On diesel locomotives this is usually referred to as dynamic braking. 11, 22, 34, 132, 133, 143, 147, 150, 153, 190

- rolling stock** is a railed, usually train or tram, vehicle. It includes both self-propelled and unpowered vehicles. xxiv, 2, 3, 5, 7, 9, 11–13, 15, 19, 30, 31, 35, 38–46, 49–51, 58, 61, 62, 73, 74, 77, 78, 82, 83, 87, 90, 94, 96, 98–101, 103, 111, 137, 141–143, 145, 147, 151, 153, 154
- Sankey diagram** is a specific type of flow diagram in which the width of the arrow is drawn proportionally to the flow quantity. 11, 12
- section** is a part of a railway line or overhead line between two geographical points. 5, 10, 13–15, 32, 46, 57–64, 66, 68, 69, 71–74, 76–80, 82, 83, 85, 111, 129, 131, 142, 143
- three-phase** refers to an electric circuit or device that is energised by three electromotive forces (alternating current) of the same frequency and voltage amplitude, relative to a common reference, but with a phase difference of one third of a cycle or  $120^\circ$ . 34, 36, 43, 110, 112, 113, 118–126
- total specific resistance,  $\rho$**  is the combined electrical resistance of the overhead line and return rail in  $\Omega/\text{km}$ . 14, 15, 52–57, 59, 62, 64–72, 74, 79, 83
- tractive effort** is the pulling or pushing force exerted by a locomotive or other powered rail vehicle. 31, 46
- Transnet** is the state owned national freight logistics company in South Africa that owns and operates the national railway network. The rail arm was previously called Spoornet, which was the successor to the South African Railways. 35, 105, 107, 108, 110

# Acronyms

**AC** alternating current. 1, 3, 9, 15–18, 23, 26, 29–31, 33–38, 40, 43, 104–108, 110–114, 127–129, 131, 133–136, 144, 152, 153

**ATM** Azienda Trasporti Milanese. 25

**ATO** automatic train operation. 8

**AUX X-F** auxiliary transformer. 128

**CAES** compressed air energy storage. 16, 17

**CSV** comma-separated values. 94, 104, 105

**CTC** centralised traffic control. 131

**Das** driver advisory system. 7, 8, 99

**DC** direct current. 1, 3, 11, 12, 16, 18, 21–24, 26, 27, 29–31, 33, 34, 36, 38–43, 51, 103–105, 110–113, 115, 116, 118, 119, 121–123, 125, 126, 129–134, 136, 142, 144, 152, 153

**DPL** DIgSILENT Programming Language. 31

**EDLC** electric double layer capacitor. 16, 17

**EL&P** electric light and power, refers to the transformer that supplies the electrical lighting and power to the substation. 128

**EMF** electromotive force. 40

**EMU** electric multiple unit. 35, 36, 42, 43

**ERS** energy recuperation system. 23, 24

- ESS** energy storage system. 4, 13, 15–17
- GMR** geometric mean radius. 110
- GPS** Global Positioning System. 163
- GUI** Graphical User Interface. 29
- Hesop** Harmonic and Energy Saving OPTimizer. 24, 25
- HMI** human machine interface. 8
- HV** high voltage. 46, 114, 127, 141
- IGBT** insulated-gate bipolar transistor. xxiv, 23, 24, 26, 36, 37
- NaS** sodium-sulfur. 16, 17
- NiCd** nickel-cadmium. 16, 17
- NiMH** nickel-metal hydride. 16, 17
- NMD** notified maximum demand, refers to the maximum power demand, calculated over a moving 30 min period, that a supply point can continuously deliver to its connected loads. 107, 127
- NS** National Railways of the Netherlands. 5–8
- OCV** open-circuit voltage, output voltage under no-load conditions. 11, 13, 18, 19, 21, 23, 28, 50
- OPF** optimal power flow. 136
- PHDC** plain hard drawn copper. 110
- Prasa** Passenger Rail Agency of South Africa. xxiii, 1, 105, 107, 108, 110, 127, 129, 153, 154
- ptcar** point caractéristique, refers to a defining point on the network and includes signals, points, change of grade, curves, etcetera. 5, 8, 31, 94
- p.u.** per unit. 107

- PWM** pulse-width modulation. 129, 133, 134
- RMS** root mean square. 110, 119, 122, 124, 132, 134
- ROI** return on investment. 26
- SAR** South African Railways. 34, 35
- SARCC** South African Rail Commuter Corporation. 168, 173–176
- Stib** Société des Transports Intercommunaux de Bruxelles, refers to the Brussels Intercommunal Transport Company, the local public transport operator in Brussels, Belgium. 18, 24, 26–28
- TCI** thyristor controlled inverter. 26, 27
- TDD** total demand distortion. 24
- THD** total harmonic distortion. 25, 26, 37
- VRB** vanadium redox. 16, 17
- WTB** Working Time Book. 90, 91, 93, 94, 104, 137, 168, 181, 183, 184, 186

# Chapter 1

## Introduction

### 1.1 Project Background

The Prasa has recently embarked on the acquisition of 600 new commuter trains from Alstom that will feature “superior regenerative braking capabilities” [1]. The first sets are due to start operating in the Western Cape by 2020.

The aim of this project is to investigate the possible energy savings that can be realised by taking the regenerative braking capabilities of these new trains into account. Thorough load-flow analysis Metrorail Western Cape’s 3 kV direct current (DC) and 33 kV alternating current (AC) feeder network will be done. The load-flow analysis will furthermore try to investigate the feasibility whether or not reversible substations will be able to add to the potential energy savings that can be realised thanks to the regenerative braking capabilities of the new trains. [1]

Some of the planned deliverables of the completed project include:

- A detailed simulation of the electrical traction network of Metrorail Western Cape. A diagram of the network is provided in Appendix A.
- An estimate of the energy savings that can be realised with the new trains.
- Whether or not reversible substations can further add to the potential energy savings that can be realised.

### 1.2 General Background

Transport is vital to the survival of the modern civilisation. The transport of people and freight is always accompanied with energy consumption. Energy is

needed for acceleration and to overcome the various forms of friction and losses in mechanical and electrical components. Luckily there is also the possibility to recoup a good proportion of this energy by harnessing the kinetic energy, that was stored in the momentum of the vehicle while accelerating, during deceleration.

Electrically powered railed vehicles, such as trains and trams, takes the energy for acceleration from the overhead line or a third-rail and convert it to mechanical energy in their traction motors. This energy is partially stored as kinetic energy by the movement of the vehicle's mass. When the vehicle needs to decelerate, it can use its traction motors as generators to convert the kinetic energy back into electrical energy. This electric energy can then be used for other applications.

Consequently, these vehicles can provide an excellent solution to mankind's search for more efficient and environmentally friendly use of earth's limited energy resources.

### 1.3 Background of the Network

The Western Cape Network on which this research study is based has a total system length of 460 km, serves 122 stations and has a daily ridership of about 621 000 [2]. The first commercial service of electric trains in this region started on 17 October 1927 [3]. The trains ran on the, now closed, line between Cape Town and Sea Point. Operation at 3 kV started in November 1954 [4].

### 1.4 Outline of Report

This study aims to develop a simulation model that can be used to determine the present and future utilisation of the equipment that make up the electrical traction network of Metrorail Western Cape.

In Chapter 2 various methods of reducing energy usage will be discussed. The concepts behind regenerative braking and how to increase the useful application of regenerated energy will be presented. Some load-flow simulation software will be explored and a historical South African perspective will be shared.

Chapter 3 provides some background on how to determine the capacity of an electrical traction network, including how moving trains can be simulated. The two types of rolling stock used on the network under investigation will be introduced. A method will be investigated to overcome PowerFactory's inability

to simulate moving loads along DC lines. This will include the definition of a relative displacement function. Lastly the method will be applied by converting the current timetable and implementing a model that accurately imitates the types of rolling stock used.

In Chapter 4 a detailed model of the AC and DC networks is constructed in PowerFactory. The AC grid consists of all utility and council feeding points, the 33 kV ring-network and all substations. In total the model will contain almost 6500 objects.

Chapter 5 describes the simulations that were executed using PowerFactory. The model will first be benchmarked against actual measurements. Once the model is proven to be a valid representation of the actual network, different scenarios will be presented. These will indicate how the energy use of the new rolling stock compares with the present rolling stock. Various alterations and improvements to the network will be investigated and discussed.

A generic driving style will be used whilst concentrating on the energy usage with and without regenerative braking and the various ways in which the network configuration will be altered in order to decide on the most effective combination.

Finally, some conclusions and recommendations are provided in Chapter 6.



# Chapter 2

## Literature study

### 2.1 Introduction

In this chapter various methods of reducing energy usage will be discussed. The concepts behind regenerative braking and how to increase the useful application of regenerated energy will be presented. Some load-flow simulation software will be explored and a historical South African perspective will be shared.

### 2.2 Economic Driving

One of the cheapest ways to reduce the amount of traction energy necessary to operate a railway is if the trains are operated in a more efficient manner. The *success* of the reduction relies heavily on the cooperation of the drivers and the amount of slack that the timetable offers. Significant reductions have been achieved without expensive hardware, such as reversible substations or energy storage systems (ESSs). More advanced applications, such as driver advisory systems, do require additional hardware. The following subsections will discuss some applications of the economic driving principle.

#### 2.2.1 Nederlandse Spoorwegen UZI

Efficient use of energy is nothing new to the Dutch railways, even in the days of steam, footplate personnel were penalised with a “kolenpremie” (coal premium) for using too much coal. After electric traction was adopted this approach was

retained. The first advice sheets with switching out points were given to drivers in 1968 [5].

The Nederlandse Spoorwegen (NS) uses one of the simplest and cheapest ways to save on their total energy bill. With their UZI methode (“Universeel Zuinig rijden Idee” — Universal Economical Driving Strategy) or eco-driving in short, they aim to reduce their energy bill by five to ten percent.

The NS defines eco-driving as “driving a train more energy-efficiently by using the slack in the timetable when driving without delay.” The method is explained as follows [6]:

- Accelerate quickly to the maximum allowable speed.
- Switch off power as soon as possible, given the timetable. This also avoids driving ahead of schedule.
- Make small adjustments during coasting, if necessary, to avoid the build-up of delay.
- Let the train roll into the next station at the exact scheduled time; punctuality always has higher priority.

Figure 2.1 shows the speed-distance relationship of an “average ride” and a trip driven according to the eco-driving principle. During the average trip, trains arrive at a certain point caractéristique (ptcar) too early and must wait at a red signal. The eco-driving strategy takes this into account by coasting for nearly 20 km, naturally reducing speed, to pass the ptcar unhindered. The estimated energy saving of the eco-driving trip is approximately 15 %.

To make it as easy as possible for the train drivers to implement eco-driving, the NS drew up a very simple reference card (Figure 2.2) to advise the drivers when they should start coasting. The reference card does not take the type of rolling stock, a specific section’s topography or possible speed restrictions into account. As a result, the achieved energy savings is not the theoretical maximum. The NS claims that theoretical energy savings of up to 30 % are achievable on individual trips [6]. “Long-term average fleet-wide savings of at least 5 % is expected” [6].

The NS further reckons that employee satisfaction and commitment will improve due to the increased craftsmanship that is expected from the drivers. Other benefits include lower maintenance costs due to less wear of components; higher punctuality (trains arrive exactly on time instead of too late or too early); more comfort due to smooth driving style; and increased customer satisfaction.

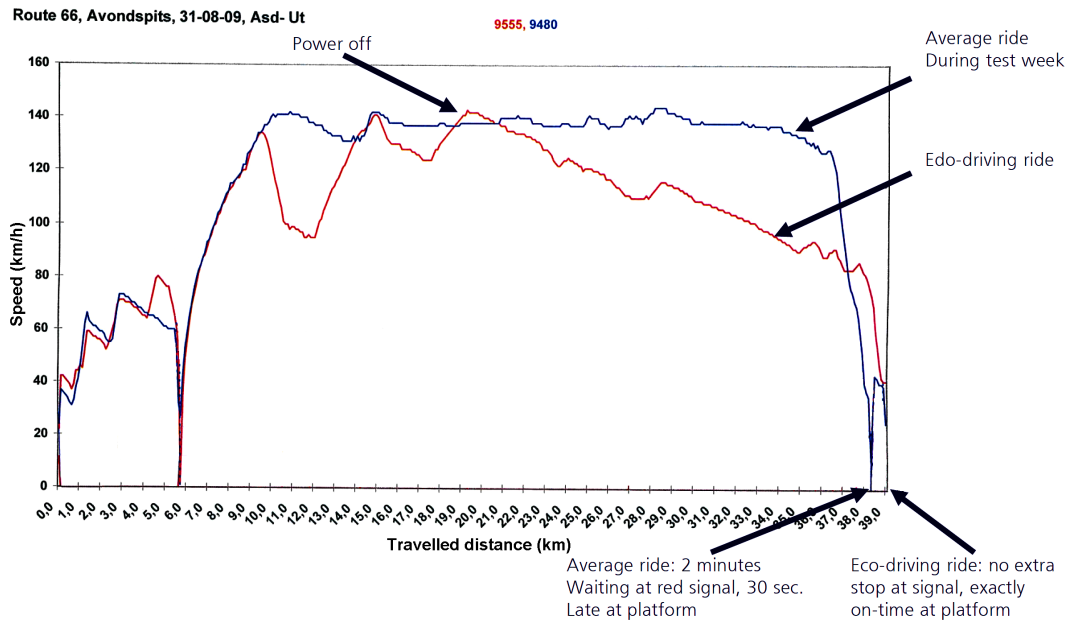


Figure 2.1: Speed-distance comparison between an average ride and a trip driven according to the eco-driving principle, adapted from [6]



Figure 2.2: Simple eco-driving tool for train driver [6]

The success of this method relies heavily on the cooperation of human beings. Some challenges that were experienced with the implementation include the culture change that was required in the personnel, especially to motivate change rather than forcing it, and the cooperation between the planning office, rail traffic control and train crew. Counter productive competition between objectives can arise and must be avoided. The NS has chosen to honour punctuality before energy saving. [6]

These challenges are handled by integrating the principles in driver training on simulators. Personnel are encouraged to buy in by making it clear that this offers

a simple, yet effective, way to make an individual contribution to sustainability, cost-savings, performance and customer satisfaction. Drivers are given tools to assess how efficient they drive their trains.

A more complicated version of static eco-driving, but with higher savings, is real-time, dynamic driver advisory system (Das).

## 2.2.2 Driver Advisory System

The goal of a Das is to enable the optimised operation of train traffic. The optimisation of goals can be diverse, even contradicting. For example, it is not easy to find a balance between minimising travelling time, delays and energy consumption [7]. Due to these contradicting goals, numerous different types of these systems have been developed to cater for each railway company's unique requirements, see [7] for some examples. The basic Das process flow is shown in Figure 2.3.

Das products are classified into three types [7]. The energy saving percentages are based on calculations by NS [8]:

- **Type A:** eco-driving principle that offers static, pre-computed advice on energy efficient driving (accelerate, coast, brake, target speed). Can be as simple as a piece of paper or an electronic screen. Maximum achievable savings of 5 % to 10 %.
- **Type B:** Das is fed with details of rolling stock and infrastructure characteristics and the ideal timetable to continually calculate the optimal, dynamic advice for punctual and economic driving. The whole process in Figure 2.3

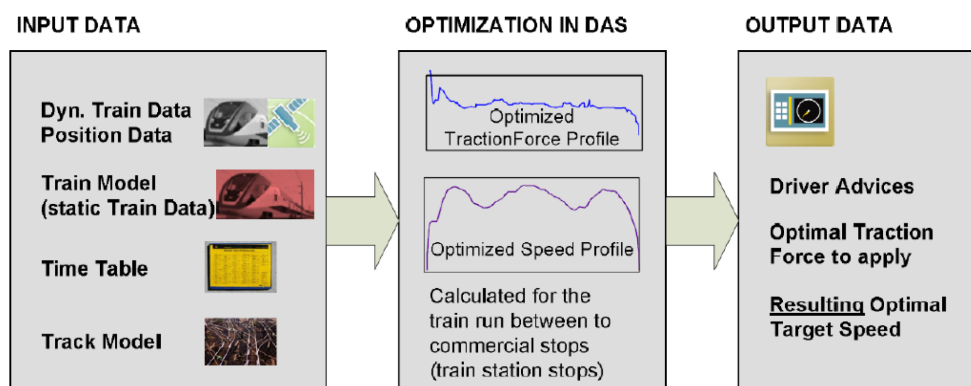


Figure 2.3: Das process flow [7]

will typically take place on the train. Such systems can offer savings of 10 % to 15 %.

- **Type C:** Das is connected to the train control systems to realise a completely dynamic system that is optimised on network-level to avoid conflicts. This type is also referred to as automatic train operation (ATO). These dynamic systems should be able to reduce energy usage by 15 % to 20 %.

The yield of Type A systems can be improved by providing drivers with real-time information about traffic conditions ahead. An example is the Routelint system developed by the NS and rail-network controller of the Netherlands, ProRail. It consists of a simple, graphical interface with the status of ptcars ahead, as shown in Figure 2.4. If the driver sees that a signal at danger will be encountered, acceleration can be stopped immediately. This saves energy and eliminates or reduces the time that the train will have to wait at the signal. In other circumstances the driver might decide to accelerate so that the train can still pass a ptcar unhindered.

The success of any Das, but especially Type A, relies heavily on the drivers' skill and willingness to cooperate.

### 2.2.3 Toshiba Greener Driving System

An example of a complete energy efficient driving solution is Toshiba's Greener Driving System. It offers in-train driver assistance with a graphical human machine interface (HMI) and the possibility of real-time updates based on schedule and

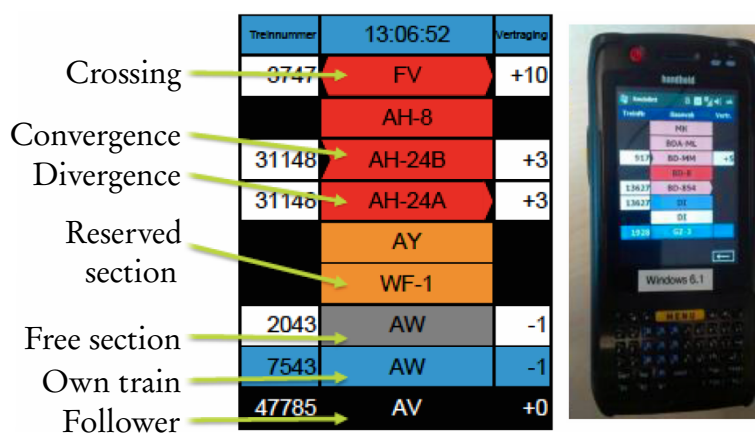


Figure 2.4: Routelint interface and device, reproduced from [7]

ground communication. Their four aspects of the operation and control Energy-Conscious Cycle are [9]:

- Driving assistance
- Energy monitoring
- Energy analysis and target setting
- Timetable and running profile planning

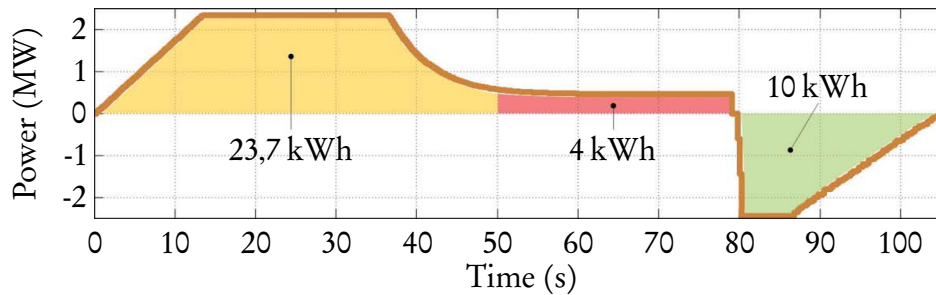
The results from the energy analysis are used to calculate an even more efficient driving profile. The improved profiles are then also included in drivers' simulator based training.

## 2.3 Energy Regeneration

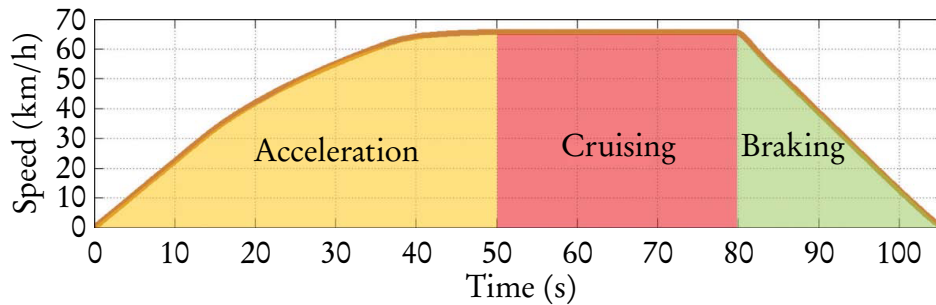
Even if drivers drive according to the most efficient plan, they will have to apply the brakes sooner or later to stop the train. Because trains are generally very heavy, the kinetic energy that must be dissipated during braking is very high. Historically this was done with mechanical friction brakes with high maintenance costs and unnecessary wastage of otherwise useful energy. Most modern (post '90s) rolling stock have regenerative braking capabilities [10]. Regenerative braking slows the train by using the traction motors as generators, partially converting the kinetic energy stored in the train back into electrical energy. The regenerated energy can be dissipated as heat in onboard rheostats or pushed back into the overhead line and used by other trains or even the AC grid, reducing the overall energy usage [11]. In addition to the energy saving, regeneration considerably reduces brake wear and the associated maintenance of the friction brake equipment [10].

The potential savings in a suburban railway environment, with a high acceleration and deceleration rate per kilometre, are very high. The potential reduction of energy consumption that regenerative braking offers is illustrated by Figure 2.5 and the example that follows [11]:

[Figure 2.5] includes the performance of a metropolitan train running between two passenger stations separated by 1,4 km without any grade and using the minimum time, the so-called flat-out speed profile. Figure 2.5a depicts the power through the pantograph, while Figure 2.5b shows the speed profile. Three different sections can be distinguished:



(a) Flat-Out Power Profile



(b) Flat-Out Speed Profile

Figure 2.5: The consumption and regeneration in a metropolitan train running between two passenger stations [11]

the first, in which the power consumed is used to accelerate the vehicle with a certain efficiency; the second, in which the energy is used to cruise; and the third, during which the train brakes and a fraction of the kinetic energy stored in it can be sent back to the system.

The energy consumption during the three phases in this example is 23,7 kWh, 4 kWh and  $-10$  kWh, respectively. The energy recovered during braking represents 44 % of the energy required to accelerate the train and 38 % of the total energy consumed. Furthermore, the energy recovered during braking can be used by another train accelerating along the same electrical section with an obvious savings [sic] in the energy taken from the electric substations. In fact, energy consumption can be up to 38 % less than without regenerative braking, if losses are neglected. These results show the enormous savings potential of regenerative braking in the total energy consumption of electrified railway systems.

The previous example give a very idealised impression of possible savings. In

reality, the theoretical energy saving is limited by several factors, including copper losses in the overhead line and conversion efficiency of the rolling stock's traction system power train [11].

Most DC based railway electrification systems are fed by unidirectional, diode based, rectifiers [12]. This means that any regenerated energy must immediately be used by other net consuming trains. Furthermore, heavy trains and relatively low voltages, 3000 V being the maximum [12], require large current and lead to high transmission losses. The overhead line resistance and high regenerated current will lead to an ohmic drop and an increased pantograph voltage. When the voltage reaches a predetermined safety level, the rolling stock's control system will switch to, partial, rheostatic braking or friction braking. Figure 2.6 shows the typical voltage—current characteristic applicable to a traction energy system. The figure is scaled for a nominal voltage of 3 kV. Rolling stock should limit the maximum current during traction,  $I_{\max_{pos}}$ , as well as the maximum current during braking,  $I_{\max_{neg}}$  [13]. The pantograph voltage of tractioning trains will be at or below the substations' open-circuit voltage (OCV). The maximum braking voltage,  $U_{\max_{brake}}$ , is limited by the technical ability of the rolling stock, but must be lower than the highest allowed non-permanent voltage of 3,9 kV for a 3 kV system [14].

The Sankey diagram diagram in Figure 2.7 shows the typical energy flow in a DC traction network. It is not drawn to scale, but it does give a good indication about the various sinks and sources in the system.

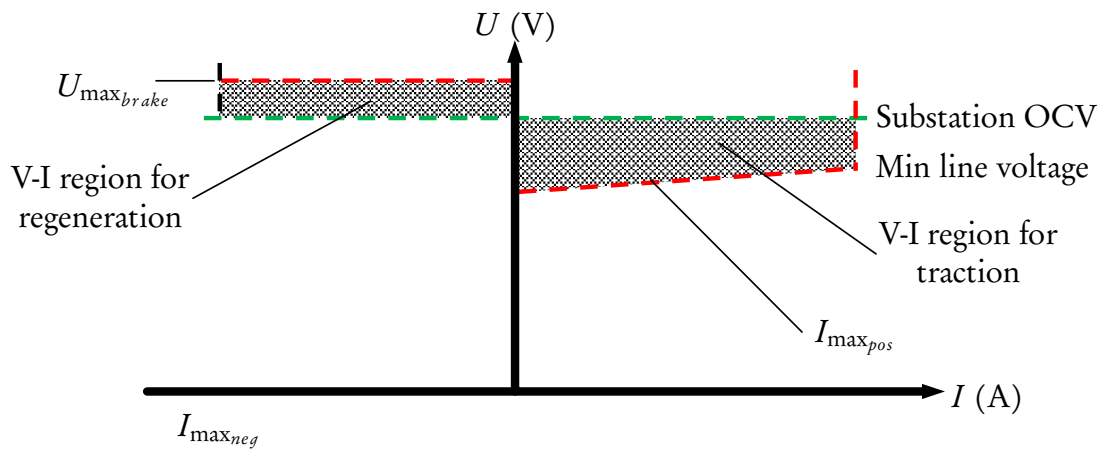


Figure 2.6: Typical V—I characteristics of a traction energy network



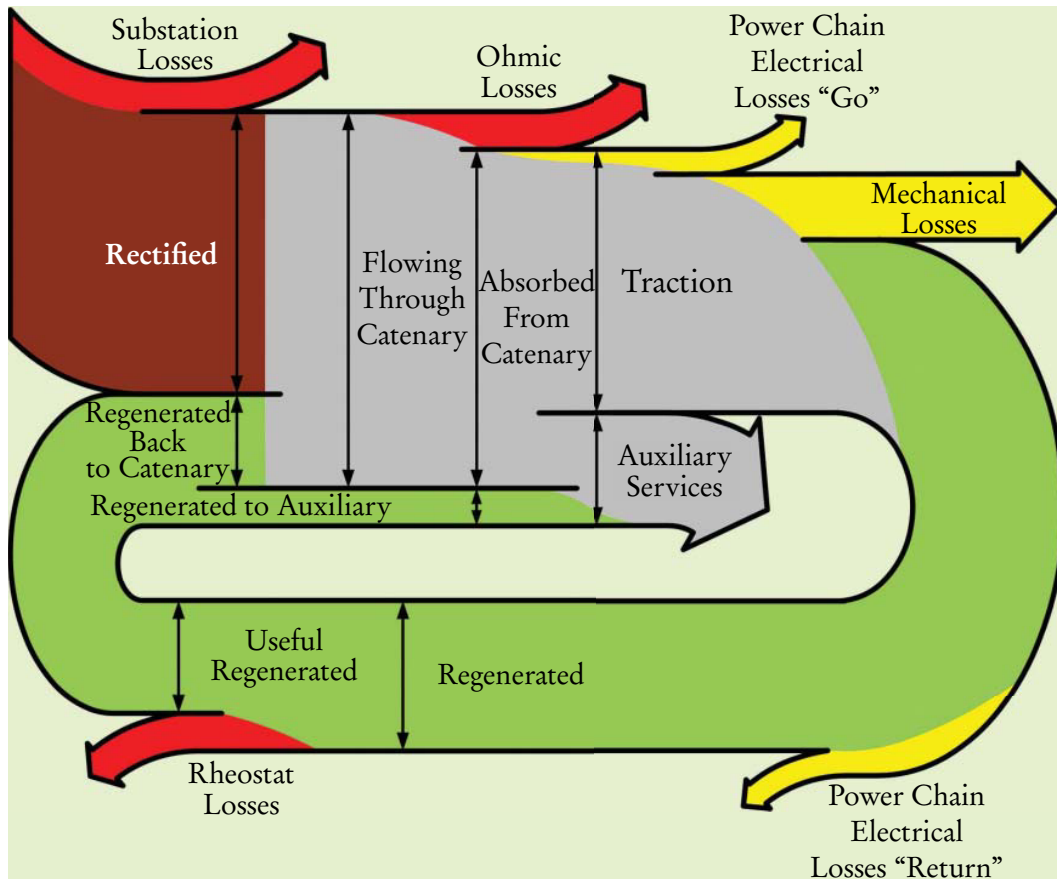


Figure 2.7: A Sankey diagram of the typical energy flow in a DC electrified railway system [11]

### 2.3.1 Receptivity and Regeneration

Receptivity is defined as a system's capacity to accept the regenerated braking energy [11]. Scenarios that reduce receptivity include:

- **Regenerated power exceeds consumption:** If the power supplied by braking trains is more than the power drawn by motoring trains in close enough electrical proximity, the network will saturate. This is characterised by a high overhead line voltage. The rolling stock will be forced to dissipate excess energy in the rheostats or use friction braking. Saturation often occurs on low density systems and during off-peak periods.
- **Distance between regeneration and utilisation:** Current flowing through the overhead line causes an ohmic drop due to the inherent conductor resistance. Long electrical distances between trains (long headways) leads to large voltage drops. This increases the chances of reaching the maximum

pantograph voltage at the regenerating side.

- **High OCV:** When no regenerating rolling stock is operating or for weak railway systems the OCV, or no-load voltage, of substations is often increased. Apart from a reduction in under-voltage situations, this practice reduces transmission losses. A higher OCV is typically not combined with a higher allowed maximum braking voltage, so the region that is available for regeneration is reduced, see Figure 2.6. This leads to low receptivity.

There are five categories of solutions that railways generally use to increase receptivity: increase service frequency, eliminate islanding, paralleling of overhead line sections, ESSs and reversible substations. The following sections provide insight into each of these solutions.

There seems to be a growing interest in all categories of solutions to increase receptivity, thanks to initiatives like the European Union's Ticket to Kyoto (T2K). Launched in 2010, it consisted of five European urban transport operators, in Bielefeld, Rotterdam, Paris, Manchester and Brussels, that actively explored different technologies to reduce their energy consumption and CO<sub>2</sub> emissions [15]. As of September 2014, some operators concluded initial testing and were installing ESSs and reversible substations on a wider scale [16].

### 2.3.2 Increased Service Frequency

By increasing the number of trains simultaneously running in a given section, the distribution of power will generally be more evenly spread. This ensures a higher probability that another train is in close electrical proximity and therefore able to absorb the regenerated energy.

### 2.3.3 Eliminate Islanding

Increased electrical meshing of a traction network means that regenerated energy has a higher chance of being absorbed by another train. Islanding refers to a situation where neighbouring electrical sections are not connected. All energy that is used and generated in that section must therefore be supplied and consumed within itself. By closing all circuit breakers at every node and installing more circuit breakers at points where there is a physical node, but no electrical node the receptivity is increased. This does not only assist trains that are braking

regeneratively, but also the substations that would otherwise have to feed the section alone.

### 2.3.4 Paralleling

Traction energy conductors (overhead lines and rails) of adjacent tracks often only connect electrically at feeder points (substations). If two trains physically pass each other mid-section, one braking and the other motoring, the regenerated energy needs to take a long detour. By connecting adjacent conductors in parallel mid-section (or more), the effective electrical distance between the trains is reduced.

Let  $\rho$ , in  $\Omega/\text{km}$ , be the typical total specific resistance of the overhead line and rails,  $d$  the distance between feeder points and  $I$  the overhead line current. The ohmic drop can be calculated as the product of these three variables. Three simple scenarios is investigated: a) where the section is fed from only one side, b) where it is fed from both ends, but without paralleling, and c) where it is paralleled midway. The ohmic drop for each of these scenarios is shown in Figure 2.8. It can be shown mathematically [17, chap. 3] that the maximum voltage drop for scenario a is  $\rho dI$ . For scenario b the maximum voltage drop is  $\frac{1}{4}\rho dI$ , a reduction of 75%. With the paralleling of scenario c the maximum voltage drop is  $\frac{1}{6}\rho dI$ , a further reduction of 33%. It can also be shown [17, chap. 3] that for a continuous

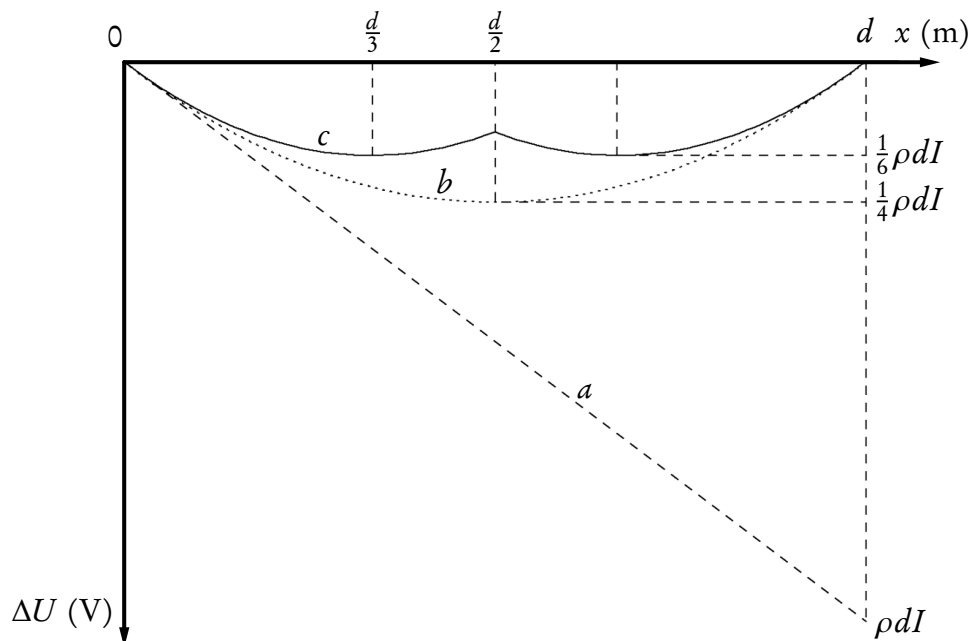


Figure 2.8: Voltage drops for different scenarios of section feeding [17, chap. 3]

load between two feeder points, the average power dissipated in the overhead line without paralleling is  $\frac{1}{12}\rho dI^2$ . With paralleling this can be reduced by 37,5 % to  $\frac{5}{96}\rho dI^2$ . These examples show that paralleling can considerably reduce voltage drops and conductor losses.

Some arguments against the wider use of paralleling stations include the additional hardware cost and operational issues. A passive, wire, connection between adjacent overhead lines is relatively cheap, but will almost certainly lead to operational problems, because running lines can not be switched off separately for maintenance purposes or in emergencies. A more expensive option is to install a high-speed circuit breaker between the lines. Modern circuit breakers can switch in as little as 20 ms [17, chap. 4]. This ensures that sections can be isolated quickly during a short-circuit.

By increasing the amount of paralleling stations on their network, the Belgian railways (3000 V<sub>DC</sub>) have been able to sufficiently increase their network's receptivity that, even with a high prevalence of regenerative braking, no reversible substations are currently deemed necessary. At half the voltage, the Dutch railways (1500 V<sub>DC</sub>) have a big problem with voltage drops and is following the Belgian example by installing more paralleling stations [18].

### 2.3.5 Energy Storage Systems

ESSs are able to capture the kinetic energy of regeneratively braking vehicles and feed it back during times of high power demand [19]. ESSs can be installed at fixed, track-side, locations or on board rolling stock [11]. When carried on board, vehicles may even be able to run on non-electrified sections of line, such as sensitive historic centres or city down-towns. One example of this is Alstom's Citadis Ecopack that allows trams to operate without overhead lines by using supercapacitors [20].

Energy storage on networks with regular accelerating—decelerating cycles offer three main advantages: a lower total energy consumption, more equalised load peaks on the energy supply (reduced maximum power or so-called peak shaving) [19] and the overhead line voltage can be boosted, increasing stability and reducing conductor losses.

ESSs can be especially useful on weak networks that suffer from frequent over- and under-voltages. It may be installed at any location and does not have to be connected to the AC grid. This is very advantageous to operators that do not have

their own medium voltage AC network. These operators have to pay for every connection to the public grid, normally relative to the installed peak load capacity. They also face a profusion of regulatory and other obstacles to discourage feeding energy back into the grid.

Various ESS technologies are available for transport purposes, but the most commonly used are: batteries (of different chemical make-up), electric double layer capacitors (EDLCs) and flywheels. The main difference between these technologies is the energy storage medium employed. Batteries convert electrical energy to chemical energy, EDLCs store energy by means of charge separation and flywheels capture the energy kinetically in a rotating mass [15]. Their implementation is generally the same: the ESS would be connected to the traction network through a power converter to capture surplus energy and the energy is stored in the relevant form. When the control system detects a shortage of energy, the stored energy is fed back to the overhead line.

The choice of technology can be a complicated trade-off between the various advantages and disadvantages of each technology and depends heavily on the application. Important characteristics include: power density, energy density, efficiency, lifetime (or cycle life) and self-discharge [15]. It is advised [15] that “other aspects such as cost, reliability, safety, required maintenance, etc. should also be considered.”

EDLCs offer a relatively high power density, high efficiency and long lifetime. Unfortunately they offer low energy density, when compared to batteries and flywheels. By nature, their voltage is a function of the state-of-charge. This is convenient to calculate the available energy, but it restricts the direct integration with the network. Due to the voltage variation, a direct connection with the overhead line would be almost pointless. A DC-DC converter is used to adapt the varying voltage to the relatively stable DC overhead line voltage [15]. Flywheels offer similar power densities to EDLCs, but a higher energy density. Due to the moving components, flywheels suffer from a high self-discharge rate (high frictional loss or windage) [21], higher maintenance requirement and additional safety measures [22].

Table 2.1 compares different ESS solutions. A comparison is made between different battery technologies (lead-acid, nickel-cadmium (NiCd), nickel-metal hydride (NiMH), lithium-ion, lithium-polymer and sodium-sulfur (NaS)), flow batteries (vanadium redox (VRB)), EDLCs, pumped hydro systems, compressed

air energy storage (CAES) and flywheels. It shows that EDLCs and composite flywheels possess a good combination of power density, efficiency and lifetime. These characteristics are very important for urban transport applications, where the ESS must endure frequent, large power flows due to the continuous acceleration and braking of vehicles. [15]

Extensive research has been done by companies and universities to determine control laws for ESSs that optimally utilise the stored energy for the set objective. Because the occurrence of accelerating and decelerating is unknown, the control must adjust in real-time [19].

### 2.3.6 Reversible Substations

Reversible substations allow surplus energy to flow back to the medium voltage AC grid. One of the first installations of a power-supply system with inverters was in 1977 on the Seishin Line of the Kobe Metro, Japan [24]. The viability of these systems have significantly improved over the last decades. This is partly due to increased consciousness about energy efficiency, because of increased energy prices and environmental concerns, and research and development of more efficient converters to maximise the energy savings [25]. Such systems can only be financially viable if the railway operator has its own medium voltage AC network to feed into or if it is compensated for the energy that is injected into an external AC grid [11].

Table 2.1: Comparison of different ESS technologies [23]

Type	Energy Efficiency (%)	Energy Density (Wh/kg)	Power Density (W/kg)	Cycle Life (cycles)	Self Discharge
Lead-Acid	70–80	20–35	25	200–2000	Low
NiCd	60–90	40–60	140–180	500–2000	Low
NiMH	50–80	60–80	220	< 3000	High
Lithium-Ion	70–85	100–200	360	500–2000	Med
Lithium-polymer	70	200	250–1000	> 1200	Med
NaS	70	120	120	2000	–
VRB	80	25	80–150	> 16 000	Negligible
EDLC	95	< 50	4000	> 50 000	Very high
Pumped hydro	65–80	0,3	–	> 20 years	Negligible
CAES	40–50	10–30	–	> 20 years	–
Flywheel (steel)	95	5–30	1000	> 20 000	Very high
Flywheel (composite)	95	> 50	5000	> 20 000	Very high

Modern reversible substations can consist of either a traditional silicon diode rectifier with an inverter in antiparallel, or a bi-directional converter that can operate in both rectifying and inverting modes. The first solution is often preferred to improve the receptivity of existing networks. Due to natural exchange between trains and transmission losses the inverter can usually be of a lower power rating than the rectifier. Fully bi-directional systems offer various other benefits and may be preferable for new installations [11]. Both configurations rely on matured technology and is in use on numerous suburban, tram and metro networks [15; 26].

### 2.3.6.1 Inverter Threshold Analysis

Barrero [15, chap. 4] illustrates that careful analysis is needed to determine the voltage level at which the inverter extracts power. When the DC bus voltage reaches the threshold voltage, the substation control system will try to clamp the voltage to this value by adjusting the amount of extracted current, see Figure 2.9. The threshold must be higher than the substations' OCV to prevent power circulation between the rectifier and inverter [15]. It must also be lower than the maximum allowed braking voltage to limit the amount of braking energy being dissipated in the rheostats [15]. Lastly, the natural exchange between trains must be promoted, but only up to a certain extent. Since the goal is to reduce overall energy use, a trade-off needs to be made between encouraging the braking energy to flow through the low voltage DC overhead line (higher threshold) and rather inverting it to medium voltage AC and then rectifying it back to DC elsewhere (lower threshold).

The results of simulations done by Barrero [15] for Metro line 6 of the Société des Transports Intercommunaux de Bruxelles (Stib) in Brussels is shown in

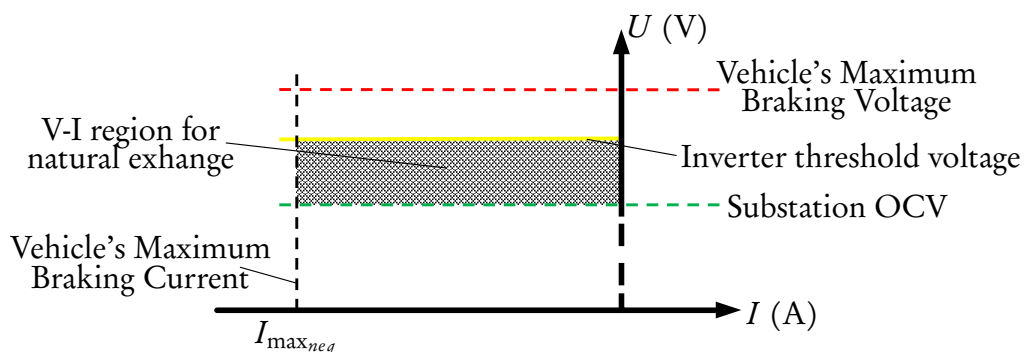


Figure 2.9: Typical V-I characteristics for reversible substation control

Figure 2.10. The OCV of the 14 substations on this line range between 819 V and 871 V.  $V_0+10$  represents a threshold voltage set to the maximum between the relevant substation's OCV and its neighbours' OCV plus 10 V. This will prevent almost all natural exchange between trains, leading to almost 25 % of the original rectified energy being inverted back to the grid, but also an increase of almost 20 % in the amount of energy that needs to be rectified elsewhere. This strategy should realise a net energy saving of almost 5 %. When the threshold voltage is higher, and OCVs set more equally, natural exchange is stimulated and net energy savings increase. According to the results, the optimum threshold level for this system is 870 V, with a possible net energy saving of more than 7 %. At a threshold of 880 V, ohmic drops will cause the pantograph voltages to often reach the maximum voltage and excessive braking energy will be lost in the rheostats, hence lower savings.

### 2.3.6.2 Inverter Placement Analysis

When a network is to be retrofitted with inverters in antiparallel with existing rectifiers, their placement and power rating should be carefully chosen. Due to power sinks, such as conductor losses, natural exchange and rolling stock losses, each inverter's installed power can be much lower than associated rectifier's rating. Because of the high cost of every inverter, the minimum amount of inverters required to realise sufficient savings must be determined. Additional simulations by Barrero [15] show that, for this network, the savings increase significantly relative to the number of inverters until six to eight inverters, see Figure 2.11. With more than eight inverters, the savings for each additional inverter is less.

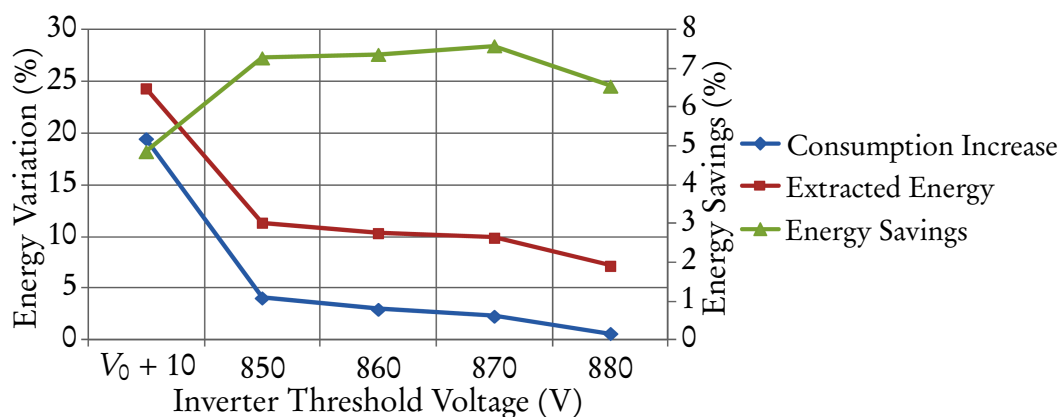


Figure 2.10: System behaviour in terms of inverter threshold voltage [15]



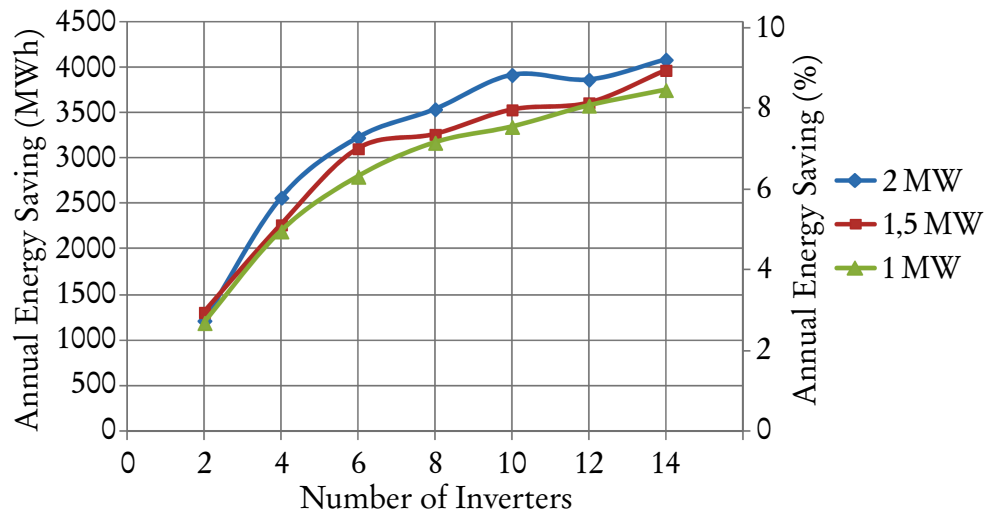


Figure 2.11: Annual energy savings as a function of the number of inverters and their power rating [15]

The simulation results also show very little difference in the savings that can be expected for different power ratings. Barrero [15] concludes that a good trade-off will be the installation of 6 to 8 inverters of 1 MW to 1,5 MW rated power.

### 2.3.6.3 Usefulness of Reversible Substations

Ohm's law dictate that the reversible substation's theoretical maximum achievable energy recuperation will be limited to the energy that would otherwise be dissipated in the rheostats and overhead conductors. Figure 2.7 on page 12 provides a visual explanation.

Figure 2.12 illustrates a scenario where a regenerating train is providing in the exact power requirement of a powering train that is far away. In order to

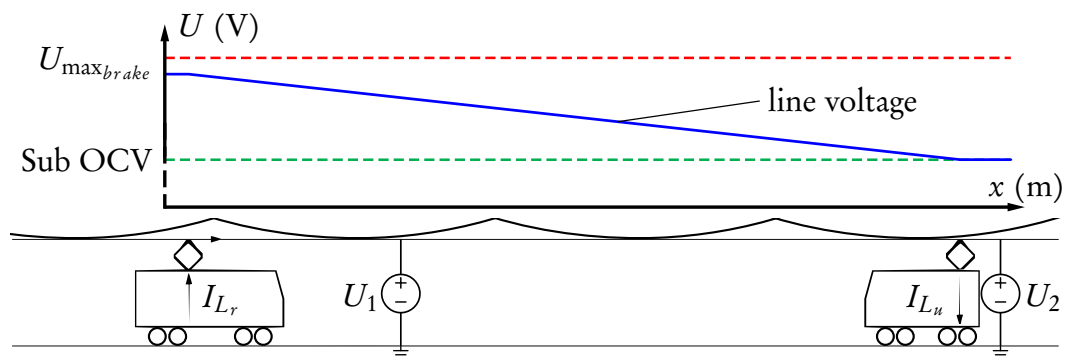


Figure 2.12: Line voltage along the overhead line when a regenerating train is providing in the full power requirement of a powering train that is far away

prevent the substations from contributing any power the pantograph voltage at the powering train will be at the substations' OCV. The pantograph voltage at the regenerating train will be increased until the full regenerated power is flowing into the overhead line or the maximum braking voltage,  $U_{\max_{brake}}$ , is reached. The amount of current injected by the regenerating train,  $I_{L_r}$ , is also the current extracted by the powering train,  $I_{L_u}$ . Because the pantograph voltages are different, the power injected by the regenerating train is higher than what is sinked by the powering train. The difference in power is the energy that is dissipated in the overhead line.

When a reversible substation is installed at  $U_1$  the ohmic drop is reduced and the pantograph voltage is much lower for the same amount of power that is regenerated. This scenario is illustrated in Figure 2.13. The full regenerated power is not absorbed by the reversible substation, because the inverter threshold voltage is higher than the other substation's OCV <sup>1</sup>. In order to provide in its energy requirement, the powering train will increase the current until the pantograph voltage is below substation  $U_2$ 's OCV. This will forward bias the diodes and allow  $U_2$  to contribute energy to the DC network. The diodes at substation  $U_1$  is reverse biased and the rectifier can not contribute any power to the DC network.

The two trains in Figure 2.14 are closer than in the scenario sketched by Figures 2.12 and 2.13. The power injected by the regenerating train,  $I_{L_r}$ , and the power sinked by the powering train,  $I_{L_u}$ , is the same as in the scenario of Figure 2.12. Because less energy is now dissipated in the overhead line, there is

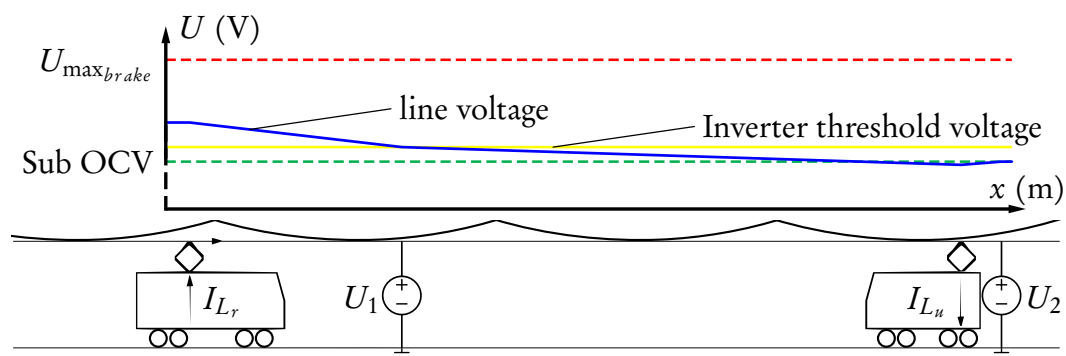


Figure 2.13: Line voltage along the overhead line when an inverter is used and trains are far

<sup>1</sup>Ohm's law states the relationship between current and voltage is:  $I = \Delta V/R$ . This implies that a difference in voltage between the reversible substation,  $U_1$ , and the powering train,  $I_{L_u}$ , will force power to flow between the two points.

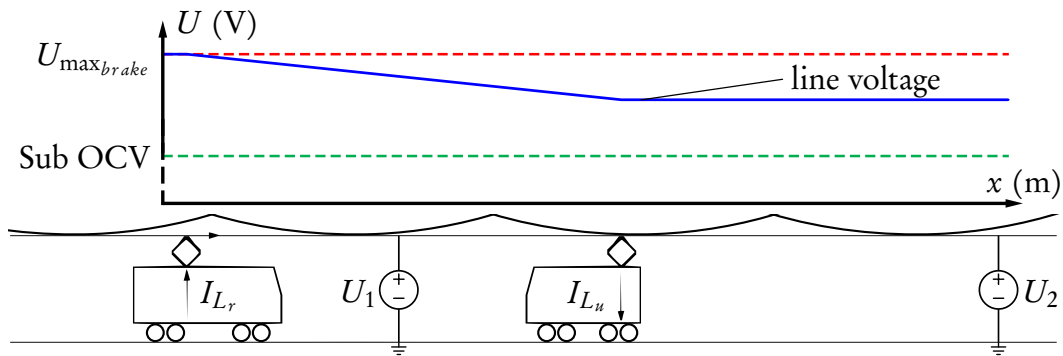


Figure 2.14: Line voltage along the overhead line when a regenerating train is providing in the full power requirement of a nearby powering train

an energy surplus in the DC network. In an attempt to dissipate the power that is being regenerated,  $I_{L_r}$  continues to increase the pantograph voltage until the maximum braking voltage,  $U_{\max_{brake}}$ , is reached. Once this voltage is reached the rheostatic braking will be used to dissipate the surplus regenerated energy. This has a counter productive effect, because the higher voltage means that less current is needed to transfer the same amount of power leading to lower conductor losses. Less energy will therefore be dissipated in the overhead line and more in the rheostats. If there were other trains cruising in stead of coasting then their energy requirement could have been supplied from the regenerated energy. This could have prevented wasting energy in the rheostats.

When a reversible substation is installed at  $U_1$  the pantograph voltage is much lower for the same amount of power that is regenerated and no rheostatic braking is necessary. This scenario is illustrated in Figure 2.15.

Even in this scenario the diodes at substation  $U_2$  will be forward biased to supply in the energy requirement of the powering train.

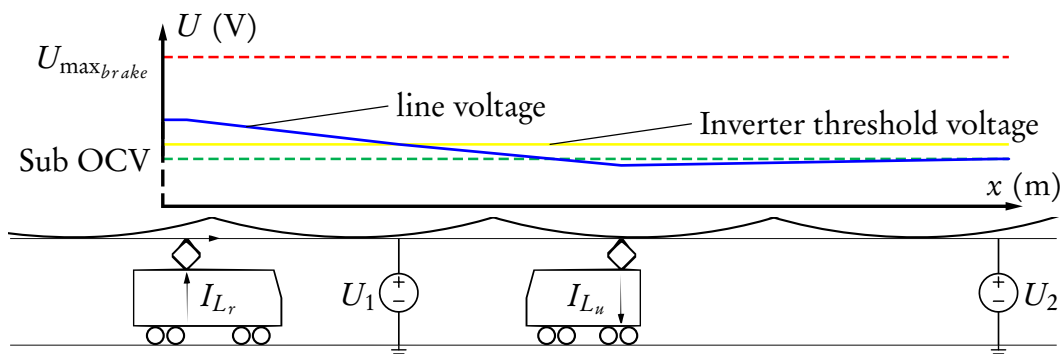


Figure 2.15: Line voltage along the overhead line when an inverter is used and trains are close

The scenario shown in Figure 2.16 is included to illustrate the situation where the regenerating train,  $I_{L_r}$ , is not able to supply the full energy requirement of the powering train,  $I_{L_u}$ . In this example the power sunk by  $I_{L_u}$  is the same, but the power generated by  $I_{L_r}$  is about 40 % less. The overhead line voltage at substation  $U_1$  will be exactly at the OCV and very little power will be contributed by this substation.

### 2.3.7 Reversible Substation Hardware

This section will briefly introduce some of the reversible substation options that is currently available. Examples of their usage will also be provided.

#### 2.3.7.1 ABB ENVILINE™ ERS

ABB's ENVILINE energy recuperation system (ERS) for DC rail transportation reduces energy costs by returning the braking energy to the AC network. This system can “mitigate the reactive power” when not inverting energy to the AC grid. It can also provide active filtering, for “reduction of harmonics effect”, and possible active rectification, to “support existing rectifiers”, thanks to the bi-directionality of the IGBT-based converter. [27]

Some key benefits highlighted in their product brochure [27]:

- **Low energy costs through energy recuperation:** Improves the energy efficiency by 10 % to 30 %
- **Improves quality of AC power network:** Harmonics and reactive power mitigation

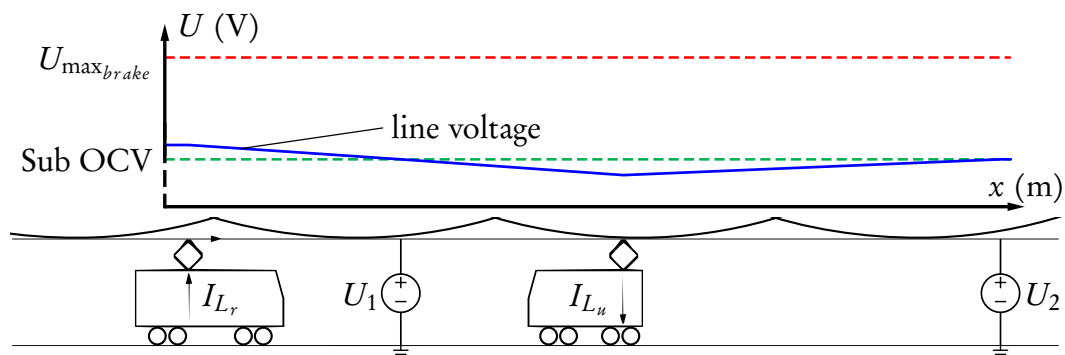


Figure 2.16: Line voltage along the overhead line when the regenerated power is too little for the power requirement of a nearby powering train

- **Lowest upfront cost and maintenance cost:** Smallest footprint, easy installation, low maintenance
- **Compatible with new and existing systems**
- **Over 50 years of experience**

Total Demand Distortion is less than 5%. ENVILINE ERS is currently available in 600 V to 750 V versions of between 500 kW and 1 MW. Systems for 1500 V and 3000 V networks, rated at 2 MW, will be available “soon”. Provision is made for an overload capability of up to 225%. The rated efficiency is 97,5%. [27]

The only known installation of this system is a pilot application in the Polish city of Łódź that was scheduled to enter service in May 2013 [28].

### 2.3.7.2 AEG Thyrobox RI

AEG Power Solutions’ Thyrobox RI inverter reacts to increased overhead line voltage and feeds excess energy back into the grid. This system uses “high quality semi-conductors” and “proven” B6 thyristor bridge to offer “tremendous robustness and high overall efficiency.” The system is currently available in 750 V and 1500 V versions of 1,2 MW with an efficiency of 96%. [29]

AEG Belgium is part of the Ticket to Kyoto initiative and supplied a unit to the Stib in Brussels during 2012 [30; 31]. The performance of this system was compared to systems by Siemens and Ingeteam over a three month period at the Stib’s Laubespain substation [32]. Information regarding the performance of each system is not in the public domain, but no additional orders for the AEG system were placed.

No additional information concerning the application of a Thyrobox RI system could be found.

### 2.3.7.3 Alstom HESOP

Alstom developed their Harmonic and Energy Saving OPTimizer (Hesop) system. They claim [33] that it is the “only ‘all-in-one’ solution that offers both traction and recovery functions in the same equipment.” The single, IGBT-based, converter offers dynamic regulation of the DC bus voltage. This optimises the power required for traction and captures more than 99% of recoverable energy during braking mode. [33]

Some “customer benefits” quoted from their product sheet [33]:

- **Infrastructure cost savings:** Hesop enables to increase the distance between substations and thereby reduces their number: 5 to 7 classic substations can be replaced by only 4 to 6 Hesop substations, depending on the line layout and operating data. This results in less infrastructure investment, i.e. real estate and civil work.
- **Best energy savings:** Thanks to dynamic voltage regulation, Hesop captures more than 99 % of the energy usually lost during braking mode. The energy recovered can be re-injected into the electricity network or re-used through the station equipment: escalators, lighting and ventilation. This results in traction energy savings of up to 40 % depending on the network's operational specificities [sic].
- **Optimised energy quality & operation:** Hesop permits high energy quality and thereby avoids penalties or allows cheaper subscription from the power supplier. The recovered energy can also be easily re-sold, if not completely used within the network. Additionally, Hesop guarantees reliable train operation via dynamic adjustment to fluctuations and allows evolution: voltage modification, traffic increase; while preserving the same equipment.
- **Less tunnel & in-station ventilation:** Thanks to full recovery of available braking energy which leads to high line receptivity, Hesop limits train heat dissipation. This leads to less tunnel and in-station ventilation or air-conditioning; and to the removal of onboard brake resistors. The train's weight is reduced which contributes to further traction energy savings.

The hardware is air-cooled, leading to lower maintenance requirements than previous, water-cooled, models. total harmonic distortion (THD) is less than 5 % with a power factor of 1. Hesop is currently available in 600 V and 750 V versions of up to 2 MW. A 1500 V system, rated at 4 MW, was developed jointly with Azienda Trasporti Milanese (ATM), the operator of the Milan metro and was available for sale as of 2015 [33]. All systems are designed for an overload capacity of 150 % for 2 hours and 300 % for 1 minute in both rectifier (traction) and inverting (recovery) modes. Current installations include Paris Tramway (1 unit at 750 V, 900 kW; Jul 2011), London Underground (1 unit at 600 V, 1 MW; Jun 2014) and Milan Metro (1 unit at 1500 V, 4 MW; 2016). Other confirmed contracts include Milan Tramway (16 units at 600 V, 1 MW; 2018), Riyadh Metro (70 units at 750 V, 1,2 MW; 2017) and Sydney Tramway (13 units at 750 V; 2016). [33; 34]

The system is adaptable to 3000 V, should the need arise [35].

#### 2.3.7.4 Ingeteam Ingeber

The Ingeteam Ingeber system allows harnessing energy from regenerative braking and feeding it back to the grid. Ingeber acts as a “pump of energy from [the] railway system.” The IGBT-based converter is installed in antiparallel with the rectifier and does not require modifications to the existing substation installations, such as rectifiers and transformers. This “transparent” configuration means it can be isolated without interrupting train services. The efficiency ratios is also optimised, because the system’s power rating is based on previewed savings, not on existing installed power. The system is designed for a 30 year lifetime. [36]

An additional benefit of using IGBT-technology is the ability to use the system as an active filter to regulate the consumption of the substation. The resultant power factor improvement will realise additional savings. [37]

Ingeteam recommends a three phased evaluation process to ensure the optimal solution and return on investment (ROI). The three phases are: data intake, mathematical analysis and simulation. The results of this process provide the recommended number, optimal power rating and location of Ingeber systems to be installed. It also gives a preview of the achievable savings for the proposed investment and the ROI rate. [36]

THD is less than 5%. Ingeber is available in 750 V, 1500 V and 3300 V versions rated at 1 MW to 2 MW. The voltage and power combination is configured according to the outcome of the evaluation process. Various Ingeber systems are in active use including Metro Bilbao (Spain 2009; 1 unit @ 750 V, 1,5 MW; 2nd phase already completed, 5 units in commercial exploitation), ADIF Suburban train (Málaga, Spain 2013; 1 unit @ 3300 V, 2 MW), Bielefeld moBiel Tram (Germany; 3 units @ 750 V, 1 MW; originally T2K initiative, now in commercial exploitation [16]) and Stib Metro (Belgium; 1 unit @ 750 V, 1,5 MW; part of T2K, order placed for 5 additional units for installation during Q3 2015 [16]). [36]

#### 2.3.7.5 Siemens Sitras<sup>®</sup> TCI

Siemens’ Sitras thyristor controlled inverter (TCI) allow DC traction substations with diode rectifiers to return surplus energy to the medium voltage AC grid. This allows braking energy to be transmitted via the AC network to “loads that are even further away”. [38]

The system is housed in a panel group of three or four cubicles, allowing easy integration into existing substations. The cubicles offer front access and is thus suitable for wall mounting. All terminals are arranged in the downward direction for easy installation. B6 thyristor bridge technology with fuses is used for robustness and reliability. The design also includes a DC choking coil to “limit the circuit [sic] currents between diode rectifiers and the thyristor inverter”. [38]

The secondary equipment includes closed looped control to meet the power requirements of DC railways in a “highly dynamic manner.” It also features an “ergonomically designed” Simantic<sup>®</sup> Touch-Panel on the panel group that provides the operating staff with “a quick and reliable overview of the operating state of the system.” Lastly, standardised communication interfaces are provided for remote link-up to allow remote parametrisation, control and diagnosis. [38]

The Sitras TCI is currently available in 750 V and 1500 V versions rated at 2,25 MW and 1,5 MW respectively for 30 s. The efficiency is stated as 96 %. [38]

This system has been tested on Oslo Metro’s Holmenkollen Line [26]. As of February 2014, Siemens is supplying the signalling and traction power supply systems for Singapore’s Downtown Line 1 [39]. The line will have a total length of 42 km and recovered electrical energy will be fed back with Sitras TCI Inverters [39]. The number and geographic distribution of the inverters along the line is not readily available. The 1500 V version has been operating since 2007 on the Bayerische Zugspitzbahn Bergbahn [40] in southern Germany. Ruling grades of 1 in 40 offer good potential for recuperation [41]. Meinert *et al.* [42] reports that “the recuperated energy can reach up to 40 % of the total primary energy demand.”

One unit was also installed at the Laubespain substation in Brussels as part of the Stib’s Ticket to Kyoto initiative and tested alongside the systems by AEG and Ingeteam [32]. The results are not in the public domain, but no additional order for the Siemens system was placed.

## 2.4 Load-flow Simulation Software

Determining the solution, or combination of solutions, that will be best suited to increase the receptivity, and consequent savings, is not a trivial process. Experience has shown that even networks that look very similar at first glance have very different optimal solutions [16]. With the presentation of his findings, Barrero [15] warns that, “these results are very particular to this metro line and cannot be



extrapolated to ‘similar lines’.”

Powerful modern computers enables engineers to determine the optimal solution through simulation. Computer simulations offer the advantage that the effect of any combination of solutions can be investigated before a single change is made to the physical infrastructure. As with any simulation, the quality of the input determines the quality of the output. Typical parameters include: vehicle mass and efficiencies; braking control strategy; maximum braking voltage; headways; substations’ OCV and internal resistance; feeders, rail and overhead line resistance; substation locations; slopes; driving cycle; occupancy rate and auxiliaries’ consumption [15].

The increased interest in the reduction of energy usage have led to the development of many different simulation suites by various role-players. Some examples are discussed in the following subsections.

### 2.4.1 Simulation from First Principles

An alternative to using a simulation suite specially designed for railway or power system applications is to use a general simulation package, such as MATLAB<sup>®</sup> Simulink<sup>®</sup>, and describe models from first principles. This method has been successfully used to create the “Multi-train simulation tool” that was used by Vrije Universiteit Brussel to simulate the Stib lines 2 and 6 [15, chap. 3]. Their simulations have proven to deliver relatively good results, with simulated total energy consumption only 6 % lower than the measured energy [15].

Due to the moving loads (trains), the topology of the system is different at every simulation time-step. The network is thus analysed at each time-step, the equations are arranged accordingly and the line resistances are calculated. The system is expressed in terms of system equations that are set in a matrix

$$AX = B \quad (2.1)$$

where  $A$  is the system matrix,  $X$  the vector containing the variables (voltage and current) that must be solved and  $B$  the system inputs. The variables are solved by inverting  $A$  and multiplying it with the input matrix,  $B$ :

$$X = A^{-1}B \quad (2.2)$$

With the solved voltages and currents known at each time-step, the data can be post-processed to create graphical outputs and calculate values for power and

energy. This system may take a long time to set up, execute and post-process the results, but does offer relatively good accuracy.

Another example of a method that models the AC and DC power flows from first principles is presented in [43]. It uses the unified Newton-Raphson method to solve the power flows. The equations are solved and applied to a commercially available Transportation System Energy Management Model simulator to enhance the performance of the electric network solutions [43].

## 2.4.2 DIgSILENT PowerFactory

DIgSILENT, a consulting and software company, provides engineering services in the electrical power systems field. They develop PowerFactory, an integrated power system analysis software for analysing generation, transmission, distribution and industrial systems. According to the product brochure it “has set standards and trends in power system modelling, analysis and simulation for more than 25 years. It covers the full range of functionality from standard features to highly sophisticated and advanced applications including wind power, distributed generation, real-time simulation and performance monitoring for system testing and

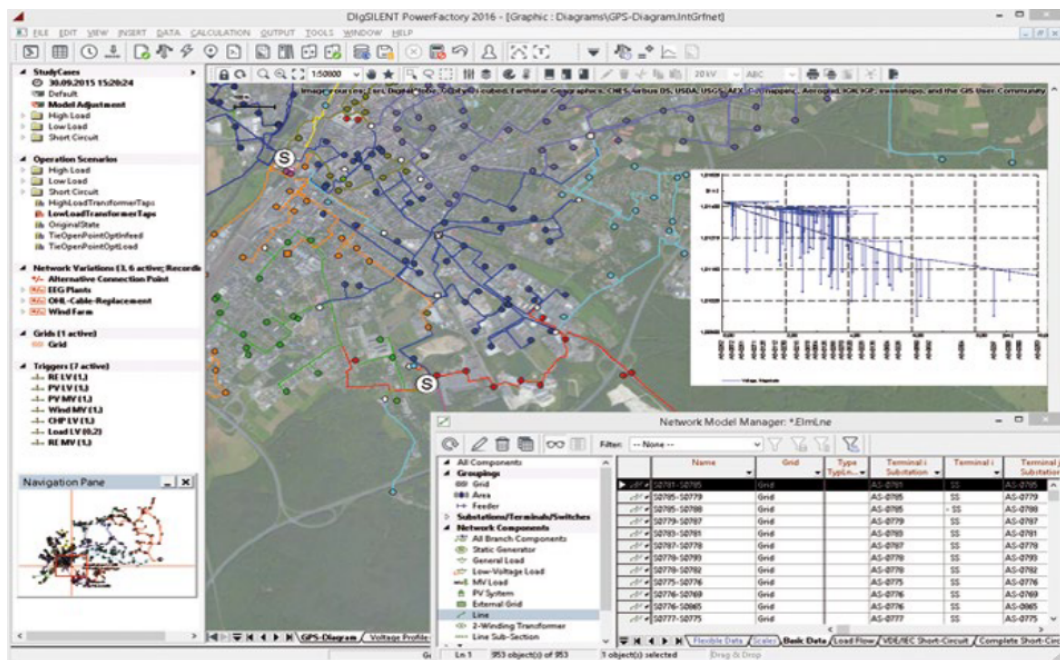


Figure 2.17: Screenshot of DIgSILENT PowerFactory showing the Graphical User Interface (GUI) with geographical representation, database manager and output graph [44]

supervision. PowerFactory is easy to use, fully Windows compatible and combines reliable and flexible system modelling capabilities with state-of-the-art algorithms and a unique database concept. For wind power applications, PowerFactory has become the power industry's de-facto standard tool, due to PowerFactory models and algorithms providing unrivalled accuracy and performance. With its rich modelling capabilities, PowerFactory is perfectly suited for network planning and operation studies of increasingly smart grids." [44]

PowerFactory is therefore designed for analysing power systems in general and does not specifically focus on railway networks. If the traction network of a railway system is analysed as an electrical power system, instead of focussing on the detail modelling of rolling stock, then PowerFactory offers the following very valuable functions [44]:

- Extensive and flexible modelling capabilities with large and comprehensive suite of power equipment models and libraries (including External grids; AC and DC voltage and current sources; cables and tower geometries; substation equipment like transformers, busbars and various switches; and power electronic devices like DC-DC converters, inverters and diodes).
- Parameter characteristics (scaling factor, vector, matrix, files) for modelling of load profiles, wind/PV infeed, temperature dependencies, etc.
- Support of any kind of meshed/radial 1-, 2-, 3- and 4-wire AC and DC networks with combined AC and DC modelling for all available analysis functions.
- Powerful network diagrams and graphic/visualisation features.
- Rich interfacing and system integration options (e.g. GIS, SCADA, EMS).
- Quasi-dynamic simulation tool which performs medium- to long-term simulations based on steady-state analysis. It can take time and time-profile characteristics as input for simplified modelling of (recurrent) time series. It can consider planned outages, network variations and expansion stages. Output includes simulation plots and tabular reports including statistical analysis. The 2016 version also provides support for parallelised simulation on multiprocessor hardware.

- Scripting and automation features including the integration of Python as programming language with full PowerFactory data model access and rich function suite. It also makes use of DIgSILENT Programming Language (DPL), a C-like syntax supporting unlimited access to PowerFactory objects, parameters and their functionality. A task automation tool was introduced with the 2016 version for parallelised execution of calculation functions and scripts.
- Various other tools for analysing protection schemes, harmonics and failure models.

DIgSILENT is therefore an economical, all-in-one solution with broad coverage of power system applications. It features support for simultaneous load flow analysis of both the AC and DC networks, but lacks the functionality to simulate moving loads along DC lines.

### 2.4.3 Infrabel Load-flow Simulation

Infrabel, the Belgian railway infrastructure manager, has developed an in-house simulation tool for load-flow analysis of its 3 kV DC traction network [45]. The original purpose was to estimate the impact of the loss of any substation in its network. This has since been extended to also simulate the influence of variables like substation no-load voltage, timetable changes and regenerating capabilities of different rolling stock classes.

The program starts by reading the inputs, which are stored in text files. These input files describe the fixed installations of the electrical traction network, rolling stock characteristics, lines and tracks (geometry and ptcars) and timetables. The text files can be created automatically by converting XML, manually or manual changes to basic structures. [45]

The input data is used to determine train movements and calculate the energy flow through the network. This is an iterative process that starts with each train's speed and position; determining the braking, power and current demands; calculating the overhead line voltages and currents; and saving the power, tractive effort, acceleration and distance. The process is repeated once for every physical second. [45]

After the simulation is done the output is provided in text file format. The files give the following for every second: all train variables per train and per

track section and all substation variables. For every 15 minutes: total energy consumption per substation and delays caused due to lack of power. [45]

Since the output data alone does not mean much, some post-processing tools have also been implemented. The tools that provide visual outputs have proven especially helpful. This includes graphs of simulated versus measured power, voltage and current (see Figure 2.18); time-space (Marvey) diagrams to compare simulation and planning; and colour coded maps to judge the prevalence of under- and over voltages, regenerative braking and power usage (see Figure 2.19). [45]

Infrabel has invested a lot of man-hours to build a product that suits its needs and assists with short- and long-term planning. The program is not commercially

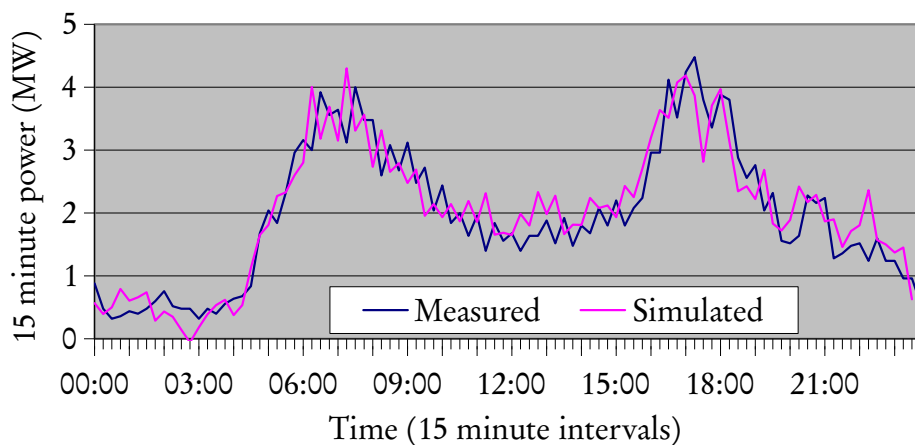


Figure 2.18: Graph showing the simulated versus measured power of Enghien substation for 24 hours [45]

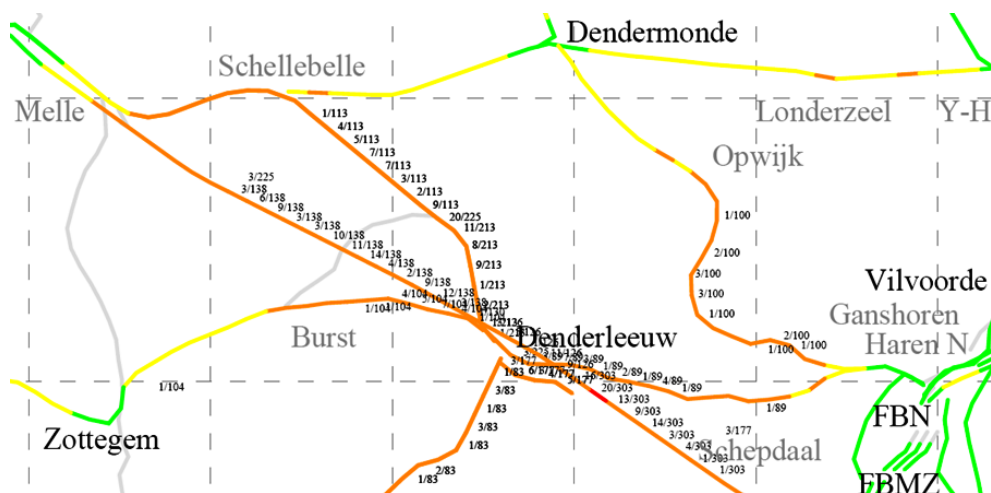


Figure 2.19: Map showing the prevalence of low line voltage during the simulation period [45]

available for use by other railways, but it has been used as part of consultation work by Transurb Technirail, a subsidiary company. [46]

#### 2.4.4 Ingeteam

Ingeteam has developed network analysing software for its internal use during consulting and development phases [16]. It analyses different data streams that influence the proposed solution, such as: schedule, train types, nominal line voltages and geographical distribution of recovery systems. The tool is based on a time variable impedance matrix that is solved through pattern calculation. This allows the analysis of voltage, current, energy and power at all points of the network. [47]

The results from this analysis is used to advise clients on their proposed solution, as discussed in Section 2.3.7.4.

#### 2.4.5 Siemens Sitras<sup>®</sup> Sidytrac

Siemens have developed the Sitras Sidytrac simulation tool to assist them with the system design of railway electrification systems. The main features are [48]:

- Detailed design of new AC or DC traction systems with electrical dimensioning of substations and overhead line systems, including system-wide economical design and power reserve calculation for further extensions.
- System comparisons and feasibility studies.
- System optimisation concerning energy consumption and erection costs.

The program provides detailed output data in both text-based and graphical formats. The customisable graphical representation of data enables the customer to easily analyse the data [48]. Sidytrac was developed for internal use by Siemens, but they have indicated that work is being done to also offer it as a stand-alone package [49].

## 2.5 Historical South African Perspective

Regenerative braking is not a new concept to South African railways. This section will provide basic insight into the use of such braking in South Africa and examples of local research that have been conducted.

### 2.5.1 Mainline Use

South Africa's difficult, mountainous terrain led to the very early adoption of electric railway traction. The Glencoe to Pietermaritzburg railway line, with some ruling gradients as steep as 1 in 66, was electrified in 1925. It is claimed that this scheme was the first to ever use regenerative braking with coupled locomotives extensively [50]. The South African Railways (SAR) initially ordered 78 of the class 1E locomotives for this scheme. At the time it was the largest order ever for a single type of electric locomotive in the world [51].

Receptivity was almost guaranteed, because the 3000 V overhead line voltage was supplied by rotary motor generator sets. Each motor generator set consisted of a 6600 V three-phase AC 50 Hz synchronous motor, directly coupled to two 1500 V DC generators designed for series operation. This allowed for full bi-directional flow of energy between the AC supply and DC overhead line. [52]

When rotary converters were replaced with mercury-arc rectifiers, between 1954 and 1958 [53], mercury-arc mutators (inverters) were connected in antiparallel to allow bi-directional flow [54]. As substations were converted to silicon-based technology <sup>2</sup>, from 1966 onwards [53], no provision was made for regeneration [54]. This meant that regenerated energy dissipation was limited to natural exchange and resistor banks at substations.

The main objective of regeneration was not to save energy, but to enable safe running at higher speeds on down grades [50]. Regeneration on the SAR was not meant to slow the trains down, but to keep the train at a constant speed during decent. The the ordinary braking system (vacuum brakes) was kept in reserve and used to stop the train [56].

All locomotive classes for DC traction up to the South African class 12E, except for the 3E [57] and 8E [58], had regenerative braking capabilities [59; 60; 61; 62; 63; 64; 65; 66; 67]. When AC electrification was introduced, locomotives used thyristor-control that did not allow for regenerative braking and large rheostatic braking capacity was installed on locomotives instead (classes 7E [68], 9E [69] and 11E [70]). The first dual voltage, 3 kV<sub>DC</sub> and 25 kV<sub>AC</sub>, locomotives, class 14E had regenerative braking on 3 kV and rheostatic braking on 25 kV [71]. The first, and only, dual mode (3 kV and diesel) locomotives in South Africa, class 38-000, had both regenerative braking and rheostatic braking [72].

---

<sup>2</sup>The SAR energised the first solid state silicon diode rectifier substation on 3 kV in the world in August 1962. After a successful trial period it adopted this form of rectification as standard. [55]

Some 136 locomotives of the 6E1 class were rebuilt by Spoornet in 1993 and reclassified to class 17E. One of the key modifications was improved regenerative braking [73]. Later rebuilds of the 6E1, and even 17E, locomotives to class 18E involved the complete removal of regenerative braking and installation of onboard rheostats [74].

This tide turned only recently with the acquisition of classes 15E, 19E and 20E. These classes feature regenerative braking on both 3 kV<sub>DC</sub> and 25 kV<sub>AC</sub> (50 kV<sub>AC</sub> for 15E). [75; 76; 77]

Transnet, the freight rail operator, applied for a power-producer licence in November 2012. This will enable it to feed energy that is regenerated on AC electrified lines back into the national grid. [78]

### 2.5.2 Suburban Usage

The use of regenerative braking on electric multiple unit (EMU) suburban trains in South African has been very limited. The first SAR suburban train to use regeneration was an experimental train set acquired in 1980 [79]. This set was based on the standard 5M2A rolling stock but was fitted with thyristor control equipment from Hitachi and air brakes from Knorr-Bremse. As per standard 5M2A configuration 25 % of the axles were motorised [79]. This was the first time that the SAR employed regenerative braking for power saving and as a stopping brake [79]. The interim report [79] states “This train is not optimum designed but suitable to prove advanced features at the test and service operation.”

Two further experimental train sets, classed 6M and 7M, were acquired in the mid '80s [73]. They were based on the latest Japanese and German technology of the time. The modular configuration and high number of powered axles, up to 66 %, gave excellent regenerative braking performance. Based on the results of extensive testing on these two classes, the class 8M was designed. Unlike the custom with mainline trains at the time, regenerative braking was specifically included for train deceleration and energy saving.

The 8M offered many advantages over the old 5M2A stock, such as lighter body, higher crush loading, higher acceleration and energy savings due to regenerative braking. Comparative testing revealed that the 8M could regenerate up to 31 % of the consumed energy. At crush load occupation, the watt-hour per passenger-kilometre usage for the 5M2A was 12,8 W h/(pass km) versus the 8M usage of 8,6 W h/(pass km) (net consumption with regen) a saving of 32,8 %. The 8M sets



consists of three modules of four coaches with automatic couplers at module ends for modular operation. This allows the splitting of modules during low occupancy periods and the resulting saving of energy consumption and wear and tear. [80]

Only eight of these sets were ever ordered and operated the commuter service between Cape Town and Khayelitsha for a number of years. They were never operated in a modular (split up) fashion.

The recent order of 600 new EMU train sets with regenerative braking have spurred renewed interest in the possibilities and challenges that it offers.

### 2.5.3 Economic Driving

The eco-driving concept is also not new to South Africa. As far back as 1966, the train operating regulations contained the following clause [81, p. 286]:

#### *Saving of Electricity and Brake blocks*

In order to utilise electric energy and brake blocks economically, Train Drivers must not run with power on for longer than necessary to maintain scheduled running times between stations. Train Drivers must coast as much as possible.

The same regulation is still part of the local operating instructions [82] and driver training manual [83]. The extent of its application or enforcement is not in the public domain.

### 2.5.4 Reversible Substation Research

An inverting DC traction substation with incorporated active power filtering aimed at the South African railway environment was designed and implemented as a low voltage, proof-of-concept demonstration in 1995 [54]. This design relied on the use of a high-frequency IGBT-type hard switched (forced commutated) inverter. The inverter was placed in antiparallel with a silicon diode rectifier. While the rectifier is delivering traction energy, the inverter would act as an active filter and inject compensation current into the AC supply, effectively ensuring that a harmonic free (up to the 25th harmonic) current is drawn from the utility. When excess power is available on the DC bus, due to regeneration, the inverter would inject a high-quality current, 180° out of phase with the utility voltage, into the secondary winding of the three-phase transformer. The proof-of-concept

model was declared a “general success”. At the time of this research, no IGBT devices were capable of operation in the 3 kV to 4 kV range and further work was necessary to produce a prototype capable of higher power and voltage levels. [54]

Renewed interest into regenerative braking by railway operator Spoornet led to the design and installation of a 1,5 MW inverter and active power filter system near the town of Wolsley, Western Cape, in 2005 [84]. An IGBT-based 7 level Series-Stacked Multilevel Inverter Topology was used. Test results proved positive and the system was able to inject high-quality AC current into the secondary winding of the substation transformer and reduce the THD for the load current from 24,93 % to 15,55 %. [84]

As of 2012, the prime motive power on the section of line was changed to class 18E locomotives. This left little to no opportunity of recuperation for the converter. The total savings that were realised with this system is not in the public domain.

## 2.6 Conclusion

In this chapter various methods of reducing energy usage was discussed. The concepts behind regenerative braking and how the useful application of regenerated energy can be increased was presented. It is clear that there are many ways a railway operator can save energy, including the way the train is driven and the infrastructure. In this study the focus will be placed on developing a method of investigating various combinations of methods.

The amount of energy that can be recovered with a specific technology first requires a detailed analysis of the network. Parameters applicable to the specific network must be known and used in calculations to ensure accurate and reliable results. Additionally, the control of the energy recovery technology will strongly influence the achieved savings. This is especially applicable to wayside systems, where the threshold voltage at which energy is extracted from the network will ultimately determine energy savings.

Some load-flow simulation software was explored. Computer simulations offer the advantage that the effect of any combination of solutions can be investigated before a single change is made to the physical infrastructure. Various simulation suites have been developed to assist in this regard. Unfortunately many are of a proprietary nature and employed as part of consulting work. Railways that

can't or don't want to utilise them usually have to undertake the tedious process of developing their own software from scratch or utilise numerical computing environments, such as MATLAB, to build models from first principles.

DIgSILENT's PowerFactory offers a stand-alone solution that is widely used by electrical network designers and power utilities around the world for power system analysis. It features support for simultaneous load flow analysis of both the AC and DC networks, but lacks the functionality to simulate moving loads along DC lines. If an alternative method of simulating the moving loads can be found, PowerFactory will be used.

Lastly, a historical South African perspective was be shared. Although South Africa was one of the first countries in the world to utilise regenerative braking, there was a lack of interest during the last few decades. New rolling stock and a shortage of energy have created renewed interest in harnessing the advantages of regenerative braking.

# Chapter 3

## Modelling moving trains

### 3.1 Introduction

This chapter will provide background on how to determine the capacity of an electrical traction network including how moving trains can be simulated. The two types of rolling stock used on the network under investigation will be introduced. A method will be investigated to overcome PowerFactory's inability to simulate moving loads along DC lines. This will include the definition of a relative displacement function. Lastly the method will be applied by converting the timetable and implementing a model that accurately models the types of rolling stock used.

Time averaged, integration based mathematical solutions have been developed to perform capacity analysis. The Average Statistical Train by Rosa [85] is a good example. These solutions work well to calculate the time averaged load that a certain number of trains per hour will place on the electrical network. The instantaneous effect of different trains accelerating and decelerating at different locations is difficult to determine using a mathematical solution, like the Average Statistical Train. Dynamic or quasi-dynamic simulations provide a solution that can be used to analyse both aspects of a network's capacity.

### 3.2 Capacity of an Electrical Traction Network

This study aims to determine the current and future utilisation of the equipment that make up the electrical traction network of Cape Metrorail. The capacity of

the electrical network typically refers to two aspects, namely the rating of the equipment and instantaneous values.

Equipment for which the rating is important include transformers, rectifiers and transmission lines. The rating is typically given in terms of time averaged values or percentage loading on a minute, hour and continuous basis. Each value is based on the ability of the equipment to dissipate heat. In this regard the maximum instantaneous power demand of the trains is not so important, since the equipment can generally handle high multiples of their nominal ratings for short periods of time (up to 350 % for 10 s for a Tamini transformer [86]). For this aspect the biggest factor to take into account is the frequency of acceleration cycles (number of trains accelerating per hour). This is because more trains will mean that equipment will be loaded for a longer continuous period of time.

Instantaneous values refer to the variables that are measured in real-time for traction control purposes. Line voltage, for example, change in real-time, so if a large current is drawn through a line with a high resistance then there will be an immediate drop in the pantograph voltage. The rate of acceleration is important, since higher acceleration requires a larger force and therefore a higher current.

### 3.3 Simulating Trains as Moving Loads

The simulation of a moving train for power flow purposes encompasses two aspects, firstly the power that is drawn from the overhead line at a specific point and secondly the movement along it. The key components of a train's propulsion system typically consists of a pantograph to collect current from the contact wire, traction motors that propel the train and a drive system that regulates the voltage applied to the traction motors. The drive system can consist of a number of resistors that are switched in or out as the back-electromotive force (EMF) changes. More modern drive systems use a chopper for DC traction motors, or an inverter for AC traction motors, to regulate the voltage and current applied to the traction motors using power electronics.

Since the main focus of this study is not the detailed working of a train, but rather the capacity of the electrical network, it is not considered necessary to model the rolling stock in detail. An alternative is to model it as a moving, time dependant power or current sink. Previous work on this subject used current values based on the following assumption [85]:

The supply voltage during all train operation modes remains virtually constant, therefore, we may state with great degree of accuracy that the instantaneous power demand of the train is directly proportional to the current profile.

The combination of an overhead line with a relatively high impedance, at low voltage and with a large current flowing through it, inevitably leads to a considerable voltage drop between supply points, whether substations or regenerating trains, and loads. It must be decided if the expected voltage variation will be sufficiently small to still define the pantograph voltage as virtually constant. In a suburban railway network the large current is not drawn for extended periods of time. If the current value is scaled for an average pantograph voltage then the total energy consumed by each train should be correct.

The operating parameters for the network under investigation state that the “nominal voltage of the overhead supply is 3,3 kV. Under normal working conditions this may vary between 2,7 kV and 3,9 kV and under abnormal conditions it may vary between 2 kV and 4 kV” [87]. From the available data of rated transformer voltages and the rectifier voltage multiplication factor one can deduce that the nominal voltage actually refers to the no-load output voltage of the substations.<sup>1</sup> Observations of cab mounted voltage meters showed that the voltage is typically around 3 kV, a deviation of about 9% from the nominal.

If the current profile is adjusted to compensate for the voltage drop, then the instantaneous power demand can still be taken as directly proportional to the current. The following sections will discuss the applicability of modelling the different types of rolling stock as moving current sinks in more detail.

An alternative would be to model the train as a moving, time dependant power sink. Unfortunately power sinks will draw the requested amount of power, irrespective of the pantograph voltage. This has the danger that the sink will increase the current until the voltage at the node is unrealistically low. In reality, the traction control system will lower the amount of power when the pantograph voltage is low. This method is therefore not considered a viable option, especially for the traction phase.

---

<sup>1</sup>The rated secondary voltage of most transformers for this network are 2,42 kV. The ideal output voltage of a six-pulse bridge rectifier is  $3\sqrt{2}\pi^{-1}U_{LLRMS}$ . This gives a nominal DC output voltage of 3,268 kV.

### 3.3.1 Present Rolling Stock

The present rolling stock, classed 5M2A, is composed of EMU sets consisting of eight to 14 coaches.<sup>2</sup> Up to three trailing coaches are normally marshalled per motor coach (four motorised axles) with a rated power output of 880 kW.<sup>3</sup> The series wound DC motors are resistor controlled and can be configured in either series (four motors in series) or parallel (two parallel circuits of two motors in series). Field weakening, for additional torque at higher speeds, are realised by connecting an inductive divert coil in parallel with the field coils. [88]

For this rolling stock, a lower voltage will lead to a lower voltage drop over the resistors and thus less power drawn. The rolling stock will be modelled as a moving current sink, with the current values based on a recording of real values, taken under similar conditions as those being modelled. For this scenario, modelling the rolling stock as a time dependant, moving current sink should be able to load the network quite realistically.

An endeavour was made to obtain current profiles recorded on different lines. These profiles could then be used to construct a representative profile of each line. Unfortunately only one out of four attempts was successful. Two attempts failed due to defective trip logger memory modules. Another was unsuccessful when technicians only downloaded the fault log. The fourth attempt was the most successful and good quality data was collected on one of the three motor coaches. The influence of various technical and operational factors resulted in the recording of only one complete acceleration cycle during the 73 km, 84 min trip. Consequently, this acceleration cycle was used as a representative profile for all lines.

Figure 3.1 shows the typical profile of the traction current drawn from the overhead line. It is based on a recording of measurements from the onboard micro controller's trip logger of motor coach 13042 during acceleration with M2 loading (estimated) on level to downhill (1:80) track. The departure point is located about 500 m from the Muldersvlei traction substation. During the acceleration only six of the 44 axles were powered (usually twelve) leading to an effective 13,6 % powered axle arrangement. The driver allowed the micro controller to automatically switch out the acceleration resistances. This led to a 18 s period in series, 24 s in parallel

---

<sup>2</sup>A diagram of the present rolling stock is included in Appendix B.

<sup>3</sup>All rated power outputs stated for rolling stock in this document is based on the sum of the traction motors' continuous rating at nominal terminal voltage.

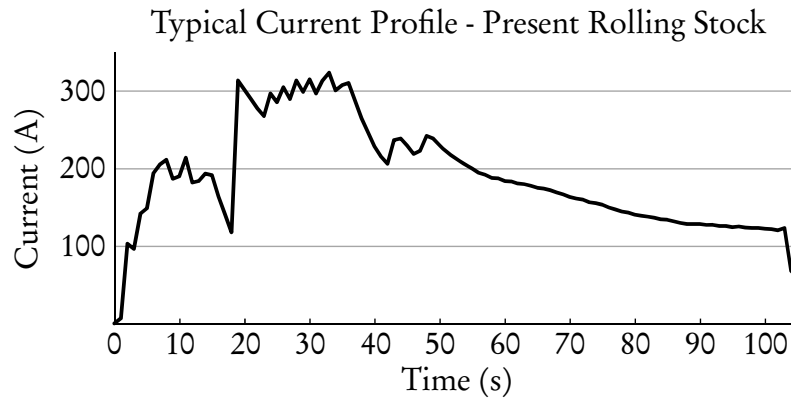


Figure 3.1: Traction current at 3 kV pantograph voltage for a single motor coach and 61 s in weak-field. Drivers normally prefer to “hand notch” the sets to delay the switching out of the acceleration resistances.

The high loading and automatic notching resulted in higher than usual traction current, reaching a maximum electrical power input of 1,421 MW during parallel. Consequently, the measurements were multiplied by a factor  $2/3$  to give the values graphically represented in Figure 3.1.

The adjusted values also correlate very well to what has been observed during a “hand notching” acceleration, video footage of which is available at [89]. The current values will further be scaled according to the number of motor coaches that are normally marshalled into a train set.

### 3.3.2 Future Rolling stock

The future rolling stock comprise of EMU modules. Each standard module will consist of six coaches.<sup>4</sup> Depending on the platform length and passenger demand, one or two modules will make up a train set. 66 % of the axles will be powered by three-phase induction motors fed by DC to AC inverters. Each module has a rated power output of 5,12 MW. [90]

Three different phases of energy use should be taken into consideration for the new rolling stock: acceleration, deceleration and cruising. Each phase will be discussed in the following subsections.

<sup>4</sup>A diagram of the future rolling stock is included in Appendix C.



### 3.3.2.1 Acceleration

The control system of the future rolling stock will adjust the amount of current drawn to compensate for changes in pantograph voltage. This is done to maintain a constant acceleration for any voltage higher than 2,7 kV (18 % lower than nominal). Figure 3.2 gives the maximum line current that can be drawn from the overhead line for different values of pantograph voltage. Figure 3.3 gives the corresponding maximum power that will be drawn from the overhead line for the different values of pantograph voltage. The current is adjusted to keep the power constant for voltages down to 2,7 kV. Below 2,7 kV the power is reduced to prevent further ohmic drop. No traction will be possible below 2,3 kV. [91]

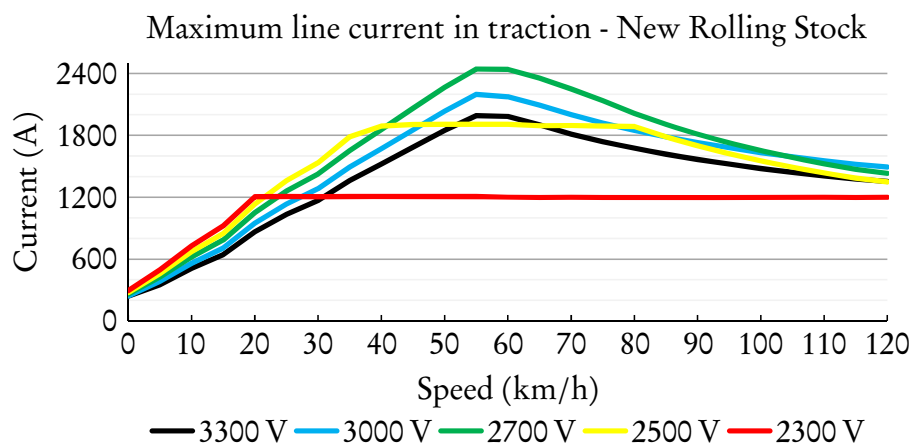


Figure 3.2: Maximum line current (traction + auxiliary) drawn by a single module during traction for different values of pantograph voltage

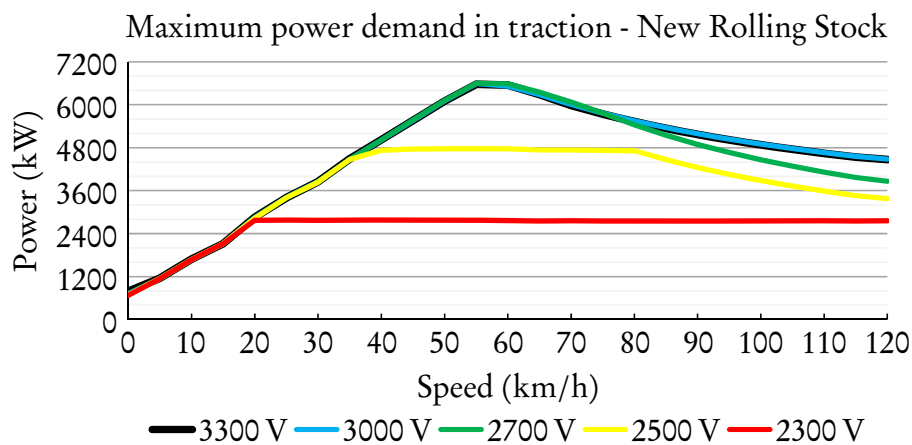


Figure 3.3: Maximum power demand (traction + auxiliary) of a single module during traction for different values of pantograph voltage

The Power column in Table 3.1 shows the maximum power that can be drawn from the overhead line by the new rolling stock at different values of pantograph voltage and speed,  $v$ . The percentage difference between the maximum power at nominal voltage and what can be drawn at lower pantograph voltages is shown under Power  $\Delta$ . The maximum power is virtually the same for 3,3 kV and 3 kV. At 2,7 kV, the maximum power diverge from what is achievable at nominal voltage for speeds above 80 km/h.

No recorded data is available yet for the new rolling stock. If it is also modelled as a current sink, the values will have to be based on simulations of the expected power requirement at a fixed pantograph voltage. The maximum pantograph-level power input is about 6,5 MW per module. A single module at nominal line voltage requires 2 kA of current. At a pantograph voltage of 2,7 kV, the pantograph current will be 2,4 kA. These high currents will inevitably lead to large voltage drops in all supply equipment; transformers, rectifiers and overhead line. Modelling the rolling stock using current values at nominal voltage would therefore not give satisfactory results, since the pantograph voltage is envisaged

Table 3.1: Comparison of the maximum power (traction + auxiliary) drawn from the overhead line for different values of pantograph voltage and speed [91]

$v$ km/h	Power (MW)			Power $\Delta$ (%)		$P$ with $I_{nom}$ (MW) <sup>5</sup>			$\Delta P_{same U}$ (%) <sup>6</sup>	
	3,3 kV	3,0 kV	2,7 kV	3,0 kV	2,7 kV	3,3 kV	3,0 kV	2,7 kV	3,0 kV	2,7 kV
0	0,792	0,723	0,702	-8,7 %	-11,4 %	0,792	0,720	0,648	-0,4 %	-7,7 %
10	1,686	1,683	1,679	-0,2 %	-0,4 %	1,686	1,533	1,380	-8,9 %	-17,9 %
20	2,858	2,847	2,838	-0,4 %	-0,7 %	2,858	2,598	2,338	-8,8 %	-17,6 %
30	3,851	3,849	3,845	-0,1 %	-0,2 %	3,851	3,501	3,151	-9,0 %	-18,1 %
40	5,023	5,016	5,017	-0,1 %	-0,1 %	5,023	4,566	4,109	-9,0 %	-18,1 %
50	6,102	6,108	6,118	0,1 %	0,3 %	6,102	5,547	4,992	-9,2 %	-18,4 %
60	6,551	6,525	6,588	-0,4 %	0,6 %	6,551	5,955	5,360	-8,7 %	-18,7 %
70	5,983	6,006	6,075	0,4 %	1,5 %	5,983	5,439	4,895	-9,4 %	-19,4 %
80	5,528	5,550	5,438	0,4 %	-1,6 %	5,528	5,025	4,523	-9,5 %	-16,8 %
90	5,171	5,193	4,892	0,4 %	-5,4 %	5,171	4,701	4,231	-9,5 %	-13,5 %
100	4,881	4,899	4,463	0,4 %	-8,6 %	4,881	4,437	3,993	-9,4 %	-10,5 %
110	4,643	4,662	4,118	0,4 %	-11,3 %	4,643	4,221	3,799	-9,5 %	-7,7 %
120	4,465	4,482	3,864	0,4 %	-13,5 %	4,465	4,059	3,653	-9,4 %	-5,5 %

<sup>5</sup>Power that will be drawn by the current sink (train) if the current value at nominal line voltage is used, while the node (pantograph) voltage is actually at 3 kV or 2,7 kV.

<sup>6</sup>The percentage difference between the power that will be delivered to the current sink when the correct current value is used (Power) and when the current value at nominal voltage is specified ( $P$  with  $I_{nom}$ ).

to be well below nominal for most operational scenarios. The  $P$  with  $I_{\text{nom}}$  and  $\Delta P_{\text{same } U}$  columns of Table 3.1 show that the simulated amount of power drawn can be almost 20 % less than what would really be drawn at 2,7 kV.

It can be assumed that the overhead line will be upgraded so that the pantograph voltage will be around 3 kV for most of the acceleration cycle, and never below 2,7 kV, even with multiple modules and maximum acceleration. For this scenario, modelling the rolling stock as current sinks, characterised by current values at 3 kV, should be able to load the network (especially the high voltage (HV) side) quite realistically.

The simulation results should also highlight quite accurately what sections are likely to experience high voltage drops. These sections can then be reinforced with additional feeder cables or substations. If the proposed overhead line upgrades are not implemented, the maximum loading on the transformers should be more or less the same, since a similar amount of current will be drawn by the trains (same loading on the transformers), but more power will be dissipated in the overhead line. In this case the acceleration will, however, be lower and hence the maximum speed will need to be higher to still cover the station-to-station trip in the same amount of time.

Figure 3.4 shows the typical profile of the current drawn from the overhead line wire by a single module during traction. It is based on simulations done by Gibela with maximum tractive effort at M3 loading at a nominal line voltage of 3,3 kV [91]. The current values shown in the figure was scaled to represent the

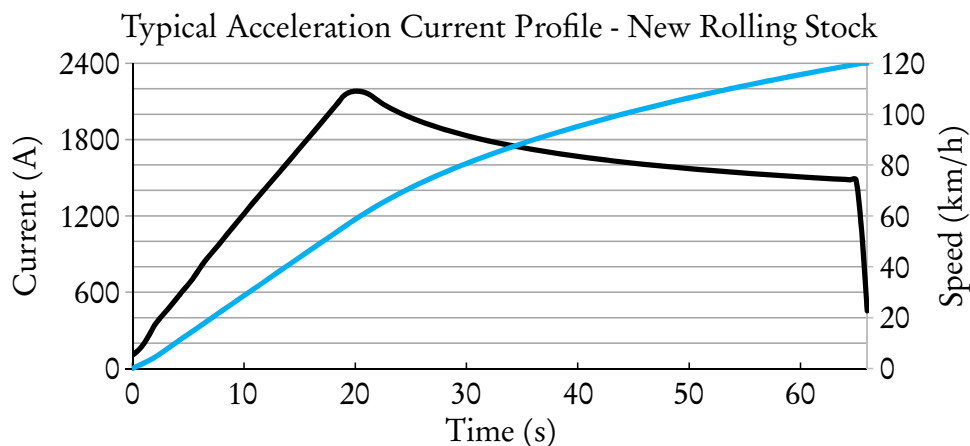


Figure 3.4: Current (black) and speed (blue) for a single module during traction with a pantograph voltage of 3 kV

simulated traction power, but at a pantograph voltage of 3 kV. It also includes provision for 310 kW of auxiliary loads. The acceleration is from standstill up to 120 km/h. This includes a near constant acceleration of  $0,81 \text{ m/s}^2$  up to 58 km/h after which there is an exponential drop in the acceleration, analogous to the drop in current. The average acceleration from 0 km/h to 68 km/h is  $0,8 \text{ m/s}^2$ .

### 3.3.2.2 Deceleration

During regenerative braking, the control system will automatically manipulate the line voltage to inject the power that is being generated by the motors into the overhead line. If the receptivity is low, the pantograph voltage will increase up to a maximum of 3,75 kV and any remaining power will be dissipated in the onboard rheostats. Figure 3.5 shows the maximum amount of current that can be injected into the overhead line for different values of pantograph voltage. Figure 3.6 gives the corresponding maximum power that will be injected for the different values of pantograph voltage. The nominal voltage during braking is 3,75 kV. The maximum power is also limited when the overhead line voltage is low due, in part, to the thermal rating of the line contactor and input filter inductor [90]. Further, even though the amplitude of the injected current varies significantly, the maximum injected power is practicably the same below 85 km/h for the normal

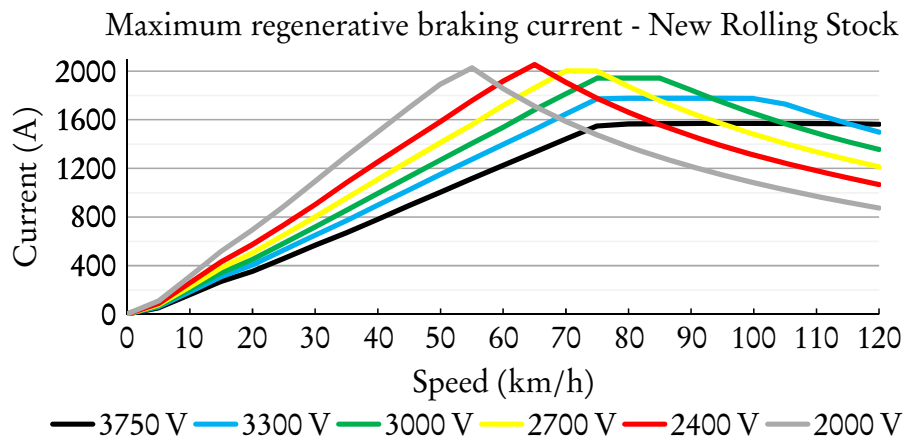


Figure 3.5: Maximum braking current (traction only) injected by a single module during regenerative braking for different values of pantograph voltage

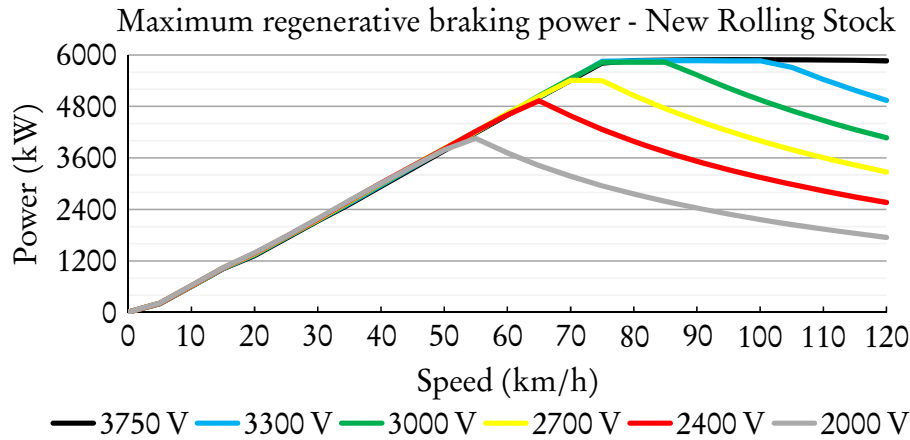


Figure 3.6: Maximum regenerative braking power (no auxiliary) injected by a single module for different values of pantograph voltage

operating voltage range during braking (3 kV to 3,75 kV).<sup>7</sup>

The Power column of Table 3.2 shows the maximum power that can be injected

Table 3.2: Comparison of the maximum power (traction only) injected into the overhead line for different values of pantograph voltage and speed [91]

$v$ km/h	Power (MW)			Power $\Delta$ (%)		$P$ with $I_{nom}$ <sup>8</sup>		$\Delta P_{same U}$ (%) <sup>9</sup>	
	3,75 kV	3,3 kV	3,0 kV	3,3 kV	3,0 kV	3,3 kV	3,0 kV	3,3 kV	3,0 kV
0	0,000	0,000	0,000	0,0 %	0,0 %	0,000	0,000	0,0 %	0,0 %
10	0,608	0,611	0,615	0,5 %	1,2 %	0,535	0,486	-12,4 %	-21,0 %
20	1,324	1,343	1,353	1,5 %	2,2 %	1,165	1,059	-13,3 %	-21,7 %
30	2,130	2,145	2,154	0,7 %	1,1 %	1,874	1,704	-12,6 %	-20,9 %
40	2,936	2,967	2,985	1,0 %	1,7 %	2,584	2,349	-12,9 %	-21,3 %
50	3,773	3,798	3,810	0,7 %	1,0 %	3,320	3,018	-12,6 %	-20,8 %
60	4,598	4,613	4,617	0,3 %	0,4 %	4,046	3,678	-12,3 %	-20,3 %
70	5,411	5,435	5,445	0,4 %	0,6 %	4,762	4,329	-12,4 %	-20,5 %
80	5,869	5,864	5,832	-0,1 %	-0,6 %	5,165	4,695	-11,9 %	-19,5 %
90	5,888	5,867	5,535	-0,3 %	-6,0 %	5,181	4,710	-11,7 %	-14,9 %
100	5,891	5,861	4,956	-0,5 %	-15,9 %	5,184	4,713	-11,5 %	-4,9 %
110	5,884	5,432	4,476	-7,7 %	-23,9 %	5,178	4,707	-4,7 %	5,2 %
120	5,865	4,943	4,068	-15,7 %	-30,6 %	5,161	4,692	4,4 %	15,3 %

<sup>7</sup>The pantograph voltage would typically only be below 3 kV during regenerative braking when the network voltage is very low (off-line substations and many trains) or when another train in close electrical proximity is drawing a very high current (pulling the line voltage down) while the regenerating train is only generating limited power (low deceleration or speed).

<sup>8</sup>Power, in MW, that will be injected by the current source (train) if the current value for nominal line voltage is used, while the node (pantograph) voltage is actually at 3,3 kV or 3 kV.

<sup>9</sup>The percentage difference between the power injected by the current source when the correct current value is used (Power) and when the current for nominal voltage is used ( $P$  with  $I_{nom}$ ).

into the overhead line during regenerative braking by the new rolling stock at different values of pantograph voltage and speed,  $v$ . The percentage difference between the maximum power at nominal voltage and what can be injected at lower pantograph voltages is shown under Power  $\Delta$ . The maximum power is virtually the same for 3,75 kV and 3,3 kV. At 3 kV, it diverges from what is achievable at nominal voltage for speeds above 80 km/h.

Suppose the new rolling stock will also be modelled as a current source during deceleration. With no recorded data available yet, the current values will have to be based on simulations of the expected power injection at a fixed pantograph voltage. The maximum pantograph-level power output is about 5,9 MW per module. For a single module at nominal line voltage, this will mean 1,57 kA of current. At a pantograph voltage of 3 kV, the pantograph current will be 1,94 kA. Modelling the rolling stock using current values at nominal voltage would therefore not give satisfactory results, since the pantograph voltage is envisaged to be well below nominal for most operational scenarios. The  $P$  with  $I_{\text{nom}}$  and  $\Delta P_{\text{same } U}$  columns of Table 3.2 show that the simulated amount of power injected can be almost 22 % less than what would actually be injected at 3 kV.

Figure 3.7 shows the typical profile of the regenerative braking current injected into the overhead line by a single module at the nominal line voltage of 3,75 kV, shown from the perspective of a current sink. It is based on simulations done by Gibela for constant braking effort corresponding to a deceleration of  $0,9 \text{ m/s}^2$  at M3 loading from 120 km/h to standstill. The maximum power output of

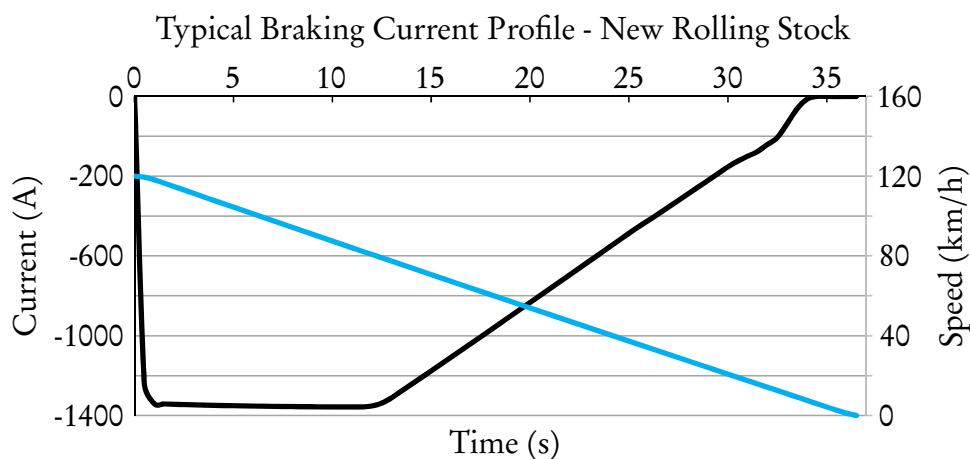


Figure 3.7: Current (black) and speed (blue) for a single module during braking with a pantograph voltage of 3,75 kV

the regenerative braking is limited to about 5,8 MW. If the requested braking effort is higher than what can be contributed by the electrical brake, then the mechanical brake is automatically blended with the electrical brake. At M3 loading the electrical brake regenerates constant power (constant current) from 120 to 80 km/h. Below 80 km/h regenerative braking can provide sufficient braking effort to fully brake the train electrically. At low speed (low power) the electrical brake is faded out and replaced by mechanical braking [92]. The current shown does not include any provision for auxiliary loads, because it will be powered directly from the regenerated power.

If the overhead line is upgraded to help during acceleration the maximum pantograph voltage will be even lower, because the receptivity is improved. In order to inject the regenerated current the pantograph voltage would need to be increased to just above the substation's OCV. For this scenario, modelling the rolling stock as current sinks, characterised by current values at 3,75 kV, will probably not be able to load the network realistically. Since receptivity is influenced by the number of trains in the vicinity, it is difficult to determine a nominal pantograph voltage that will be valid for the whole day. Regeneration will initially be modelled using current sources, but power sources will be investigated if needed.

### 3.3.2.3 Cruising

Gibela also did simulations to determine the current needed to cruise so that a constant velocity on flat and straight track can be maintained. Results were only available for M2 loading and at discrete speeds (10 km/h interval) for the range 40 to 100 km/h. The current value includes provision for 310 kW of auxiliary load. Since the constant speed can be any value between 1 and 120 km/h, an exponential function was fitted around the known points using Microsoft Excel. Figure 3.8 shows the original simulation values and the fitted exponential trend-line. The estimated line current, in ampere, as a function of the train speed  $v$ , in km/h, was calculated as:

$$I_L(v) = 86,065\,394 e^{0,013\,138 v} \quad (3.1)$$

It was decided that the constant current values would not be scaled to represent M3 loading since not all trains will be loaded at M3 at the same time. For the system under review, peak traffic is very one-directional, with a large flow of commuters away from residential areas in the morning. The high acceleration rate

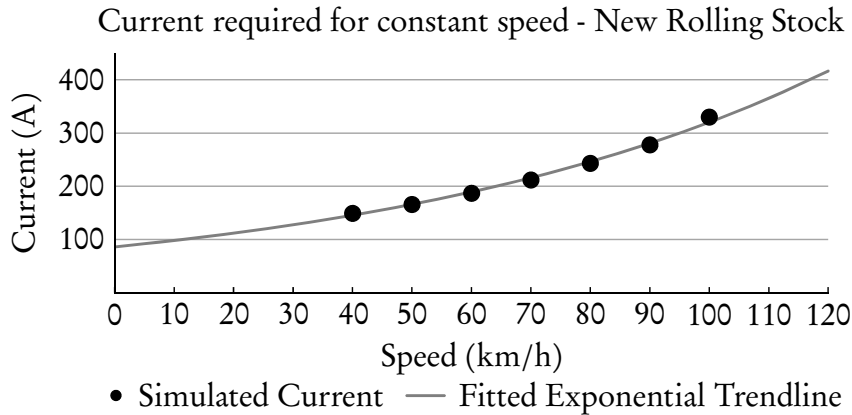


Figure 3.8: Line current drawn from overhead line by a single M2 loaded module to maintain a constant speed at a pantograph voltage of 3,3 kV

of the new rolling stock also mean that the period of constant speed running will be much longer than acceleration during a station-to-station journey. The simulation results is expected to create a general impression of the power requirement. Current values have also not been scaled for 3 kV, since the current magnitude is not so high as during acceleration and the voltage drop will not be so large.

### 3.4 Simulating Moving Loads

PowerFactory lacks the functionality to dynamically move a load along a DC line. An alternative method had to be sought that would be able to realistically simulate the amount of power that each substation contributes whilst the load is moving along the line. As already discussed, each moving load will be modelled as an ideal current source<sup>10</sup> with a time-dependant current value. One possibility is to place a single current source mid-way between stations. This model will only represent the real power division<sup>11</sup> at a single point in time, i.e. when the train passes the location of the current source.

Another possibility is to use two stationary current sources and vary the amount of current that is allocated to each source in a way that would produce the same system response as a single, moving load. Typically a source will be placed at every departure and arrival point.

<sup>10</sup>The terms current source and current sink are used interchangeably and both refer to the “DC - Current Source” element in PowerFactory (ElmDci). This element, by definition, sinks (draws) current for positive setpoint values (dissipates power). For negative setpoint values it is a source and injects current into the node to which it is connected (generates power).

<sup>11</sup>Amount of power contributed by individual substations.



By using superposition, the system response of all trains operating together will equal the sum of the responses caused by each train acting alone, where all the other independent sources are replaced by their internal impedances. Since the trains are modelled as ideal current sources, their internal impedances are infinite and they have no influence whenever their current is zero. If it is therefore proven that the system response to a single train modelled as two stationary dynamic loads will be the same as a single train modelled as a single, moving load, then the amount of trains that will eventually be operating in the system should have no effect on the validity of the model.

### 3.4.1 Moving Train on an Open Section

The diagram in Figure 3.9 represents a load, moving between points A and B along an overhead line of length  $d$ , fed by two substations. Each substation's transformers and rectifiers are replaced by a Thévenin equivalent circuit. Between each substation and the extremes of movement is a piece of overhead line, of length  $x_1$  and  $x_2$  respectively. The combined resistance of the overhead line and return rail is called the total specific resistance, represented by  $\rho$  and expressed in  $\Omega/\text{km}$ . In the diagram the straight line suspended below the parabolic line represents the total specific resistance. Using the superposition theorem, the system response of a single, moving train drawing current can be calculated by solving a simple equivalent circuit.

The relative displacement of the train is represented by the function  $m(t)$ . The typical form of this function is shown in Figure 3.10. It represents three stages of the journey between two stations: acceleration (quadratic change in displacement), constant speed (linear change in displacement) and braking (quadratic change in displacement). For the equations below  $m(0) = 1$  indicates that the train is 100 %

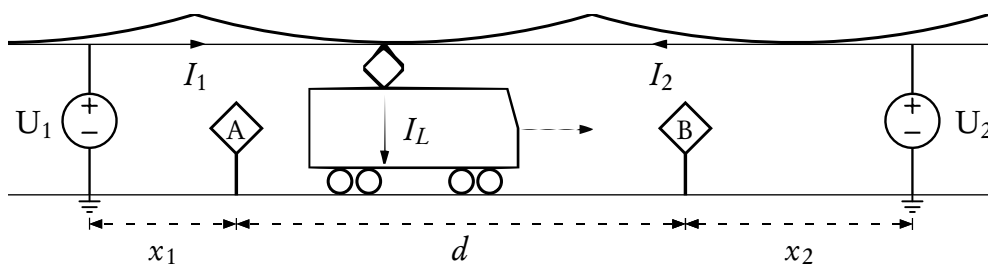


Figure 3.9: Diagram of a train moving between two points, supplied by two substations

at the departure station and 0% at the destination. Similarly,  $m(t_f) = 0$  indicates that the train is 0% at the departure station, but 100% at the destination.

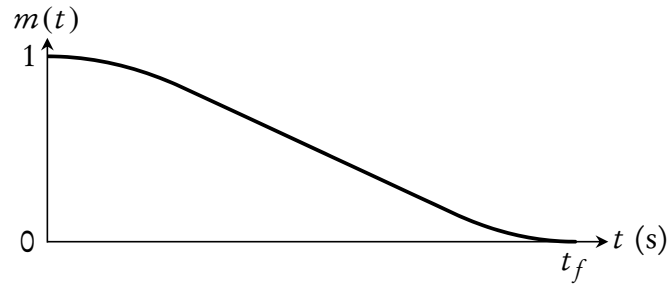


Figure 3.10: Typical form of the displacement function  $m(t)$

### 3.4.1.1 Single Moving Load

In Figure 3.11 the load movement is represented by changing the resistance of the overhead wire with a function,  $m(t)$ , that represents the position of the train in time.  $I_{U_1}$ , the amount of current that is contributed by substation 1 to supply the moving load  $I_L$ , can be calculated using circuit analysis:

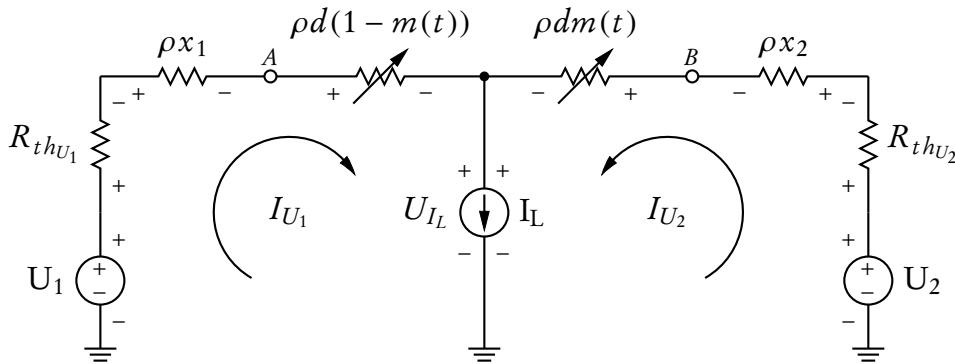


Figure 3.11: Circuit of a single, moving load fed by two substations

Node voltage equation:

$$I_L = I_{U_1} + I_{U_2} \quad (3.2)$$

Mesh current equations:

$$-U_1 + I_{U_1} [R_{thU_1} + \rho x_1 + \rho d (1 - m(t))] + U_L = 0 \quad (3.3a)$$

$$-U_2 + I_{U_2} (R_{thU_2} + \rho x_2 + \rho d m(t)) + U_L = 0 \quad (3.3b)$$

Writing (3.3a) in terms of  $U_L$  and substituting in (3.3b) gives

$$-U_2 + I_{U_2} (R_{th_{U_2}} + \rho x_2 + \rho dm(t)) + U_1 - I_{U_1} [R_{th_{U_1}} + \rho x_1 + \rho d (1 - m(t))] = 0. \quad (3.4)$$

From (3.2) it is known that  $I_{U_2} = I_L - I_{U_1}$  and let  $\Delta U = U_1 - U_2$ , then it follows:

$$\begin{aligned} I_{U_1} [R_{th_{U_1}} + \rho x_1 + \rho d (1 - m(t)) + \rho dm(t) + R_{th_{U_2}} + \rho x_2] \\ = I_L (R_{th_{U_2}} + \rho x_2 + \rho dm(t)) + \Delta U \end{aligned} \quad (3.5)$$

To give the current contribution of substation 1 as:

$$I_{U_1} = \frac{I_L (R_{th_{U_2}} + \rho x_2 + \rho dm(t)) + \Delta U}{R_{th_{U_1}} + R_{th_{U_2}} + \rho (x_1 + x_2 + d)} \quad (3.6)$$

The power that will be dissipated by the moving load can be calculated from (3.3a) and (3.6):

$$\begin{aligned} P_{I_L} &= U_{I_L} I_L \quad (3.7) \\ &= I_L \left\{ U_1 - \frac{[R_{th_{U_1}} + \rho (x_1 + d - dm(t))] [I_L (R_{th_{U_2}} + \rho x_2 + \rho dm(t)) + \Delta U]}{R_{th_{U_1}} + R_{th_{U_2}} + \rho (x_1 + x_2 + d)} \right\} \end{aligned} \quad (3.8)$$

### 3.4.1.2 Two Stationary Dynamic Loads

Now consider Figure 3.12, where there is two current loads: one at the departure point, A, and one at the destination point, B. Load movement is represented by changing the amount of current allocated to each source using the same relative displacement function,  $m(t)$ . By setting  $I_1 = I_L m(t)$  and  $I_2 = I_L (1 - m(t))$ , it is foreseen that the full load current will initially be allocated to  $I_1$  and gradually transferred until it is fully allocated to  $I_2$  at  $t = m^{-1}(0)$ .  $I_{U_1}$ , the amount of current that is contributed by substation 1 to feed the stationary loads  $I_1$  and  $I_2$ , can then be calculated using circuit analysis:

Node voltage equation:

$$I_1 = I_{U_1} + I_d \quad (3.9a)$$

$$I_2 = I_{U_2} - I_d \quad (3.9b)$$

$$\therefore I_d = I_{U_2} - I_2 \quad (3.9c)$$

$$\text{and } I_1 + I_2 = I_{U_1} + I_{U_2} \quad (3.9d)$$

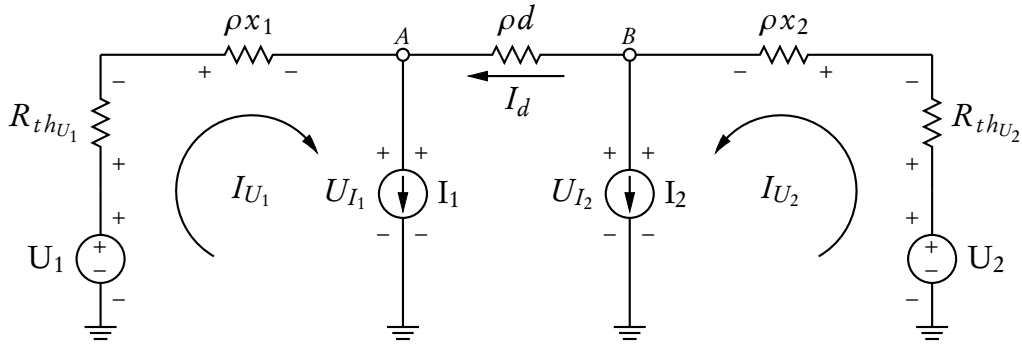


Figure 3.12: Circuit of two stationary dynamic loads fed by two substations

Let

$$I_1 = I_L m(t) \quad \text{and} \quad I_2 = I_L (1 - m(t)), \quad (3.10)$$

so that

$$I_1 + I_2 = I_L m(t) + I_L (1 - m(t)) \quad (3.11a)$$

$$= I_L (m(t) - m(t) + 1) \quad (3.11b)$$

$$= I_L \quad (3.11c)$$

and from (3.9d) it follows that

$$I_L = I_{U_1} + I_{U_2}. \quad (3.12)$$

Mesh current equations:

$$-U_1 + I_{U_1} (R_{thU_1} + \rho x_1) + U_{I_1} = 0 \quad (3.13a)$$

$$-U_2 + I_{U_2} (R_{thU_2} + \rho x_2) + U_{I_2} = 0 \quad (3.13b)$$

$$-U_{I_2} + \rho d I_d + U_{I_1} = 0 \quad (3.13c)$$

Rearranging (3.13a), (3.13b) and (3.13c) gives:

$$-U_{I_1} = -U_1 + I_{U_1} (R_{thU_1} + \rho x_1) \quad (3.14a)$$

$$U_{I_2} = U_2 - I_{U_2} (R_{thU_2} + \rho x_2) \quad (3.14b)$$

$$0 = -U_{I_1} - \rho d (I_{U_2} - I_2) + U_{I_2} \quad (3.14c)$$

Substituting (3.14a) and (3.14b) in (3.14c):

$$I_{U_1} (R_{thU_1} + \rho x_1) - U_1 - \rho d (I_{U_2} - I_2) + U_2 - I_{U_2} (R_{thU_2} + \rho x_2) = 0 \quad (3.15)$$

From (3.12) and (3.10) let

$$I_{U_2} = I_L - I_{U_1}, \quad (3.16)$$

$$I_{U_2} - I_2 = -I_{U_1} + I_L m(t) \text{ and} \quad (3.17)$$

$$\Delta U = U_1 - U_2 \text{ (the difference in supply voltage),} \quad (3.18)$$

then

$$I_{U_1} (R_{th_{U_1}} + \rho x_1) - \Delta U - \rho d (I_L m(t) - I_{U_1}) - (I_L - I_{U_1}) (R_{th_{U_2}} + \rho x_2) = 0. \quad (3.19)$$

Simplifying (3.19) yields:

$$I_{U_1} (R_{th_{U_1}} + \rho x_1 + \rho d + R_{th_{U_2}} + \rho x_2) - I_L (R_{th_{U_2}} + \rho x_2 + \rho d m(t)) - \Delta U = 0 \quad (3.20)$$

Finally, (3.20) is written in terms of the current contribution of substation 1:

$$I_{U_1} = \frac{I_L (R_{th_{U_2}} + \rho x_2 + \rho d m(t)) + \Delta U}{R_{th_{U_1}} + R_{th_{U_2}} + \rho (x_1 + x_2 + d)} \quad (3.21)$$

The power that will be dissipated by the moving load itself can be calculated as the sum of the power dissipated in both stationary loads. The power dissipated in  $I_1$  can be calculated using (3.13a) and (3.21):

$$P_{I_1} = U_{I_1} I_1 \quad (3.22)$$

$$= U_{I_1} I_L m(t) \quad (3.23)$$

$$= I_L m(t) [U_1 - I_{U_1} (R_{th_{U_1}} + \rho x_1)] \quad (3.24)$$

$$= I_L m(t) \left\{ U_1 - \frac{(R_{th_{U_1}} + \rho x_1) [I_L (R_{th_{U_2}} + \rho x_2 + \rho d m(t)) + \Delta U]}{R_{th_{U_1}} + R_{th_{U_2}} + \rho (x_1 + x_2 + d)} \right\} \quad (3.25)$$

Similarly, the power dissipated in  $I_2$  can be calculated using (3.14b), (3.16) and

(3.21):

$$P_{I_2} = U_{I_2} I_2 \quad (3.26)$$

$$= U_{I_2} I_L (1 - m(t)) \quad (3.27)$$

$$= I_L (1 - m(t)) \left[ U_2 - I_{U_2} (R_{th_{U_2}} + \rho x_2) \right] \quad (3.28)$$

$$= I_L (1 - m(t)) \left\{ U_2 - I_L (R_{th_{U_2}} + \rho x_2) \right. \\ \left. + \frac{(R_{th_{U_2}} + \rho x_2) \left[ I_L (R_{th_{U_2}} + \rho x_2 + \rho dm(t)) + \Delta U \right]}{R_{th_{U_1}} + R_{th_{U_2}} + \rho (x_1 + x_2 + d)} \right\} \quad (3.29)$$

By summing (3.25) and (3.29) together, the total power that will be dissipated by the train,  $I_L$ , is given by (3.31).

$$P_{I_L} = P_{I_1} + P_{I_2} \quad (3.30)$$

$$= I_L \left\{ U_2 + (R_{th_{U_2}} + \rho x_2) \left\{ \frac{I_L (R_{th_{U_2}} + \rho x_2 + \rho dm(t)) + \Delta U}{R_{th_{U_1}} + R_{th_{U_2}} + \rho (x_1 + x_2 + d)} - I_L \right\} \right\} \\ + I_L m(t) \left\{ \Delta U + I_L (R_{th_{U_2}} + \rho x_2) \right. \\ \left. - [R_{th_{U_1}} + R_{th_{U_2}} + \rho (x_1 + x_2)] \frac{I_L (R_{th_{U_2}} + \rho x_2 + \rho dm(t)) + \Delta U}{R_{th_{U_1}} + R_{th_{U_2}} + \rho (x_1 + x_2 + d)} \right\} \quad (3.31)$$

### 3.4.1.3 Comparison of Two Methods

The current supplied by substation 1 to the two stationary loads (3.21) is exactly the same as the current that will be delivered to the moving load (3.6). From (3.2) and (3.16), the current supplied by substation 2 will also be the same. Since the power delivered by each substation is directly proportional to the current flowing through it, the power that each substation contribute will also be identical. This proves that the response of substations due to moving trains along an open section can be mimicked by manipulating the current profiles with an external script. These profiles can then be used as input for the stationary current loads in PowerFactory.

Comparing (3.8) and (3.31), it is clear that the power dissipated in the load itself will be different for the two methods. The extent to which they differ was evaluated using Microsoft Excel with sample values of  $m(t)$  and  $I_L$ . All calculations are based on current values generated by the processing algorithm, discussed in Sections 3.5.2 and 3.5.3. Three methods were investigated for each evaluation: moving load, two stationary dynamic sources (placed at departure and arrival stations) and one stationary source (placed mid-section). Negative current represents regenerative braking. Bi-directional substations with no threshold voltage are assumed. This assumption is akin to a load in the vicinity of the substation, drawing exactly the amount of current that will otherwise flow to the substation.

The node voltage at each load can be calculated using (3.3a) for the moving load, (3.14a) for stationary load 1 and (3.12) substituted in (3.14b) for stationary load 2. The minimum and maximum voltage calculated during each evaluation will be given for the future rolling stock in a table, such as Table 3.4. This will give an indication about the expected difference in pantograph voltage of a moving load and the voltage recorded at each stationary load.

The results are encouraging and the total power dissipated by two stationary dynamic sources is deemed close enough to that of a moving load. The recorded values of minimum and maximum voltage also compares very well.

**Power comparison — Future load on short open section** Figure 3.13 shows the amount of power dissipated by the load for the three different methods of load representation. It represents the movement and load current of the future rolling stock (single module) along a short, uninterrupted section. There is virtually no difference between the three methods. The parameters used for the calculations are given in Table 3.3. A summary of the calculated values is provided in Table 3.4.

**Power comparison — Present load on short open section** Figure 3.14 shows the amount of power dissipated by the load for the three different methods of load representation. It represents the movement and load current of the present rolling stock (two motor coaches) along a short, uninterrupted section. There is virtually no difference between the three methods. The parameters used for the calculations are given in Table 3.3. A summary of the calculated values is provided in Table 3.5.

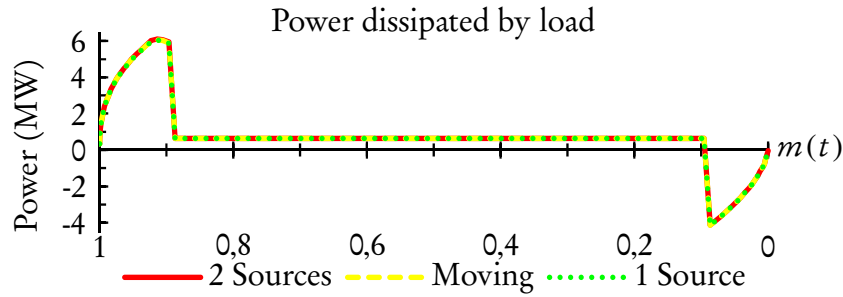


Figure 3.13: Power dissipated by load along short open section for different load representations — Future rolling stock

Table 3.3: Parameters used in calculation

Component	Value
$U_1, U_2$	3268 V
$R_{th_{U_1}}, R_{th_{U_2}}$	0,228 $\Omega$
$x_1$	2,399 km
$x_2$	3,088 km
$d$	1,87 km
$\rho$	0,063 14 $\Omega/\text{km}$

Table 3.4: Load representation comparison — Future loading, short open section

Calculated Value	Moving Load	2 Sources	1 Source
Total energy dissipated (kWh)	38,772	38,882	38,700
Total energy generated (kWh)	10,128	10,113	10,130
Net energy dissipated (kWh)	28,768	28,644	28,570
Difference net energy		+0,434 %	-0,256 %
Minimum difference in power		-0,310 %	-0,390 %
Maximum difference in power		+0,827 %	+0,014 %
Minimum voltage (V)	2778	2791	2767
Difference in minimum voltage		+0,457 %	-0,386 %
Maximum voltage (V)	3537	3530	3537
Difference in maximum voltage		-0,180 %	+0,009 %

**Power comparison — Constant current load on short open section** Figure 3.15 shows the amount of power dissipated by a constant current load of 500 A moving along a short open section at a constant speed for the three different methods of load representation. This example is included to show the difference in form of



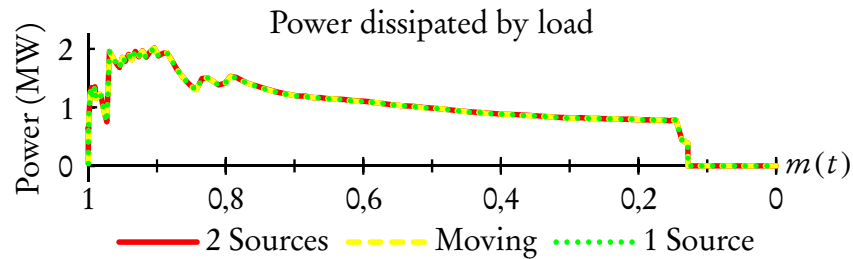


Figure 3.14: Power dissipated by load along short open section for different load representations — Present rolling stock

Table 3.5: Load representation comparison — Present loading, short open section

Calculated Value	Moving Load	2 Sources	1 Source
Total energy dissipated (kWh)	34,967	35,032	34,950
Difference total energy		+0,186 %	-0,049 %
Minimum difference in power		0,000 %	-0,119 %
Maximum difference in power		0,307 %	0,004 %

the power curve as the load representations move along the line. The effect is amplified by the graph and that the real difference in power is actually very small. The parameters used for the calculations are given in Table 3.3. A summary of the calculated values is provided in Table 3.6.

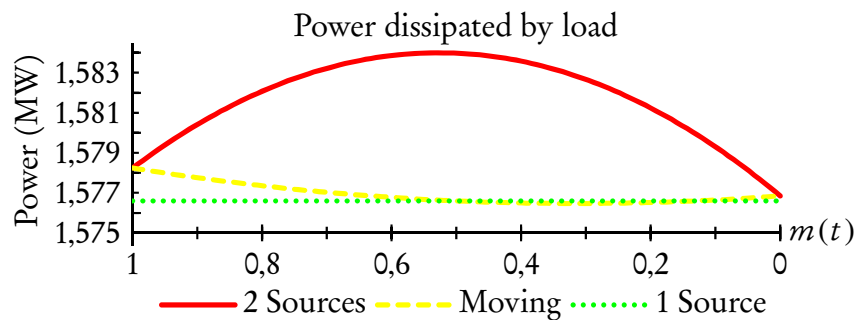


Figure 3.15: Power dissipated by load along short open section for different load representations — Constant current 500 A

The lowest point on the moving load's curve correspond to the mid-point between two substations. For sections that do not include the mid-point, the power demand of the single stationary load will only be the correct at a single point, namely halfway between the two stations (like in Figure 3.18). This is normally the point where the power demand of a real train would be at its lowest.

Table 3.6: Load representation comparison — Constant current on short open section

Calculated Value	Moving Load		2 Sources	1 Source
Total energy dissipated (kWh)	55,192	55,363	55,181	
Difference total energy		+0,310 %	-0,020 %	
Minimum difference in power		0,000 %	-0,104 %	
Maximum difference in power		0,468 %	0,008 %	

Also, the power dissipation of the moving and two stationary loads are exactly the same at the departure and arrival stations. These correspond better with the points where the power demand of a real train would be at its highest (as per Figure 3.13).

**Power comparison — Future load on long open section** Figure 3.16 shows the amount of power dissipated by the load for the three different methods of load representation. It represents the movement and load current of the future rolling stock (two modules) along a long, uninterrupted section. The difference between the three methods are relatively small.<sup>12</sup> The single stationary load does have a large error when current is drawn close to the departure and arrival points. The parameters used for the calculations are given in Table 3.7. A summary of the calculated values is provided in Table 3.8.

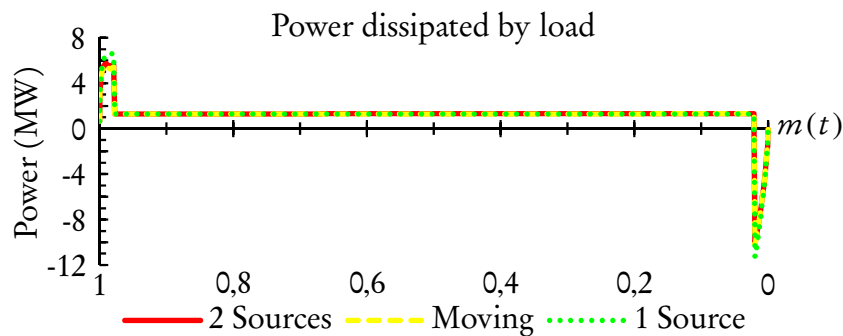


Figure 3.16: Power dissipated by load along long open section for different load representations — Future rolling stock

<sup>12</sup>The “long open section” is included purely for illustrative purposes. For the network under review, the longest open section is 6,47 km long and consequently, the largest error should be much smaller than 4 %.

Table 3.7: Parameters used in calculation

Component	Value
$U_1, U_2$	3268 V
$R_{thU_1}, R_{thU_2}$	0,228 $\Omega$
$x_1$	12,186 km
$x_2$	0,487 km
$d$	10,21 km
$\rho$	0,063 14 $\Omega/\text{km}$

Table 3.8: Load representation comparison — Future loading, long open section

Calculated Value	Moving Load		
	2 Sources	1 Source	
Total energy dissipated (kWh)	217,955	221,208	221,585
Total energy generated (kWh)	26,797	26,691	29,069
Net energy dissipated (kWh)	191,158	194,516	192,516
Difference net energy		+1,757 %	+0,711 %
Minimum difference in power		-0,828 %	-2,229 %
Maximum difference in power		4,059 %	25,407 %
Minimum voltage (V)	1203	1223	1508
Difference in minimum voltage		+1,723 %	25,407 %
Maximum voltage (V)	3876	3848	4323
Difference in maximum voltage		-0,724 %	11,533 %

**Power comparison — Present load on long open section** Figure 3.17 shows the amount of power dissipated by the load for the three different methods of load representation. It represents the movement and load current of the present rolling stock (three motor coaches) along a long, uninterrupted section. The difference between the three methods are relatively small. The single stationary load does have a larger error when current is drawn close to the departure point. The error is much smaller than for the future rolling stock, due to the smaller maximum current demand. The parameters used for the calculations are given in Table 3.7. A summary of the calculated values is provided in Table 3.9

Table 3.9: Load representation comparison — Present loading, long open section

Calculated Value	Moving Load		
	2 Sources	1 Source	
Total energy dissipated (kWh)	131,594	132,450	132,179
Difference total energy		+0,650 %	+0,445 %
Minimum difference in power		0,000 %	-1,030 %
Maximum difference in power		1,011 %	2,411 %

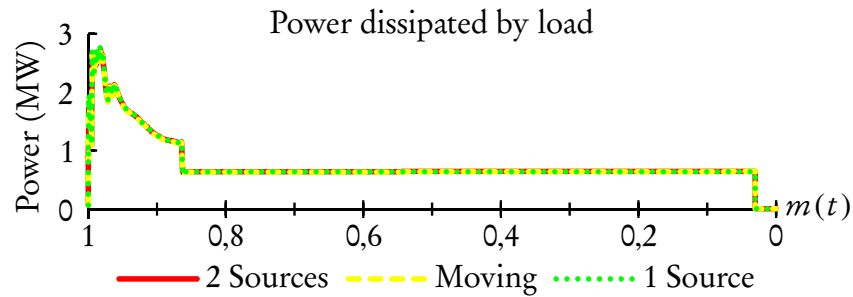


Figure 3.17: Power dissipated by load along long open section for different load representations — Present rolling stock

**Power comparison — Constant current load on long open section** Figure 3.18 shows the amount of power dissipated by a constant current load of 500 A moving along a long open section at a constant speed for the three different methods of load representation. This example is included to show the difference in form of the power curve as the load representations move along the line. The effect is amplified by the graph and that the real difference in power is relatively very small. The parameters used for the calculations are given in Table 3.7. A summary of the calculated values is provided in Table 3.10.

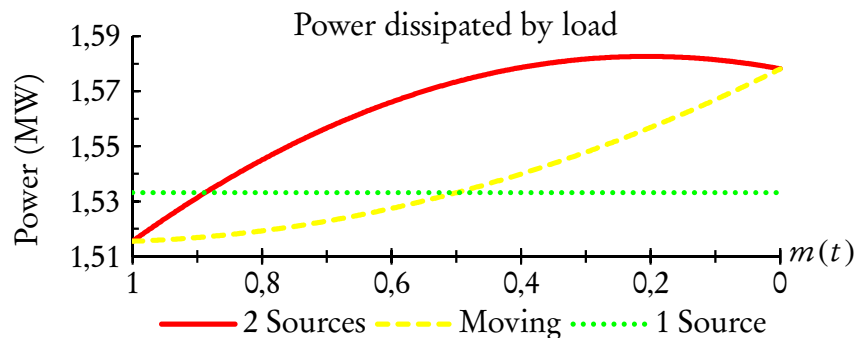


Figure 3.18: Power dissipated by load along long open section for different load representations — Constant current 500 A

Table 3.10: Load representation comparison — Constant current on long open section

Calculated Value	Moving Load	2 Sources	1 Source
Total energy dissipated (kWh)	242,617	246,847	241,895
Difference total energy		+1,744 %	-0,297 %
Minimum difference in power		0,000 %	-2,850 %
Maximum difference in power		2,628 %	1,165 %

In this instance, where the mid-point between the two substations is not part of the section, the power demand of the single stationary load will only be the correct at a single point, namely halfway between the two stations.

Also, the power dissipation of the moving and two stationary loads are exactly the same at the departure and arrival stations. These correspond better with the points where the power demand of a real train would be at its highest (as per Figure 3.16).

### 3.4.2 Moving Train on an Interrupted Section

The previous section showed that the system response of a moving load along a section with only two substations can be modelled quite well by manipulating the current allocated to two stationary loads. Another scenario exists, illustrated in Figure 3.19, where the train will depart from point A, between substation 1 and 2, but arrive at point B, between substation 2 and 3. The circuit of Figure 3.11 is not applicable any more, since a third substation now divides our previously uninterrupted line of length  $d$ . The variable  $k$  is introduced to denote the relative position of substation 2 along  $d$ . By definition the distance from point A to substation 2 is  $d/k$ . The combined resistance of the overhead line and return rail is called the total specific resistance, represented by  $\rho$  and expressed in  $\Omega/\text{km}$ . The current contribution of each substation will need a piece-wise continuous function to explain the time period  $0 \leq t \leq m^{-1}(0)$ .

#### 3.4.2.1 Single Moving Load

This scenario requires two circuits, one for the case where the load is between substation 1 and 2 (Figure 3.20) and another when the load is between substation

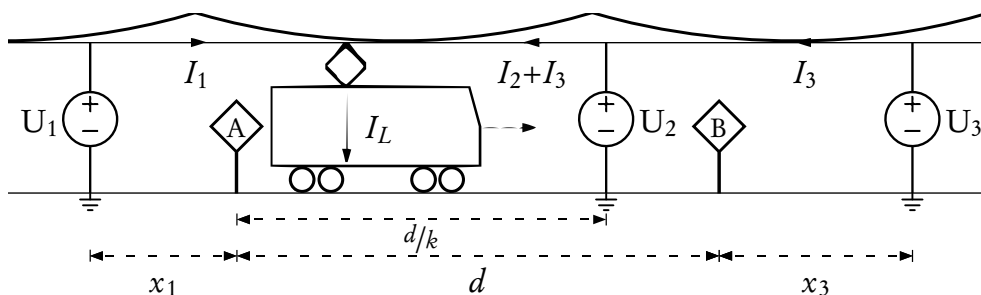


Figure 3.19: Diagram of a train moving between two points, supplied by three substations

2 and 3 (Figure 3.21).

**Between substation 1 and 2** Consider Figure 3.20, where the load is between

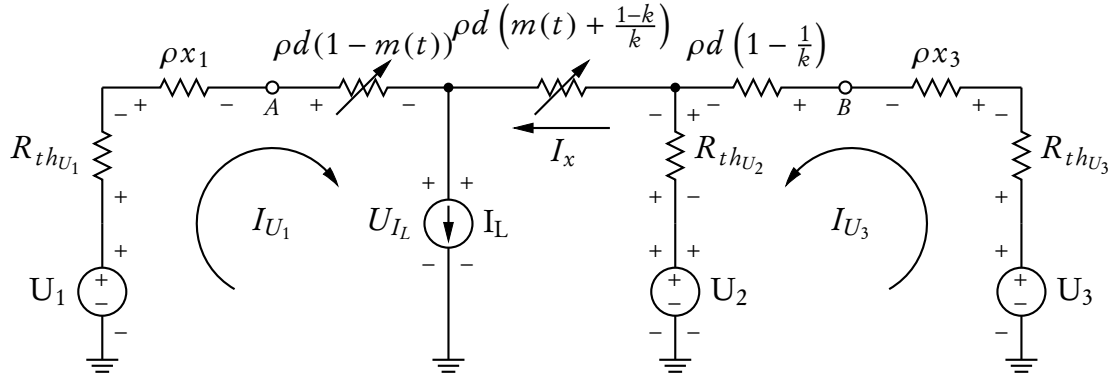


Figure 3.20: Circuit of a single, moving load located between substations 1 and 2, but supplied by three substations

substation 1 and 2 and movement is represented by changing a portion of the interrupted line of total length  $d$ . The function  $m(t)$  still represents the position of the train along  $d$  in time, so Figure 3.20 is only valid for  $0 \leq t \leq m^{-1} \left( \frac{k-1}{k} \right)$ ,  $k \in \mathbb{R}^+$ .  $I_{U_1}$ , the amount of current that is contributed by substation 1 to feed the moving load  $I_L$  during this time interval, can be calculated using circuit analysis: Node voltage equation:

$$I_{U_2} = I_x - I_{U_3} \quad (3.32a)$$

$$\text{and } I_L = I_x + I_{U_1} \quad (3.32b)$$

$$\therefore I_x = I_{U_2} + I_{U_3} = I_L - I_{U_1} \quad (3.32c)$$

$$\text{and } I_{U_3} = I_L - I_{U_1} - I_{U_2} \quad (3.32d)$$

Mesh current equations:

$$-U_1 + I_{U_1} \left[ R_{thU_1} + \rho x_1 + \rho d(1 - m(t)) \right] + U_{I_L} = 0 \quad (3.33a)$$

$$-U_2 + (I_x - I_{U_3}) R_{thU_2} + I_x \rho d \left( m(t) - 1 + \frac{1}{k} \right) + U_{I_L} = 0 \quad (3.33b)$$

$$-U_3 + I_{U_3} \left[ R_{thU_3} + \rho x_3 + \rho d \left( 1 - \frac{1}{k} \right) \right] + (I_{U_3} - I_x) R_{thU_2} + U_2 = 0 \quad (3.33c)$$

Substituting (3.33a) in (3.33b) and using (3.32a) and (3.32c) gives:

$$U_1 - U_2 + I_{U_2} R_{th_{U_2}} + (I_L - I_{U_1}) \rho d \left( m(t) - 1 + \frac{1}{k} \right) - I_{U_1} \left[ R_{th_{U_1}} + \rho x_1 + \rho d (1 - m(t)) \right] = 0 \quad (3.34)$$

With further simplification resulting in:

$$U_1 - U_2 + I_{U_2} R_{th_{U_2}} + I_L \rho d \left( m(t) - 1 + \frac{1}{k} \right) - I_{U_1} \left( \frac{\rho d}{k} + \rho x_1 + R_{th_{U_1}} \right) = 0 \quad (3.35)$$

Similarly, substituting (3.32a) and (3.32d) in (3.33c) gives:

$$-U_3 + (I_L - I_{U_1} - I_{U_2}) \left[ R_{th_{U_3}} + \rho x_3 + \rho d \left( 1 - \frac{1}{k} \right) \right] - I_{U_2} R_{th_{U_2}} + U_2 = 0 \quad (3.36)$$

This yields the following equation for  $I_{U_2}$ :

$$I_{U_2} = \frac{U_2 - U_3 + (I_L - I_{U_1}) \left[ R_{th_{U_3}} + \rho x_3 + \rho d \left( 1 - \frac{1}{k} \right) \right]}{R_{th_{U_2}} + R_{th_{U_3}} + \rho x_3 + \rho d \left( 1 - \frac{1}{k} \right)} \quad (3.37)$$

Finally, by substituting (3.37) in (3.35) and then solving for the current contribution of substation 1,  $I_{U_1}$ :

$$I_{U_1} = \frac{1}{c} \left\{ I_L \left\{ \frac{R_{th_{U_2}} \left[ R_{th_{U_3}} + \rho x_3 + \rho d \left( 1 - \frac{1}{k} \right) \right]}{R_{th_{U_2}} + R_{th_{U_3}} + \rho x_3 + \rho d \left( 1 - \frac{1}{k} \right)} + \rho d \left( m(t) - 1 + \frac{1}{k} \right) \right\} + U_1 - U_2 + \frac{R_{th_{U_2}} (U_2 - U_3)}{R_{th_{U_2}} + R_{th_{U_3}} + \rho x_3 + \rho d \left( 1 - \frac{1}{k} \right)} \right\},$$

where  $c = \frac{R_{th_{U_2}} \left[ R_{th_{U_3}} + \rho x_3 + \rho d \left( 1 - \frac{1}{k} \right) \right]}{R_{th_{U_2}} + R_{th_{U_3}} + \rho x_3 + \rho d \left( 1 - \frac{1}{k} \right)} + R_{th_{U_1}} + \rho x_1 + \frac{\rho d}{k}$  (3.38)

The power that will be dissipated by the moving load for this section can be calculated from (3.33a).

$$P_{I_L} = U_{I_L} I_L \quad (3.39)$$

$$= I_L U_1 - I_L I_{U_1} \left[ R_{th_{U_1}} + \rho x_1 + \rho d (1 - m(t)) \right] \quad (3.40)$$

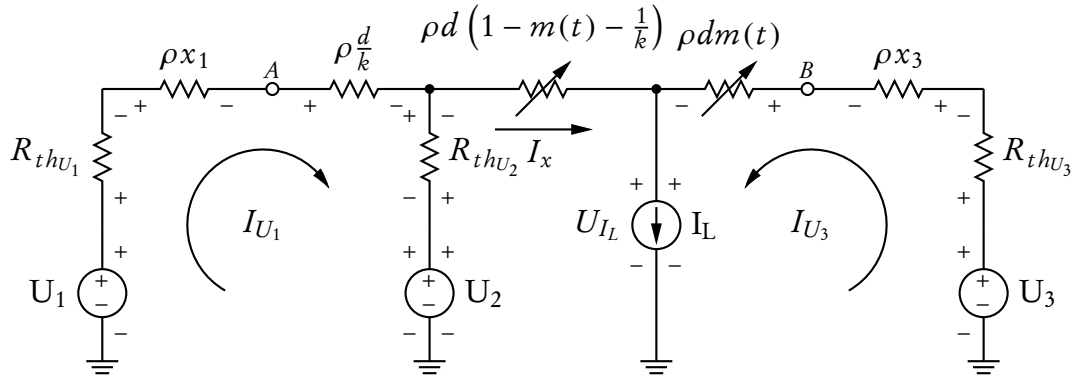


Figure 3.21: Circuit of a single, moving load fed by three substations, located between substation 2 and 3

**Between substation 2 and 3** Similarly, consider Figure 3.21, where the load is between substation 2 and 3 and  $t$  is valid for  $m^{-1}\left(\frac{k-1}{k}\right) \leq t \leq m^{-1}(0)$ ,  $k \in \mathbb{R}^+$ .  $I_{U_1}$ , the amount of current that is contributed by substation 1 to feed the moving load  $I_L$  during this time-interval, can be calculated using circuit analysis:

Node voltage equation:

$$I_{U_2} = I_x - I_{U_1} \quad (3.41a)$$

$$\text{and } I_L = I_x + I_{U_3} \quad (3.41b)$$

$$\therefore I_x = I_{U_1} + I_{U_2} = I_L - I_{U_3} \quad (3.41c)$$

$$\text{and } I_{U_3} = I_L - I_{U_1} - I_{U_2} \quad (3.41d)$$

Mesh current equations:

$$-U_1 + I_{U_1} \left( R_{thU_1} + \rho x_1 + \rho \frac{d}{k} \right) + R_{thU_2} (I_{U_1} - I_x) + U_2 = 0 \quad (3.42a)$$

$$-U_2 + R_{thU_2} (I_x - I_{U_1}) + I_x \rho d \left( 1 - m(t) - \frac{1}{k} \right) + U_{I_L} = 0 \quad (3.42b)$$

$$-U_3 + I_{U_3} \left[ R_{thU_3} + \rho x_3 + \rho d m(t) \right] + U_{I_L} = 0 \quad (3.42c)$$

Substituting (3.42c) in (3.42b) and using (3.41a), (3.41c) and (3.41d) gives:

$$\begin{aligned} U_3 - U_2 + I_{U_1} \left[ R_{thU_3} + \rho x_3 + \rho d \left( 1 - \frac{1}{k} \right) \right] \\ + I_{U_2} \left[ \rho d \left( 1 - \frac{1}{k} \right) + \rho x_3 + R_{thU_2} + R_{thU_3} \right] \\ - I_L \left( R_{thU_3} + \rho x_3 + \rho d m(t) \right) = 0 \end{aligned} \quad (3.43)$$



Similarly, substituting (3.41a) in (3.42a) yields:

$$-U_1 + I_{U_1} \left( R_{th_{U_1}} + \rho x_1 + \rho \frac{d}{k} \right) - R_{th_{U_2}} I_{U_2} + U_2 = 0 \quad (3.44)$$

This yields the following equation for  $I_{U_2}$ :

$$I_{U_2} = \frac{1}{R_{th_{U_2}}} \left[ U_2 - U_1 + I_{U_1} \left( R_{th_{U_1}} + \rho x_1 + \rho \frac{d}{k} \right) \right] \quad (3.45)$$

Finally, by substituting (3.45) in (3.43) and then solving for the current contribution of substation 1,  $I_{U_1}$  yields the equation:

$$I_{U_1} = \frac{1}{c} \left\{ I_L \frac{R_{th_{U_2}} (R_{th_{U_3}} + \rho x_3 + \rho d m(t))}{R_{th_{U_2}} + R_{th_{U_3}} + \rho x_3 + \rho d \left( 1 - \frac{1}{k} \right)} + U_1 - U_2 + \frac{R_{th_{U_2}} (U_2 - U_3)}{R_{th_{U_2}} + R_{th_{U_3}} + \rho x_3 + \rho d \left( 1 - \frac{1}{k} \right)} \right\}$$

where  $c = \frac{R_{th_{U_2}} [R_{th_{U_3}} + \rho x_3 + \rho d \left( 1 - \frac{1}{k} \right)]}{R_{th_{U_2}} + R_{th_{U_3}} + \rho x_3 + \rho d \left( 1 - \frac{1}{k} \right)} + R_{th_{U_1}} + \rho x_1 + \rho \frac{d}{k}$  (3.46)

The power that will be dissipated by the moving load for this section can be calculated from (3.42b) and (3.45).

$$P_{I_L} = U_{I_L} I_L \quad (3.47)$$

$$= I_L U_2 - I_L I_{U_1} \rho d \left( 1 - m(t) \frac{1}{k} \right) - I_L \left[ U_2 - U_1 + I_{U_1} \left( R_{th_{U_1}} + \rho x_1 + \rho \frac{d}{k} \right) \right] \left[ 1 + \frac{\rho d}{R_{th_{U_2}}} \left( \frac{k-1}{k} - m(t) \right) \right] \quad (3.48)$$

Equations (3.38) and (3.46) together give the piece-wise continuous function for  $I_{U_1}$ :

$$I_{U_1} = \begin{cases} \frac{I_L}{c} \left\{ \frac{R_{thU_2} [R_{thU_3} + \rho x_3 + \rho d (1 - \frac{1}{k})]}{R_{thU_2} + R_{thU_3} + \rho x_3 + \rho d (1 - \frac{1}{k})} + \rho d \left( m(t) - 1 + \frac{1}{k} \right) \right\} \\ \quad + c^{-1} \left[ U_1 - U_2 + \frac{R_{thU_2} (U_2 - U_3)}{R_{thU_2} + R_{thU_3} + \rho x_3 + \rho d (1 - \frac{1}{k})} \right] & \forall 0 \leq t \leq m^{-1} \left( \frac{k-1}{k} \right), \\ I_L c^{-1} \frac{R_{thU_2} (R_{thU_3} + \rho x_3 + \rho d m(t))}{R_{thU_2} + R_{thU_3} + \rho x_3 + \rho d (1 - \frac{1}{k})} \\ \quad + c^{-1} \left[ U_1 - U_2 + \frac{R_{thU_2} (U_2 - U_3)}{R_{thU_2} + R_{thU_3} + \rho x_3 + \rho d (1 - \frac{1}{k})} \right] & \forall m^{-1} \left( \frac{k-1}{k} \right) \leq t \leq m^{-1}(0) \end{cases}$$

where  $c = \frac{R_{thU_2} [R_{thU_3} + \rho x_3 + \rho d (1 - \frac{1}{k})]}{R_{thU_2} + R_{thU_3} + \rho x_3 + \rho d (1 - \frac{1}{k})} + R_{thU_1} + \rho x_1 + \rho \frac{d}{k}$  (3.49)

Equations (3.40) and (3.48) together give the piece-wise continuous function for  $P_{I_L}$ :

$$P_{I_L} = \begin{cases} I_L U_1 - I_L I_{U_1} [R_{thU_1} + \rho x_1 + \rho d (1 - m(t))] & \forall 0 \leq t \leq m^{-1} \left( \frac{k-1}{k} \right), \\ I_L U_2 - I_L I_{U_1} \rho d \left( 1 - m(t) \frac{1}{k} \right) \\ \quad - I_L \left[ U_2 - U_1 + I_{U_1} \left( R_{thU_1} + \rho x_1 + \rho \frac{d}{k} \right) \right] \\ \quad \left[ 1 + \frac{\rho d}{R_{thU_2}} \left( \frac{k-1}{k} - m(t) \right) \right] & \forall m^{-1} \left( \frac{k-1}{k} \right) \leq t \leq m^{-1}(0) \end{cases}$$

(3.50)

### 3.4.2.2 Two Stationary Dynamic Loads

Now consider the circuit in Figure 3.22, where substation 2 is located between two stationary dynamic current sources,  $I_1$  and  $I_2$ . These are placed at the departure, A, and the destination, B. Load movement is represented by changing the amount of current allocated to each source using the function,  $m(t)$ , as in Section 3.4.1.2.

Once again  $I_1 = I_L m(t)$  and  $I_2 = I_L (1 - m(t))$ . This method does not consider the, almost binary, shift of the load from the section between substations 1 and 2 to the section between 2 and 3. Consequently, only one circuit needs to be solved

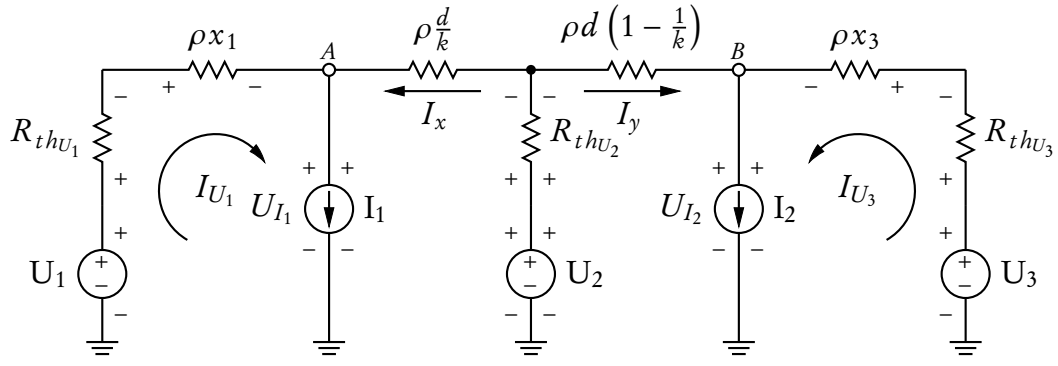


Figure 3.22: Circuit of two stationary dynamic loads fed by three substations

for the whole time period  $0 \leq t \leq m^{-1}(0)$ .  $I_{U_1}$ , the amount of current that is contributed by substation 1 at time instance  $t$  to feed the stationary loads  $I_1$  and  $I_2$ , can then be calculated using circuit analysis:

Node voltage equation:

$$I_1 = I_{U_1} + I_x \quad (3.51a)$$

$$I_2 = I_{U_3} + I_y \quad (3.51b)$$

$$I_{U_2} = I_x + I_y \quad (3.51c)$$

Let

$$I_1 = I_L m(t) \quad \text{and} \quad I_2 = I_L (1 - m(t)), \quad (3.52)$$

so that

$$I_1 + I_2 = I_L m(t) + I_L (1 - m(t)) \quad (3.53a)$$

$$= I_L [m(t) - m(t) + 1] \quad (3.53b)$$

$$= I_L \quad (3.53c)$$

and from (3.51), it follows that

$$I_L = I_{U_1} + I_{U_2} + I_{U_3}. \quad (3.54)$$

Mesh current equations:

$$-U_1 + I_{U_1} (R_{thU_1} + \rho x_1) + U_{I_1} = 0 \quad (3.55a)$$

$$-U_2 + I_{U_2} R_{thU_2} + (I_1 - I_{U_1}) \rho \frac{d}{k} + U_{I_1} = 0 \quad (3.55b)$$

$$-U_2 + I_{U_2} R_{thU_2} + (I_{U_2} + I_{U_1} - I_1) \rho d \left(1 - \frac{1}{k}\right) + U_{I_2} = 0 \quad (3.55c)$$

$$-U_3 + I_{U_3} (R_{thU_3} + \rho x_3) + U_{I_2} = 0 \quad (3.55d)$$

Substituting (3.52), (3.54) and (3.55d) in (3.55c):

$$I_{U_2} \left( R_{th_{U_2}} + \rho d \frac{k-1}{k} + R_{th_{U_3}} + \rho x_3 \right) = U_2 - U_3 \\ - I_{U_1} \left( \rho d \frac{k-1}{k} + R_{th_{U_3}} + \rho x_3 \right) + I_L \left( m(t) \rho d \frac{k-1}{k} + R_{th_{U_3}} + \rho x_3 \right) \quad (3.56)$$

Substituting (3.52) and (3.55b) in (3.55a):

$$-U_1 + I_{U_1} (R_{th_{U_1}} + \rho x_1) + U_2 - I_{U_2} R_{th_{U_2}} - (I_L m(t) - I_{U_1}) \rho \frac{d}{k} = 0 \quad (3.57)$$

Substituting  $I_{U_2}$  from (3.56) into (3.57) gives the current contribution of substation 1 as:

$$I_{U_1} = \left\{ \frac{R_{th_{U_2}} \left[ R_{th_{U_3}} + \rho x_3 + \rho d \left( 1 - \frac{1}{k} \right) \right]}{R_{th_{U_2}} + R_{th_{U_3}} + \rho x_3 + \rho d \left( 1 - \frac{1}{k} \right)} + R_{th_{U_1}} + \rho x_1 + \rho \frac{d}{k} \right\}^{-1} \\ \left\{ I_L \left[ \frac{R_{th_{U_2}} \left[ R_{th_{U_3}} + \rho x_3 + m(t) \rho d \left( 1 - \frac{1}{k} \right) \right]}{R_{th_{U_2}} + R_{th_{U_3}} + \rho x_3 + \rho d \left( 1 - \frac{1}{k} \right)} + m(t) \rho \frac{d}{k} \right] \right. \\ \left. + U_1 - U_2 + \frac{R_{th_{U_2}} (U_2 - U_3)}{R_{th_{U_2}} + R_{th_{U_3}} + \rho x_3 + \rho d \left( 1 - \frac{1}{k} \right)} \right\} \quad (3.58)$$

In this instance (3.58) is not equal to (3.49). This means that the power contributed by each substation to two stationary dynamic loads on an interrupted section will not be exactly same as the contribution towards a single, moving load. The stations will typically be spaced much closer together than the substations, i.e.  $d$  will be relatively short compared to the  $x_1$  and  $x_2$ . Consequently, the difference between the two cases should be acceptably small. The extent to which it differs is explored in Section 3.4.2.3

The power that will be dissipated by the moving load itself can be calculated as the sum of the power dissipated in both stationary loads. The power dissipated in  $I_1$  can be calculated using (3.55a):

$$P_{I_1} = U_{I_1} I_1 \quad (3.59)$$

$$= I_L m(t) U_{I_1} \quad (3.60)$$

$$= I_L m(t) \left[ U_1 - I_{U_1} (R_{th_{U_1}} + \rho x_1) \right] \quad (3.61)$$

Similarly, the power dissipated in  $I_2$  can be calculated using (3.52) and (3.55c):

$$P_{I_2} = U_{I_2} I_2 \quad (3.62)$$

$$= I_L (1 - m(t)) U_{I_2} \quad (3.63)$$

$$= I_L (1 - m(t)) \left[ U_2 - I_{U_2} R_{th_{U_2}} - (I_{U_1} + I_{U_2} - I_L m(t)) \rho d \left( 1 - \frac{1}{k} \right) \right] \quad (3.64)$$

By summing (3.61) en (3.64) together the total power that will be dissipated by the train at time instance  $t$  is given by (3.66).

$$P_{I_L} = P_{I_1} + P_{I_2} \quad (3.65)$$

$$\begin{aligned} &= I_L m(t) \left[ U_1 - I_{U_1} (R_{th_{U_1}} + \rho x_1) \right] \\ &\quad + I_L (1 - m(t)) \left[ U_2 - I_{U_2} R_{th_{U_2}} - (I_{U_1} + I_{U_2} - I_L m(t)) \rho d \left( 1 - \frac{1}{k} \right) \right] \end{aligned} \quad (3.66)$$

### 3.4.2.3 Comparison of Two Methods

In the case of an interrupted section, the current supplied by substation 1 to the two stationary loads (3.49) is not the same as the current that will be delivered to the moving load (3.58). This also implies that the power contribution of each substation will not be the same. For an interrupted section, the response of substations due to moving trains along it can thus not be perfectly mimicked by manipulating the current profiles using the relative displacement function and an external script.

From mere observation of the equations for current contribution ((3.49) and (3.58)) and power dissipation in the load ((3.50) and (3.66)), it is not immediately clear to what extent the two methods will vary for the network under review. This was evaluated using Microsoft Excel with sample values of  $m(t)$  and  $I_L$ . All calculations are based on current values generated by the processing algorithm, discussed in Sections 3.5.2 and 3.5.3. Three methods were investigated for each evaluation: moving load, two stationary dynamic sources (placed at departure and arrival stations) and one stationary source (placed mid-section). Negative current represents regenerative braking. Bi-directional substations with no threshold voltage are assumed.

The node voltage at each load can be calculated using (3.33a) and (3.45) substituted in (3.42b) for the moving load, (3.61) for stationary load 1 and (3.64) for

stationary load 2. The minimum and maximum voltage calculated during each evaluation will be given for the future rolling stock. This will give an indication about the expected difference in pantograph voltage of a moving load and the voltage recorded at each stationary load.

The results are encouraging and the total power dissipated by two stationary dynamic sources is deemed close enough to that of a moving load. The recorded values of minimum and maximum voltage also compares very well.

This proves that the movement of the trains can be sufficiently mimicked by manipulating the current profiles with an external script. These profiles can then be used as input for the stationary current sources in PowerFactory.

**Power comparison – Future load on short interrupted section** Figure 3.23 shows the amount of power dissipated by the load for the three different methods of load representation. It represents the movement and load current of the future rolling stock (single module) along a short, interrupted section. Substation 2 is located almost in the middle of the section. From a power dissipation perspective there is virtually no difference between the three methods.

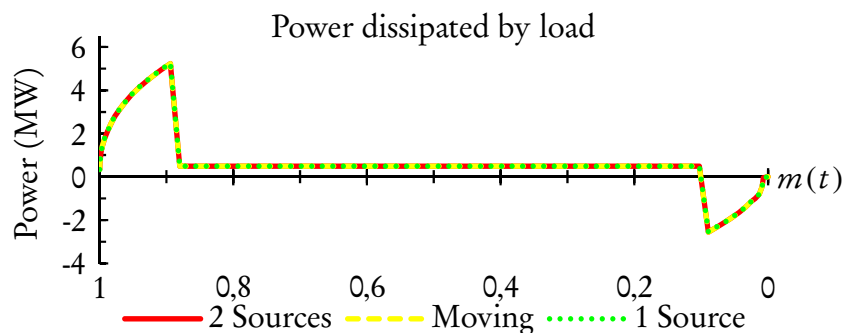


Figure 3.23: Power dissipated by load along short interrupted section for different load representations — Future rolling stock

Figure 3.24 shows the current contribution of substation 1 for the three different methods of load representation. The difference between the two stationary loads and a moving load is very small, especially close to the departure and arrival points. The maximum error during acceleration is 1%. By comparison, the system response to the single load does not correspond very well to that of the moving load. During acceleration, about 13% less current is allocated to substation 1, 3% more to substation 2 and 6% more to substation 3.

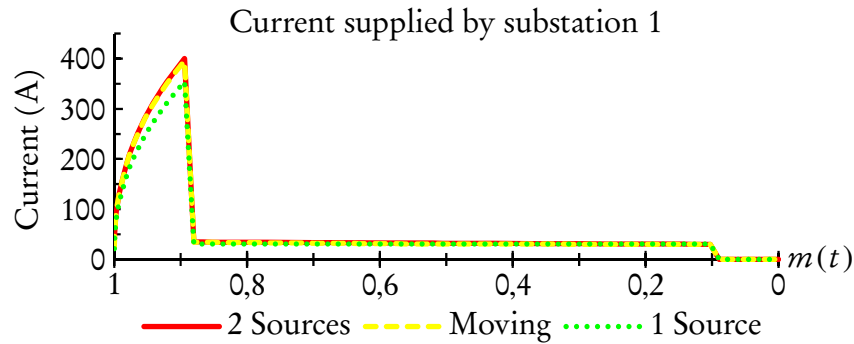


Figure 3.24: Current contribution of substation 1 for different load representations — Future rolling stock

The parameters used for the calculations are given in Table 3.11. A summary of the calculated values is provided in Table 3.12.

Table 3.11: Parameters used in calculation

Component	Value
$U_1, U_2, U_3$	3268 V
$R_{thU_1}, R_{thU_2}, R_{thU_3}$	0,228 $\Omega$
$\rho$	0,063 14 $\Omega/\text{km}$
$x_1$	6,199 km
$x_3$	5,691 km
$d$	0,85 km
$k$	2,219

**Power comparison — Present load on short interrupted section** Figure 3.25 shows the amount of power dissipated by the load for the three different methods of load representation. It represents the movement and load current of the present rolling stock (two motor coaches) along a short, interrupted section. Substation 2 is located almost in the middle of the section. From a power dissipation perspective there is virtually no difference between the three methods.

Figure 3.26 shows the current contribution of substation 1 for the three different methods of load representation. The difference between the two stationary loads and a moving load is very small, especially close to the departure point. The maximum error during parallel is 3 %. By comparison, the system response to the single load does not fare as well. During acceleration, about 13 % less current is allocated to substation 1, 3 % more to substation 2 and 6 % more to substation 3.

Table 3.12: Load representation comparison — Future loading, short interrupted section

Calculated Value	Moving Load		2 Sources	1 Source
Total energy dissipated (kWh)	20,579	20,585	20,631	
Total energy generated (kWh)	4,249	4,248	4,240	
Net energy dissipated (kWh)	16,330	16,337	16,391	
Difference net energy		+0,042 %	+0,373 %	
Minimum Difference in Power		-0,043 %	-0,263 %	
Maximum Difference in Power		0,092 %	0,515 %	
Minimum voltage (V)	3021	3020	3036	
Difference in minimum voltage		-0,024 %	+0,515 %	
Maximum voltage (V)	3378	3378	3369	
Difference in maximum voltage		+0,001 %	-0,263 %	

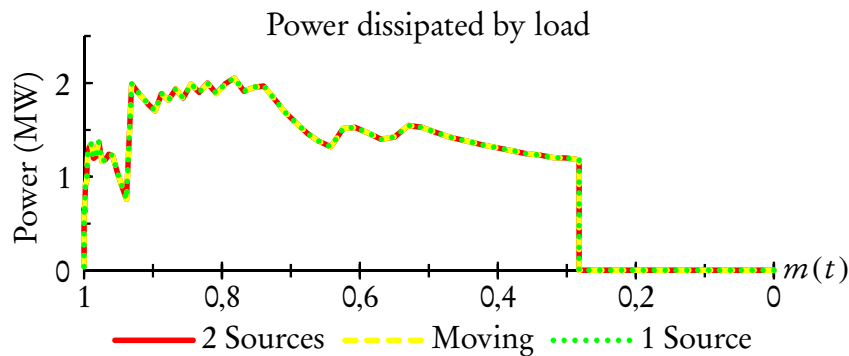


Figure 3.25: Power dissipated by load along short interrupted section for different load representations — Present rolling stock

The parameters used for the calculations are given in Table 3.11. A summary of the calculated values is provided in Table 3.13.

Table 3.13: Load representation comparison — Present loading, short interrupted section

Calculated Value	Moving Load		2 Sources	1 Source
Total energy dissipated (kWh)	24,071	24,076	24,093	
Difference total energy		+0,018 %	+0,093 %	
Minimum Difference in Power		-0,024 %	-0,021 %	
Maximum Difference in Power		0,040 %	0,198 %	

### Power comparison — Constant current load on short interrupted section

Figure 3.27 shows the amount of power dissipated by a constant current load of



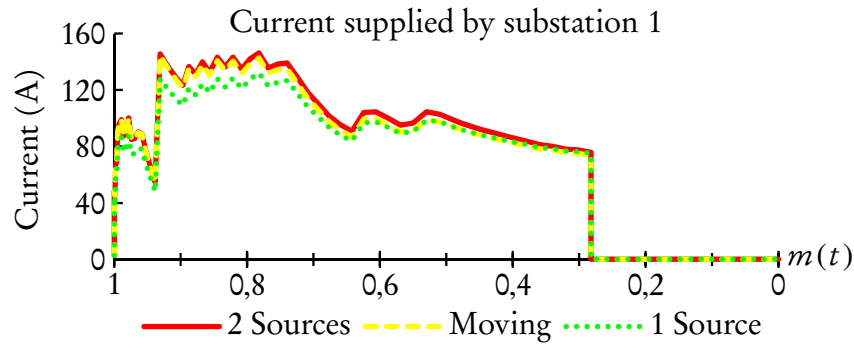


Figure 3.26: Current contribution of substation 1 for different load representations — Present rolling stock

500 A moving along a short interrupted section at a constant speed for the three different methods of load representation. This example is included to show the difference in form of the power curve as the load representations move along the line. The effect is amplified by the graph and that the real difference in power is actually very small, as shown in Table 3.14.

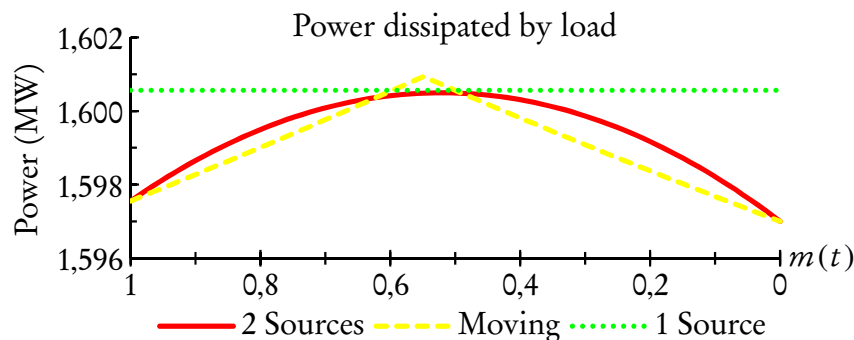


Figure 3.27: Power dissipated by load along short interrupted section for different load representations — Constant current 500 A

The vertex on the moving load's curve correspond to the location of substation 2. Even though the two stationary dynamic loads do not use a piece-wise continuous function, the difference between the two methods is relatively small.

Also, the power dissipation of the moving and two stationary loads are once again exactly the same at the departure and arrival stations. These correspond better with the points where the power demand of a real train would be at its highest.

Figure 3.28 shows the current contribution of substation 1 for the three different methods of load representation. The maximum difference between

the two stationary loads and the moving load is 5,827 % (where the load passes substation 2). By comparison, the largest difference between the single stationary load and the moving load is at the departure point when 13 % less current will be contributed by substation 1.

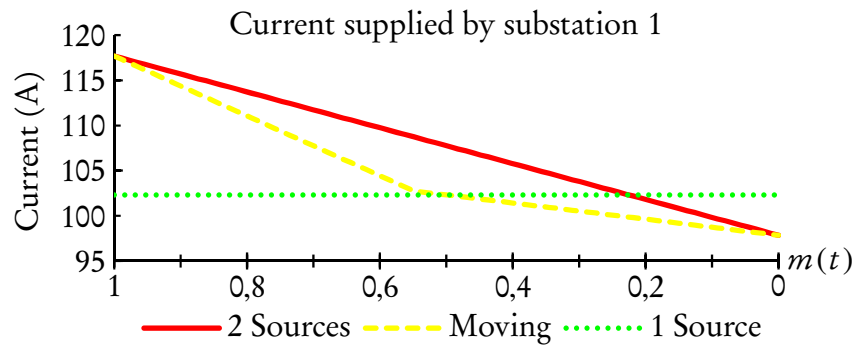


Figure 3.28: Current contribution of substation 1 for different load representations — Constant current 500 A

The parameters used for the calculations are given in Table 3.11. A summary of the calculated values is provided in Table 3.14.

Table 3.14: Load representation comparison — Constant current on short interrupted section

Calculated Value	Moving Load	2 Sources	1 Source
Total energy dissipated (kWh)	39,088	39,096	39,125
Difference total energy		+0,023 %	+0,096 %
Minimum Difference in Power		-0,027 %	-0,022 %
Maximum Difference in Power		0,052 %	0,223 %

**Power comparison — Future load on longer interrupted section** Figure 3.29 shows the amount of power dissipated by the load for the three different methods of load representation. It represents the movement and load current of the future rolling stock (two modules) along a longer, interrupted section. Substation 2 is located about 200 m from the departure point, an eighth of the section length. From a power dissipation perspective there is virtually no difference between the three methods.

Figure 3.30 shows the current contribution of substation 1 for the three different methods of load representation. The difference between the two stationary

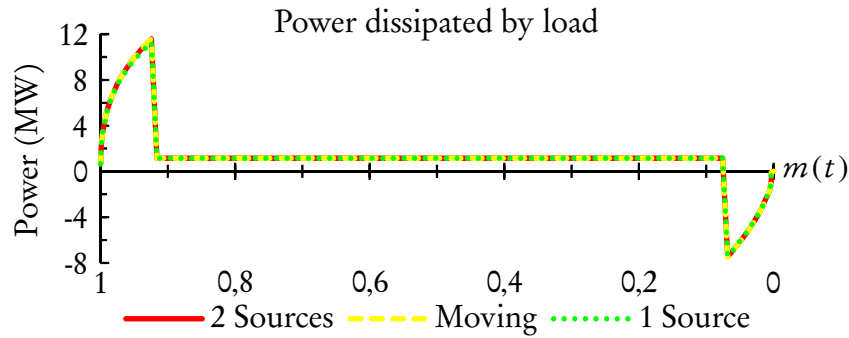


Figure 3.29: Power dissipated by load along longer interrupted section for different load representations — Future rolling stock

loads and a moving load is very small, especially close to the departure and arrival points. The maximum error during acceleration is 2 %. By comparison, the system response to the single load does not correspond very well to that of the moving load. During acceleration, about 11 % less current is allocated to substation 1, 4 % less to substation 2 and 23 % more to substation 3.

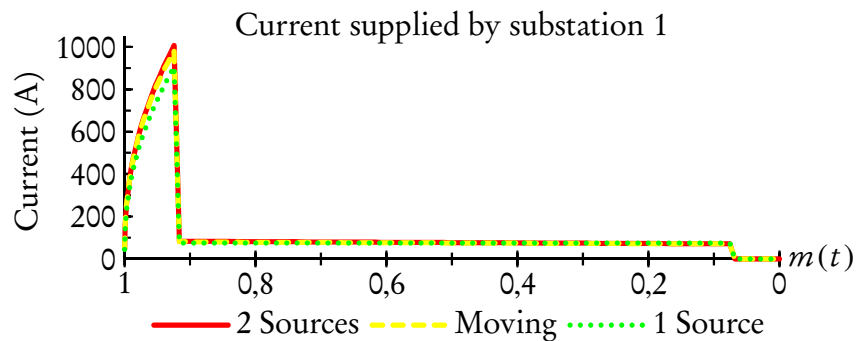


Figure 3.30: Current contribution of substation 1 for different load representations — Future rolling stock

The parameters used for the calculations are given in Table 3.15. A summary of the calculated values is provided in Table 3.16.

**Power comparison — Present load on longer interrupted section** Figure 3.31 shows the amount of power dissipated by the load for the three different methods of load representation. It represents the movement and load current of the present rolling stock (four motor coaches) along a longer, interrupted section. From a power dissipation perspective there is virtually no difference between the three methods.

Table 3.15: Parameters used in calculation

Component	Value
$U_1, U_2, U_3$	3268 V
$R_{thU_1}, R_{thU_2}, R_{thU_3}$	0,228 $\Omega$
$\rho$	0,047 54 $\Omega/\text{km}$
$x_1$	7,259 km
$x_3$	6,9 km
$d$	1,91 km
$k$	8,4141

Table 3.16: Load representation comparison — Future loading, longer interrupted section

Calculated Value	Moving Load		
	2 Sources	1 Source	
Total energy dissipated (kWh)	70,031	70,066	69,452
Total energy generated (kWh)	16,152	16,130	16,029
Net energy dissipated (kWh)	53,879	53,937	53,423
Difference net energy		+0,108 %	-0,846 %
Minimum Difference in Power		-0,286 %	-2,666 %
Maximum Difference in Power		0,192 %	0,196 %
Minimum voltage (V)	2699	2691	2627
Difference in minimum voltage		-0,290 %	-2,666 %
Maximum voltage (V)	3613	3610	3576
Difference in maximum voltage		-0,083 %	-1,018 %

Figure 3.32 shows the current contribution of substation 1 for the three different methods of load representation. The difference between the two stationary loads and a moving load is small, especially when there is a big power demand close to the departure point. The maximum error during parallel is 3 %. By comparison, the system response to the single stationary load does not correspond as well: about 11 % less current is allocated to substation 1, up to 5 % less to substation 2 and 23 % more to substation 3.

The parameters used for the calculations are given in Table 3.15. A summary of the calculated values is provided in Table 3.17.

#### Power comparison — Constant current load on longer interrupted section

Figure 3.33 shows the amount of power dissipated by a constant current load of 500 A moving along a longer interrupted section at a constant speed for the three different methods of load representation. This example is included to show the

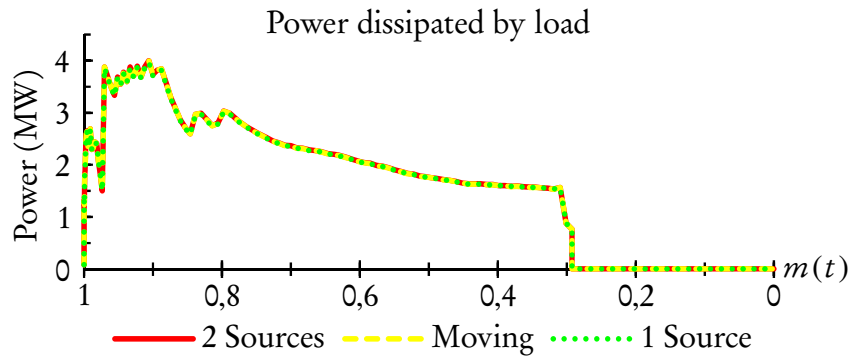


Figure 3.31: Power dissipated by load along longer interrupted section for different load representations — Present rolling stock

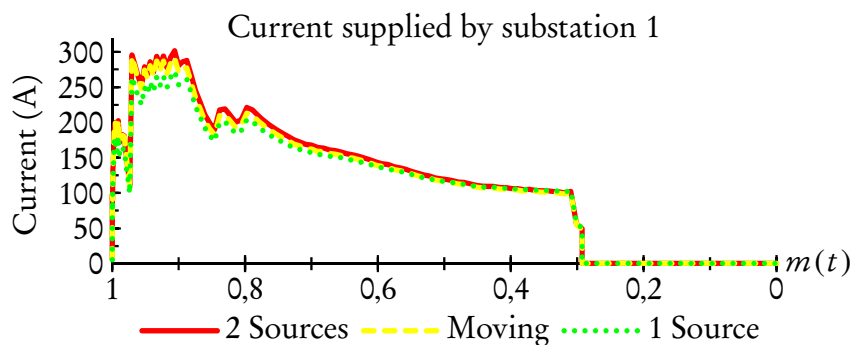


Figure 3.32: Current contribution of substation 1 for different load representations — Present rolling stock

Table 3.17: Load representation comparison — Present loading, longer interrupted section

Calculated Value	Moving Load	2 Sources	1 Source
Total energy dissipated (kWh)	69,483	69,566	69,252
Difference total energy		+0,120 %	-0,332 %
Minimum Difference in Power		-0,044 %	-0,739 %
Maximum Difference in Power		0,306 %	0,127 %

difference in the form of the power curve as the load representations move along the line. The effect is amplified by the graph and that the real difference in power is actually very small, as shown in Table 3.18.

The vertex on the moving load's curve correspond to the location of substation 2. The difference in power is larger than in the case of the short section (as shown in Figure 3.27). The difference in instantaneous power between two static loads and a moving load is smaller than between one static load and a moving load.

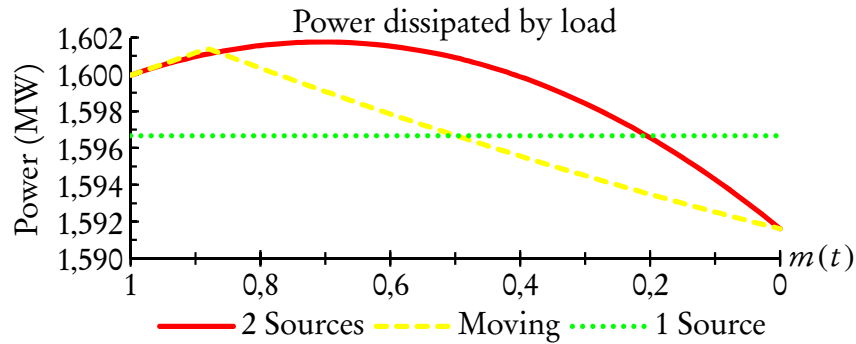


Figure 3.33: Power dissipated by load along longer interrupted section for different load representations — Constant current 500 A

Also, the power dissipation of the moving and two stationary loads are once again exactly the same at the departure and arrival stations. These correspond better with the points where the power demand of a real train would be at its highest.

Figure 3.34 shows the current contribution of substation 1 for the three different methods of load representation. The maximum difference between the two stationary loads and the moving load is 4,16 % (where the load passes substation 2). By comparison, the largest difference between the single stationary load and the moving load is when 11 % less current will be contributed by substation 1 (departure point), 8 % more by substation 2 (arrival point) and 23 % more by substation 3 (departure point).

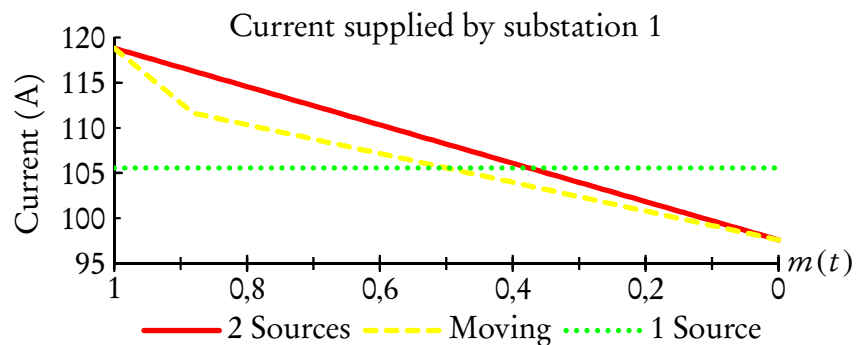


Figure 3.34: Current contribution of substation 1 for different load representations — Constant current 500 A

The parameters used for the calculations are given in Table 3.15. A summary of the calculated values is provided in Table 3.18.

Table 3.18: Load representation comparison — Constant current on longer interrupted section

Calculated Value	Moving Load		2 Sources	1 Source
Total energy dissipated (kWh)	62,538	62,634	62,536	
Difference total energy		+0,155 %	−0,002 %	
Minimum Difference in Power		−0,017 %	−0,294 %	
Maximum Difference in Power		0,271 %	0,318 %	

**Power comparison — Future load on long interrupted section** Figure 3.35 shows the amount of power dissipated by the load for the three different methods of load representation. It represents the movement and load current of the future rolling stock (two modules) along a long, interrupted section. Substation 2 is located about 310 m from the departure point, after a thirtieth of the section length. From a power dissipation perspective the overall difference between the three methods are relatively small. The single stationary load does have a large error when current is drawn close to the departure and arrival points.

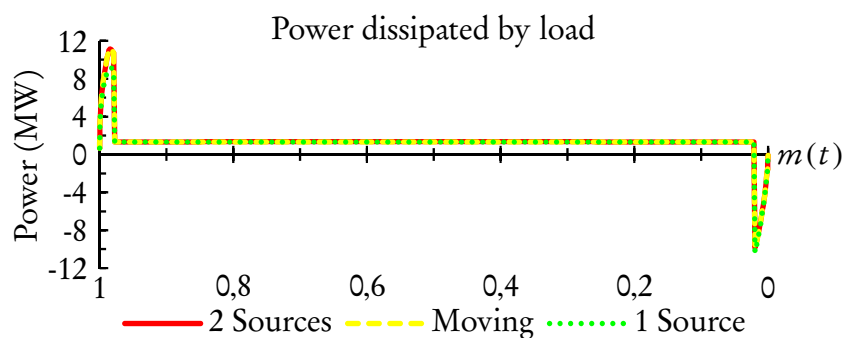


Figure 3.35: Power dissipated by load along long interrupted section for different load representations — Future rolling stock

Figure 3.36 shows the current contribution of substation 1 for the three different methods of load representation. The difference between the two stationary loads and a moving load is very small, especially close to the departure and arrival points.<sup>13</sup> The maximum error during acceleration is 5%. By comparison, the system response to the single load does not correspond very well to that of the moving load. During acceleration, about 40% less current is allocated to substation 1, 33% less to substation 2 and up to 168% more to substation 3.

<sup>13</sup>The “long interrupted section” described here does exist on the network under review, but represents the worst case. Consequently, the largest error will typically be much smaller than 5%.

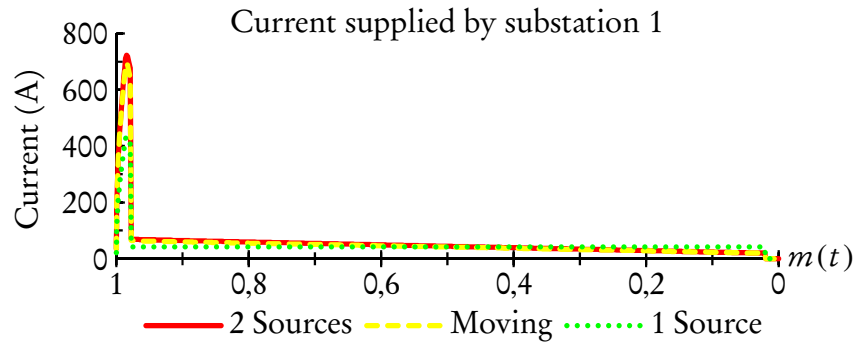


Figure 3.36: Current contribution of substation 1 for different load representations — Future rolling stock

The parameters used for the calculations are given in Table 3.19. A summary of the calculated values is provided in Table 3.20.

Table 3.19: Parameters used in calculation

Component	Value
$U_1, U_2, U_3$	3268 V
$R_{thU_1}, R_{thU_2}, R_{thU_3}$	0,228 $\Omega$
$\rho$	0,063 14 $\Omega/\text{km}$
$x_1$	12,186 km
$x_3$	0,487 km
$d$	10,21 km
$k$	32,85

**Power comparison — Present load on long interrupted section** Figure 3.37 shows the amount of power dissipated by the load for the three different methods of load representation. It represents the movement and load current of the present rolling stock (three motor coaches) along a long, interrupted section. From a power dissipation perspective there is little difference between the three methods. The single stationary load does have a larger error when current is drawn close to the departure and arrival points. The error is much smaller than for the future rolling stock, due to the smaller maximum current demand.

Figure 3.38 shows the current contribution of substation 1 for the three different methods of load representation. The difference between the two stationary loads and a moving load is relatively small. The maximum error during parallel is 6%. By comparison, the system response to the single load does not correspond



Table 3.20: Load representation comparison — Future loading, long interrupted section

Calculated Value	Moving Load		2 Sources	1 Source
Total energy dissipated (kWh)	239,754	242,187		233,030
Total energy generated (kWh)	26,416	26,312		27,268
Net energy dissipated (kWh)	213,338	215,875		205,762
Difference net energy		+1,189 %		-3,551 %
Minimum Difference in Power		-0,830 %		-17,857 %
Maximum Difference in Power		2,015 %		4,344 %
Minimum voltage (V)	2568	2547		2110
Difference in minimum voltage		-0,830 %		-17,857 %
Maximum voltage (V)	3798	3773		3962
Difference in maximum voltage		-0,634 %		+4,344 %

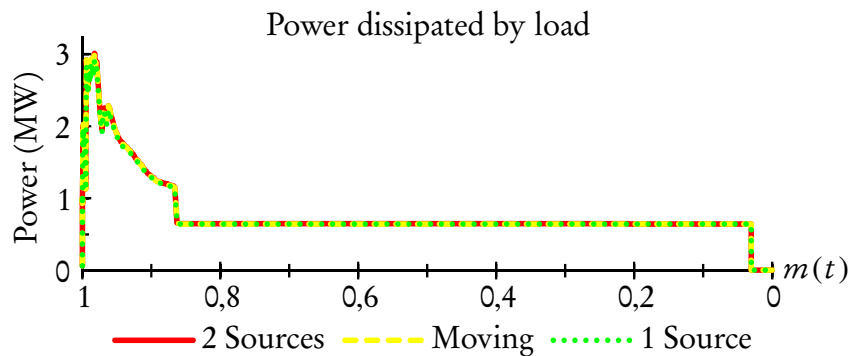


Figure 3.37: Power dissipated by load along long interrupted section for different load representations — Present rolling stock

as well: about 40 % less current is allocated to substation 1, 33 % less to substation 2 and 167 % more to substation 3.

The parameters used for the calculations are given in Table 3.19. A summary of the calculated values is provided in Table 3.21.

Table 3.21: Load representation comparison — Present loading, long interrupted section

Calculated Value	Moving Load		2 Sources	1 Source
Total energy dissipated (kWh)	135,509	136,158		134,343
Difference total energy		+0,479 %		-0,861 %
Minimum Difference in Power		-0,134 %		-3,298 %
Maximum Difference in Power		0,955 %		0,015 %

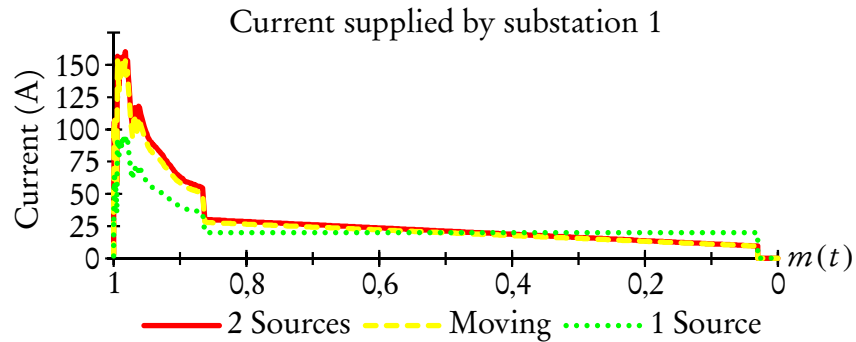


Figure 3.38: Current contribution of substation 1 for different load representations — Present rolling stock

**Power comparison — Constant current load on long interrupted section** Figure 3.39 shows the amount of power dissipated by a constant current load of 500 A moving along a long interrupted section at a constant speed for the three different methods of load representation. This example is included to show the difference in the form of the power curve as the load representations move along the line. The effect is amplified by the graph and that the real difference in power is actually very small. The parameters used for the calculations are given in Table 3.19. A summary of the calculated values is provided in Table 3.22.

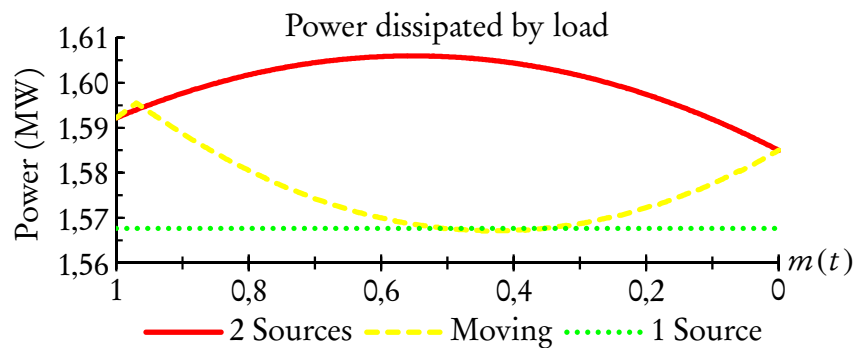


Figure 3.39: Power dissipated by load along long interrupted section for different load representations — Constant current 500 A

The vertex on the moving load's curve correspond to the location of substation 2. The difference in power is larger than in the case of the short and longer section (as shown in Figures 3.27 and 3.33). This section is the longest on the network, so represents the maximum expected difference. For this instance, the maximum difference in instantaneous power between two static loads and a moving load is larger than between one static load and a moving load.

Table 3.22: Load representation comparison — Constant current on long interrupted section

Calculated Value	Moving Load	2 Sources	1 Source
Total energy dissipated (kWh)	261,797	265,665	260,404
Difference total energy		+1,477 %	-0,532 %
Minimum Difference in Power		-0,097 %	-1,747 %
Maximum Difference in Power		2,439 %	0,036 %

Also, the power dissipation of the moving and two stationary loads are once again exactly the same at the departure and arrival stations. These correspond better with the points where the power demand of a real train would be at its highest.

Figure 3.40 shows the current contribution of substation 1 for the three different methods of load representation. The maximum difference between the two stationary loads and the moving load is 8,60% (where the load passes substation 2). By comparison, the largest difference between the single stationary load and the moving load is at the arrival point when 125% more current will be contributed by substation 1 and 2 and at the departure point when 168% more current will be contributed by substation 3.

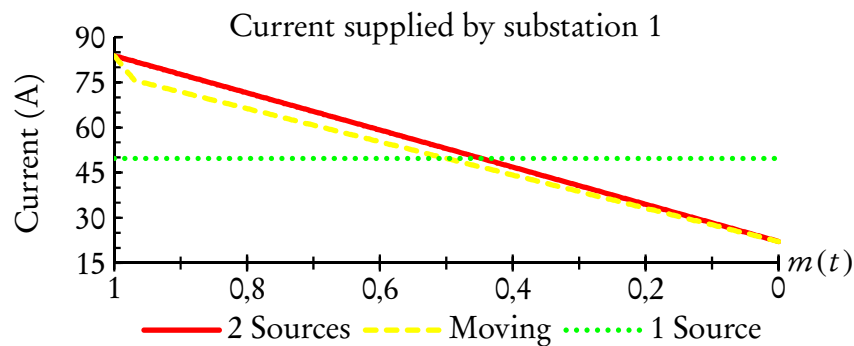


Figure 3.40: Current contribution of substation 1 for different load representations — Constant current 500 A

### 3.4.3 Defining the Relative Displacement Function

Irrespective of the load representation, the location of the load along the line at a certain time instance will play a significant role in the amount of power that each substation will contribute. This was exemplified in the previous sections,

where the error for a single source was almost always larger than the two sources. In Section 3.4.1 the concept of a relative displacement function,  $m(t)$ , was first mentioned. In this section this function will be defined.

As stated earlier,  $m(t)$  must represent the relative displacement of the train between two stations. By definition  $m(0) = 1$  should indicate that the train is 100 % at the departure station and 0 % at the destination. Similarly,  $m(t_f) = 0$  indicate that the train is 0 % at the departure station, but 100 % at the destination.

One possibility that was investigated was to use recorded values of location and electrical current data. This method would be able to model the true energy demand very well. The quality of data depends strongly on the conditions on the day the recording is made, such as delays, driver behaviour, train loading and state of the rolling stock and traction power network. It proved very difficult to gather the recorded values of especially the electrical current data, as discussed in Section 3.3.1. A model of the future rolling stock can also not be constructed using this method. As a result it did not prove practical to pursue this method further.

In order to evaluate the different classes of rolling stock that will be operating on the network, a more idealised model was rather investigated. By using simple equations of motion and the average acceleration and deceleration rate of the different classes of rolling stock, an idealised displacement function can be calculated. Since the network under review is relatively flat the influence of the track gradient was considered to be negligible.<sup>14</sup>

As described in Section 2.2.1, some believe that the ideal is to accelerate to maximum line speed and then coast as much as possible, with only limited intervention to the train speed to consider line conditions and timekeeping. The extent to which coasting can be utilised, however, depends a lot on track gradient and curvature. This strategy needs a very detailed model of the aerodynamic properties of the rolling stock and the topographical layout of the network.

The future rolling stock has a speed control driving mode that allows the driver to set a target speed [96]. The train will then automatically accelerate to the target speed and adjust the traction and braking effort in order to continue cruising at this

---

<sup>14</sup>The steepest grade of most lines are in the order of 1:80. All lines servicing the southern and south eastern parts of Cape Town traverse an area known as the Cape Flats, a vast sheet of aeolian sand [93]. Lines servicing the northern parts were originally constructed as a standard gauge (1435 mm) line with large embankments and deep cuttings to limit gradients to around 1:100 [94; 95].

speed [96]. This strategy conforms to the idealised model described above. The train will accelerate at a constant rate up to the velocity which is needed to cover the distance between stations in the amount of time allowed in the timetable. It will then travel at that velocity until commencing a constant deceleration, so that the train arrives the destination station at exactly the scheduled time. Allowance can be made to over the distance in less time, say 5 %, to cover delays.

The maximum train speed is based purely on the amount of time allocated to the station-to-station journey in the official timetable and the distance between the stations. It can therefore not take individual speed restrictions, nor the associated deceleration and acceleration, into consideration.

Figure 3.41 illustrates the acceleration  $a(t)$ <sup>15</sup>, speed  $v(t)$  and displacement  $x(t)$  of a typical station-to-station journey. The train departs and continues to accelerate at  $a_v$  m/s<sup>2</sup> until reaching a speed of  $v_{max}$  m/s after  $t_v$  seconds. It then maintains this speed until  $t_f - t_s$  seconds after departure. From this time it

Typical station-to-station acceleration, speed and displacement

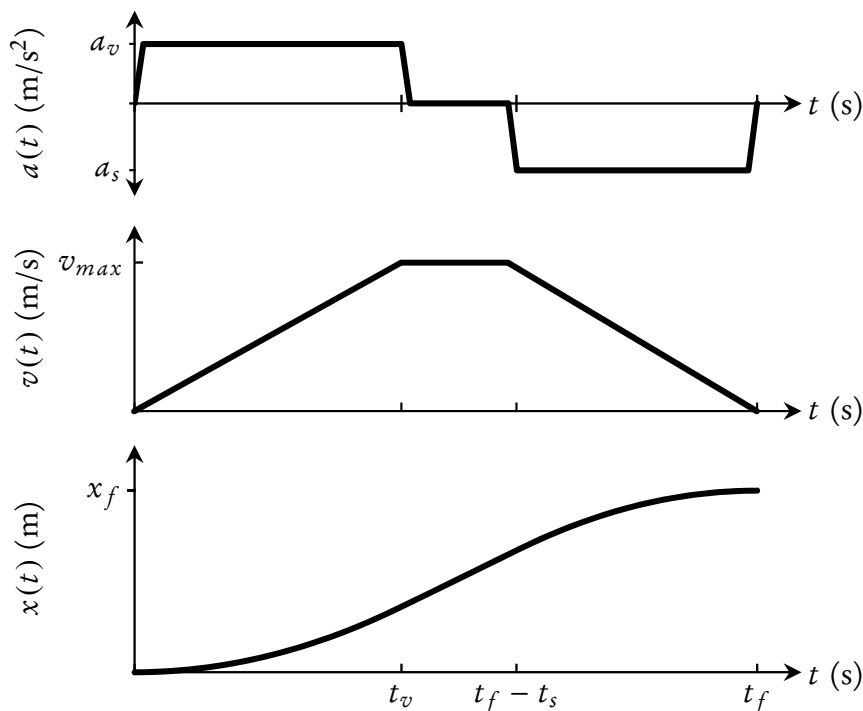


Figure 3.41: Idealised acceleration, speed and displacement curve of a single station-to-station journey

<sup>15</sup>In reality the acceleration and deceleration will be adjusted to limit the jerk. The effect is deemed negligible and the equivalent acceleration will be used.

accelerates at  $a_s$  m/s<sup>2</sup> (deceleration) and continues to do so (for  $t_s$  seconds) until reaching the destination. The journey is  $x_f$  metres long and takes  $t_f$  seconds to complete.

Substituting these variables into the standard motion equation

$$x(t) = x_0 + v_0 t + \frac{1}{2} a t^2 \quad (3.67)$$

yields the following piecewise continuous function for the displacement  $x(t)$

$$x(t) = \begin{cases} \frac{1}{2} a_v t^2 & \forall 0 \leq t \leq t_v, \\ \frac{1}{2} a_v t_v^2 + v_{max} (t - t_v) & \forall t_v \leq t \leq t_f - t_s, \\ \frac{1}{2} a_v t_v^2 + v_{max} (t - t_v) + \frac{1}{2} a_s (t - t_f + t_s)^2 & \forall t_f - t_s \leq t \leq t_f \end{cases} \quad (3.68)$$

where

$$t_v = \frac{v_{max}}{a_v}, a_v > 0 \quad \text{and} \quad t_s = -\frac{v_{max}}{a_s}, a_s < 0. \quad (3.69)$$

Substituting (3.69) into (3.68), one can solve the maximum speed:

$$v_{max} = \frac{-t_f + \sqrt{t_f^2 + 2 \left( \frac{1}{a_s} - \frac{1}{a_v} \right) x_f}}{\frac{1}{a_s} - \frac{1}{a_v}} \quad (3.70)$$

If the allocated time is too short, then the term under the square root will be negative. The shortest time allowed will be when acceleration is immediately superseded by deceleration and the term under the square root is zero. As a result (3.70) must be defined as:

$$v_{max} = \frac{-t_f + \sqrt{t_f^2 + 2 \left( \frac{1}{a_s} - \frac{1}{a_v} \right) x_f}}{\frac{1}{a_s} - \frac{1}{a_v}} \iff t_f^2 + 2 \left( \frac{1}{a_s} - \frac{1}{a_v} \right) x_f \geq 0 \quad (3.71)$$

It can happen that the time allowed in the timetable will be too short for normal acceleration. This may be as a result of certain network characteristics, such as departure on a decline, or if the time allocated is rounded, for example to the closest 15 s. Under these circumstances the condition associated with (3.71) will not be met. A workaround is to temporarily assign the minimum value to  $a_v$  that is necessary to complete the journey within the allocated time:

$$a_v = \left( \frac{t_f^2}{2x_f} + \frac{1}{a_s} \right)^{-1} \quad (3.72)$$

Also, the function for  $x(t)$  in (3.68), and its graphical representation in Figure 3.41, does not conform to the definition for  $m(t)$  stated at the start of this section. In order for  $m(0) = 1$  and  $m(t_f) = 0$  to hold true,  $m(t)$  can be defined in terms of  $x(t)$  as follow:

$$m(t) = 1 - \frac{x(t)}{x_f} \quad (3.73)$$

For more information regarding the determination of the acceleration and deceleration rates for the present rolling stock and validation of the relative displacement function against measured data, see Appendix D.

## 3.5 Implementation of Model

The previous sections showed that it should prove quite accurate to model the system response of a moving train by allocating its current demand dynamically to two stationary current sources. A Python based processing algorithm was developed<sup>16</sup> that takes the official timetable and calculates the current that should be allocated to each current source for every time-step of the simulation. This section will discuss how this was implemented for the present and future rolling stock.

### 3.5.1 Converting the Timetable

The official timetable, known as the Working Time Book (WTB), was acquired in spreadsheet format.<sup>17</sup> It describes the working of all scheduled commuter trains, revenue earning and non-revenue trips, for the network under review. The line from Cape Town to Muldersvlei via Century City and Kraaifontein forms part of the mainline from Cape Town to De Aar and Johannesburg. In addition to the scheduled commuter service it also carries some freight and long distance traffic. These trains do not run to a very tight schedule, don't stop at intermediate stations and mainly run in the off-peak period. Their main energy use is therefore the initial acceleration and then overcoming rolling resistance on the relatively flat

<sup>16</sup>The processing algorithm source code itself can be found in Appendix E.

<sup>17</sup>Three files make up the complete WTB. The files used for this study are:  
DOCS\_CMR3-#232282-v1-Southern\_lines\_train\_service\_Current\_Service.xls  
DOCS\_CMR3-#264103-v17-WTB\_NORTH\_2014.xlsx  
DOCS\_CMR3-#272937-v5-WTB\_AREA\_CENTRAL\_MARCH\_2014\_SERVICE.XLS

terrain<sup>18</sup>. For the purpose of this study, the focus is on commuter trains and no mainline trains were taken into account.

An extract of the WTB is shown in Table 3.23. It contains the arrival (A) and departure (D) times at second level accuracy for all stations where a train must stop at. These times are mostly calculated by adding the time in column two to the preceding cell. If a train is not scheduled to stop at a particular station, no arrival time is indicated. For empty trains (indicated by EC), the times given should act as a guide to drivers and train control officers.

The model that will be implemented, must determine the amount of current drawn or injected by a train for every time instance and allocate that current to two current sources. One source will typically be placed at each station platform on the network. For this reason, the model will have to know when a train arrives and departs, or pass through, each consecutive point. This implies that any omitted departure time, indicated by an ellipsis, would have to be sourced or calculated.

It is not clear what source is used to determine the running times for the WTB. The official document that was supplied gives “distances in kilometres and running times of Electrical Motor coach sets. Running times reflect tested passenger trains stopping at all stations.” [99] The original document is given in Appendix F. Unfortunately it was found that this document contained a number of errors in terms of point to point kilometre distance and feasibility of running times. The running times were assessed in terms of the maximum speed that would have to be achieved to cover the station-to-station distance in the allocated time. It was also compared with actual running times recorded during footplate observations. Some running times were found to be too short and others very lenient. Additionally, in some cases the values do not correspond to the running times given in the WTB. An improved table of running times is included in Appendix F.

The travel time of empty coaches were also found to be inconsistent. Firstly, travel times do not correspond to those given for express working in the official running times. Secondly, the amount of time allocated to different instances of the same working (different trains of the same type and with the same origin and destination) were not always the same. The reason for this could not be determined.

---

<sup>18</sup>The steepest gradient between Cape Town and Bellville is a short 1:90 section [97]. Between Bellville and Muldersvlei there are some 1:80 sections [98].



Table 3.23: Extract of the official timetable for the network under review

DESCRIPTION TRAIN NO.		EC 9899	EC 9703	EC 9803	METRO 9001	EC 9713	EC 9811	METRO 9501	METRO 9911	METRO 9003
PLATFORM NO.		21	20					16	17	19
CAPE TOWN	D		02:15:00	03:45:00				05:00:00	05:05:00	05:10:00
WOODSTOCK	A	00:03:00						05:03:00		
	D	00:00:30						05:03:30		
SALT RIVER	A	00:02:30		STOP YST				05:06:00		
	D	00:00:45		FOR STAFF			05:00:00	05:06:45		
KOEBERG RD	A	00:01:45					...	05:08:30		
	D	00:00:30					...	05:09:00		
MAITLAND	A	00:01:30					...	05:10:30		
	D	00:00:30					05:05:00	05:11:00		
NDABENI	A	00:02:30					...	05:13:30		
	D	00:00:30					...	05:14:00		
PINELANDS	A	00:01:45					...	05:15:45		
	D	00:00:30					...	05:16:15		
ESPLANADE	A	00:03:30	...	...					05:08:30	05:13:30
	D	00:00:30	...	...					05:09:00	05:14:00
P/EILAND	A	00:02:30	...	...					...	...
	D	00:00:15	02:20:00	...	04:15:00	04:55:00	04:50:00		...	...
YSTERPLAAT	A	00:04:45	...	03:50:00	...	...	...		05:13:45	05:18:45
	D	00:00:30	...	03:51:00	...	...	...		05:14:15	05:19:15
MUTUAL	A	00:04:00	...	...	05:00:00	...	...		05:18:15	05:23:15
	D	00:00:30	...	...	05:00:30	...	...		05:18:45	05:23:45
LANGA	A	00:03:15	...	...	05:04:30	...	...	05:20:30	05:22:45	05:27:45
	D	00:00:30	02:33:00	03:58:00	04:23:00	05:05:00	05:00:00	05:21:00	05:23:15	05:28:15
BONTEHEUWEL	A	00:03:00	...	...	...	05:08:00	...	05:24:00	05:26:15	05:31:15
	D	00:01:00	...	...	...	05:09:00	...	05:25:00	05:27:15	05:32:15
NETREG	A	00:02:30	...	...	...	...	...	05:27:30	05:29:45	
	D	00:00:30	...	...	...	...	...	05:28:00	05:30:15	
HEIDEVELD	A	00:02:30	...	...	...	...	...	05:30:30	05:32:45	
	D	00:00:30	...	...	...	...	...	05:31:00	05:33:15	
NYANGA	A	00:03:30	...	...	...	...	...	05:34:30	05:36:45	
	D	00:00:30	...	...	...	...	...	05:35:00	05:37:15	
PHILIPPI	A	00:04:00	...	...	...	...	...	05:39:00	05:42:15	
	D	00:00:30	02:48:00	...	...	...	...	05:39:30	05:42:45	
LENTEGEUR	A	00:04:45	...	...	...	...	...	05:44:15		
	D	00:01:00	...	...	...	...	...	05:45:15		
MITCHELLS PL.	A	00:02:30	...	...	...	...	...	05:47:45		
	D	00:00:30	...	...	...	...	...	05:48:15		
KAPTEINSKLIP	A	00:02:30	02:55:00	04:43:00	...	...	05:35:00	05:50:45		
STOCK ROAD	A	00:01:45	...	...	...	...	...		05:44:30	
	D	00:00:30	...	...	...	...	...		05:45:00	
MANDALAY	A	00:02:00	...	...	...	...	...		05:47:00	
	D	00:01:00	...	...	...	...	...		05:48:00	
NOLUNGILE	A	00:02:45	...	...	...	...	...		05:50:45	
	D	00:00:30	...	...	...	...	...		05:51:15	
NONKQUBELA	A	00:02:30	...	...	...	...	...		05:53:45	
	D	00:00:30	...	...	...	...	...		05:54:15	
KHAYELITSHA	A	00:03:15	...	...	...	...	...		05:57:30	
	D	00:00:30	04:22:00	...	...	05:23:00	...		05:58:00	
KUYASA	A	00:03:30	...	...	...	...	...		06:01:30	
	D	00:00:30	...	...	...	...	...		06:02:00	
CHRIS HANI	A	00:03:45	04:28:00	...	...	05:30:00	...		06:05:45	
LAVISTOWN	A	00:03:30	...	...	05:12:30	...	...			05:35:45
	D	00:00:30	...	...	05:13:00	...	...			05:36:15
BELHAR	A	00:03:00	...	...	05:16:00	...	...			05:39:15
	D	00:00:30	...	...	05:16:30	...	...			05:39:45
UNIBELL	A	00:02:15	...	...	05:18:45	...	...			05:42:00
	D	00:00:30	...	...	05:19:15	...	...			05:42:30
PENTECH	A	00:03:15	...	...	05:22:30	...	...			05:45:45
	D	00:00:30	...	...	05:23:00	...	...			05:46:15
SAREPTA	A	00:02:30	...	...	05:25:30	...	...			05:48:45
	D	00:00:30	...	...	05:28:00	...	...			05:49:15
BELLVILLE	A	00:06:30	...	...	05:34:30	...	...			05:55:45

It was decided that using equations of movement would give the most credible values of unknown departure times. The acceleration was based on the type of train and location. An empty coach working would typically take longer to leave a yard or siding than an express train departing from a platform. The departure and arrival time stated in the WTB and distance between stations were used to calculate a departure time for all unspecified instances. If a train is not scheduled to stop at a particular station, an “E” would be placed in the arrival field.

Certain short-haul empty coach workings were removed. They are in essence yard movements between Cape Town station and the staging yards at Salt River, Cape Town and Paardeneiland. This was regarded as an acceptable simplification of the WTB, mainly because their short distance and relatively low speed should not have an adverse impact on the general loading of traction energy supply equipment. Similarly, shunting manoeuvres during the crossing of two trains on a single line is not included. Commuter trains that are hauled by diesel locomotive were also removed. A complete list of workings removed from the simulation is given in Appendix G.

After further analysis of the WTB, some additional matters were highlighted. The first appertains to the way that the individual times are determined. The departure time from the origin station is normally predetermined and manually entered into the spreadsheet. Subsequent arrival and departure times are then calculated by adding the amount of time in column two to the preceding time instance. A number of cases were found where the wrong cell reference for the preceding time instance was entered. For example, occasionally the arrival time at station B would be calculated by adding the running time to the arrival time at station A (thus ignoring the time that the train dwelt at station A). Other oddities include some instances where very long or very short running times are allowed due to manual manipulation of arrival or departure times. In one instance only 75 s is allowed to cover 4,7 km, requiring an average speed of 225,6 km/h. In other instances the amount of running time allocated is much more than what would be needed, for example 5 min for 1,31 km, an average of 15,72 km/h. . .

Whenever a discrepancy was discovered, through manual inspection or the processing algorithm, it was evaluated and amended to reflect what would offer a more realistic representation of the train service. Care was taken to keep adjustments as small as possible. Superfluous running times were typically not altered, except to balance other instances where the allocated time was too short.

A summary of some discrepancies that were discovered and the amendments that were made can be found in Appendix H.

Other preparation-work included the removal of all notes between the times. Each station's name was replaced with its official three character abbreviation and a reference code to the route. The algorithm will use these codes to determine what current pair a station-to-station trip's current demand will be allocated to. Finally, the WTB was split up according to individual routes so that consecutive stations along the route are listed directly below one another. An example to illustrate the format of a cleaned-up timetable is shown in Table 3.24. The first three lines are for traceability purposes only and is not used by the algorithm. The split files were saved in comma-separated values (CSV)-format to use as input for the processing algorithm.

It was noted that older WTBs also contained the "departure" times at all intermediate large junctions, i.e. ptcars between stations where trains from different lines converge and diverge. The simulation results should be more accurate if the model also contains current sources at all of these intermediate points. Unfortunately the present WTB does not contain this level of detail.<sup>19</sup> The additional time that it would have taken to calculate departure times for all of the junctions on the network could not be justified by the forecasted improvement of the simulation results.

### 3.5.2 Present Rolling Stock

The processing algorithm for the rolling stock that is presently used will be described in this section. After reading the departure and arrival time, the running time is calculated. For the system under review, it is highly unlikely that the train will depart exactly at its scheduled time. The departure time is shifted by adding a random amount of seconds to it. This number can be any integer in the interval  $[-5, 5]$  and is drawn from a discrete uniform distribution.

The station-to-station distance and running time is used to calculate the relative displacement function, as described in Section 3.4.3. For the purpose of this calculation, a constant acceleration of  $0,35 \text{ m/s}^2$  and deceleration of  $0,65 \text{ m/s}^2$  was

---

<sup>19</sup>Most ptcars that previously required very careful planning to prevent bottlenecks are now less important due to additional routes, bridges and quadrupling or sextupling completed in the '80s. Today Kasselsvlei, midway between the stations Bellville, Kuilsrivier and Sarepta, is one of the only major junctions left that is not situated close to a station.

Table 3.24: Example of a cleaned-up timetable, with the format of station codes and use of “E” to indicate that the train will not be stopping at that station

DESCRIPTION	EC	METRO	METRO	EC	METRO
TRAIN NO.	9811	9501	9507	9843	9509
PLATFORM NO.		16	16	15	16
CWNV1-V		05:00:00	06:30:00	06:45:00	06:52:00
WDCV1-A		05:03:00	06:33:00	E	06:55:00
WDCV1-V		05:03:30	06:33:30	06:49:52	06:55:30
SRXV1-A		05:06:00	06:36:00	E	06:58:00
SRXV1-V	05:00:00	05:06:45	06:36:45	06:51:26	06:58:45
KOBV1-A	E	05:08:30	06:38:30	E	07:00:30
KOBV1-V	05:04:17	05:09:00	06:39:00	06:52:36	07:01:00
MLDV1-A	E	05:10:30	06:40:30	E	07:02:30
MLDK1-V	05:05:19	05:11:00	06:41:00	06:53:19	07:03:00
NBIK1-A	E	05:13:30	06:43:30	E	07:05:30
NBIK1-V	05:07:04	05:14:00	06:44:00	06:54:31	07:06:00
PNDK1-A	E	05:15:45	06:45:45	E	07:07:45
PNDK1-V	05:08:54	05:16:15	06:46:15	06:55:47	07:08:15
LAGK1-A	E	05:20:30	06:50:30	E	07:12:30
LAGK1-V	05:15:00	05:21:00	06:51:00	07:00:00	07:13:00
BTLK1-A	E	05:24:00	06:54:00	E	07:16:00
BTLK1-V	05:16:53	05:25:00	06:55:00	07:02:13	07:17:00
NTGK1-A	E	05:27:30	06:57:30	E	07:19:30
NTGK1-V	05:18:55	05:28:00	06:58:00	07:04:36	07:20:00
HEDK1-A	E	05:30:30	07:00:30	E	07:22:30
HEDK1-V	05:20:45	05:31:00	07:01:00	07:06:45	07:23:00
NAGK1-A	E	05:34:30	07:04:30	07:10:00	07:26:30
NAGK1-V	05:23:18	05:35:00	07:05:00		07:27:00
PPIK1-A	E	05:39:00	07:09:00		07:31:00
PPIK1-V	05:27:13	05:39:30	07:09:30		07:31:30
LENK1-A	E	05:44:15	07:14:15		07:36:15
LENK1-V	05:30:56	05:45:15	07:15:15		07:37:15
MTPK1-A	E	05:47:45	07:17:45		07:39:45
MTPK1-V	05:32:48	05:48:15	07:18:15		07:40:15
KTEK1-A	05:35:00	05:50:45	07:20:45		07:42:45

used.<sup>20</sup> The current profile presented in Section 3.3.1 (replicated in Figure 3.42) is used to represent the current demand for an acceleration from 0 to 90 km/h in 105 s. Measurements recorded during footplate observations showed that the maximum braking time for the present rolling stock is around 30 s.<sup>21</sup> The observations also showed that the time spent accelerating is also fairly constant. The following three different scenarios were identified:

- When stations are located fairly close together the master controller is kept in the powering state until deceleration has to start (almost no coasting).
- For more distant stations, the train is allowed to accelerate up to line speed and the traction power switched off. The train momentum is utilised to coast until deceleration has to commence.
- If stations are located very far from one another, the train is accelerated up to line speed after which the speed is maintained by moving the master controller to full-field parallel operation until deceleration has to commence. For this study it was decided that all trips of 4 min 45 s or longer would utilise full-field parallel. The current in full-field parallel has been set at 66 A per motor coach, a compromise between the real value, which is closer to 100 A, and the fact that the master controller will typically not be set to power throughout.

Express trains are dealt with similarly, but the algorithm also determines how long the train should still accelerate for (if the running time between the previous stations was less than the accelerating time). All express trains continue in full field parallel after acceleration.

The network under review utilise numbers to identify trains uniquely and the route that will be travelled. Trains operating on a specific route generally use a predetermined number of motor coaches per train set. The current demand of empty trains were taken as 80 % of normal load. The prefix (first two digits) of the train number is used to determine the factor with which the typical current profile will be adjusted. A summary of the prefixes and factor used is provided in Table 3.25.

---

<sup>20</sup>For more information regarding the determination of acceleration and deceleration rates for the present rolling stock and validation of the relative displacement function, see Appendix D.

<sup>21</sup>Since this rolling stock does not brake regeneratively, the exact amount of time that is spent decelerating is not so important. The value of 30 s is rather a place-holder for the time period before arrival when no power is used.

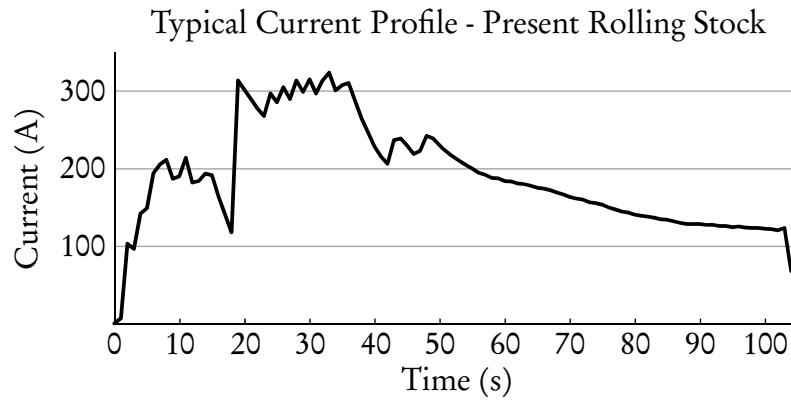


Figure 3.42: Traction current at 3 kV pantograph voltage for a single motor coach

Table 3.25: Loading factors used for different train number prefixes

Route and Service Type	Prefix	Loading Factor
Southern Empty	00	1,6 (80 % of 2)
Southern Normal	01, 02	2
Cape Flats Normal	05	2
Cape Flats Empty	07	1,6 (80 % of 2)
Northern Empty	08	2,4 (80 % of 3)
Northern Express	27	1,6 (80 % of 2)
Monte Vista Normal	28	2
North Normal	23, 25, 32, 34, 35	3
Lavistown Normal	90	3
Lavistown Empty	91	2,4 (80 % of 3)
Central Normal	92, 93, 94, 95, 99	4
Central Empty	97, 98	3,2 (80 % of 4)

The processing algorithm determines what the current profile for the journey should look like. It then divides this value between the two current sources applicable to the journey according to the relative displacement function. These values are summed<sup>22</sup> to the values already assigned to the current sources for the specific time period.

Figure 3.43 gives an example of the current demand calculated for a journey between two stations. The distance between the stations is 1,845 km. The timetable allows 120 s to complete the journey. Since this journey is shorter than the acceleration time of 105 s, the current profile is truncated to 90 s. The last 30 s is reserved for coasting and braking.

<sup>22</sup>In line with the superposition principle, the system response to all trains is the sum of the individual trains.

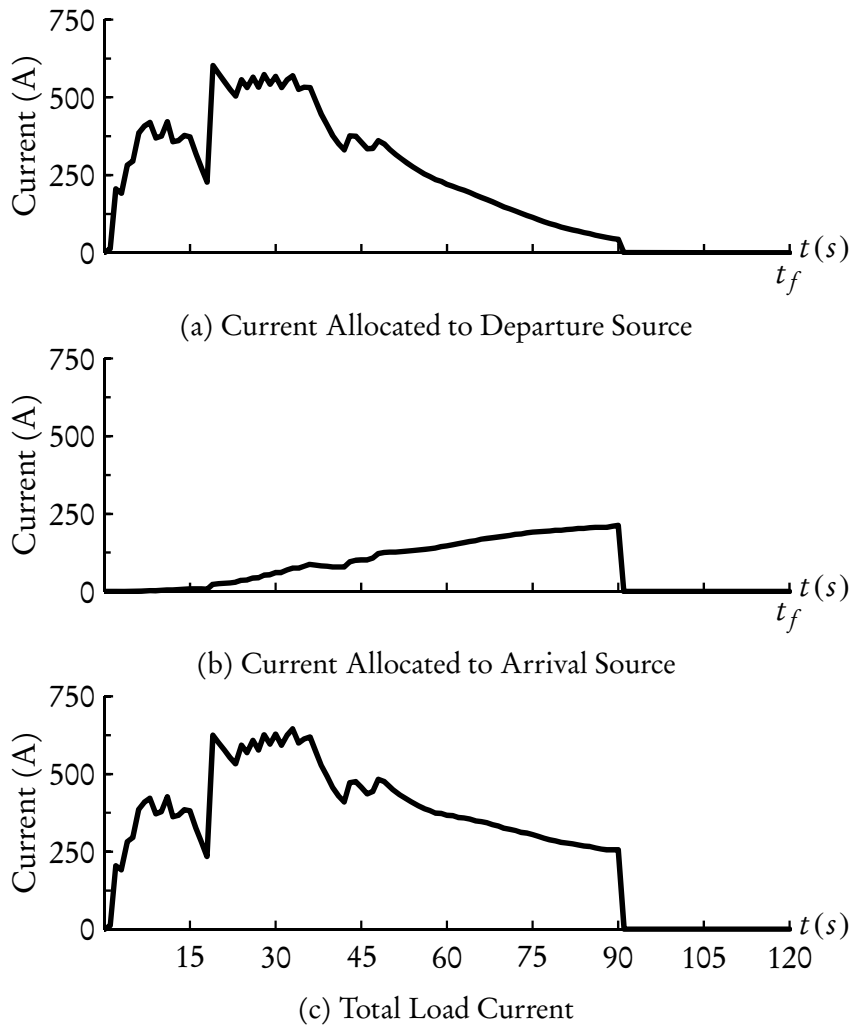


Figure 3.43: Current demand of a station-to-station journey

Figure 3.43a shows the current that will be allocated to the current source at the departure station. It is large during acceleration and decreases as the train “moves” along the line. Similarly, Figure 3.43b shows the current that will be allocated to the current source at the destination. The total load current, that will flow through the pantograph, is shown in Figure 3.43c.

### 3.5.3 Future Rolling Stock

The processing algorithm for the rolling stock that will be used in future will be described in this section. The performance of this rolling stock is more constant for different load conditions and over a wider speed spectrum. This can be attributed to its modern control and propulsion system. Gibela’s simulation results show

that acceleration from 0 to 90 km/h at M3 loading takes only 36 s [91]. As a result, a more detailed model of its current demand could, and had to, be implemented. The biggest difference is that this model will utilise the same parameters used to calculate the relative displacement function to determine exactly how long the train will have to draw current (accelerate) and inject current (brake) for.

The algorithm once again reads the departure and arrival time and calculates the running time. A random amount of seconds is again added. This number can be any integer in the interval  $[-5, 5]$  and is drawn from a discrete uniform distribution. The running time is reduced by 5%. This is done for the following three reasons:

1. The constant speed calculated for the relative displacement function,  $v_{max}$ , will be used to determine the current demand necessary to maintain that speed. In the absence of a  $D_{as}$ , drivers will typically not accelerate to the exact  $v_{max}$  needed to cover the trip distance in the timetable's running time and then adjust the traction to keep the train moving at that speed. They will rather accelerate to a bit higher speed and arrive the destination a bit earlier.
2. The running time stipulated in the timetable generally includes a 5% to 10% allowance to increase the robustness against delays. The 5% that is subtracted can therefore be regarded as the situation where the train is delayed and the driver has to make up some time.
3. Due to the higher performance capability of this rolling stock, it is likely that the running times will be shortened. Long term plans include increasing the line speed to 120 km/h. In the absence of a timetable that represents this, the 5% can also be seen as a shortcut to take the likely, initial, increase in speed into account.

The station-to-station distance and running time is used to calculate the relative displacement function, as described in Section 3.4.3. For the new rolling stock, a constant acceleration of  $0,8 \text{ m/s}^2$  and deceleration of  $0,9 \text{ m/s}^2$  was used, as described in Section 3.3.2.

Figure 3.44 is similar to what was presented in Figure 3.4 (Section 3.3.2) and includes provision for 310 kW of auxiliary load. Figure 3.45 is a replication of Figure 3.7 and does not consider auxiliary loads, similar to what Gibela did in



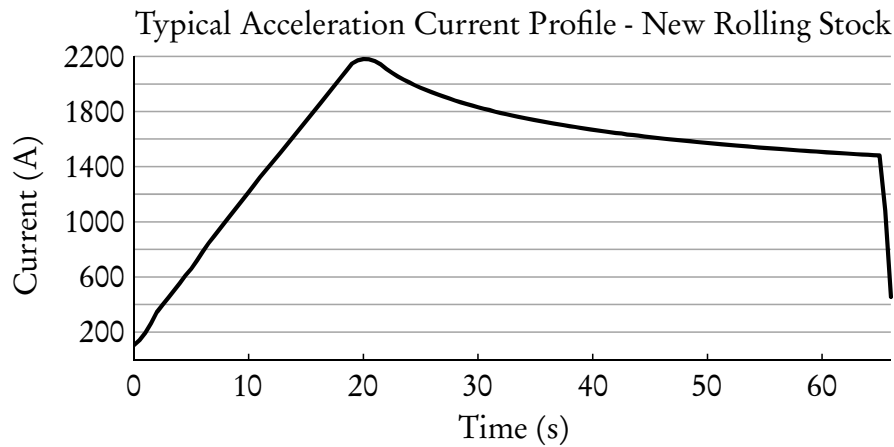


Figure 3.44: Total line current for a single module accelerating with an M3 load from standstill to 120 km/h and a pantograph voltage of 3 kV

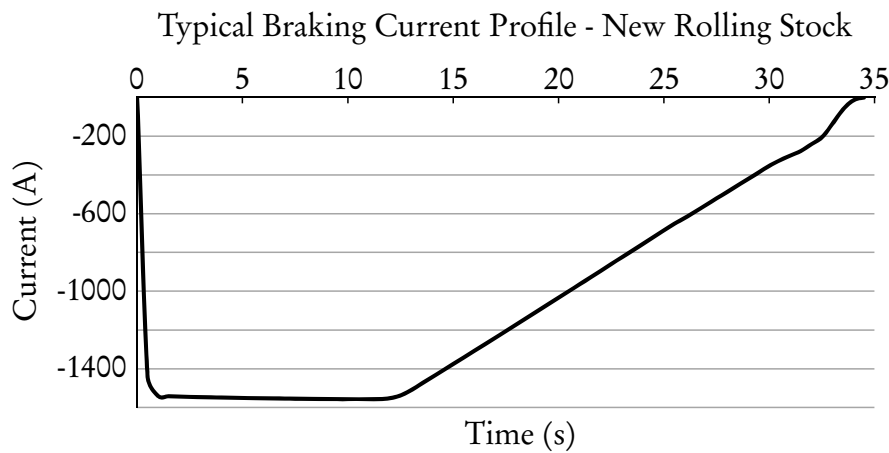


Figure 3.45: Regenerative braking current for a single module decelerating with an M3 load from 120 km/h to standstill and a pantograph voltage of 3,75 kV

their simulations [91]. For this model, only the section of the current profile (accelerating and braking) that are relevant to the specific trip are used. The first  $t_v$  seconds (acceleration duration) of the acceleration current profile is used. Similarly, the last  $t_s$  seconds (deceleration duration) of the braking current profile is used. The current demand during constant speed running is calculated using (3.1), the formula that was estimated in Section 3.3.2.

Express trains are treated similarly, but due to the high acceleration of this rolling stock, it will always finish accelerating before the next station is reached. These trains accelerate to the speed necessary to reach the next station at the specified time (without stopping) and then continue at constant speed. If the train

is already moving (accelerated during a previous iteration of the algorithm), the current demand is based on the speed that must be maintained to reach the next station at the specified time (with or without stopping), irrespective of the speed that the train is already travelling at.

The amount of modules that will be utilised per train is based on the train numbers. All modules will initially consist of six coaches. One module will be equal in length to seven coaches of the current rolling stock. The assumption is made that all trains currently operated by eight coach trains will in future be operated by a single module and that all trains that are currently longer than eight coaches will be operated by two modules. No simulation data was available for M1 loading (empty coaches), so it was regarded as a standard, M3 loaded train.<sup>23</sup> The train number prefix is again used to determine the factor with which the current demand (acceleration, constant speed and braking) will be adjusted. A summary of the prefixes and factor used is provided in Table 3.26.

The processing algorithm calculates what the current profile should look like for each second of the journey. It then divides this value between the two current sources applicable to the journey according to the relative displacement function. These values are summed<sup>24</sup> to the values already assigned to the current sources for the specific time period.

Figure 3.46 gives an example of the current demand calculated for a journey between two stations. The distance between the stations is 1,845 km. The timetable allows 120 s to complete the journey, but with the 5 % reduction, it will complete the journey in 114 s. The processing algorithm calculated that 27 s will be spent accelerating up to a maximum speed of 74 km/h. To maintain this speed a constant

Table 3.26: Loading factors (amount of modules) used for different train number prefixes

Route and Service Type	Prefix	Loading Factor
Southern	00, 01, 02	1
Cape Flats	05, 07	1
Northern Express	27	1
Monte Vista Normal	28	1
North Rest	08, 23, 25, 32, 34, 35	2
Central	90, 91, 92, 93, 94, 95, 97, 98, 99	2

<sup>23</sup>More information regarding this decision can be found in Appendix I.

<sup>24</sup>In line with the superposition principle, the system response to all trains is the sum of the individual trains.

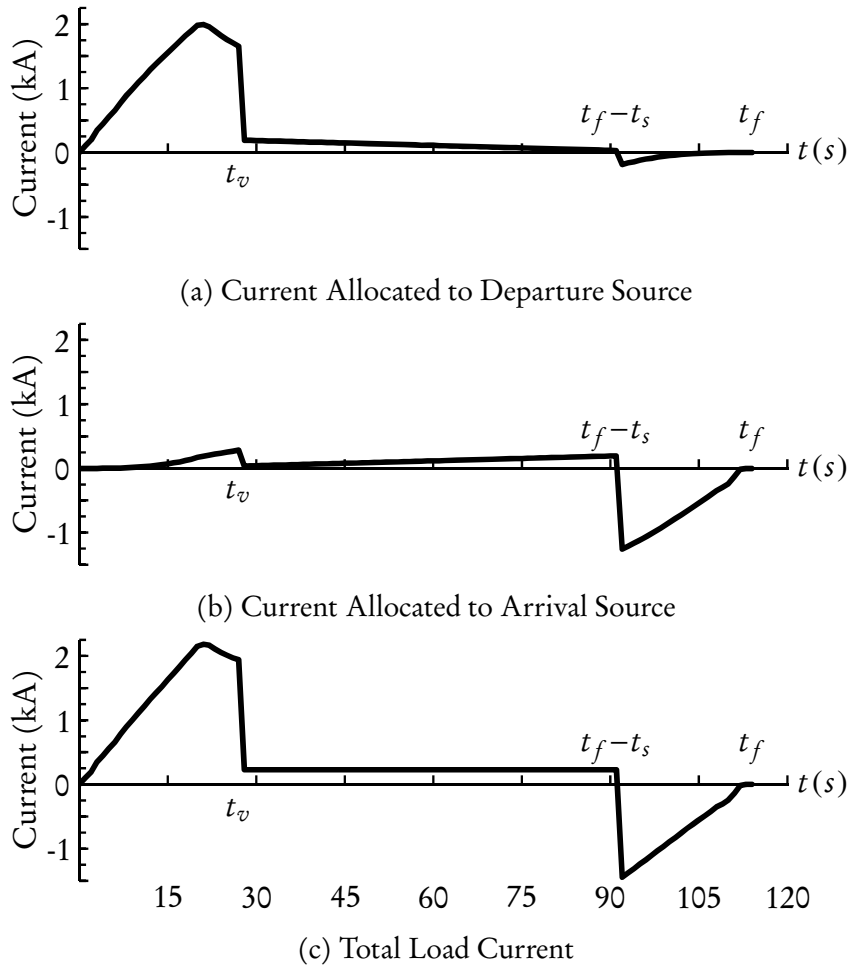


Figure 3.46: Current demand of a station-to-station journey

current of 228 A will be drawn. This speed will be sustained until deceleration will commence 23 s before arrival.

The total load current that will flow through the pantograph is shown in Figure 3.46c. Figure 3.46a shows the current that will be allocated to the current source at the departure station. It is large during acceleration and decreases as the train “moves” along the line. When braking commences, very little of the braking current is still allocated to this source.

Similarly, Figure 3.46b shows the current that will be allocated to the current source at the destination. The quadratic change in displacement during acceleration also causes a quadratic increase in the current. During the constant speed period, there is a linear change in the current allocated to each source. This is exactly what is expected and indicates that the processing algorithm works correctly.

## 3.6 Conclusion

In this chapter background on how to determine the capacity of an electrical traction network was provided. Various ways of simulating a moving train load was investigated and mathematically analysed. A method was devised on how this could be done in PowerFactory, the simulation package of choice for this project.

PowerFactory's lack of support for dynamic load movement along DC lines will be addressed by using two stationary current sources. The results of the investigation in Section 3.4.1 and 3.4.2 shows that the system response to a single train modelled as two stationary dynamic loads will be very similar to that of a single train modelled as a single, moving load. The relative displacement function, defined in Section 3.4.3, will be used to vary the amount of current allocated to each source. A source will be placed at every departure and arrival point.

Ways to model the present and future rolling stock were devised by taking each type's properties and abilities into consideration. A processing algorithm was developed to allocate the current or power values to each source for each second of the simulation based on the rolling stock and timetable.

# Chapter 4

## PowerFactory model

### 4.1 Introduction

The previous chapter explained how moving trains can be modelled using current profiles. It also explained how a Python algorithm is used to process the WTB and automatically determine the current profile for each station platform. This chapter will explain how a simulated model of the electrical network was constructed in DIGSILENT's PowerFactory. The CSV output of the processing algorithm is used as input for the PowerFactory simulation. The simulation output will be post-processed using Microsoft Excel in order to summarise the results for comparison of the different strategies. This process is illustrated in Figure 4.1.

As discussed in Chapter 2, DIGSILENT's PowerFactory was chosen as the simulation package for this project. As discussed in Section 2.4.2, it offers very good integration of AC and DC networks. Various power system components are included, negating the need to build anything from first principles.

Almost all element parameters can be assigned a time characteristic. This

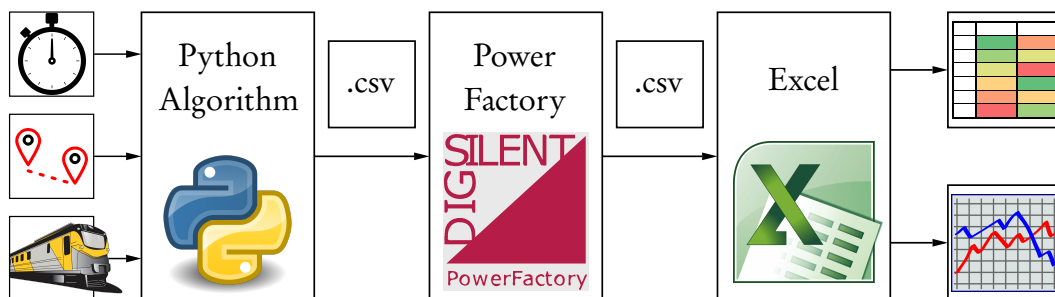


Figure 4.1: Flowdiagram of the simulation process

allows time dependant current or power values to be assigned to load elements. These values can be read in from a CSV file. Unfortunately PowerFactory does not offer the built-in functionality to change the position of a DC load element <sup>1</sup> quasi-dynamically. With the help of the Quasi-dynamic simulation tool a series of consecutive load flow calculations, considering different scenarios (such as passage of time), can be executed.

From this departure point, a detailed model of the AC and DC networks can be constructed in PowerFactory. The AC grid consists of all utility and council feeding points, the 33 kV ring-network and all substations. The model of each substation includes all circuit breakers, transformers, rectifiers, DC bus-bars and miscellaneous loads. The DC grid consists of all DC bus-bars (connected to AC grid), DC circuit breakers, tie stations, 3 kV transmission lines and DC loads. As explained in Section 3.4, all trains will be modelled as stationary dynamic current sources. In total the model contains almost 6500 objects.

The parameters that describe each element was sourced from a variety of technical documentation [81; 100], drawings [101; 102; 103; 104; 105], Prasa and Transnet technical officials [106; 107; 108; 109] and external consultants [110; 111]. When conflicting data was received, a value would be chosen based on the date, source credibility and data value. When no data could be sourced, a value was determined from another element with similar specifications.

## 4.2 AC grid

The AC grid modelled in PowerFactory consists of three main components: high voltage AC supply points, the 33 kV ring-network and all substations. Each of these will be described in more detail in the subsections that follow. An outline of the network in its normal state [101] and as it is modelled in PowerFactory is shown in Figure 4.2. The colours represent the cross section of the transmission line conductors.

### 4.2.1 Supply Points

The substations that form part of the network under review are supplied with high voltage AC electric power either via Prasa's private AC ring-network or

---

<sup>1</sup>This includes all types of elements that can act as a load on a DC network, including Current Sources (ElmDci) and the General Load element (ElmLod).

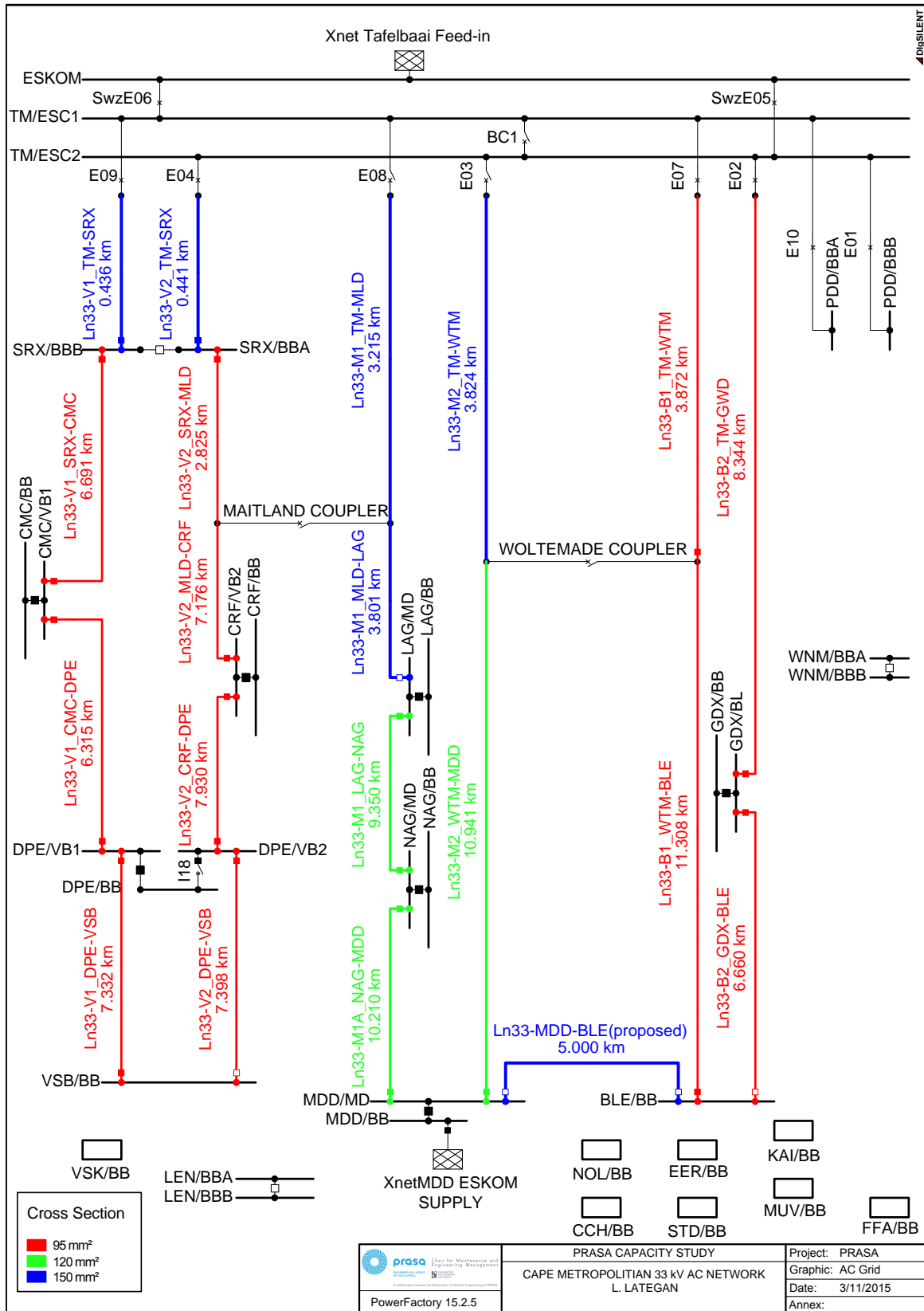


Figure 4.2: AC network, as modelled in PowerFactory

directly from the national, Eskom, grid or the Cape City Council's sub-grid. The 33 kV ring-network is supplied by Eskom at two locations: the primary feed at Traction Main (close to Paardeneiland) and a secondary feed at Modderdamweg (close to Belhar). Six substations are directly supplied by Eskom at 33 kV or 66 kV. Three are owned and operated by Prasa and another three by Transnet. The three Transnet substations are included in the model, because they directly supply Prasa owned lines or are adjacent to Prasa substations. Provision has been made for an additional Eskom supplied substation at Chris Hani, but at the time of this study, it was not yet in use. Two substations are supplied through the council's 11 kV local network. A summary of the supply points and their Notified Maximum Demand (NMD) is shown in Table 4.1.

The supply points are modelled in PowerFactory by the external grid element (ElmXnet)<sup>2</sup>. For load flow purposes it is modelled as an SL (slack) bus, referenced to a local busbar. The external grid controls the voltage and angle of the reference busbar [112]. All supply points were modelled with the busbar they are connected to as reference, a voltage setpoint of 1 per unit (p.u.) and an angle of 0°. The NMD is not entered into PowerFactory, since it is a time-averaged value. It can be used during post-processing to determine if the supply points are operating within

Table 4.1: High voltage AC supply point parameters

Supplier	Substation	Voltage	NMD
Council	Lentegeur	11,66 kV	10 MVA <sup>3</sup>
	Vishoek	11,66 kV	3,5 MVA <sup>3</sup>
Eskom	Chris Hani	66 kV	5 MVA <sup>3 4</sup>
	Eersterivier	33 kV	5,5 MVA
	Modderdam	33 kV	40 MVA
	Nolungile	66 kV	5 MVA
	Strand	66 kV	4,5 MVA
	Traction Main	33 kV	60 MVA
Transnet	Kraaifontein	66 kV	5 MVA <sup>3</sup>
	Muldersvlei	66 kV	10 MVA <sup>3</sup>
	Windermere	33 kV	10 MVA <sup>3</sup>
Total notified demand			158,5 MVA <sup>5</sup>

<sup>2</sup>The value between parentheses refers to the PowerFactory object extension.

<sup>3</sup>Estimated based on Traction Transformer Rating

<sup>4</sup>Future supply point

<sup>5</sup>Including future supply point



their agreed-upon limits.

For the simulation output, the total active power, `m : Psum : bus1` in MW, and line-to-line voltage magnitude, `n : U1 : bus1` in kV, output variables were selected.<sup>6</sup>

## 4.2.2 Ring-network

Eleven substations are connected to Prasa's private AC distribution network. As mentioned in the previous section, it is supplied from the national power grid at two locations. The network form three rings: Bellville (30,184 km), False Bay (46,544 km) and Modderdam (41,341 km). The rings are normally not closed (complete), but can be remotely coupled together in a number of configurations for operational requirements. Additionally, Paardeneiland substation is supplied directly from Traction Main switching station. [81; 101]

The normal switching arrangement is shown in Figure 4.2. Closed couplers are indicated by solid boxes while normally open couplers are indicated by square outlines. The False Bay (left) and Bellville (right) rings are normally supplied from the Tafelbaai supply at Traction Main (TM). The Modderdam ring (center) is normally supplied from the Modderdam supply. Langa (LAG) is supplied via Nyanga (NAG) 19,56 km from the external supply while a direct line of 7,016 km is unused. No reasons could be supplied as to why this is the case and the alternative switching arrangement will be investigated.

Bellville substation (BLE) is supplied from Traction Main with a 15,18 km transmission line, but it is less than 5 km from the Modderdam supply. Bellville station is the second largest railway junction in the region (Cape Town station is the largest). Should the supply at Traction Main fail, Bellville substation would have to be supplied via 22,249 km of transmission line from Modderdam. The viability of an additional transmission line will be investigated.

Three different options are possible, as indicated on Figure 4.3. The most direct route, via Transnet owned land, will be 5 km long. Another possibility is to first follow the Prasa railway line and then continue along the rail reserve of a

---

<sup>6</sup>In this chapter, the values in typewriter font refer to the PowerFactory signal name.

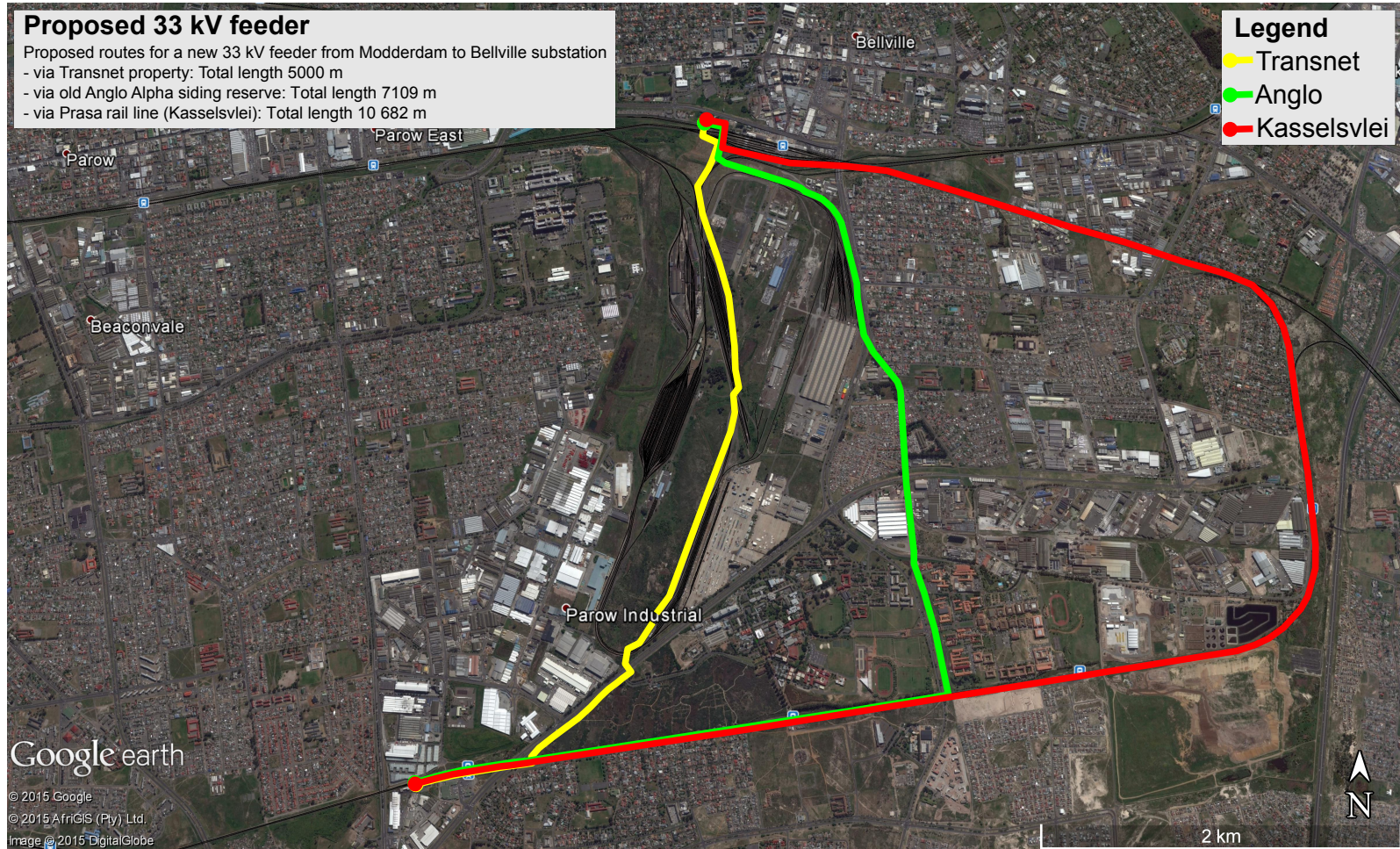


Figure 4.3: Proposed routes for a new 33 kV transmission line from Modderdam to Bellville substation

disused railway siding. This option does not need to cross as many active Transnet installations as the first one. The longest option is to follow the Prasa rail reserve all the way from Modderdam substation to Bellville via the Kasselsvlei junction. This route will be more than double the length of the first option, but still provide a shorter route than the current arrangement.

The transmission lines of the ring-network are modelled in PowerFactory as line elements (ElmLne) with a tower geometry type (TypGeo) equipment type. The three-phase conductors are specified as being fixed 1,3 m apart on 8 m high structures with a maximum conductor sag between structures of 0,6 m. Conductors are transposed according to the optimal arrangement. The conductors used are plain hard drawn copper (PHDC) conductors of 95 mm<sup>2</sup>, 120 mm<sup>2</sup> or 150 mm<sup>2</sup> cross section. Table 4.2 gives a summary of the parameters specified for each conductor type. Nominal Current refers to the continuous current rating of the conductor.

Table 4.2: 33 kV AC conductor parameters

Cross Section	Nominal Current	DC Resistance	GMR Equivalent Radius	Outer Diameter
95 mm <sup>2</sup>	0,387 kA	0,18 Ω/km	4,600 mm	12,7 mm
120 mm <sup>2</sup>	0,475 kA	0,12 Ω/km	6,063 mm	16,0 mm
150 mm <sup>2</sup>	0,427 kA	0,15 Ω/km	5,381 mm	14,2 mm

For the simulation output the output variables for loading, `c : loading` in %, and losses, `c : LOSSES` in kW, were selected. Loading refers to the percentage of the nominal root mean square (RMS) current flowing through the conductor.

### 4.2.3 Substations

Each substation typically consists of high voltage AC couplers and circuit breakers, traction transformer(s), traction rectifier(s), DC busbar, DC couplers and circuit breakers and an auxiliary transformer to supply the substation's own needs. In some cases there is also a transformer to feed the 11 kV signalling network. All of these components have been modelled in PowerFactory. A typical substation diagram, as produced by PowerFactory, is shown in Figure 4.4. Due to bugs in the PowerFactory software, two additional components had to be included in each substation model: a constant current source to model rectifier losses and a

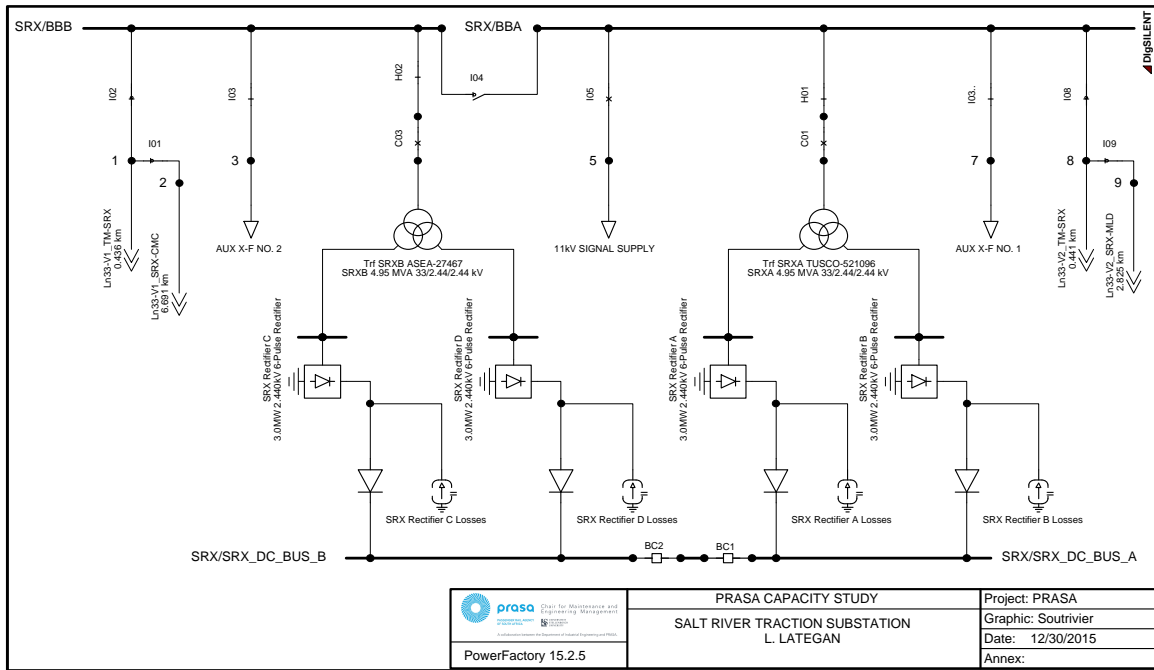


Figure 4.4: Soutrivier substation, as modelled in PowerFactory

diode at each rectifier output to ensure that the biasing of the rectifier diodes are correct. The following subsections describe the design choices that were made for the model in more detail.

#### 4.2.3.1 Couplers and Circuit Breakers

All AC couplers and circuit breakers are modelled as ideal switches (TypSwitch) with no losses and no current rating. The main reason for this design choice is that no information regarding the switches was available. Since the values are negligibly small, compared to the other components, this choice is deemed acceptable.

For the simulation output the total active power,  $m: P_{sum}: bus1$  in MW, and line-ground voltage magnitude,  $U: bus1$  in kV, were selected.

All DC circuit breakers that connect the DC bus with the individual overhead line sections are modelled as ideal switches (TypSwitch) with no losses, but with a current rating specified at 2,5 kA. The current rating is specified because there was a question regarding the ability of the existing switches to supply the high current requirement of the future rolling stock, both in powering and braking. The current rating is not used in the calculation of the load flow, but the value is used to calculate the loading of the switch.

For the simulation output the loading, `c : loading` in %, total active power, `m : Psum : bus 1` in MW, and line-ground voltage magnitude, `n : U : bus 1` in kV, were selected. Loading refers to the percentage of the DC current rating flowing through the switch.

#### 4.2.3.2 Transformers and Rectifiers

Traction transformers and diode rectifiers form the interface between the AC and DC networks. All of the transformers that form part of this study have at least three windings, one primary for the high voltage AC input and two secondary windings for low voltage AC output. The secondary outputs are connected to the traction rectifiers. Some transformers also have an additional auxiliary winding to supply electric light and power for the substation.

PowerFactory supports a variety of different transformers, including: 2- and 3-winding transformers, auto-transformers and booster transformers [113, app. C.1]. It also supports current and voltage transformers to simulate protection schemes [113, chap. 40].

**The PowerFactory rectifier element** There are two rectifier models available. They differ only in terms of the number of DC connections [113, app. C.3.2]. The first, `ElmRecmono`, has one AC and one positive DC terminal. The negative DC terminal is connected to ground, see Figure 4.5a. The second model, `ElmRec`, has one AC and two DC terminals, to allow the series connection of rectifiers, see Figure 4.5b. Internally, both models have a three-phase, six diode, full-wave rectifier, see Figure 4.6. The technical reference documentation shows the DC reactance,  $L_d$  but this reactance is not actually part of the model [114]. Both models can be configured to use thyristors, for a controlled rectifier or inverter.

The PowerFactory technical reference documentation describe the working of the diode rectifier as follows:

The diode rectifier is a full-bridge diode rectifier, which is rectifying

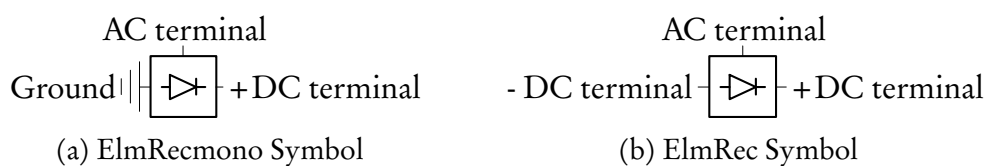


Figure 4.5: PowerFactory symbols of the two rectifier elements

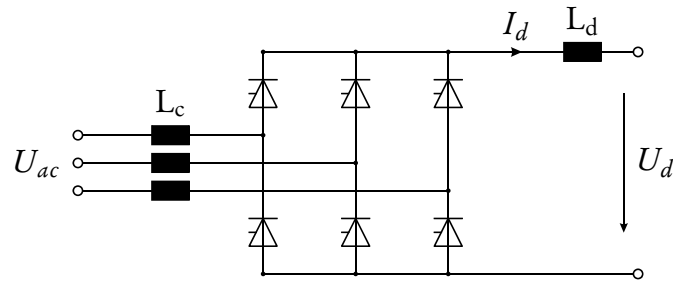


Figure 4.6: Detailed circuit of PowerFactory rectifier element with Commutation Reactance and DC Reactance (not part of the model), reproduced from [114]

the three-phase AC voltage to a 6-pulse DC voltage. Due to the usage of diodes, which can neither be turned-on or turned-off externally, the DC voltage or DC current of the rectifier cannot be controlled. [114]

The ideal DC output voltage,  $U_d$ , is defined as ( $U_{\phi\phi}$  denotes the phase-to-phase AC input voltage of the rectifier):

$$U_d = \frac{3\sqrt{2}}{\pi} U_{\phi\phi} \quad (4.1)$$

In real rectifiers, the commutation reactance of the transformer leads to a time delay between the transfer of the current from one diode to the next. This commutation leads to a drop in the DC output voltage,  $\Delta U_d$ , see Figure 4.7. The sign convention of the DC current,  $I_d$ , is an anomaly.<sup>7</sup> The DC output voltage of the rectifier can then be written as:

$$U_{dr} = U_d - \Delta U_d, \quad (4.2)$$

where  $\Delta U_d$  is defined as a function of  $I_d$  and the commutation reactance,  $X_c$ <sup>8</sup>:

$$\Delta U_d = -R_{cr} I_d = -\frac{3}{\pi} \omega L_c I_d = -\frac{3}{\pi} X_c I_d. \quad (4.3)$$

<sup>7</sup>The technical reference states “the DC current is negative for the rectifier operation due to the representation with load-orientation.” [114] PowerFactory uses “load-orientation” to determine the sign of the current and power. This means that a positively measured I, P or Q flows into the relevant element. This also explains why the “DC - Current Source” consumes energy when a positive current setpoint value is entered. It is unclear why Figure 4.6 does not also follow this convention.

<sup>8</sup>In the Parameter Definitions section of [114, app. A] and PowerFactory itself, the parameter Xd is described as the “Converter Transformer: Commutation Reactance” with the unit Ohm. When no converter transformer is used, the commutation reactance is still an active field, with parameter name Xd, and the value is used during load flow calculations.

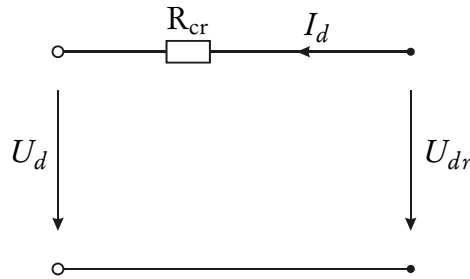


Figure 4.7: Equivalent rectifier element circuit with commutation reactance  $R_{cr}$ , reproduced from [114]

The rectifier element can be configured to include a built-in converter transformer or it can be connected to an external transformer. The built-in transformer features a tap-changer on the HV side to control the secondary voltage that is used for rectifier input. The commutation reactance is always assumed to be on the secondary side of the transformer. The following formula for  $X_c$  is provided: [114]

$$X_c = \frac{u_{kr}}{100\%} \frac{U_{r,sec}^2}{S_r} \quad (4.4)$$

It is understood that  $u_{kr}$  refers to the short circuit impedance of the transformer,  $U_{r,sec}$  the rated secondary voltage of the transformer and  $S_r$  the rated apparent power. The technical reference documentation states:

If an external transformer is used for the converter model, the AC voltage drop over the transformer is estimated using the commutation reactance specified. Here the model is not able to calculate the AC voltage directly from the parameters given. When the parameters specified in the external transformer and in the rectifier fit together, the same results are obtained as with the built-in transformer. [114]

No equation is provided to define how the AC voltage drop over the transformer is estimated. It is also not clear what is meant by “fit together”, since the same output voltage could not be achieved by testing the two arrangements in a small test project in PowerFactory.

Some of the older transformers that is used on this network contain a commutating reactance value, in Ohm, on their nameplate in addition to an impedance value, in %. It is unknown if this value was determined through measurement after installation or through calculation. Four transformers have known commutation reactance values. Table 4.3 shows these values and the corresponding values that was calculated by using (4.4). There is no clear relation between the known and

Table 4.3: Known and calculated commutation reactance values

Transformer	$X_c$ known	$U_{r,sec}$	$S_r$	$u_{kr}$	$X_c$ calculated
CMC-A	0,230 $\Omega$	2420 V	2831 kW	5,72 %	0,118 $\Omega$
CMC-B	0,232 $\Omega$	2420 V	2831 kW	5,60 %	0,116 $\Omega$
GWD-A	0,223 $\Omega$	2420 V	2831 kW	6,00 %	0,124 $\Omega$
VSB-A	0,228 $\Omega$	2420 V	2831 kW	6,05 %	0,125 $\Omega$

calculated values. The average value of the known values is 0,228  $\Omega$ .

The circuit in Figure 4.8 was used to further investigate the relationship between the input and output voltage of the rectifier element and the role of the commutation reactance. The parameters of transformer GWD-A was used as example. Five scenarios were investigated. The results and a description of the five scenarios are shown in Table 4.4 on page 117.

The load current for the investigation was based on the reference voltages for low and full loading. [115] states that a traction transformer's tap switch "should always be left in a position to give a low (100 A) load voltage of about 3150 V (or a full load voltage of 3000 V) [or, if not obtainable, a] position giving a DC voltage as close as possible to this value." The full load rating of GWD-A is 3,5 MVA, so that the full load DC current can be calculated as:

$$I_{DC} = \frac{P_r}{U_{fl}} = \frac{3\,500\,000\text{ VA}}{3000\text{ V}} \approx 1166\text{ A} \quad (4.5)$$

The five scenarios were evaluated twice, first with the low load current and then with the full load current from (4.5). The Theoretical Output column of Table 4.4

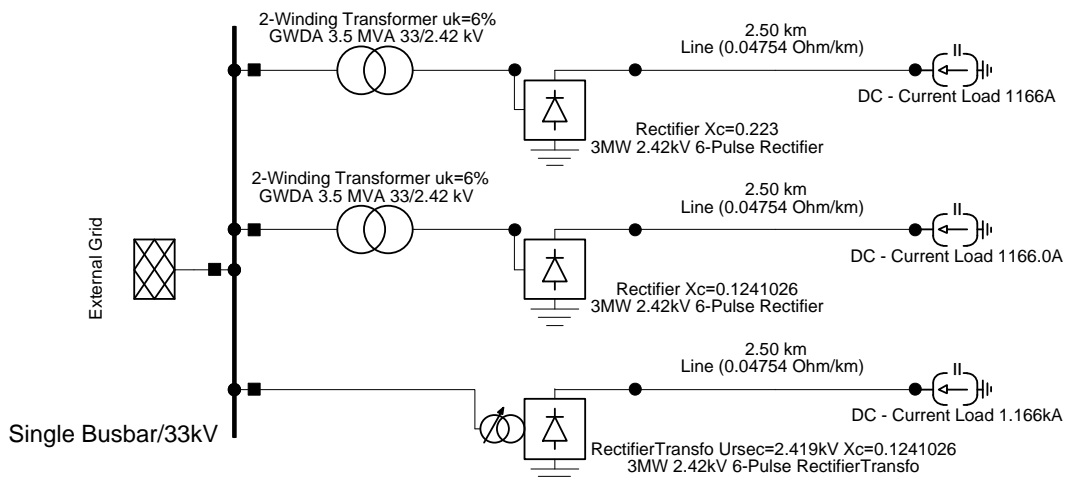


Figure 4.8: Commutation reactance investigation test circuit



gives the values that were calculated using the equations discussed earlier in this subsection:  $U_d$  refers to the ideal DC output voltage of the rectifier, calculated using (4.1);  $\Delta U_d$  refers to the drop in DC output voltage, calculated using (4.3); and  $U_{dr}$  refers to the theoretical DC output voltage of the rectifier, calculated using (4.2). The column  $\Delta U_{dr}$  gives the difference between the value of  $U_{dr}$  that was measured and the calculated value.

The measured and theoretical values are equal only when no  $X_c$  value is specified (scenario 2) or when an internal transformer is used (scenario 5). When the parameters fit together (scenario 3), the same results (Power and  $U_{dr}$  at rectifier output) are not obtained, especially at full load. In scenario 3 and 4 the same  $X_c$  value is specified, but the impedance of the external transformer in scenario 4 is almost 0%. In this case, the measured  $U_{dr}$  values differ quite significantly, but  $\Delta U_{dr}$  is almost exactly the same. This indicates that the real  $\Delta U_d$  value was also the same: 1,74 V for low load and 61 V for full load. This value is not equal to the  $\Delta U_d$  value that was used in scenario 5, even though  $I_d$  and the rectifier models were exactly the same, bar the use of an internal transformer. This indicates that the model is not behaving according to what is understood from the technical reference documentation.

The measured rectifier output voltage,  $U_{dr}$ , is shown in Table 4.4. The values for all scenarios are much higher than the reference voltages. The measured output for the scenarios that utilise the calculated commutation reactance is very high, even at full load conditions. The output voltage values of scenario 1 are deemed more realistic.

Similar results were obtained when the other three transformers with a known commutation reactance were investigated. Consequently, it was decided to use the average value of the known reactances, 0,228  $\Omega$ , for all rectifiers in the simulation model. Where rectifiers are connected in series, a value of 0,114  $\Omega$  will be used.

Table 4.4: Commutation reactance investigation results

#	Transfo Input		Transfo Out / Rect In			Rectifier Output			Theoretical Output			Total	
	Current	Power	Current	Power	$U_{LL}$	$-I_d$	Power	$U_{dr}$	$U_d$	$\Delta U_d$	$U_{dr}$	Losses	$\Delta U_{dr}$
1	5,796 A	328,5 kW	77,913 A	324,7 kW	2416,9 V	100 A	324,7 kW	3246,8 V	3264,0 V	21,3 V	3242,7 V	3,855 kW	4,1 V
2	5,785 A	330,4 kW	77,970 A	326,6 kW	2418,2 V	100 A	326,6 kW	3265,7 V	3265,7 V	0,0 V	3265,7 V	3,857 kW	0,0 V
3	5,795 A	329,3 kW	77,938 A	325,4 kW	2417,2 V	100 A	325,4 kW	3254,2 V	3264,4 V	11,9 V	3252,5 V	3,855 kW	1,7 V
4	5,795 A	329,5 kW	77,938 A	325,6 kW	2418,6 V	100 A	325,6 kW	3256,2 V	3266,3 V	11,9 V	3254,5 V	3,858 kW	1,7 V
5	5,715 A	325,6 kW	n/a	n/a	2420,0 V	100 A	325,6 kW	3256,3 V	3268,1 V	11,9 V	3256,3 V	0,000 kW	0,0 V
1	66,201 A	3623,0 kW	901,39 A	3595 kW	2364,3 V	1166 A	3595 kW	3083,1 V	3193,0 V	248 V	2944,7 V	28,10 kW	138 V
2	66,733 A	3805,6 kW	909,13 A	3777 kW	2398,6 V	1166 A	3777 kW	3239,3 V	3239,3 V	0 V	3239,3 V	28,56 kW	0 V
3	66,445 A	3669,0 kW	904,78 A	3641 kW	2368,9 V	1166 A	3641 kW	3122,4 V	3199,1 V	138 V	3060,9 V	28,29 kW	62 V
4	66,452 A	3724,9 kW	904,84 A	3697 kW	2404,6 V	1166 A	3697 kW	3170,3 V	3247,3 V	138 V	3109,1 V	28,35 kW	61 V
5	66,351 A	3649,5 kW	n/a	n/a	2420,0 V	1166 A	3650 kW	3130,0 V	3268,1 V	138 V	3130,0 V	0,000 kW	0,0 V

Let  $u_{kr}$  refer to the short-circuit voltage (short-circuit impedance) entered into the 2-winding transformer type data page and  $X_c$  refer to the commutation reactance entered into the rectifier element data page, then # denotes the following setup:

1. External transformer with  $u_{kr} = 6,0\%$  and  $X_c = 0,223\ \Omega$  (Figure 4.8: top circuit)
2. External transformer with  $u_{kr} = 6,0\%$  and  $X_c = 0\ \Omega$  (not shown)
3. External transformer with  $u_{kr} = 6,0\%$  and  $X_c = 0,124\ 102\ 6\ \Omega$  (Figure 4.8: middle circuit)
4. External transformer with  $u_{kr} = 0,6\%$  and  $X_c = 0,124\ 102\ 6\ \Omega$  (not shown)
5. Internal transformer only with  $X_c = 0,124\ 102\ 6\ \Omega$  (Figure 4.8: bottom circuit)

**Rectifier topologies** The previous part highlighted the fact that PowerFactory only makes provision for a full-bridge, six pulse rectifier. It also mentioned that two six-pulse elements can be connected in series. This is done to realise a 12-pulse rectifier that delivers a DC output with less ripple. There are four basic rectifier topologies that is used on the network under investigation:

1. Two three-phase half-wave rectifiers in series
2. Two three-phase half-wave rectifiers in parallel
3. Two three-phase full-wave rectifiers in series
4. Two three-phase full-wave rectifiers in parallel

Because PowerFactory does not contain a half-wave rectifier element, transformer-rectifier pairs that utilise a half-wave rectifier topology will have to be converted to an equivalent full-wave rectifier topology. Each topology and how it was implemented in PowerFactory will be discussed in the following paragraphs.

**A three-phase half-wave rectifier** is shown in Figure 4.9. Let the input voltage be a balanced, three-phase source, with the sinusoidal voltage wave form of each phase separated by  $120^\circ$  or  $2\pi/3$  radians. Because the three phases are connected in parallel, only the phase with the largest voltage will be active at any moment in time. Consequently, each phase will contribute one voltage pulse over a period of  $2\pi$  radians.

In order to calculate the ideal average DC output voltage,  $U_d$ , the circuit in Figure 4.9 is simplified to only represent the period  $[-\frac{\pi}{3}, \frac{\pi}{3}]$  (one voltage pulse), as

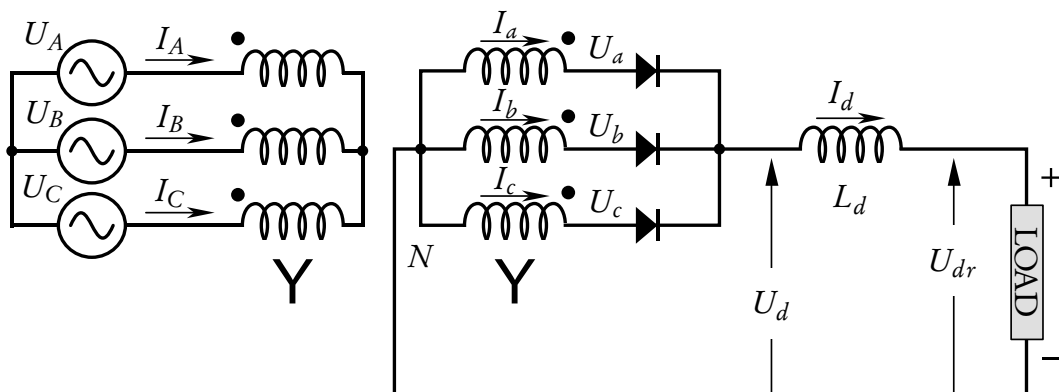


Figure 4.9: Three-phase half-wave rectifier, adapted from [116]

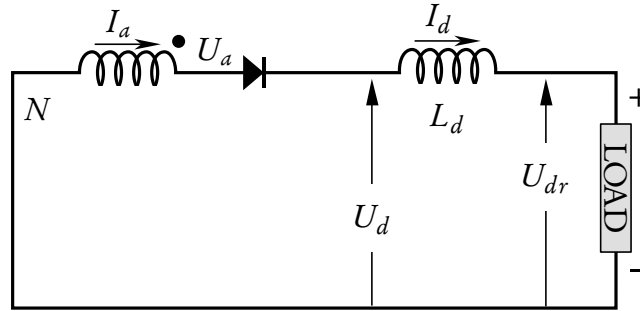


Figure 4.10: Three-phase half-wave rectifier equivalent circuit for one voltage pulse period, adapted from [116]

shown in Figure 4.10. When a phase is active, its diode is forward biased, the full secondary phase-to-neutral voltage is applied across the load.

With the secondary phase-to-neutral peak voltage,  $U_{\phi N}^{max}$ , its RMS value,  $U_{\phi N}^{rms}$ , and the angular frequency of the power supply,  $\omega$ ,  $U_d$  is calculated as:

$$U_d = \frac{U_{\phi N}^{max}}{\frac{2}{3}\pi} \int_{-\frac{\pi}{3}}^{\frac{\pi}{3}} \cos \omega t \, d\omega t \quad (4.6)$$

$$= U_{\phi N}^{max} \frac{\sin \frac{\pi}{3}}{\frac{\pi}{3}} \quad (4.7)$$

$$= U_{\phi N}^{max} \frac{3\sqrt{3}}{2\pi} \quad (4.8)$$

$$= U_{\phi N}^{rms} \sqrt{2} \frac{3\sqrt{3}}{2\pi} = U_{\phi N}^{rms} \frac{3\sqrt{6}}{2\pi} \quad (4.9)$$

$$\approx 1,17 U_{\phi N}^{rms} \quad (4.10)$$

A **three-phase full-wave rectifier** is shown in Figure 4.11. Let the input voltage be a balanced, three-phase source, with the sinusoidal voltage wave form of each phase separated by  $120^\circ$  or  $2\pi/3$  radians. Two phases will have to be active simultaneously in order to create a closed current path. Each phase-to-phase combination will contribute two voltage pulses over a period of  $2\pi$  radians.

In order to calculate the average DC output voltage,  $U_d$ , the circuit in Figure 4.11 is simplified to only represent the period  $[-\frac{\pi}{6}, \frac{\pi}{6}]$  (one voltage pulse), as shown in Figure 4.12. When a phase group is active, one diode of each phase is forward biased, the full secondary phase-to-phase voltage is applied across the load. With the secondary phase-to-phase peak voltage,  $U_{\phi\phi}^{max}$ , its RMS value,  $U_{\phi\phi}^{rms}$ ,

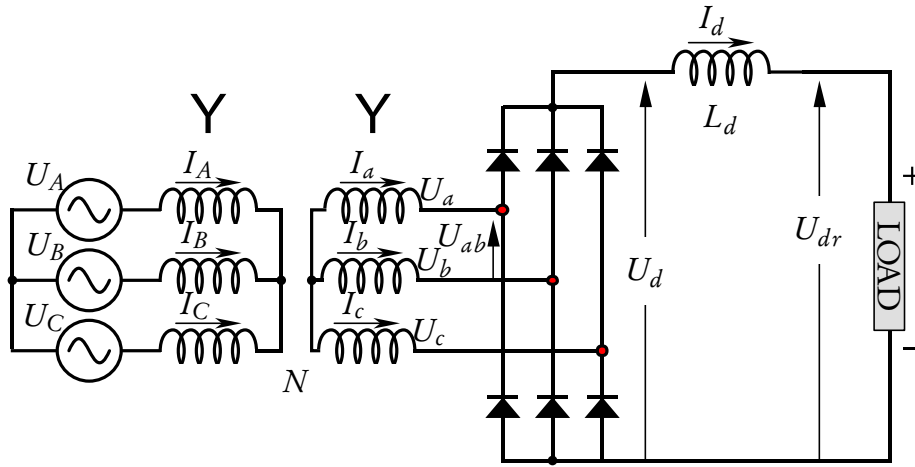


Figure 4.11: Three-phase full-wave rectifier, adapted from [116]

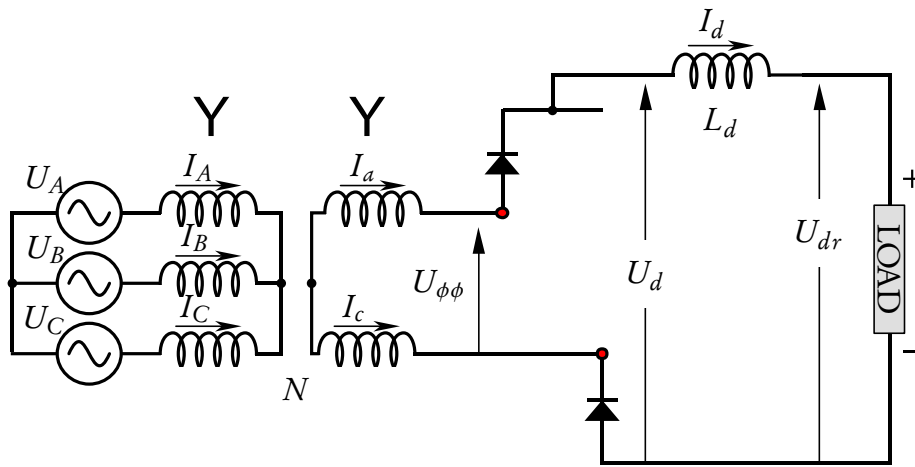


Figure 4.12: Three-phase full-wave rectifier equivalent circuit for one voltage pulse period, adapted from [116]

and the angular frequency of the power supply,  $\omega$ ,  $U_d$  is calculated as:

$$U_d = \frac{U_{\phi\phi}^{max}}{\frac{\pi}{3}} \int_{-\frac{\pi}{6}}^{\frac{\pi}{6}} \cos \omega t \, d\omega t \quad (4.11)$$

$$= U_{\phi\phi}^{max} \frac{\sin \frac{\pi}{6}}{\frac{\pi}{6}} \quad (4.12)$$

$$= U_{\phi\phi}^{max} \frac{3}{\pi} \quad (4.13)$$

$$= U_{\phi\phi}^{rms} \frac{3\sqrt{2}}{\pi} \approx 1,35 U_{\phi\phi}^{rms} \quad (4.14)$$

$$\text{and } = U_{\phi N}^{rms} \sqrt{3} \sqrt{2} \frac{3}{\pi} = U_{\phi N}^{rms} \frac{3\sqrt{6}}{\pi} \quad (4.15)$$

$$\approx 2,34 U_{\phi N}^{rms} \quad (4.16)$$

Two three-phase half-wave rectifiers in series are shown in Figure 4.13. It utilises a transformer with a star- or delta-connected three-phase primary and two star-connected three-phase secondaries. The two secondary windings have a phase difference of  $180^\circ$ . Each three-phase secondary winding is connected to a three pulse half-wave rectifier. The two half-wave rectifiers are connected in series to form the equivalent of one three-phase six pulse full-wave rectifier. Each half-wave rectifier contributes three voltage pulses over a period of  $2\pi$  radians.

The average output voltage of the rectifier can be calculated as the sum of the average output voltage of the individual half-wave rectifiers. If it is accepted that the voltage magnitude of all secondary windings are equal, then the total average DC output voltage,  $U_d$ , will be double the output voltage of a half-wave rectifier. From (4.9) it follows that  $U_d$  will be:

$$U_d = 2 \left( U_{\phi N}^{rms} \frac{3\sqrt{6}}{2\pi} \right) \quad (4.17)$$

$$= U_{\phi N}^{rms} \frac{3\sqrt{6}}{\pi} \quad (4.18)$$

$$\approx 2,34 U_{\phi N}^{rms} \quad (4.19)$$

$U_d$  for the two three-phase half-wave rectifiers in series is the same as the value that was calculated in (4.15) for a full-wave rectifier. This means that, in terms of DC output voltage, two three-phase half-wave rectifiers connected in series will be equal to a single three-phase full-wave rectifier. A three-winding transformer with

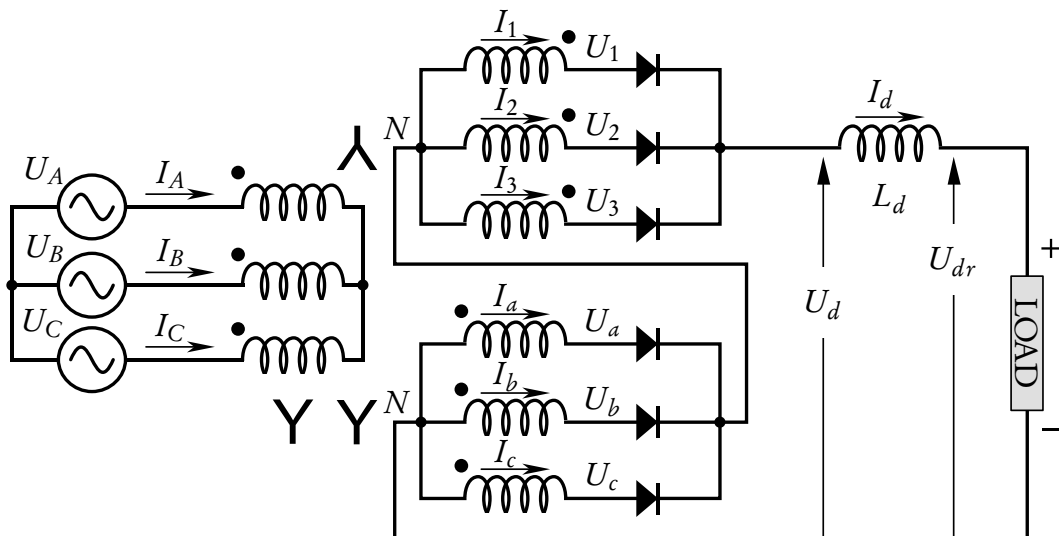


Figure 4.13: Two three-phase half-wave rectifiers in series, adapted from [116]

two three-phase half-wave rectifiers in series can be modelled in PowerFactory as a single two-winding transformer connected to a three-phase full-wave rectifier.

**Two three-phase half-wave rectifiers in parallel** are shown in Figure 4.14. It is also called a six-pulse or double star rectifier, since it utilises a transformer with a delta-connected three-phase primary and two star-connected three-phase secondaries. The two secondary windings have a phase difference of  $180^\circ$ . Each of the six secondary windings are connected to diode, forming a one-pulse rectifier. The six one-pulse rectifiers are connected in parallel. Each one-pulse rectifier contributes a single voltage pulse over a period of  $2\pi$  radians.

In order to calculate the average DC output voltage,  $U_d$ , the circuit in Figure 4.14 is simplified to only represent the period  $[-\frac{\pi}{6}, \frac{\pi}{6}]$  (one voltage pulse), as shown in Figure 4.10. When a phase is active, its diode is forward biased, the full secondary phase-to-neutral voltage is applied across the load. With the secondary phase-to-neutral peak voltage,  $U_{\phi N}^{max}$ , its RMS value,  $U_{\phi N}^{rms}$ , and the angular

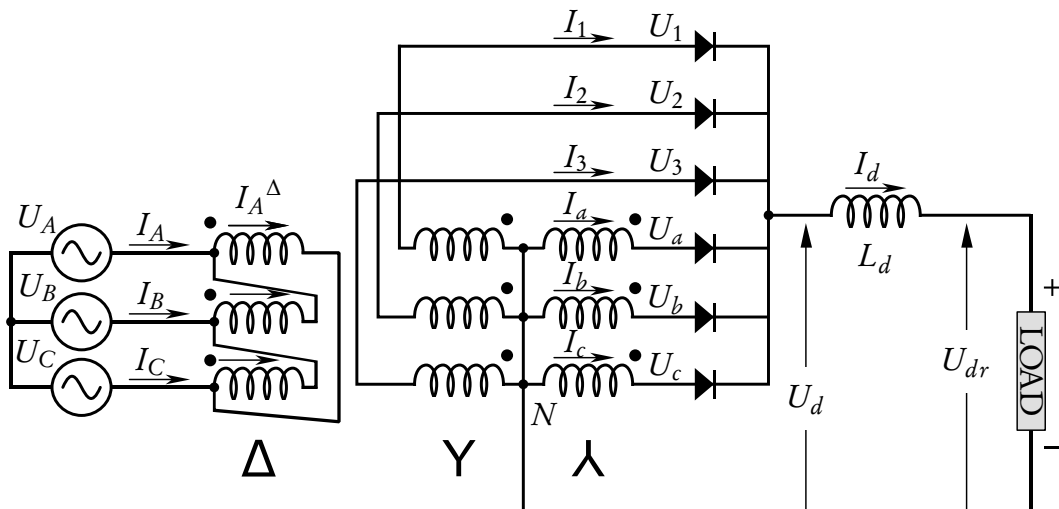


Figure 4.14: Two three-phase half-wave rectifiers in parallel, adapted from [116]

frequency of the power supply,  $\omega$ ,  $U_d$  is calculated as:

$$U_d = \frac{U_{\phi N}^{max}}{\frac{\pi}{3}} \int_{-\frac{\pi}{6}}^{\frac{\pi}{6}} \cos \omega t d\omega t \quad (4.20)$$

$$= U_{\phi N}^{max} \frac{\sin \frac{\pi}{6}}{\frac{\pi}{6}} \quad (4.21)$$

$$= U_{\phi N}^{max} \frac{3}{\pi} \quad (4.22)$$

$$= U_{\phi N}^{rms} \frac{3\sqrt{2}}{\pi} \approx 1,35 U_{\phi N}^{rms} \quad (4.23)$$

In (4.14) it was determined that for a three-phase full-wave rectifier  $U_d$  will be approximately  $1,35 U_{\phi\phi}^{rms}$ . From (4.23) it follows that  $U_d$  will be approximately  $1,35 U_{\phi N}^{rms}$ . This implies that no combination of three-phase full-wave rectifiers (in series or parallel) will be able to model two three-phase half-wave rectifiers connected in parallel.

For the PowerFactory model, it was decided to use the secondary phase-to-neutral voltage value of the real three-winding transformer as the phase-to-phase voltage value of a two-winding transformer model. This means that there is still a 1,35 multiplication factor between the transformer's rated "output" voltage and the rectifier's average DC output voltage.

**Two three-phase full-wave rectifiers in series** are shown in Figure 4.15. It utilises a transformer with a star-connected three-phase primary and two three-phase secondary windings, one connected in star and the other in delta. A three-phase full-wave rectifier is connected to each three-phase secondary winding. The two full-wave rectifiers are connected in series. Twelve-pulse operation is obtained with a  $30^\circ$  phase-shift between the two secondary windings. By using superposition, it can be seen that the total average output voltage of the two full-wave rectifiers will be the sum of the individual average output voltages. The output voltage of both full-wave rectifiers can be calculated by using (4.14) to yield the total average output voltage,  $U_d$ :

$$U_d = U_{\phi\phi}^{rms} \frac{3\sqrt{2}}{\pi} + U_{\phi\phi}^{rms} \frac{3\sqrt{2}}{\pi} \quad (4.24)$$

$$U_d = U_{\phi\phi}^{rms} \frac{6\sqrt{2}}{\pi} \approx 2,70 U_{\phi\phi}^{rms} \quad (4.25)$$

$$(4.26)$$



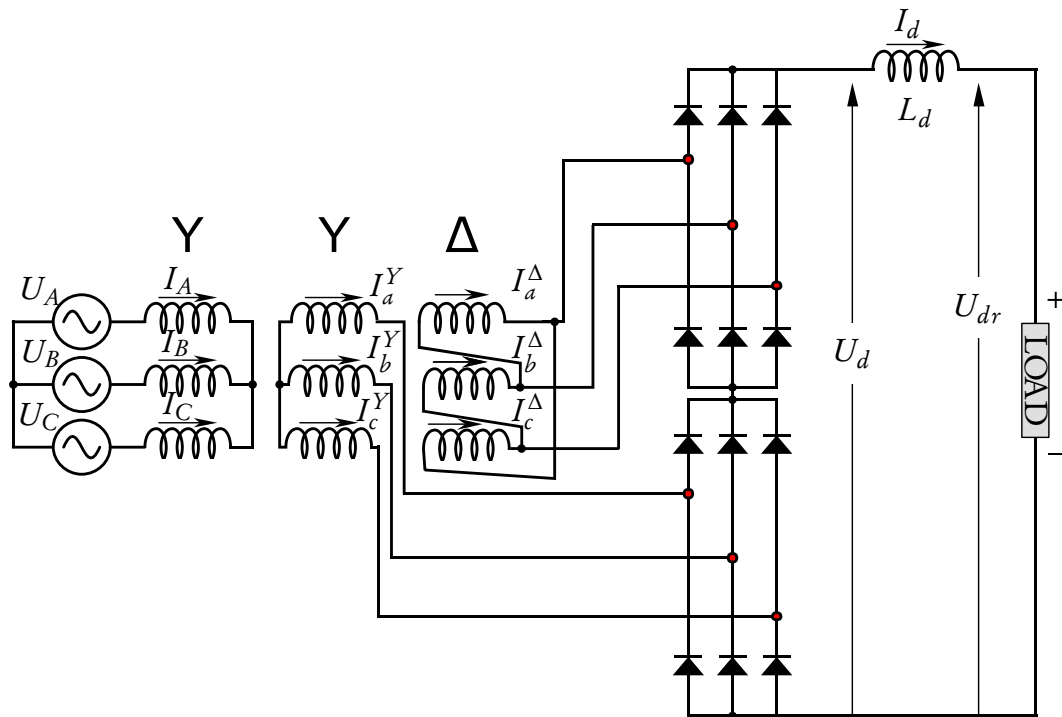


Figure 4.15: Two three-phase full-wave rectifiers in series, adapted from [116]

All the components required to model this rectifier topology is available in PowerFactory. As discussed in paragraph 4.2.3.2, a commutation reactance value of  $0,114 \Omega$  will be specified for each rectifier element.

**Two three-phase full-wave rectifiers in parallel** are shown in Figure 4.16. It utilises a transformer with a star-connected three-phase primary and two three-phase secondary windings, one connected in star and the other in delta. A three-phase full-wave rectifier is connected to each three-phase secondary winding. The two full-wave rectifiers are connected in parallel. The winding ratio of the secondary windings are calculated so that the phase-to-phase output voltages are equal. Twelve-pulse operation is obtained with a  $30^\circ$  phase-shift between the two secondary windings. The  $30^\circ$  phase-shift means that only two diodes will be conducting at a specific moment in time. The biasing will change every  $30^\circ$  ( $\pi/6$  radians). During each  $30^\circ$  period, say  $[-\frac{\pi}{12}, \frac{\pi}{12}]$ , the circuit will be similar to the diagram for a single voltage pulse of a three-phase full-wave rectifier that was shown in Figure 4.12. With the secondary phase-to-phase peak voltage,  $U_{\phi\phi}^{max}$ , its RMS value,  $U_{\phi\phi}^{rms}$ , and the angular frequency of the power supply,  $\omega$ ,  $U_d$  is

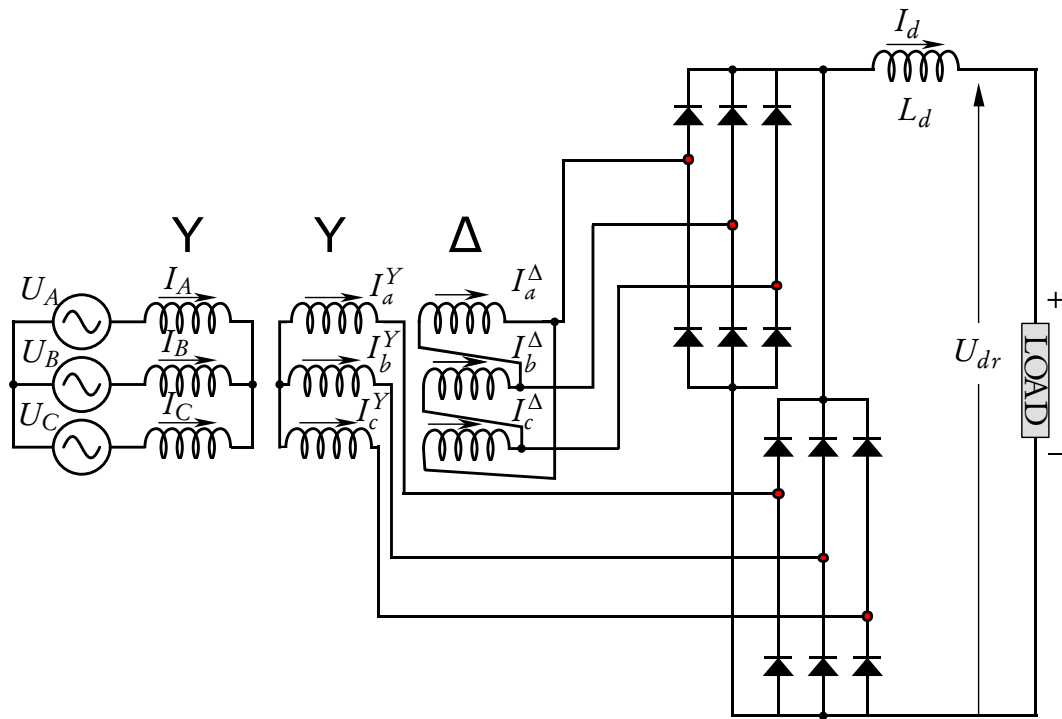


Figure 4.16: Two three-phase full-wave rectifiers in parallel, adapted from [116]

calculated as:

$$U_d = \frac{U_{\phi\phi}^{max}}{\frac{\pi}{6}} \int_{-\frac{\pi}{12}}^{\frac{\pi}{12}} \cos \omega t \, d\omega t \quad (4.27)$$

$$= U_{\phi\phi}^{max} \frac{\sin \frac{\pi}{12}}{\frac{\pi}{12}} \quad (4.28)$$

$$= U_{\phi\phi}^{max} \frac{12 \sqrt{3} - 1}{\pi \, 2\sqrt{2}} \quad (4.29)$$

$$= U_{\phi\phi}^{max} \frac{6\sqrt{3} - 6}{\pi \sqrt{2}} \quad (4.30)$$

$$= U_{\phi\phi}^{rms} \frac{6\sqrt{3} - 6}{\pi} \approx 1,398 U_{\phi\phi}^{rms} \quad (4.31)$$

The ideal average DC output voltage of two three-phase full-wave rectifiers in parallel that was calculated in (4.31) is slightly higher than the value for a single three-phase full-wave rectifier that was calculated in (4.14) ( $1,398 U_{\phi\phi}^{rms}$  vs.  $1,35 U_{\phi\phi}^{rms}$ ). These values correspond to what is given in [117, chap. 10.4].

The components that are necessary to model this rectifier topology in PowerFactory, three-winding transformer and two three-phase full-wave rectifier elements, are all available as standard. One can also specify the phase shift of the

secondary windings. Figure 4.17 shows a test circuit that was used to test the topology in PowerFactory. The three-winding transformer is defined with a Y0y0d1 topology, as required for 12-pulse operation. The load flow results shows that the phase-to-phase voltage at the secondary terminal of the transformer is 2,437 kV. From (4.31), the DC output voltage should be 3,407 kV. The DC output voltage calculated by PowerFactory, however, is 3,291 kV. This value is the value expected for a single three-phase full-wave rectifier (4.14):

$$2437 \frac{3\sqrt{2}}{\pi} = 3291 \quad (4.32)$$

This points to an error in the way PowerFactory use transformer phase shift to calculate the rectifier output voltage. There is only one substation on the network with this topology, namely Salt River. It has two three-winding transformers, each connected to a two three-phase full-wave rectifiers in parallel topology that normally feeds two separate DC buses, as shown in Figure 4.4. The rated secondary voltage for both of the transformers is 2,44 kV. If (4.31) is used, this implies a no-load DC output voltage of 3,411 kV, much higher than the voltage at most other substations of around 3,268 kV. If (4.14) is used, the ratio that PowerFactory uses, then a no-load DC output voltage of 3,295 kV is expected (as proved in the test above). It was felt that this value is more realistic, since in reality the transformer tap changers can be used to set the no-load voltage closer to that of the other substations. The total rated installed capacity of this substation is 12 MW,

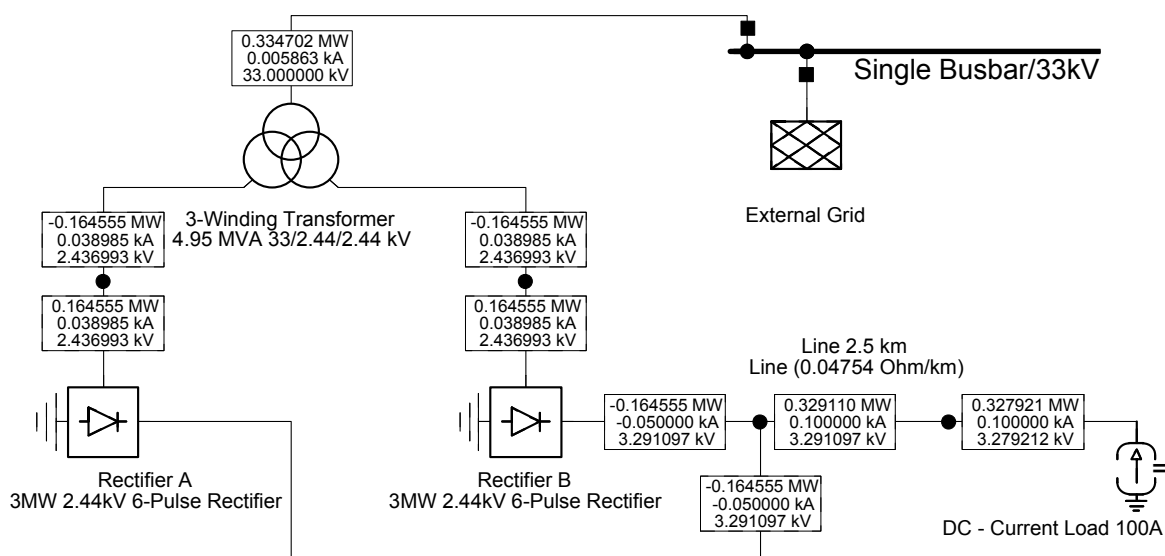


Figure 4.17: Two three-phase full-wave rectifiers in parallel test circuit

so a slightly higher no-load voltage, was also deemed acceptable. Consequently, all transformer parameter values, as indicated on the rating plate, was used in the PowerFactory model. A commutation reactance value of  $0,228 \Omega$  will be specified for each rectifier element.

For the simulation output the loading, `c : loading` in %, and total active power on HV side, `m : Psum : bushv` in MW, were selected. Loading refers to the percentage of the AC current rating flowing through the HV terminals.

### 4.2.3.3 Auxiliary Loads

Some substations have additional transformers to supply auxiliary equipment within the substation itself, for example battery chargers, or other external loads. Prasa owns and operates a private 11 kV AC network to supply its signalling system. This network covers a larger geographical area than the 33 kV ring-network. It is supplied from traction substations, including those connected to the ring-network, and local supply points connected to the national grid or municipal sub-grid. It allows for a high level of redundancy to maintain a high level of signalling power reliability. [118]

The 11 kV network is not part of the scope of this study. It does, however, demand a small, but nonetheless significant, load from the supply points and ring-network. This subtracts from the NMD available for traction purposes and adds to the loading of the ring-network's conductors.

A summary of the auxiliary equipment included in the simulation model is provided in Table 4.5. The "Auxiliary Load" column shows the component name, as indicated on the substation drawing. Power Rating refers to the nameplate capacity of the transformer. In PowerFactory, the auxiliary transformers are modelled as pure resistive general loads (ElmLod).

Due to the high level of redundancy, the auxiliary equipment will almost never operate continuously at full capacity. The scaling factor in PowerFactory is used to scale the active power operating point to a more realistic value. No data is available regarding the loading of individual auxiliary transformers. Royal Haskoning DHV used a scaling factor of 0,5 in their capacity study [110]. Their measurements of the power flow through the ring-network supply points during times of no, or very little, train traffic was compared with the total load that each supply point is supposed to supply. The results are shown in Table 4.6. For the Modderdam supply, only 23,4 % of the rated power was measured during periods with no traffic.

Table 4.5: Auxiliary AC load parameters

Substation Name	Auxiliary Load	Power Rating	Scaling Factor	Effective Load Power
Bellville	AUX X-F NO. 1	100 kW	0,45	45 kW
Bellville	AUX X-F NO. 2	100 kW	0,45	45 kW
Bellville	EL&P & SIG. X-F 33/11kV	2000 kW	0,45	900 kW
Bellville	SIG. SUPPLY X-F 33/2.2kV	80 kW	0,45	36 kW
Chris Hani	SIGNALS	1000 kW	0,44	440 kW
Crawford	AUX X-F NO. 1	100 kW	0,45	45 kW
Dieprivier	SIGNAL SUPPLY	500 kW	0,45	225 kW
Eersterivier	AUX X-F	100 kW	0,45	45 kW
Goodwood	AUX X-F NO. 1	100 kW	0,45	45 kW
Goodwood	AUX X-F NO. 2	100 kW	0,45	45 kW
Langa	SIGNALS	2000 kW	0,25	500 kW
Lentegeur	SIGNAL SUPPLY	2000 kW	0,45	900 kW
Modderdam	AUX X-F NO. 1	0,1 kW	0,25	0,025 kW
Nolungile	SIGNALS	1000 kW	0,45	450 kW
Nyanga	SIGNALS	500 kW	0,25	125 kW
Soutrivier	11kV SIGNAL SUPPLY	500 kW	0,45	225 kW
Soutrivier	AUX X-F NO. 1	100 kW	0,45	45 kW
Soutrivier	AUX X-F NO. 2	100 kW	0,45	45 kW
Valsbaai	AUX X-F NO1	100 kW	0,45	45 kW
Valsbaai	AUX X-F NO2	100 kW	0,45	45 kW
Vishoek	SIGNAL SUPPLY	500 kW	0,45	225 kW
Total load		11 080,1 kW		4476,025 kW

Table 4.6: Scaling of auxiliary AC loads

Supply Point	Total Power (rated)	Total Power (measured)	Loading Factor	Scaling Factor used
Modderdam	2500,1 kW	584 kW	0,234	0,25
Traction Main	3980 kW	1770 kW	0,445	0,45

At Traction Main, the power flowing during similar periods was 44,5 % of the rated capacity. The difference in loading is deemed acceptable, since the network is more dense in the parts that are supplied from Traction Main. Consequently, all auxiliary loads connected to Modderdam was scaled to 0,25, while all other loads were scaled to 0,45 of their rated power value.

No output variables were selected for the simulation output of the auxiliary loads.

#### 4.2.3.4 Reversible Substation

The ideal placement for an inverter unit, to feed regenerated energy back into the AC network, will be at one of the substations connected to the private 33 kV AC network. This is due to various regulatory and technical factors. Unfortunately the railway network is also very meshed around these substations and consequently very little regenerated energy is dissipated. To harness a meaningful amount of energy, that would otherwise be wasted, the reversible substation(s) would therefore need to be placed on the periphery of the system. This necessitates pushing energy into the national grid.

One substation was fitted with an ideal inverter to extract regenerated energy to the AC grid. Nolungile substation was chosen, because simulations showed that the section around this substation had the highest energy dissipation in the rheostats. A diagram of the substation, with inverting equipment, is shown in Figure 4.18.

The inverting equipment consists of an ideal pulse-width modulation (PWM) converter that maintains the DC-node voltage at 3,4 kV. The voltage is maintained by an ideal 1 F capacitor. Whenever the substation's DC bus voltage is above 3,4 kV the diode will conduct and the PWM converter will inject current into the substation's AC bus to maintain the DC-node voltage at the setpoint.

This substation is connected to the municipal 66 kV supply and not Prasa's own AC distribution network. It is envisaged that the inverter will mainly inject quite a large amount of energy for relatively short periods. It is unlikely that Prasa will be able to get permission to inject this inverted energy into the municipal supply. The railway network fed directly by Prasa's own AC distribution network is very meshed and it is envisaged that an inverting substation at a substation fed by this network will not be viable. More detail about the choice of location for the reversible substation is given in Section 4.2.3.4.

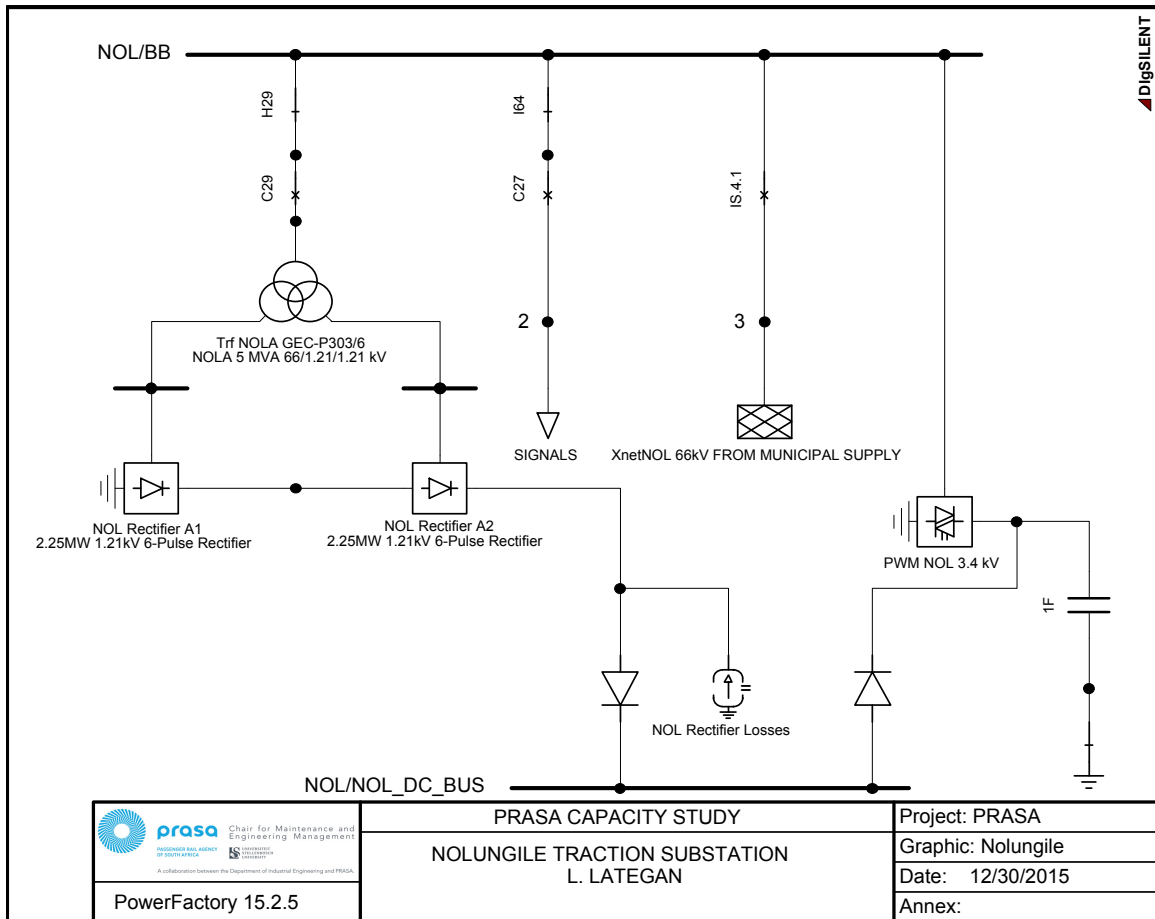


Figure 4.18: Nolungile substation, with inverting unit, as modelled in PowerFactory

For the simulation output the total active power on DC-side, m : Psum : busdc in MW, and line-ground voltage magnitude at the DC terminal, m : U1 : busdc in kV, were selected.

#### 4.2.3.5 Workarounds Required

DIgSILENT's PowerFactory version 15.2.5 was used to conduct the simulations. Various flaws were uncovered during the project. Some include problems with the Quasi-Dynamic tool, non-convergence when there is a net generation on the DC grid and issues with the rectifier element. With the help of DIgSILENT support, workarounds were found for most of the problems.

One of the workarounds that was necessary, was to model the rectifier losses with a constant current source. Issues with the biasing of the rectifiers were

overcome by placing a diode between the rectifier output and the DC busbar.

## 4.3 DC grid

The 3 kV DC grid modelled in PowerFactory represents the network layout of the traction conductors and busbars. Care was taken to model the distance and conductor type of each overhead line section correctly. The DC busbar of each substation is included in the DC grid to form the interface between the AC and DC networks. As discussed in Section 3.4, trains are modelled by placing a current source at each station platform. The DC grid alone consists of almost 2000 elements.

A diagram of the DC network, in its normal state [103] and as it is modelled in PowerFactory, is shown in Appendix J. The layout is based on the diagram in Appendix A.

### 4.3.1 Overhead lines

The DC conductors of the traction network consists of the overhead line and the rails that the train runs on. PowerFactory does not support current return conductors for the DC elements, only earth return. An equivalent resistance was calculated for each wire combination that also includes the resistance of the return rail.

Sections that are controlled by centralised traffic control (CTC) generally use only one rail for current return and the other for train detection. In these areas there are usually also multiple running lines in parallel. All the current return rails of parallel running lines are periodically connected in parallel, reducing the effective resistance of the current return. On single line sections, where there are no CTC, both rails are used for current return. The assumption was made that there will always be two rails in parallel available for current return. UIC C rail of 48 kg/m with a resistance of 0,0396  $\Omega$ /km was used throughout [104; 105].

Eight wire combinations are used on the network. Table 4.7 gives a summary of the parameters specified for each conductor type. Wire Combination refers to the cross-sections of the combination of conductors that make up the overhead line.



Table 4.7: Wire combinations used for DC network [104; 105]

Wire Combination	Continuous Current Rating	Total Resistance
161+100	0,9627 kA	0,088 28 $\Omega$ /km
161+100+160	1,2991 kA	0,070 55 $\Omega$ /km
161+100+250	1,5671 kA	0,061 84 $\Omega$ /km
161+100+500	1,5916 kA	0,050 12 $\Omega$ /km
161+160	1,1496 kA	0,076 42 $\Omega$ /km
161+160+250	1,7474 kA	0,057 05 $\Omega$ /km
161+160+500	1,7392 kA	0,047 54 $\Omega$ /km
161+250	1,2184 kA	0,063 14 $\Omega$ /km
161+250+800	2,0663 kA	0,038 66 $\Omega$ /km

For the simulation output the output variables for loading, `c : loading` in %, and losses, `c : Losses` in kW, were selected. Loading refers to the percentage of the nominal RMS current flowing through the conductor.

### 4.3.2 Train Representation

Each station platform contains three elements to model the trains' traction, regenerative braking and rheostatic braking. These are a current source, a power source and a diode connected to a communal constant voltage node. Figure 4.19 shows the graphical representation of this setup. The orange line represents the overhead line and the black dot the node to which the elements are connected to. PowerFactory does not put the node dot above other layers. The symbol labelled `DciNOLC1` represents the DC - Current Source element in PowerFactory

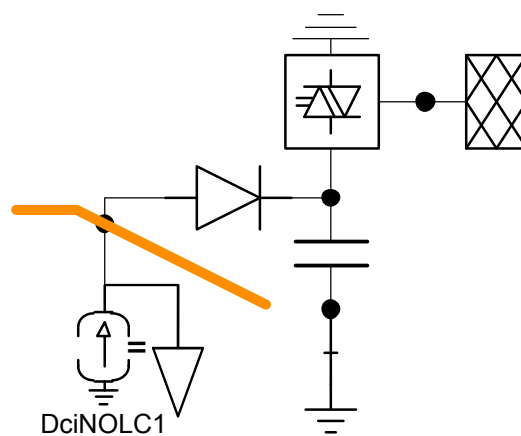


Figure 4.19: Model of a single node

(ElmDci). NOLC1 refers to the source placed at Nolungile station at the number 1 platform servicing the Central line. The triangle next to it represents the General Load element (ElmLod). This element is characterised by the active power flow defined for it and can be specified as a constant value or a time characteristic. The third element connected to the node is a diode or DC Valve as it is called in PowerFactory (ELMValve).

The cathode of the diode is connected to the positive terminal of a Series Capacitor (ElmScap)<sup>9</sup> and the DC output terminal of a PWM Converter (ElmVsc-mono). The technical reference documentation [119] for the PWM converter states, “The PWM converter model represents a self-commutated, voltage source AC/DC converter (with a capacitive DC-circuit included).” The caption given below Figure 4.20 reads “Equivalent Circuit, with DC-Capacitance (not part of the model)”. This implies that the capacitance is not really included in the model. This was tested and it was found that the external series capacitor is indeed necessary. The control condition of the PWM converter is set to  $V_{dc} \cdot \cos(\phi)$ . The DC Voltage Setpoint is set to 3750 V so that the DC node is controlled to the trains’ threshold voltage for rheostatic braking. Whenever the node voltage reaches the threshold voltage, the diode will be forward bias and surplus energy will be extracted by the converter. The extracted energy is injected into an imaginary external AC network with a power factor of 1.

The current source is linked to a time characteristic defining a current value that should be sunk from the node (positive setpoint) or injected into the node (negative setpoint), as calculated by the processing algorithm explained in Section 3.5. Initially both powering and braking will be represented by using a time-current characteristic. During further simulations regeneration will be modelled using a power source (general load element) with a time-power characteristic, as

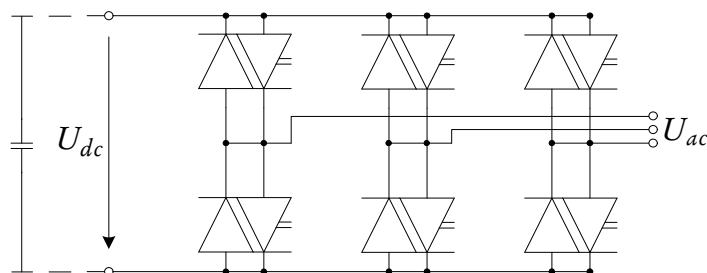


Figure 4.20: Equivalent Circuit of the PWM Converter, reproduced from [119]

<sup>9</sup>Ideal capacitor with a capacitance of 1 F.

mentioned in Section 3.3.2.2.

Due to space limitations, the power source is not included in the graphical representation. It is defined and connected to the appropriate node using PowerFactory's database manager. The same PWM converter, capacitor and external grid is used for all nodes. The diode is included in the graphical representation, but not the connection from the anode to the communal constant voltage node.

Different current sources are used in the up and down direction for trains running on single lines. This is to simplify the processing algorithm. Figure 4.21 shows an example of the graphical representation of such a node.

For the simulation output the following output variables were selected: current sources Total Active Power, m: Psum: bus1 in MW; general loads Total Active Power, m: Psum: bus1 in MW; DC valve Total Active Power, m: Psum: bus1 in MW, and Line-Ground Voltage, n:U: bus1 in V. Loading refers to the percentage of the nominal RMS current flowing through the conductor.

### 4.3.3 Substations and Ties

The DC busbars (ElmTerm) of substations and ties is the interface between the AC and DC grid, as explained in the chapter. Figure 4.22 shows how the graphical representation in PowerFactory looks like. No output variables are defined for these elements.

## 4.4 Load Flow Calculation Parameters

The following options were selected in PowerFactory when executing the load flow calculations:

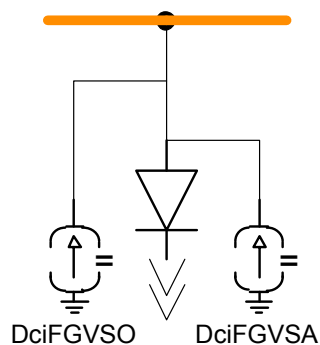


Figure 4.21: Model of a single node on a single line section

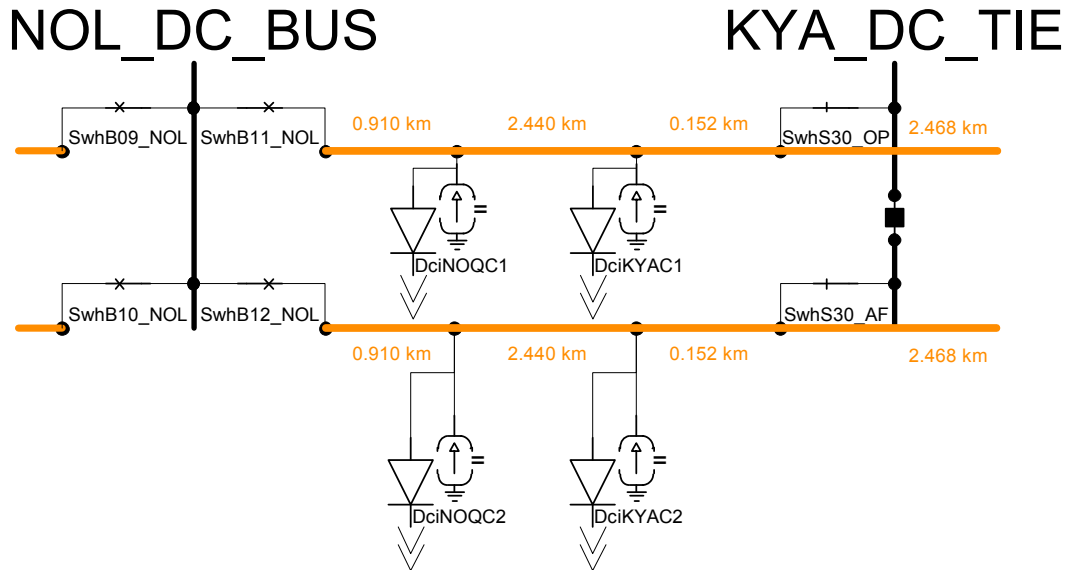


Figure 4.22: Model of substation and tie busbars

- Basic Options
  - Calculation Method: AC load flow, balanced, positive sequence
  - Reactive Power Control: no automatic tap adjust of transformers and no consideration of reactive power limits
  - Temperature Dependency: line/cable resistances = at 20 °C
  - Load Options: no consideration of voltage dependency of loads; no feeder load scaling
- Active Power Control
  - Active Power Control: as dispatched
  - Balancing: by reference machine
- Advanced Options
  - Load Flow Method: Newton-Raphson (current equations)
  - Load Flow Initialisation: no topology rebuild; initialisation (flat-start); consideration of transformer winding ratio
  - Tap Adjustment: Method = direct; minimum controller relaxation factor = 1
  - Station Controller: standard
  - Modelling Method of Towers: equation in lines

- Do not use this load flow for initialisation of OPF
- Iteration Control
  - Max. Number of Iterations for: Newton-Raphson iteration = 1000; outer loop = 5000; number of steps = 5
  - Max Acceptable Load Flow Error for: nodes = 1 kVA; model equations = 0,1 %
  - Convergence Options: automatic adaption of iteration step size
  - Automatic Model Adaptation for Convergence
  - Settings - Automatic step size: trim unreasonable Newton-Raphson steps and break if no progress in 10 000 iterations
- Outputs
  - Show 'Outer Loop' messages
  - Show Convergence Progress Report and report on 3 buses/models per iteration
  - Do not show Verification Report
  - Check Control Conditions for: generator, transformer, shunt and SVC station controller, tap-controller, others
- Advanced Simulation Options: consider protection devices = none

A step size of 1 s or  $2,777 \times 10^{-4}$  h was used. This means that each simulation contained data for 75 601 s and 1741 output variables, a total of 131 621 341 output values per simulation.

## 4.5 Conclusion

In this chapter it was explained how the AC and DC electrical networks was modelled in PowerFactory. All of the supply points, transmission network, substations, overhead line and trains have been modelled. The parameters have been defined for the load flow calculation.

# Chapter 5

## Results

### 5.1 Introduction

This chapter will describe the simulations that were executed using PowerFactory. The model is first benchmarked against actual measurements. Once the model is proven to be a valid representation of the actual network, different scenarios will be presented. These will indicate how the energy use of the new rolling stock compares with the present rolling stock. Various alterations and improvements to the network will be investigated and discussed.

### 5.2 Benchmarking the Model

Before using the model to do any predictions it was validated by benchmarking simulation results of the present network layout and rolling stock model against power data logger measurements. The measurements were done as part of a study by Royal Haskoning DHV in 2013 [110]. The present rolling stock's model was based on a current profile that was recorded by one of the motor coaches' on board trip logger, as described in Section 3.5.2. The WTB used during the measurements is the same as what was presented in Section 3.5.1.

The power data loggers were installed at all substations connected to the 33 kV network. Assumptions of the network's phase conductor loading was made during an earlier phase of Royal Haskoning DHV's project. The study focussed on confirming these assumptions in the shortest time and using existing instrument transformers. A total of 31 meters were used. At the ring-network's supply points the loggers were connected to the incoming feeds and outgoing transmission lines.

At all intermediate substations a logger was connected to each traction transformer. At the terminus of each ring<sup>1</sup> only the incoming transmission lines were measured, not individual transformers. [110]

The raw data recorded during this study was obtained, imported into a database using PQSCADA Management Studio and analysed using Elspec Investigator. This data was analysed and it was found that parameters like power and voltage measurements were not available for all substations. This is due to the request to use only existing instrument transformers. The parameter that displayed the highest availability across substations was the “Positive Sequence Current”. The parameter “Average Total Active Power (Fundamental) (Cycle by Cycle)” was available for the Eskom supply points at Traction Main (two supplies) and Modderdam.

Figure 5.1 shows the averaged power flowing through the two main bus bars at Traction Main.<sup>2</sup> This is the most important feeding point to the ring-network. The measured data of 22 August was chosen as reference, due to the availability of

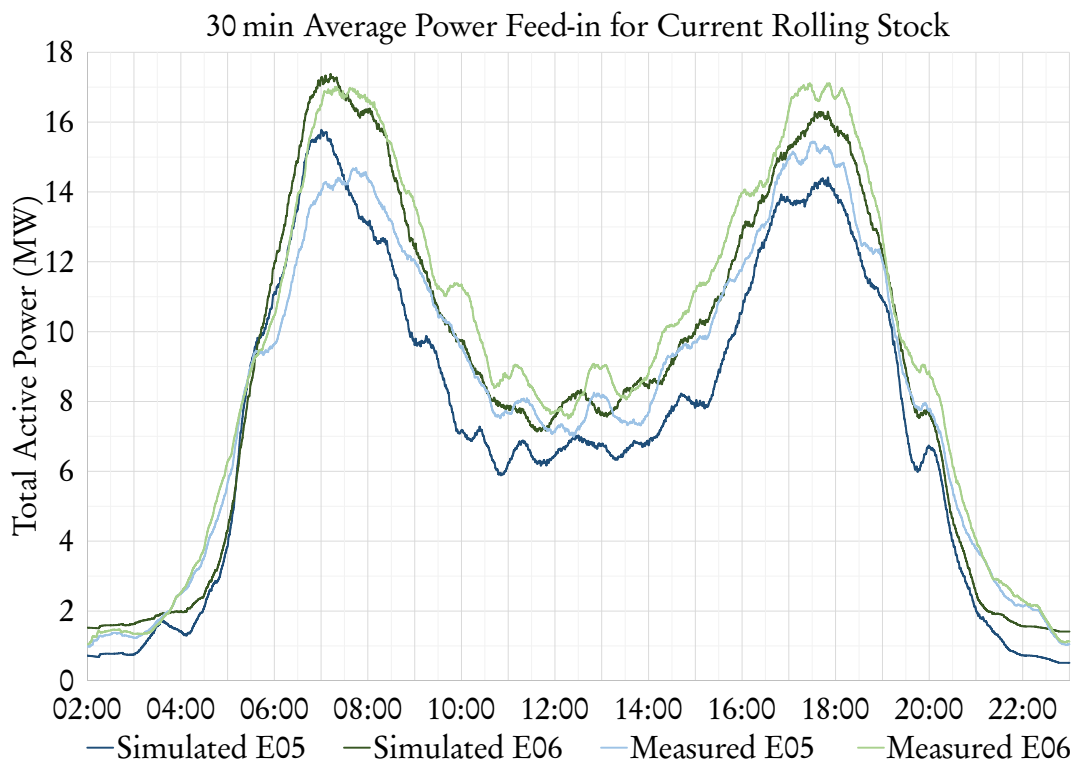


Figure 5.1: Averaged Power measured and simulated for the two feeds into Traction Main

<sup>1</sup>Bellville, Valsbaai and Modderdam substations.

<sup>2</sup>Indicated by E05 and E06 in Figure 4.2.

substations on this day. The output data from the measurement and simulation was exported at a resolution of one sample per second. Each data series was then averaged over a period of 30 min. The dark blue and dark green was the simulated values, while the light blue and light green resembles the measured values. The correlation between the simulated and measured values is quite good, both in terms of form and magnitude. The largest error, of about 1 MW, is less than the energy demand of a single train. This can be attributed to operational factors, such as delays.

Figure 5.2 shows the total averaged power at Traction Main in blue. In dark green is the simulated averaged power flow at the Modderdam feeding point (SATS) and the measured values in light green. This graph shows excellent overall correlation.

Table 5.1 compares the simulated loading of individual traction transformers with values given by Royal Haskoning DHV. The outcome report states, “The daily load profiles for each meter were analysed and a representative peak load tabulated for each day.” [110]

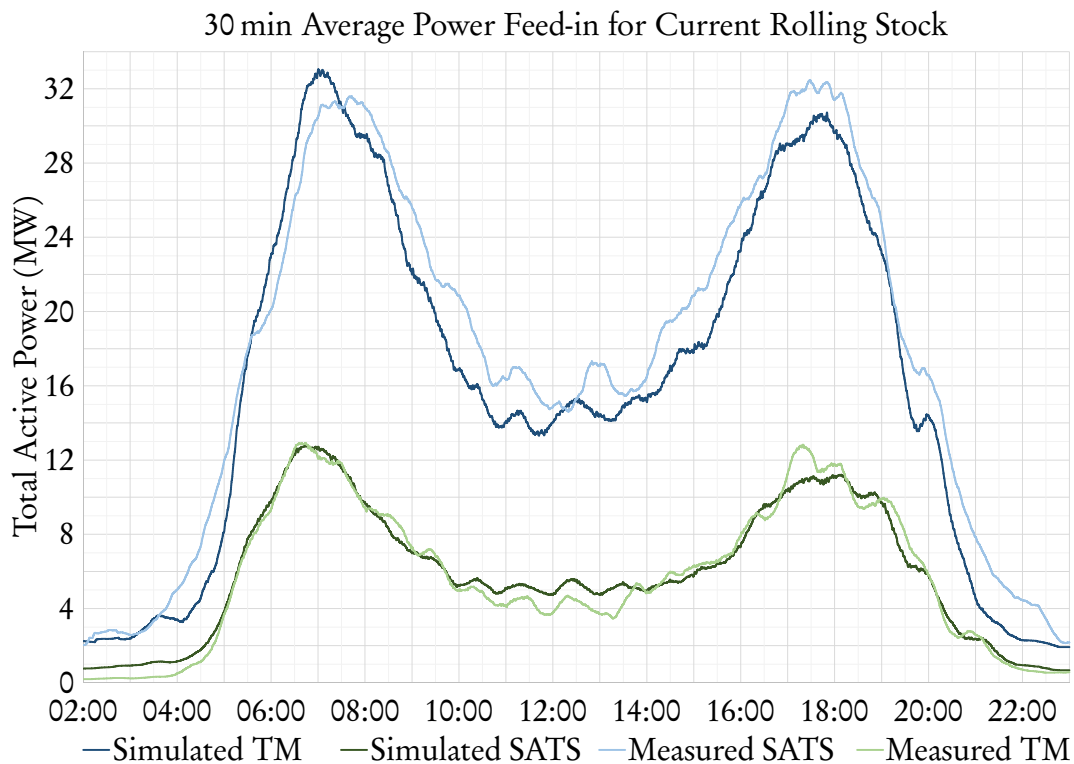


Figure 5.2: Averaged Power measured and simulated for Modderdam feed (SATS) and the total feed into Traction Main (TM)



Table 5.1: Comparison of measured and simulated values of maximum current and transformer loading

Basic Data		Measured Values			Simulation Results			
Substation Transformer	Rated Capacity	Max Measured RMS Current	Calculated Apparent Power Demand	Max Loading	Max 1 min RMS Current	Calculated Apparent Power Demand	Max 1 min Loading	Max 30 min Loading
Bellville A + B	7000 kVA	87 A	4968 kVA	71 %	105 A	5987 kVA	86 %	56 %
Claremont A	3500 kVA	32 A	1800 kVA	51 %	39 A	2248 kVA	64 %	45 %
Claremont B	3500 kVA	30 A	1715 kVA	49 %	40 A	2262 kVA	65 %	45 %
Crawford A	3500 kVA	43 A	2458 kVA	70 %	44 A	2491 kVA	71 %	53 %
Crawford B	3500 kVA	46 A	2629 kVA	75 %	45 A	2583 kVA	74 %	54 %
Dieprivier A	3340 kVA	34 A	1943 kVA	58 %	39 A	2245 kVA	67 %	39 %
Dieprivier B	3340 kVA	28 A	1600 kVA	48 %	39 A	2219 kVA	66 %	39 %
Goodwood A	3500 kVA	60 A	3429 kVA	98 %	61 A	3479 kVA	99 %	71 %
Goodwood B	3500 kVA	56 A	3201 kVA	91 %	62 A	3538 kVA	101 %	72 %
Langa A	3340 kVA	50 A	2858 kVA	86 %	46 A	2647 kVA	79 %	59 %
Langa B	3340 kVA	60 A	3429 kVA	103 %	46 A	2630 kVA	79 %	59 %
Modderdam A + B	7840 kVA	93 A	5316 kVA	68 %	102 A	5814 kVA	74 %	51 %
Nyanga A	3340 kVA	48 A	2744 kVA	82 %	61 A	3483 kVA	104 %	70 %
Nyanga B	3340 kVA	56 A	3201 kVA	96 %	68 A	3868 kVA	116 %	76 %
Paardeneiland A	3340 kVA	42 A	2401 kVA	72 %	68 A	3901 kVA	117 %	87 %
Paardeneiland B	3340 kVA	42 A	2401 kVA	72 %	68 A	3901 kVA	117 %	87 %
Soutrivier A	4950 kVA	100 A	5716 kVA	115 %	108 A	6153 kVA	124 %	93 %
Soutrivier B	4950 kVA	96 A	5487 kVA	111 %	77 A	4423 kVA	89 %	69 %
Valsbaai A	3500 kVA	35 A	2001 kVA	57 %	37 A	2126 kVA	61 %	40 %

It could not be determined how the “representative peak load” was determined. The data in the Measured Values column is quoted from the outcome report. The Max 1 min RMS Current column gives the maximum 1 min averaged current, measured on the HV side of the relevant transformer(s) during the simulation period.

The Calculated Apparent Power Demand values are based on the maximum current and the nominal input voltage of 33 kV. A calculated value is used, because the real measured voltage is not available. The Max Loading is calculated by comparing the maximum current to the rated current value for the specific transformer(s). The measured Max Loading generally lie between the simulated 1 min and 30 min counterparts.

Transformers installed at the same substation is generally of the same make and model. The transformers at Modderdam and Soutrivier substations are the only exceptions. The actual measurements shows that some of the transformer pairs are not loaded evenly. The two worst examples are Dieprivier and Langa. The maximum loading of Dieprivier A is 121 % higher than that of Dieprivier B. At Langa the maximum loading of unit B is 120 % higher than that of unit A. The simulated results, using the nameplate inductance and no tap changing exhibits a more evenly distributed load. This discrepancy may be due to the tap changers of the real transformers that is not set correctly.

The graphs and table illustrate a good correlation between the simulation results and the measured data. The simulation results of the network with altered configuration and the new rolling stock should also prove to be equally accurate.

## 5.3 Results from Further Simulation

The output data from PowerFactory includes values for all variables that were specified in Chapter 4. It was written to a CSV file and post-processed using Microsoft Excel. This data is used to evaluate the various components in terms of loading and losses.

### 5.3.1 Scenarios Investigated

A number of simulations were done to test different scenarios regarding the network response to the future trains and their regenerative braking capabilities.

As explained in Section 3.5.3, the simulation model of the future rolling stock is more advanced than the present stock. By using equations of motion, the algorithm determines how long the trains must accelerate for, drive at a constant speed and brake to reach the arrival station at the prescribed time. It uses these results to calculate the current or power value at each second of the journey.

The scenarios that were investigated is used to illustrate that the simulation model can be used to explore different solutions. Some scenarios are based on others, for example:  $^m + Fding$  (<sup>b</sup>) refers to the New simulation, but with some altered feeding. This arrangement is defined as <sup>b</sup>. The following list explains each scenario in more detail:

- Old: This is the benchmark case, with the present rolling stock and network configuration.
- New (<sup>m</sup>): Also uses the present network configuration, but with the future rolling stock, including regenerative braking.
- New (<sup>m</sup>) noRegen: Same network configuration as in New, but without any regenerative braking power injected into the network.
- <sup>d</sup>+Sub noRegen: This scenario uses the same network configuration as <sup>d</sup>+Sub, below, but without any regenerative braking power injected into the network.
- All further simulations utilises the future rolling stock with regenerative braking.
- $^m + Fding$  (<sup>b</sup>): Langa substation is fed using the 33 kV network from Modderdam, which is 20 km away. A 7 km transmission line from Traction Main is available. The more direct route is used for this simulation.
- <sup>b</sup> + Sctng (<sup>d</sup>): This scenario utilises the more direct feeding, but additionally the DC bus couplers at Soutrivier and Lenteguur are closed. At the moment the rectifier units at these substations are connected to separate overhead line sections. By closing the DC couplers a tie is created.
- <sup>d</sup>+Sub (<sup>e</sup>): For this simulation the altered feeding and sectioning arrangement is retained, but the substation at Chris Hani is energised <sup>3</sup>. It is the

---

<sup>3</sup>This substation is already built, but no supply from the Eskom grid has been provided.

last station of a line that was extended in 2010. Initial simulations show that if this substation is not energised before the future rolling stock is deployed, low pantograph voltages can be expected.

- <sup>d</sup>+Sub3,7: This scenario uses the same network configuration as <sup>d</sup>+Sub, but the threshold voltage for rheostatic braking is reduced from 3,75 kV to 3,7 kV.
- <sup>e</sup>+Feedr: This scenario utilises the substation at Chris Hani, but Bellville is supplied using the shorter 33 kV transmission line from Modderdam proposed in Section 4.2.2.
- <sup>e</sup>+OHL (<sup>§</sup>): This scenario also utilises the additional substation at Chris Hani, but with upgraded 3 kV overhead line conductors on sections with high copper losses, low pantograph voltages and low receptivity. The upgraded conductor is equivalent to a copper contact wire of 161 mm<sup>2</sup> with a copper catenary of 250 mm<sup>2</sup> and an aluminium feeder cable of 800 mm<sup>2</sup>. The upgraded sections are Goodwood substation to Bellville substation and Bellville substation via Eersterivier to Muldersvlei substation and Strand station. The section Bellville to Eersterivier benefits from the substation at Modderdam, through the tie at Kasselsvlei, but is included for increased receptivity and to make provision for a future line from Kuilsrivier to Nolungile.
- <sup>§</sup>+Invrtr: The final scenario is used to investigate the viability of a reversible substation, as described in Section 4.2.3.4. It uses the network with the upgraded conductors, but with an ideal inverting unit placed at Nolungile substation.

In all of the scenarios presented the regenerated energy was modelled using power sources (ElmLod). Initial simulations were conducted by modelling regeneration using current sources (ElmDci). Upon analysis of the data it was found that almost 10 % less regenerated energy was being simulated than what was implied by the input file. During the same initial simulations the simulated energy consumption by trains differed by only about 0,3 % from what was implied by the input file. This is in line with the prediction made in Section 3.3.2.2, page 50. The pantograph voltage during regeneration seems less predictable than during power consumption.

### 5.3.2 Comparison of Statistics

A comparison of various statistics is presented below. It discusses the effect of the changes introduced by the various scenarios on the simulated network.

Figure 5.3 compares the total energy consumed by all trains during the simulation period with the total amount of energy that was implied by the current values used at input. The largest deviation is for the New <sup>(m)</sup> noRegen case, where the high currents and no assistance from regenerating trains cause large ohmic drops between the substations and the simulated trains. This means that the required amount of power does not reach the trains. As more improvements are made to the network, the regenerated energy can flow more easily between braking and accelerating trains. The average line voltage will be higher and more power is consumed for the same current value. With improved overhead line conductors almost 1 % more energy reaches the trains than for the New <sup>(m)</sup> scenario.

Figure 5.4 shows the total energy delivered to all AC and DC loads from the power utility for one day, relative to the 711 MWh consumed during the New <sup>(m)</sup> simulation. With the present trains 2,18 % less energy is delivered in total. If the new trains did not have regenerative braking, the energy bill would have been about 18 % higher. For the case with an inverter, even though almost 1 % more

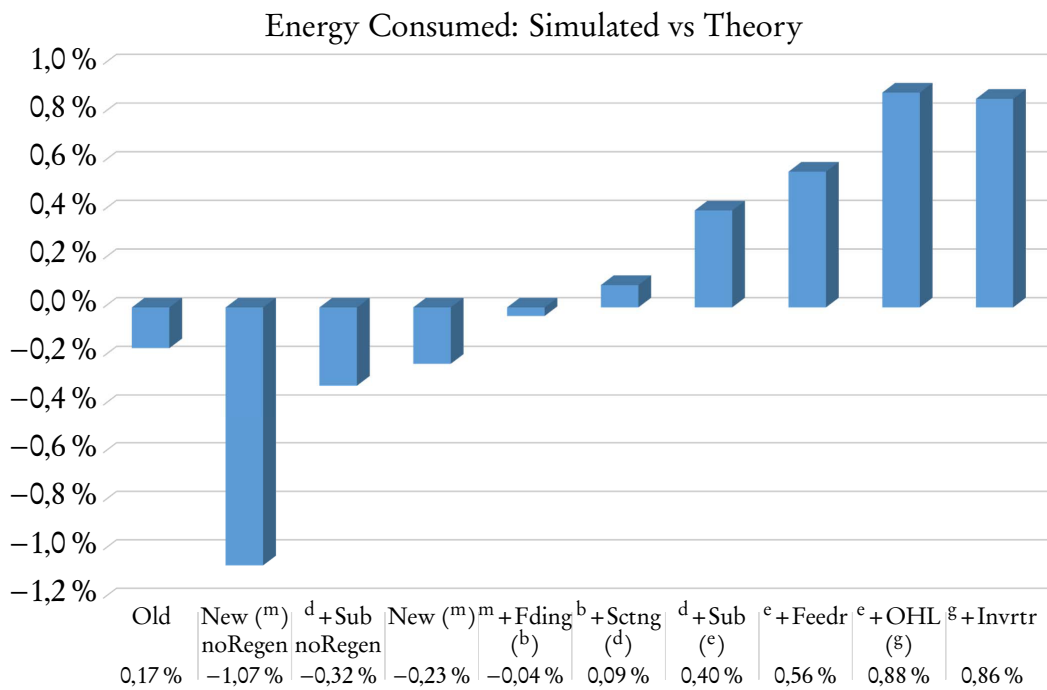


Figure 5.3: Comparison between the total amount energy consumed during the simulation and what was implied by the input

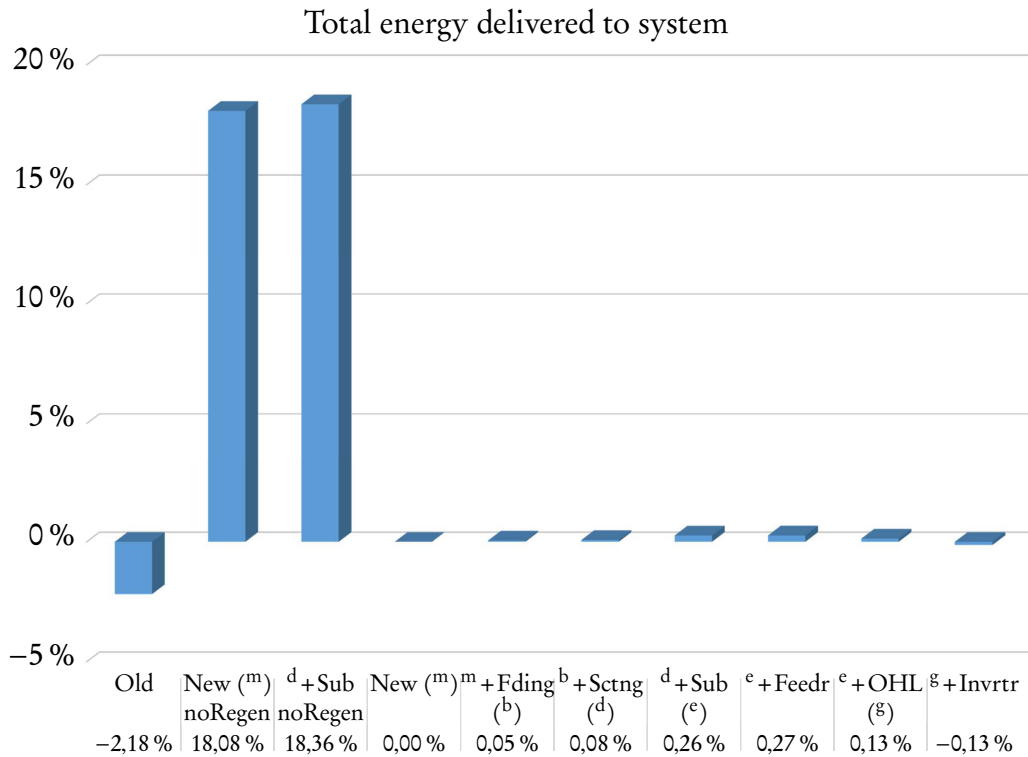


Figure 5.4: Total energy delivered to system expressed as a percentage of the 711 232 kWh that is delivered for New (<sup>m</sup>)

energy reaches the trains, the net energy delivered is less. This indicates that some savings can be achieved with such a system.

Figure 5.5 shows the prevalence of low pantograph voltages relative to New (<sup>m</sup>) counted at the 247 current sources. It shows that by simply altering the feeding and switching arrangement, <sup>b</sup> + Sctng (<sup>d</sup>), the total number of seconds that the pantograph voltage will be below 3 kV, in orange, can be reduced by 15 %. The prevalence of pantograph voltages below 2,7 kV, in blue, can be reduced by 40 % through energising one substations and more than 50 % by upgrading the overhead line conductors.

Figure 5.6 shows the total 3 kV transmission-line losses, relative to the losses of around 40 MWh per day for the New (<sup>m</sup>) simulation. Not shown is that the low maximum current demand of the present trains incur 70 % less line losses than what is expected to be incurred by the new rolling stock running on the same network. It is interesting that the losses for the noRegen cases are also significantly lower. This is because about 4 % of the regenerated energy is dissipated in the overhead lines. The losses can be reduced by almost 13 % by upgrading the overhead line conductors.

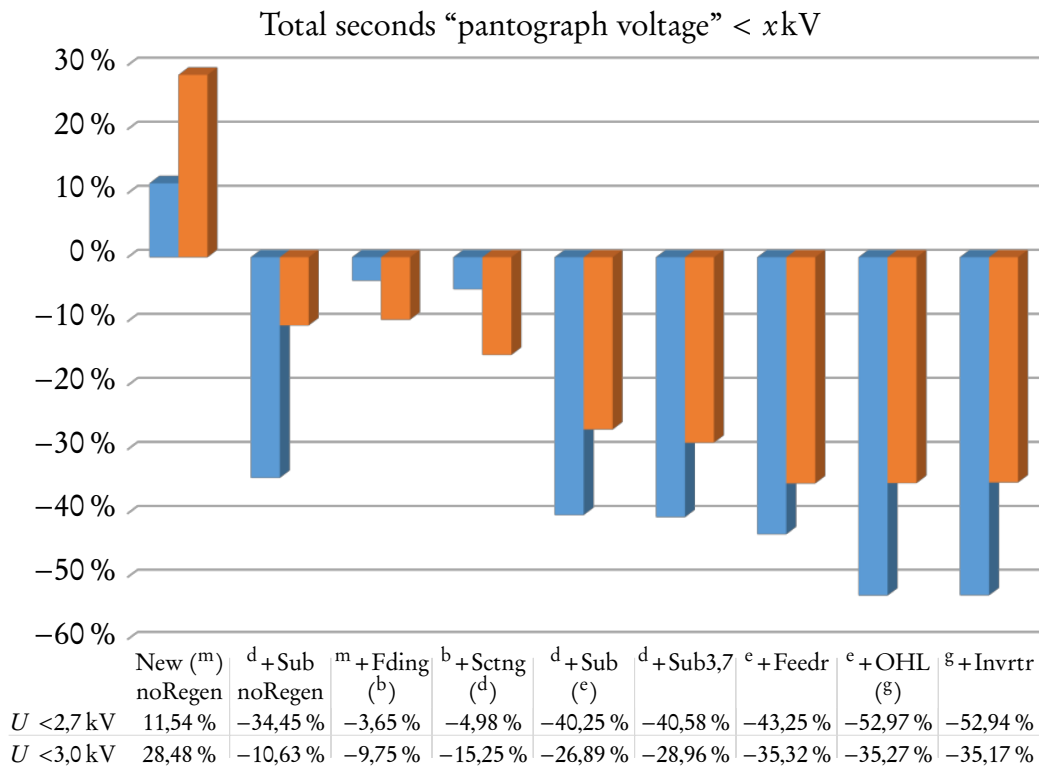


Figure 5.5: Total seconds that node voltages were below 2,7 kV, in blue, and 3 kV, in orange, relative to the 75 414 s and 721 610 s respectively counted for New <sup>(m)</sup>

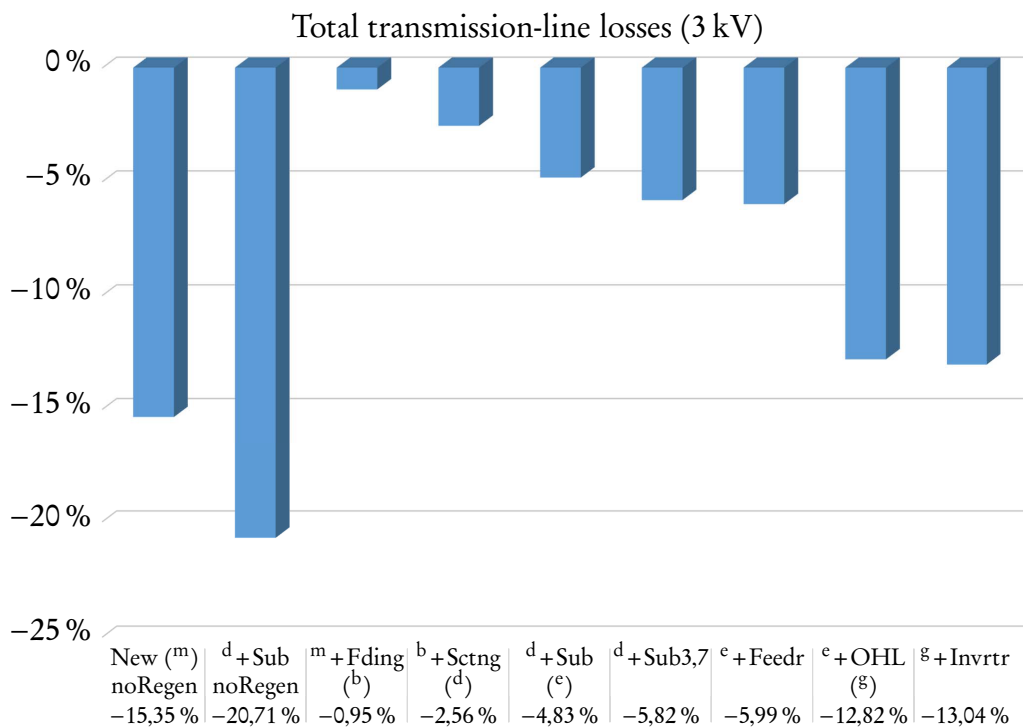


Figure 5.6: Total 3 kV transmission-line losses relative to the 40 638 kWh lost during the New <sup>(m)</sup> simulation

Figure 5.7 shows the 33 kV transmission-line losses, using the 2852 kWh lost during New <sup>(m)</sup> as base. By changing the switching arrangement alone, no capital expenditure, a 23 % reduction in losses can be achieved. If the 5 km feeder is installed between Modderdam and Bellville the losses can be reduced by almost 45 %.

Figure 5.8 shows the median power that is dissipated in the rheostats whilst a train is dissipating. For all cases the median dissipation is around 2 MW. This value is quite low, because the future rolling stock makes provision for 100 % rheostatic braking; 12 MW per 2 module train. The high regeneration current means that even trains in relative close electrical proximity to the reversible substation still needs to dissipate some of the regenerated power in their onboard rheostats.

Figure 5.9 shows the percentage of regenerated energy dissipated in the rheostats for each scenario. About 3,98 % of regenerated energy will be dissipated for the New <sup>(m)</sup> scenario. By upgrading the overhead line, almost 15 % less energy will be dissipated. If the maximum braking voltage is reduced by just 50 V, 19 % more energy will be dissipated. Using a single inverter will reduce the energy dissipation to only 2,76 % of total regenerated energy or 46 % less than New <sup>(m)</sup>.

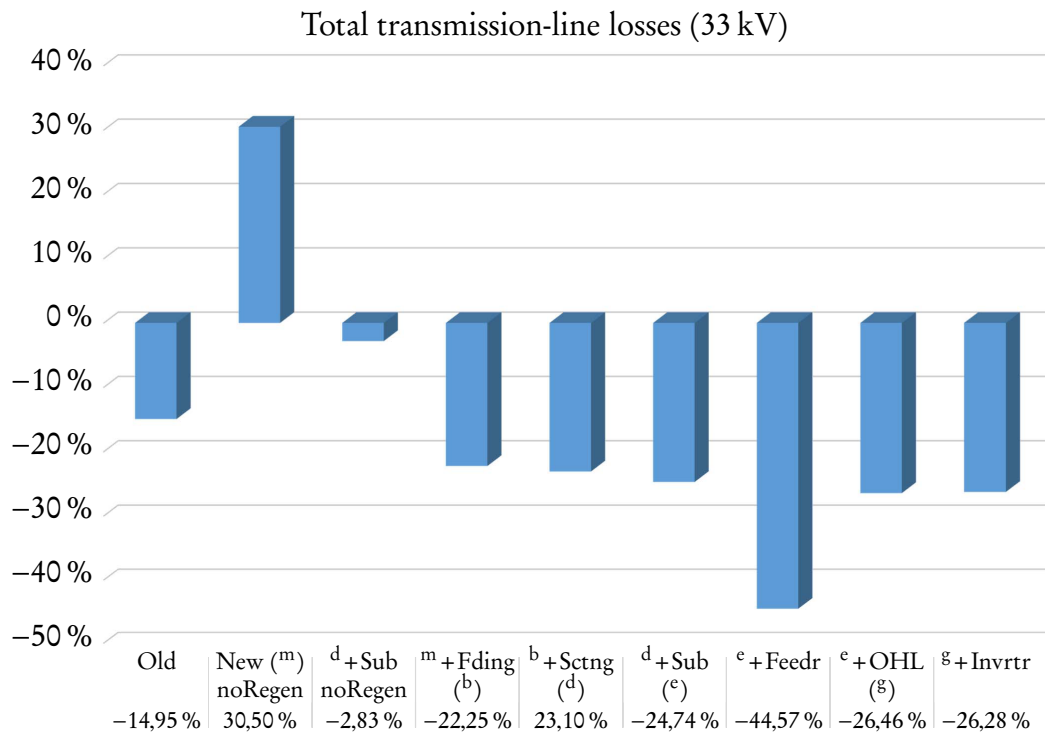


Figure 5.7: Total 33 kV transmission-line losses relative to the 2852 kWh lost during the New <sup>(m)</sup> scenario



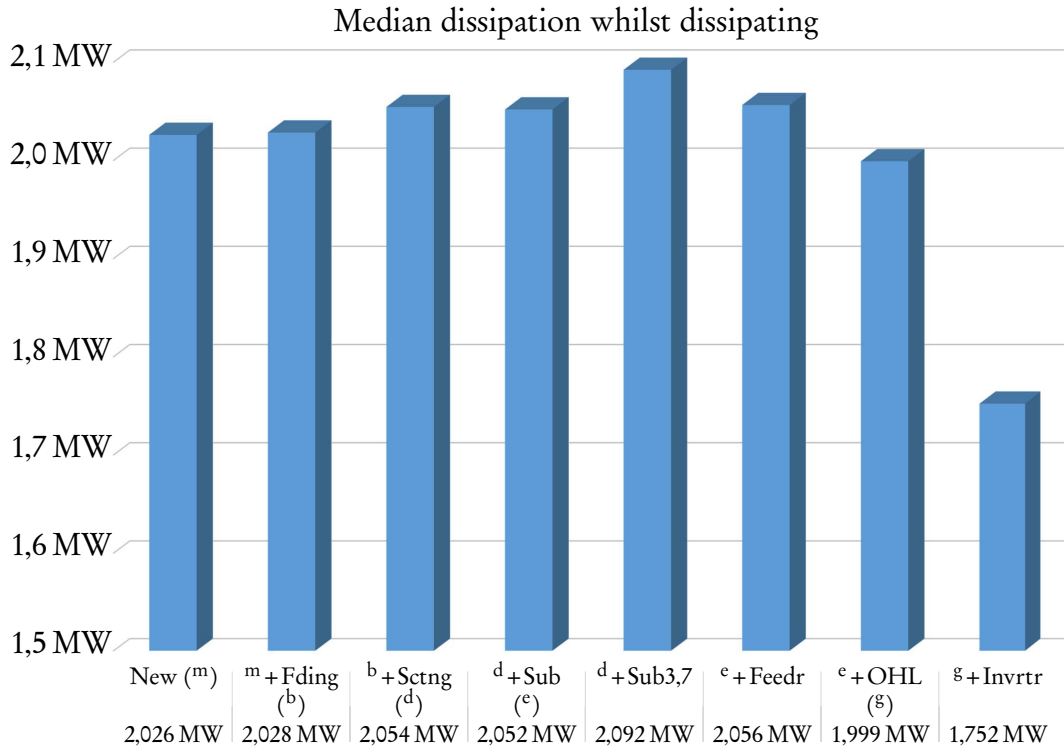


Figure 5.8: Median dissipation in onboard rheostats whilst a train is dissipating

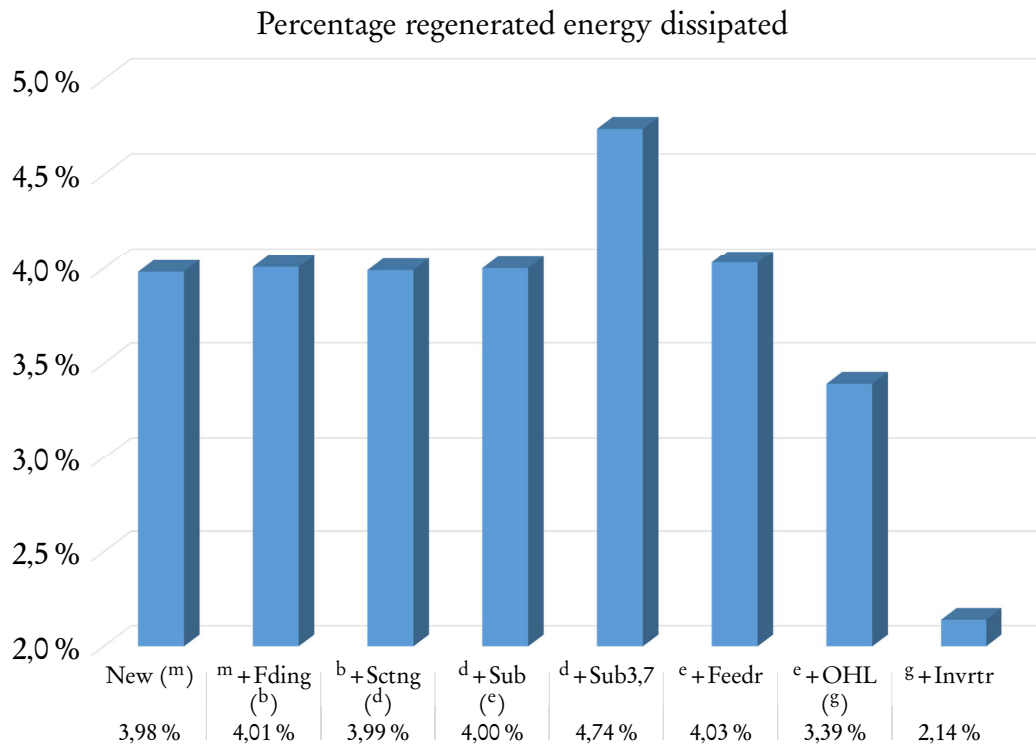


Figure 5.9: Percentage of regenerated energy dissipated in onboard rheostats

Figure 5.10 shows the total energy consumption by trains as a percentage of the total energy supplied to the network. For this network and the simulated timetable the energy that is regenerated makes up for almost all the losses in the system.

Table 5.2 gives a summary of results for the various scenarios. New(\*) refers to the New (<sup>m</sup>) noRegen scenario. <sup>d</sup>+Sub noRegen is not shown, due to space constraints.

More detailed results can be found in Appendix K.

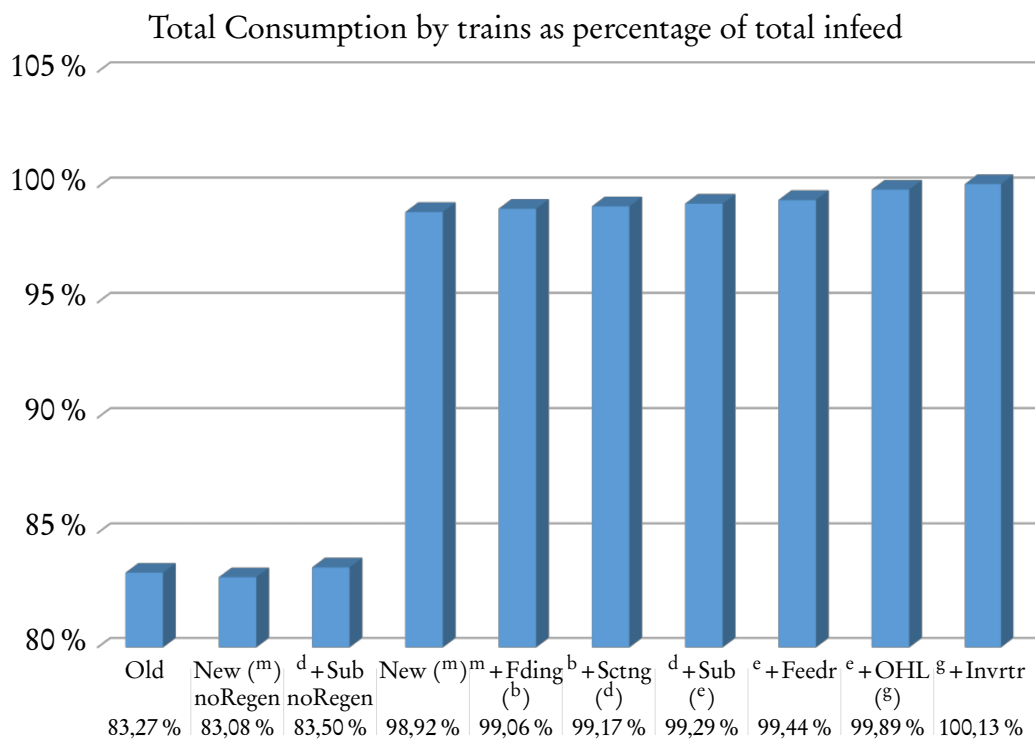


Figure 5.10: Total energy consumption by trains as a percentage of the total energy infeed

Table 5.2: Summary of results for the various scenarios

Description	Old	New(*)	New <sup>(m)</sup>	m + Fding <sup>(b)</sup>	b + Sctng <sup>(d)</sup>	d + Sub <sup>(e)</sup>	d + Sub <sup>3,7</sup>	e + Feedr	e + OHL <sup>(g)</sup>	g + Invrtr
Total energy infeed (kWh)	695 761	839 820	711 232	711 604	711 771	713 104	713 758	713 118	712 192	710 303
33 kV transmission losses (kWh)	2426	3722	2852	2217	2193	2147	2141	1581	2097	2103
Miscellaneous loads (kWh)	93 998	93 998	93 879	93 915	93 907	93 906	93 910	93 948	93 917	93 920
Transformer consumption (kWh)	599 337	742 100	614 501	615 472	615 671	617 051	617 707	617 589	616 177	617 729
3 kV line losses (kWh)	11 728	34 400	40 638	40 250	39 599	38 675	38 273	38 203	35 430	35 338
Trains consumed (kWh)	579 386	697 688	703 566	704 950	705 847	708 010	708 153	709 133	711 424	711 243
Trains consumed vs infeed	83,27 %	83,08 %	98,92 %	99,06 %	99,17 %	99,29 %	99,21 %	99,44 %	99,89 %	100,13 %
Trains regenerated (kWh)			144 711	144 719	144 717	144 582	144 723	144 738	144 692	144 501
% energy regenerated			20,57 %	20,53 %	20,5 %	20,42 %	20,44 %	20,41 %	20,34 %	20,32 %
Net use by trains (kWh)	579 386	697 688	558 855	560 231	561 130	563 429	563 430	564 394	566 732	566 741
Energy dissipated rheostats (kWh)			5763	5801	5776	5785	6862	5836	4911	3094
% regenerated energy dissipated			3,98 %	4,01 %	3,99 %	4,00 %	4,74 %	4,03 %	3,39 %	2,14 %
Effective % energy regenerated			19,75 %	19,71 %	19,68 %	19,6 %	19,47 %	19,59 %	19,65 %	19,88 %
Inverter energy recovered (kWh)										3448
Transformer & rectifier losses (kWh)	8223	10 012	9245	9190	9166	9162	9142	9156	9105	9108
Seconds rheostatic dissipation			7777	7824	7745	7766	9057	7833	6766	4897
% of day dissipating			10,29 %	10,35 %	10,24 %	10,27 %	11,98 %	10,36 %	8,95 %	6,48 %
Seconds inverter active										5382
% of day recovering										7,12 %
Seconds recov&dissip										1279
% of recov recov&dissip										23,76 %
Maximum instant dissipation (MW)			21,742	21,742	21,741	21,741	21,934	21,741	21,733	21,41
Average dissipation (MW)			2,668	2,669	2,685	2,682	2,727	2,682	2,613	2,274
Median dissipation (MW)			2,026	2,028	2,054	2,052	2,092	2,056	1,999	1,752
Maximum instant recovered (MW)										19,775
Average recovery (MW)										2,306
Median recovery (MW)										1,852
“Line voltage” < 2,7 kV (total s)	0	84 120	75 414	72 662	71 662	45 061	44 810	42 795	35 465	35 488
“Line voltage” < 3 kV (total s)	6640	927 126	721 610	651 287	611 585	527 581	512 606	466 751	467 120	467 833

## 5.4 Conclusion

This chapter described the simulations that were executed using PowerFactory. The model was first benchmarked against actual measurements. The simulated values compared very well with their measured counterparts. Once the model proved to be a valid representation of the actual network, different scenarios were presented and could be investigated further. The scenarios indicated how the energy use of the new rolling stock compares with the present rolling stock. Various alterations and improvements to the network could be investigated using the model that was developed.

# Chapter 6

## Conclusion

### 6.1 Synopsis

This study investigated various methods of reducing energy usage. The concepts behind regenerative braking and how the useful application of regenerated energy can be increased was presented. Two ways through which the railway operator can save energy is by change the way the train is driven and the improve the energy flow through the infrastructure on which the trains are running. In this study the focus was placed on developing a method of investigating various combinations of methods.

To determine the amount of regenerated energy that can be recovered with a specific technology first required a detailed analysis of the network. Parameters applicable to the network that was part of this study was acquired to ensure accurate and reliable results.

Some options for load-flow simulation software was explored. Computer simulations offer the advantage that the effect of any combination of solutions can be investigated before a single change is made to the physical infrastructure. Unfortunately a lot of the simulation suites are of a proprietary nature and employed as part of consulting work. If the railway can't or don't want to utilise them, it has to undertake the tedious process of developing software from scratch or build models from first principles.

DIgSILENT's PowerFactory offers a stand-alone solution that is widely used by electrical network designers and power utilities around the world for power system analysis. It features support for simultaneous load flow analysis of both the AC and DC networks, but lacks the functionality to simulate moving loads

along DC lines. This was addressed by developing a model where a moving train's dynamically changing traction current is allocated to two stationary dynamic current sources. It was validated using a mathematical approach and proved to be sufficiently close to a fully dynamic model. The relative displacement function will be used to vary the current allocated to each source according to the train's actual position.

Ways to model the present and future rolling stock were devised by taking each type's properties and abilities into consideration. A processing algorithm was developed to allocate the current or power values to each source for each second of the simulation based on the rolling stock and timetable.

The simulation results showed that an off-the-shelf simulation package, such as PowerFactory, can be successfully used to conduct dynamic capacity and contingency studies. It contains sufficient elements to accurately model a railway traction network and simultaneously solve the AC and DC networks. Several issues with the simulation software were encountered, but the results are satisfactory nonetheless. The model that was presented can be used to represent any timetable and rolling stock.

This outcome of this study into the possibilities that are available to reduce railway traction energy usage are very positive. Other studies and real-life experience of railway operators have shown that by using the technology that is available today, large savings in energy usage and money can be realised.

Further investigation into the application of these principles by railway operators in South Africa, and Prasa in particular, is definitely justified and should deliver some exciting results.

## 6.2 Future Work and Recommendations

The following issues can be addressed as part of future work on the subject:

- The post-processing of simulation results need some streamlining, including the ability to colour PowerFactory diagrams from external files, so that it is possible to graphically indicate which areas suffer from low voltages or high prevalence of rheostatic braking.
- The current and power values should be obtained for all load conditions. This should be used to predict the energy use and exchange between trains

at different times of the day.

- It is well known that something that is not measured, can also not be managed. Prasa should install power data loggers at all of the important points in their traction network. This will make it possible to track deviations in energy use much faster and improve the quality of studies like this.
- A thorough study should be done of the real time that it takes trains to run between stations, also at different times of the day. These times must then be used to develop a timetable on a second level, with a buffer for robustness.
- If it is not possible to perform physical tests, then the rolling stock's characteristics should be used to calculate running times. These times can be used to design a timetable that is more suited to the increased performance of the future rolling stock. The solution proposed in this study can then be used to find an improved network configuration and driving style even before the new trains enter service.

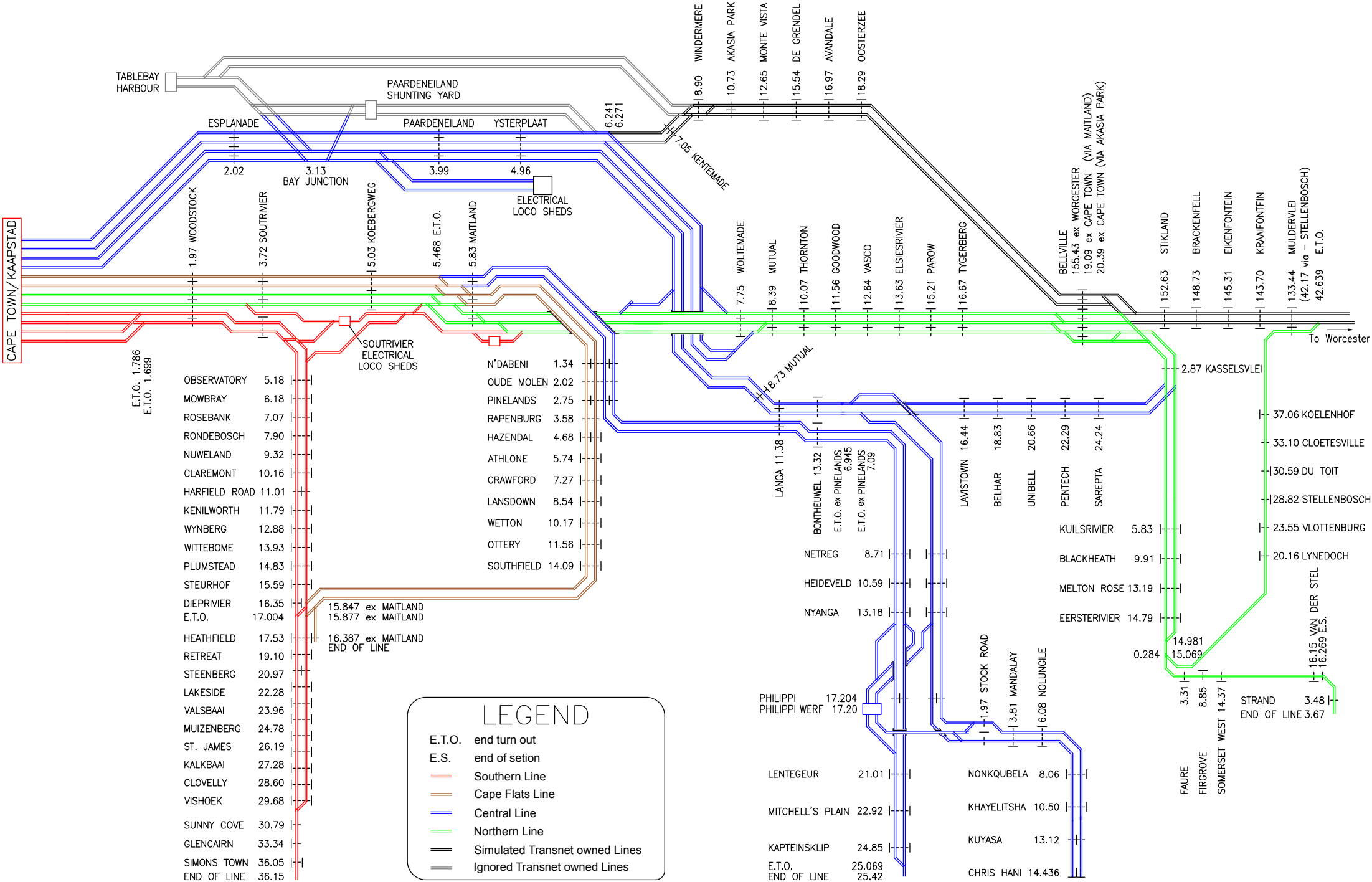
# Appendices



# Appendix A

## Network Diagram

A diagram of the railway network that was investigated as part of this study can be found on the following page. It shows the different lines of the network and a distance reference for each station.



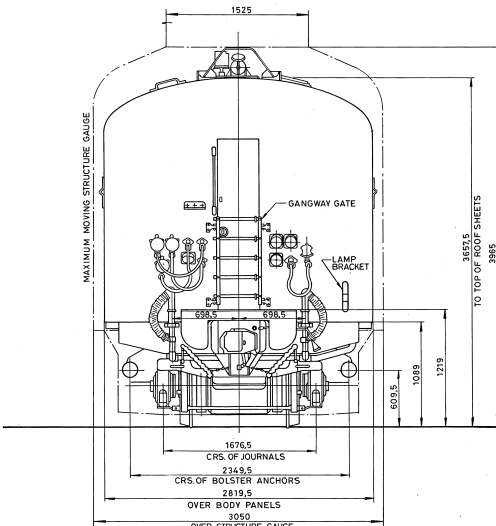
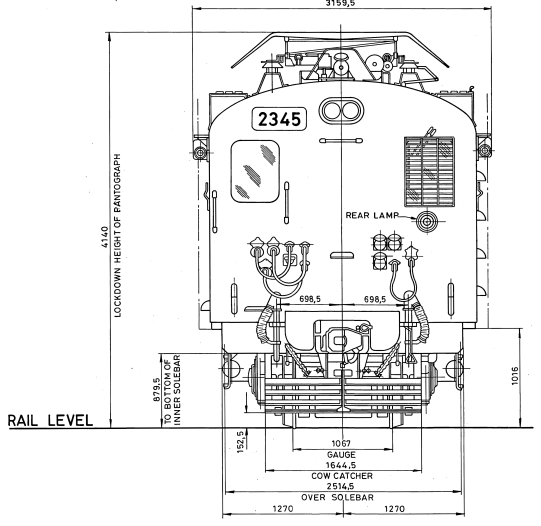
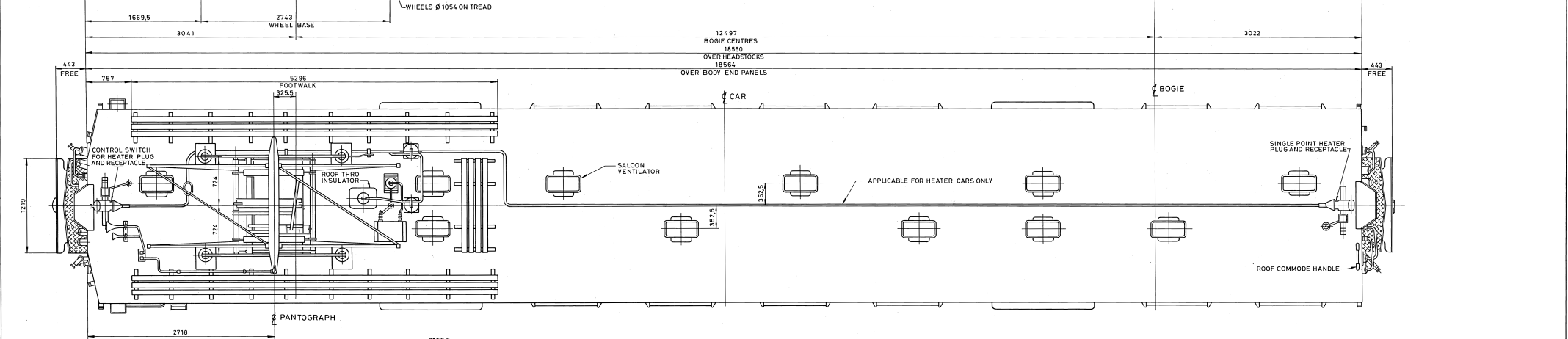
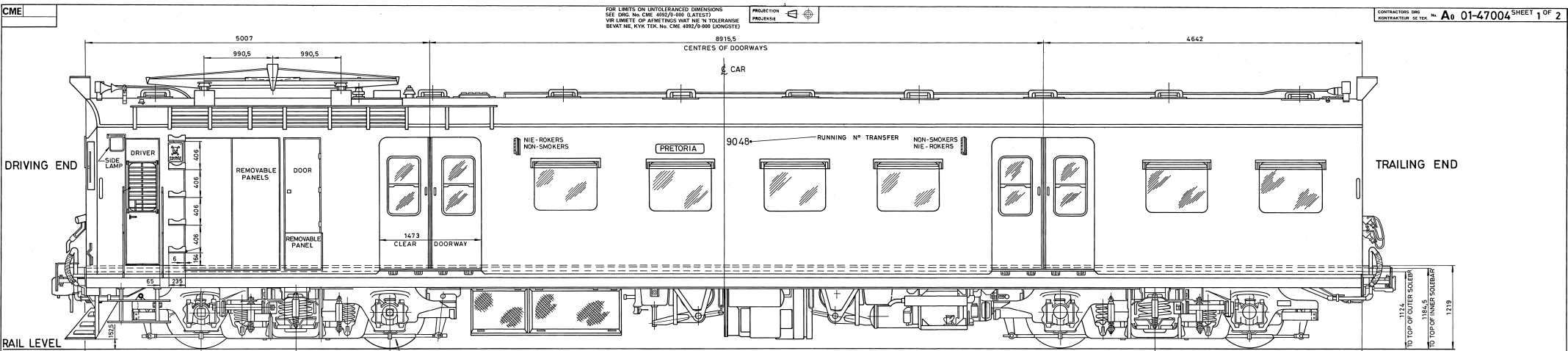
### LEGEND

- E.T.O. end turn out
- E.S. end of setion
- Southern Line
- Cape Flats Line
- Central Line
- Northern Line
- Simulated Transnet owned Lines
- Ignored Transnet owned Lines

## Appendix B

### Diagram of Present Rolling Stock

Diagrams of the present rolling stock can be found on the following pages. A motor coach is shown first and then a trailer coach. There are many variants of these coaches in use. This includes different configurations of saloon doors, inclusion of a guards compartment, inclusion of a toilet and different seating arrangements.



NOTE:  
FOR MATERIAL LIST SEE DRG.No.A01-47004 SHEET 2 OF 2.

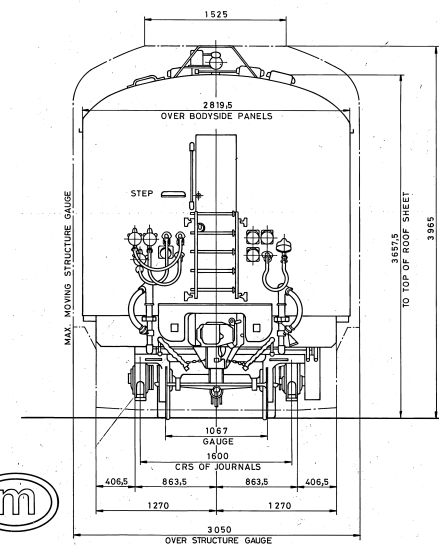
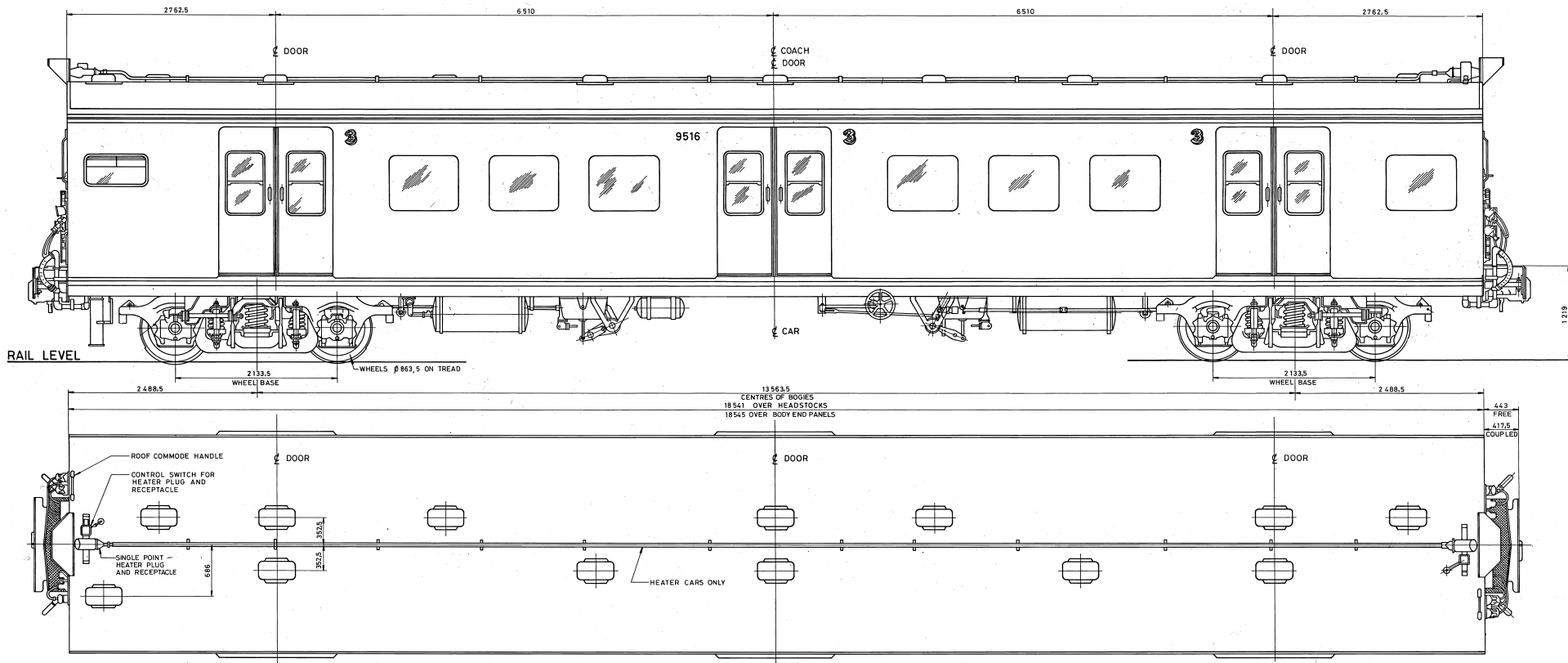
ITEM	NAME	NUMBER	MATERIAL	SPEC.	QTY	DESCRIPTION / SET	QUANTITY	REMARKS
ASSEMBLY DRG. No. 2345		SUBURBAN MOTOR COACHES		UNION		S.A.R.-S.A.S. GENERAL ARRANGEMENT OF SUBURBAN MOTOR COACHES TYPE L2MH AND L2MX		
SUPERSEDED BY DRG. No. A0 01-40002		L2MH L2MX		DATE: MARCH 79		DRAWN: 1/20		
SEPA TO XL		SUBURBAN MOTOR COACHES		DATE: MARCH 79		DIMENSIONS IN mm EXCEPT WHERE OTHERWISE INDICATED		
SEPA TO XL		SUBURBAN MOTOR COACHES		DATE: MARCH 79		DIMENSIONS IN mm EXCEPT WHERE OTHERWISE INDICATED		



SEE SHEET 2  
REMARKS  
MATERIAL: MATERIAL

UNION  
S.A.R.-S.A.S.  
GENERAL ARRANGEMENT  
OF SUBURBAN MOTOR COACHES  
TYPE L2MH AND L2MX

NIGEL  
No. CME 12 01  
47004  
SHT 10F2



**TYPE S11T SUBURBAN TRAILER COACHES**

- COACH RUNNING Nos:- 9516 - 9561 - WESTERN TRANSVAAL SYSTEM  
 9558 - 9592 - WESTERN TRANSVAAL SYSTEM  
 9761 - 9769 - WESTERN TRANSVAAL SYSTEM  
 9770 - 9800 - NATAL SUBURBAN SYSTEM  
 9951 - 10011 - NATAL SUBURBAN SYSTEM  
 10032 - 10067 - NATAL SUBURBAN SYSTEM  
 10058 - 10069 - EASTERN TRANSVAAL SYSTEM  
 10081 - 10100 - EASTERN TRANSVAAL SYSTEM

**MAIN VARIATIONS FROM PREVIOUS CONTRACTS:-**

- PRESSURE VENTILATION SYSTEM FITTED ON COACH 10058
- 'WONEY' DOOR GEAR FITTED ON ABOVE P.V. SYSTEM COACH
- HALF-DROP WINDOWS FITTED ON ABOVE P.V. SYSTEM COACH AND COACH Nos. 9516 - 9523.
- COUPLER RELEASE WIRES - DISCONTINUED ON ALL COACHES
- SALOON PASSENGER DOOR GRABHANDLES FITTED ON COACHES 10051 AND 10100 - IN LIEU OF DOORWAY GRABPOLES
- SAB TYPE AAR-DRV-2A-9DJ SLACK ADJUSTERS, FITTED ON COACHES..... 10041 - 10057

ITEM	NAME NAAM	NUMBER WHEEL ASSIGNMENT GETAL WIEL WAGTEL	MATERIAL MATERIAAL	SPEC. SPESIF.	QTY. MENGTE	DESCRIPTION / OOR BESKRYWING/PROOFTE	STOCKS / IN OP. ORG. NO. WAG. NO.	QUANTITY IN STOCK MENGTE WAG. NO.	REMARKS OPMERKINGS	STATIONERS STASIONERS
UNION										
SAR-SAS										
GENERAL ARRANGEMENT										
OF TRAILER COACHES - TYPE S11TH AND S11TX										
DATE: MARCH 79										
SCALE: 1:20										
DIMENSIONS IN mm EXCEPT WHERE OTHERWISE INDICATED METRICS IN mm BEHALWE WAG. ANDER. AANGEDE										
SEE TABLE										
CME No. 01-47001										

## Appendix C

### Diagram of New Rolling Stock

A diagram of the new rolling stock can be found on the following page [120]. It shows the standard six coach configuration.



## Appendix D

# Determination and Validation of Acceleration Parameters

The processing algorithm calculates the relative displacement function by using the rolling stock's acceleration and deceleration parameters. A 14 coach trainset of the present rolling stock is stated to have a crush load acceleration of  $0,44 \text{ m/s}^2$  [80]. To validate this and determine the typical deceleration rate various GPS recordings were made on different lines across the network.

The data was analysed using Microsoft Excel and an acceleration of  $0,35 \text{ m/s}^2$  was found to be more realistic. The difference in acceleration might be attributed to driver behaviour under normal operating conditions versus test circumstances and the condition of the rolling stock. For deceleration a value of  $-0,5 \text{ m/s}^2$  was calculated for the Southern Line and  $-0,65 \text{ m/s}^2$  for all other lines.

Figure D.1 shows the measured and ideal relative displacement graphs of station-to-station trips along the Southern Line between Cape Town and Vishoek. Measured values, denoted by a subscript M, are based on the displacement that was recorded by the GPS-receiver at one second intervals and is drawn with solid lines. Ideal values are based on the displacement that was calculated using the typical acceleration and deceleration rate for the present rolling stock and the relative displacement function, defined in Section 3.4.3. As stated in that section, the function only use the station-to-station distance and running time and can not take speed restrictions into account. The graph shows that there is good overall correlation, but that especially speed restrictions necessitate that drivers accelerate slower when departing a station (for example MZM) or departing with high acceleration and then slowing down (for example SRX).



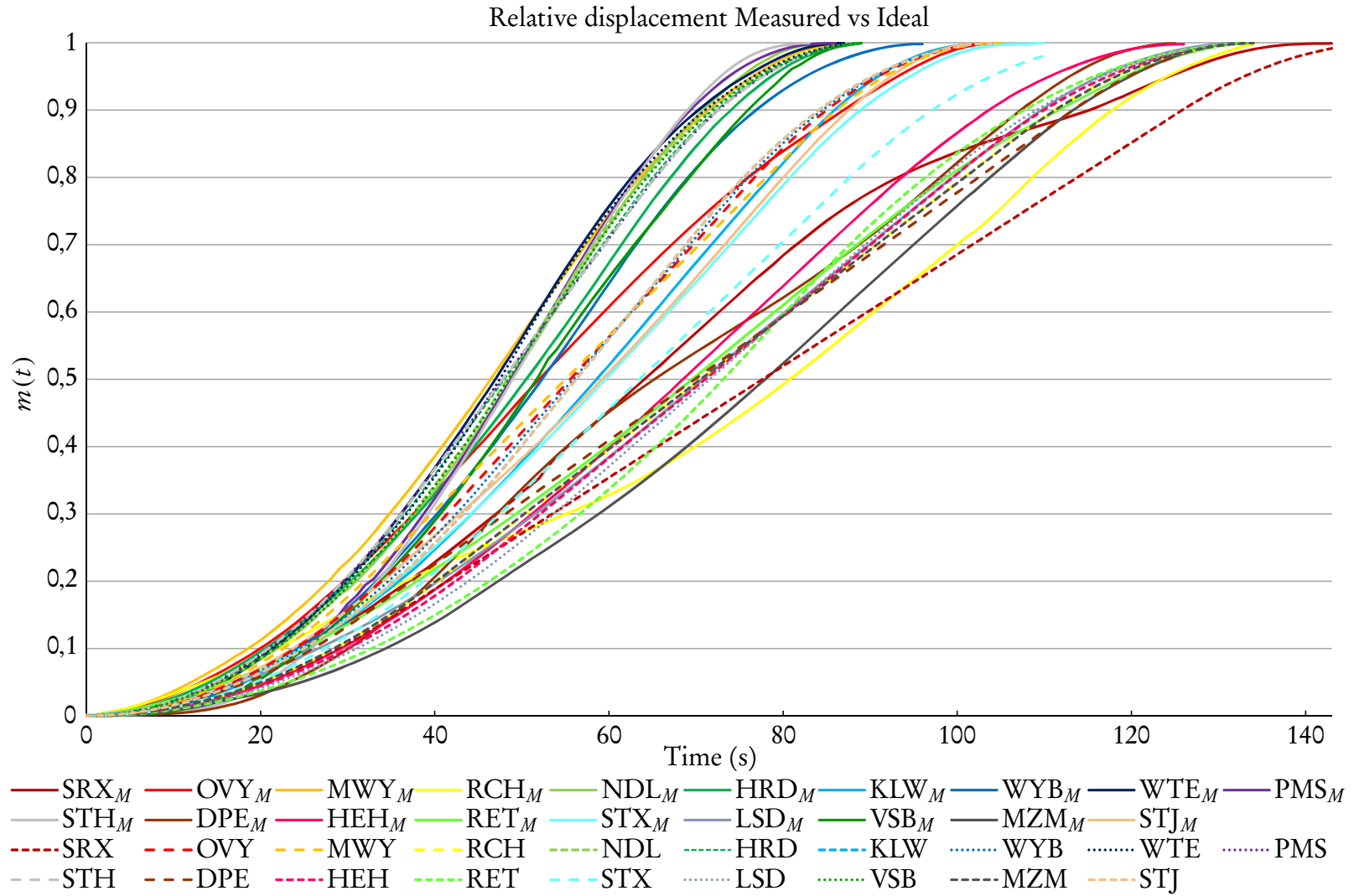


Figure D.1: Comparison of measured and calculated values of the relative displacement function for old rolling stock: Cape Town to Vishoek

Figure D.2 shows the measured, denoted by a subscript M, and ideal relative displacement graphs of station-to-station trips along the Northern Line between Cape Town and Du Toit. The same method was followed as in Figure D.1. This graph also shows good overall correlation between the measured and ideal curves. Notice that once again the biggest difference is when a train departed with good acceleration, but then had to slow down due to speed restrictions, for example MET and TYG. The high measured acceleration rate (of nearly  $0,5 \text{ m/s}^2$ ) when departing WTM can be attributed to the station being located on a 1:80 gradient. This station is one of only a very few such exceptional case on the network and hence the ignoring of gradients is deemed acceptable.

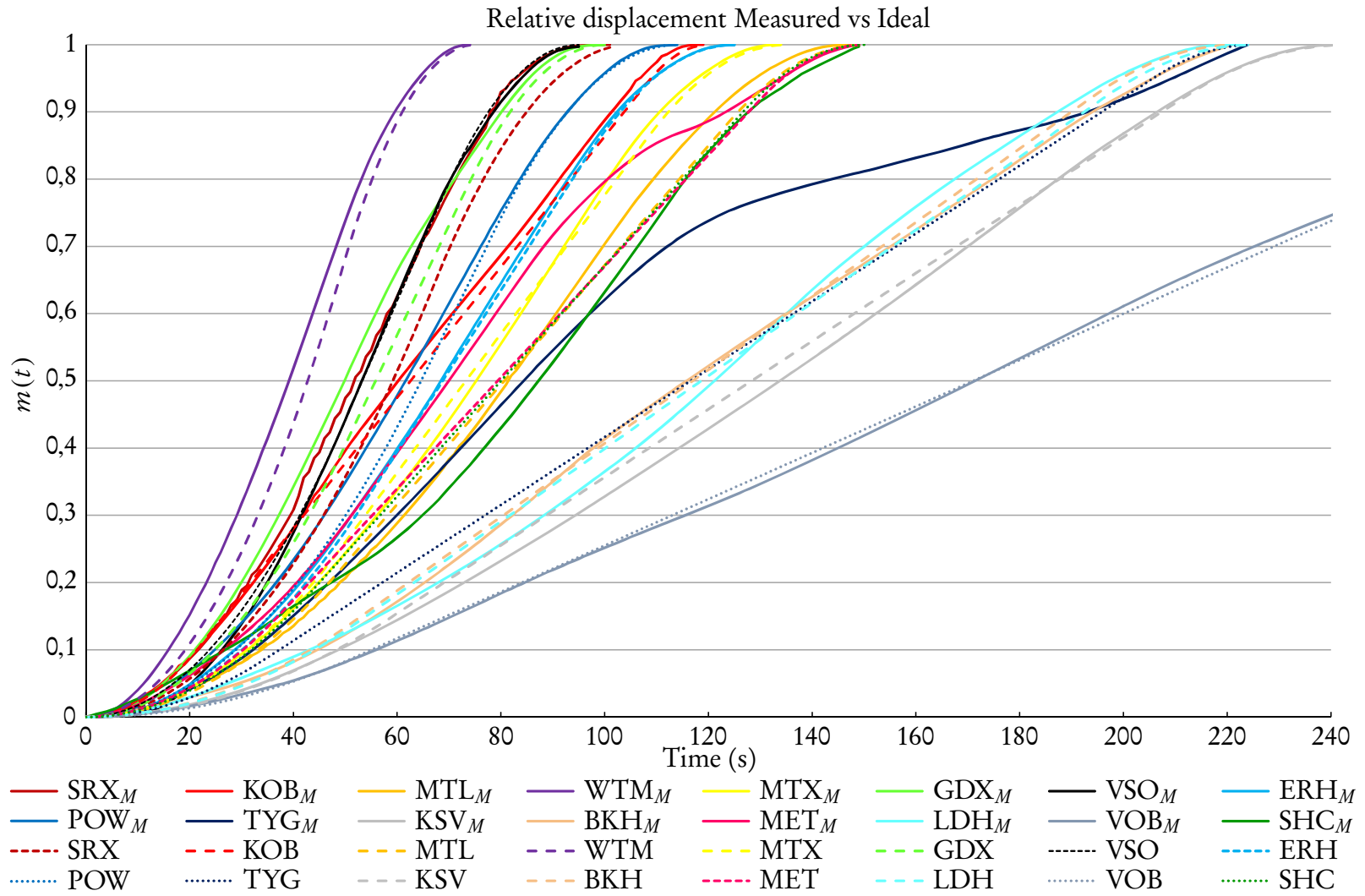


Figure D.2: Comparison of measured and calculated values of the relative displacement function for old rolling stock: Cape Town to Du Toit

# Appendix E

## Python Processing Algorithm

The processing algorithm was written in Python. The source code and input files are available at the following URL:

[https://www.dropbox.com/sh/zou97hrtpwpuyii/AAA0kk7ZbEwznmCI\\_M8XATFa?dl=0](https://www.dropbox.com/sh/zou97hrtpwpuyii/AAA0kk7ZbEwznmCI_M8XATFa?dl=0)

Password: pythonAlgorithm2016

# Appendix F

## Train Running Times

Tables F.1 to F.4 give the official Metrorail running times. It is included here for the sake of completeness. Only the formatting was altered, to improve readability. A time of “5.30” refers to 5 min 30 s. These values were, however, added as if they are decimal numbers, so the totals given for each column is not correct.

Tables F.5 to F.8 give another version of the official Metrorail running times, compiled by the former South African Rail Commuter Corporation (SARCC). It is also included only for the sake of completeness. These tables include the junctions Bay, Kasselsvlei, Kensington and Windermere.

Tables F.9 to F.12 have been reworked from the official Metrorail running times. It includes the official three letter abbreviation for each station. Times have been converted to decimal minutes. A value of “5.50”, for example, now refers to 5 min 30 s. The point-to-point distances have also been verified and updated, where necessary. The tables are by no means provided as a definitive list of what is practically possible, but should prove more realistic than those given in the official versions. It is proposed that all times are reviewed through an iterative process where it is evaluated with equations of motion (to determine maximum line speed), addition of time for robustness and conduction of line tests. The column “SAR 73/74” was obtained from the WTB for 1973-1974 and shows the running times that was used to compile it. It is included here for comparison. Running times were generally faster than what can be achieved today, utilising the same rolling stock, but without technological “advancements” such as centralised traffic control.

Table F.1: Official Metrorail running times for Southern Lines [99]

## CAPE METRORAIL: TRAIN RUNNING TIMES

STATIONS	KILOMETRE DISTANCE	ALL STATION TRAINS	EXPRESS TRAINS	DWELL TIMES	STATIONS	ALL STATION TRAINS	EXPRESS TRAINS	DWELL TIMES	
CAPE TOWN					SIMONSTAD				
WOODSTOCK	1.97	2.45	2.30	0.20	GLENCAIRN	4.30	4.30	0.20	
SALT RIVER	1.75	3.00	2.00	0.30	SUNNY COVE	4.15	3.45	0.20	
OBSERVATORY	1.46	2.30	1.45	0.20	FISH HOEK	2.15	1.30	0.20	
MOWBRAY	1.00	1.45	1.00	0.20	KALK BAY	4.30	3.30	0.20	
ROSEBANK	0.89	1.45	0.45	0.20	ST JAMES	1.45	1.15	0.20	
RONDEBOSCH	0.83	1.30	0.45	0.20	MUIZENBERG	2.15	1.30	0.20	
NEWLANDS	1.42	2.15	1.15	0.20	FALSE BAY	1.30	1.00	0.20	
CLAREMONT	0.84	1.30	0.45	0.30	LAKESIDE	2.15	1.30	0.20	
HARFIELD RD	0.85	1.30	0.45	0.20	STEENBERG	2.00	1.15	0.20	
KENILWORTH	0.78	1.30	1.00	0.20	RETREAT	1.30	1.15	0.30	
WYNBERG	1.09	1.45	1.00	0.35	HEATHFIELD	3.00	2.00	0.30	
WITTEBOME	1.05	1.45	1.00	0.20	DIEP RIVER	1.45	1.15	0.20	
PLUMSTEAD	0.90	1.30	0.45	0.30	STEURHOF	1.15	0.45	0.20	
STEURHOF	0.76	1.30	0.45	0.20	PLUMSTEAD	1.30	0.45	0.20	
DIEP RIVER	0.76	1.30	0.45	0.20	WITTEBOME	1.30	1.00	0.20	
HEATHFIELD	1.18	2.15	1.30	0.30	WYNBERG	1.45	1.00	0.30	
RETREAT	1.57	2.15	1.30	0.30	KENILWORTH	1.45	1.15	0.20	
STEENBERG	1.87	2.15	1.45	0.20	HARFIELD RD	1.30	0.45	0.20	
LAKESIDE	1.31	2.00	1.15	0.20	CLAREMONT	1.30	0.45	0.30	
FALSE BAY	1.68	2.15	1.45	0.20	NEWLANDS	1.30	0.45	0.20	
MUIZENBERG	0.82	1.30	1.00	0.20	RONDEBOSCH	2.00	1.15	0.20	
ST JAMES	1.41	2.15	1.45	0.20	ROSEBANK	1.30	0.45	0.20	
KALK BAY	1.09	1.45	1.15	0.20	MOWBRAY	1.45	0.45	0.20	
FISH HOEK	1.08	4.45	4.15	0.20	OBSERVATORY	1.30	0.45	0.20	
SUNNY COVE	1.11	2.15	2.00	0.20	SALT RIVER	2.45	1.45	0.30	
GLENCAIRN	2.55	4.45	3.45	0.20	WOODSTOCK	2.15	2.00	0.20	
SIMONSTAD	2.71	4.00	4.15	0.20	CAPE TOWN	3.15	3.00	0.20	
	34.73	55.35	38.05	5.85		54.05	36.90	5.70	
<b>CAPE TOWN - RETREAT VIA CAPE FLATS</b>					<b>RETREAT - CAPE TOWN VIA CAPE FLATS</b>				
CAPE TOWN					RETREAT				
WOODSTOCK	1.97	3.00	2.30	0.20	HEATHFIELD	2.30	1.30	0.30	
SALT RIVER	1.75	2.30	1.30	0.30	SOUTHFIELD	3.30	2.45	0.20	
KOEBERG RD	1.31	1.45	1.15	0.20	OTTERY	3.00	2.15	0.20	
MAITLAND	0.80	2.00	1.15	0.30	WETTON	2.00	1.15	0.20	
N'DABENI	1.34	2.30	2.00	0.20	LANSDOWNE	2.15	1.30	0.20	
PINELANDS	1.41	1.45	1.15	0.25	CRAWFORD	2.00	1.15	0.20	
HAZENDAL	1.91	2.30	1.45	0.20	ATHLONE	2.00	1.15	0.30	
ATHLONE	1.08	2.00	1.00	0.20	HAZENDAL	1.45	1.00	0.20	
CRAWFORD	1.53	2.00	1.15	0.20	PINELANDS	2.30	1.45	0.30	
LANSDOWNE	1.27	2.00	1.15	0.20	N'DABENI	2.00	1.00	0.20	
WETTON	1.63	2.15	1.30	0.20	MAITLAND	2.45	1.45	0.30	
OTTERY	1.39	2.00	1.15	0.20	KOEBERG RD	1.45	1.30	0.20	
SOUTHFIELD	2.53	3.00	2.15	0.20	SALT RIVER	2.00	1.15	0.30	
HEATHFIELD	2.30	4.00	3.15	0.30	WOODSTOCK	3.15	2.30	0.20	
RETREAT	1.57	1.45	1.30	0.30	CAPE TOWN	3.15	2.15	0.20	
	23.79	33.40	22.85	3.15		34.70	22.45	3.30	

Table F.2: Official Metrorail running times for Northern Lines (1 of 2) [99]

## CAPE METRORAIL: TRAIN RUNNING TIMES

STATIONS	KILOMETRE DISTANCE	ALL STATION TRAINS	EXPRESS TRAINS	DWELL TIMES	STATIONS	ALL STATION TRAINS	EXPRESS TRAINS	DWELL TIMES	
CAPE TOWN					WELLINGTON				
ESPLANADE	2.02	3.15	2.45	0.30	MBEKWENI	5.00	4.30	0.45	
YSTERPLAAT	2.94	4.45	3.15	0.45	DAL JOSAFAT	4.30	2.30	0.30	
WOLTEMADE	3.77	4.30	3.45	0.30	HUGUENOT	3.15	2.00	0.30	
					PAARL	4.15	3.15	0.30	
WOODSTOCK	1.97	3.00	2.45	0.30	KLAPMUTS	9.30	8.30	0.30	
SALT RIVER	1.75	3.30	2.15	1.00	MULDERSVLEI	6.15	4.30	0.30	
KOEBERG RD	1.31	1.45	1.15	0.30	KRAAIFONTEIN	10.00	8.00	1.00	
MAITLAND	0.8	2.00	1.15	0.30	EIKENFONTEIN	2.15	1.15	0.45	
WOLTEMADE	1.92	2.30	2.3	0.30	BRACKENFELL	4.00	2.30	0.30	
MUTUAL	0.64	1.15	1	0.45	STIKLAND	4.15	3.00	0.45	
THORNTON	1.68	2.15	1.3	0.30	BELLVILLE	3.30	2.45	1.00	
GOODWOOD	1.49	2.00	1.15	0.30	TYGERBERG	3.30	3.00	0.45	
VASCO	1.08	1.45	1.3	0.30	PAROW	2.00	1.15	0.30	
ELSIES RIVER	0.99	1.45	1	0.30	ELSIES RIVER	2.00	1.15	0.45	
PAROW	1.58	2.15	1.3	0.30	VASCO	1.30	1.00	0.30	
TYGERBERG	1.46	2.00	1	0.30	GOODWOOD	1.45	1.30	0.30	
BELLVILLE	2.42	3.15	3	1.00	THORNTON	2.00	1.15	0.30	
STIKLAND	2.82	3.45	3.15	0.45	MUTUAL	2.00	1.15	0.45	
BRACKENFELL	3.83	3.45	2.45	0.45	WOLTEMADE	1.15	1.15	0.30	
EIKENFONTEIN	3.47	4.00	2.45	0.45	MAITLAND	2.30	1.45	0.45	
KRAAIFONTEIN	1.67	2.15	1.15	1.00	KOEBERG RD	1.45	1.15	0.30	
MULDERSVLEI	10.21	10.00	8.3	0.45	SALT RIVER	1.45	1.15	1.00	
KLAPMUTS	5.8	5.30	4.3	0.30	WOODSTOCK	2.45	2.30	0.30	
PAARL	10.69	8.30	8	0.30	CAPE TOWN	3.45	3.15		
HUGUENOT	4.24	4.00	3	0.30					
DAL JOSAFAT	2.53	3.00	2	0.30	YSTERPLAAT	5.45	5.00	0.30	
MBEKWENI	3.58	3.30	2.45	0.30	ESPLANADE	4.45	3.00	0.30	
WELLINGTON	4.53	4.30	4	0.00	CAPE TOWN	3.45	3.30		
VIA ESP	73.44	78.65	61.35	8.60		84.20	63.60	8.60	
VIA SRX	72.46	78.80	61.50	9.75		81.95	61.50	10.05	
<b>BELLVILLE - STRAND</b>					<b>STRAND - BELLVILLE</b>				
BELLVILLE					STRAND				
KUILS RIVER	5.83	6.15	6	0.30	VAN DER STEL	5.00	4.30	0.30	
BLACKHEATH	4.08	4.15	3.3	0.30	SOMERSET W	3.00	2.00	0.30	
MELTONROSE	3	3.30	2.15	0.30	FIRGROVE	5.15	4.15	0.30	
EERSTE RIVER	2	2.30	1.3	1.00	FAURE	5.15	4.15	0.30	
FAURE	3.31	4.15	3.3	0.45	EERSTE RIVER	4.30	3.15	1.00	
FIRGROVE	5.54	5.30	5	0.45	MELTONROSE	2.30	1.30	0.45	
SOMERSET W	5.52	5.15	4.15	0.45	BLACKHEATH	4.00	2.30	0.45	
VAN DER STEL	1.78	2.30	2	0.30	KUILS RIVER	4.30	3.00	0.30	
STRAND	3.48	4.45	4.3		BELLVILLE	6.00	7.15	1.00	
	34.54	37.25	31.50	3.55		39.20	31.50	4.40	
<b>BELLVILLE - MULDERSVLEI VIA SCH</b>					<b>MULDERSVLEI - BELLVILLE VIA SCH</b>				
BELLVILLE					MULDERSVLEI				
KUILS RIVER	5.83	6.15	6	0.30	KOELLENHOF	4.30	4.00	0.30	
BLACKHEATH	4.08	4.15	3.3	0.30	DU TOIT	5.30	4.45	0.30	
MELTONROSE	3	3.30	2.15	0.30	STELLENBOSCH	2.30	1.30	0.30	
EERSTE RIVER	2	2.30	1.3	1.00	VLOTTENBURG	5.00	4.00	0.30	
LYNEDOCH	5.36	5.30	5	0.30	LYNEDOCH	3.30	2.45	0.30	
VLOTTENBURG	3.4	3.45	3	0.30	EERSTE RIVER	5.30	4.45	1.00	
STELLENBOSCH	5.27	5.30	4.3	0.30	MELTONROSE	2.30	1.30	0.45	
DU TOIT	1.77	2.30	1.45	0.30	BLACKHEATH	4.00	2.30	0.45	
KOELLENHOF	6.47	6.00	4.45	0.30	KUILS RIVER	4.30	3.00	0.30	
MULDERSVLEI	5.11	5.15	4.45		BELLVILLE	6.00	7.15	1.00	
	42.29	43.40	35.40	3.40		42.10	34.40	4.70	

Table F.3: Official Metrorail running times for Northern Lines (2 of 2) [99]

WELLINGTON - WORCESTER				WORCESTER - WELLINGTON			
WELLINGTON				1.00	WORCESTER		
MALAN	8.2	7.00		1.00	CHAVONNES	6.00	0.00
SOETENDAL	8.61	6.00		1.00	GOUDINI RD	5.00	1.00
HERMON	9.62	7.00		1.00	BOTHA	5.00	1.00
VOELVLEI	7.68	8.00		1.00	BREE RIVER	5.00	1.00
GOUDA	6.99	6.00		1.00	ROMANS RIVER	4.00	1.00
TULBAGH RD	8.63	9.00		1.00	WOLSELEY	7.00	1.00
ARTOIS	6.28	11.00		1.00	ARTOIS	5.00	1.00
WOLSELEY	4.84	7.00		1.00	TULBAGH RD	9.00	1.00
ROMANS RIVER		8.00		1.00	GOUDA	9.00	1.00
BREE RIVER		4.00		1.00	VOELVLEI	6.00	1.00
BOTHA		6.00		1.00	HERMON	8.00	1.00
GOUDINI RD		5.00		1.00	SOETENDAL	8.00	1.00
CHAVONNES		4.00		1.00	MALAN	7.00	1.00
WORCESTER		8.00		1.00	WELLINGTON	8.00	1.00
	60.85	96.00	0.00	13.00		92.00	0.00
							13.00

CAPE TOWN - BELLVILLE VIA MTV				BELLVILLE - CAPE TOWN VIA MTV			
CAPE TOWN				0.30	BELLVILLE		
ESPLANADE	2.02	3.15	3	0.30	OOSTERZEE	3.00	2.30
YSTERPLAAT	2.94	4.45	3.3	0.30	AVONDALE	2.30	1.45
KENTEMADE	2.05	3.15	2.3	0.30	DE GRENDDEL	2.00	1.15
AKASIAPARK	3.68	4.45	4	0.30	MONTE VISTA	3.00	2.00
MONTE VISTA	1.91	2.30	1.3	0.30	AKASIAPARK	2.30	1.30
DE GRENDDEL	2.9	3.15	2.15	0.30	KENTEMADE	4.15	3.30
AVONDALE	1.43	2.00	1.15	0.30	YSTERPLAAT	3.15	2.00
OOSTERZEE	1.32	2.00	1.15	0.30	ESPLANADE	4.45	3.15
BELLVILLE	2.17	3.00	2.15	0.30	CAPE TOWN	3.45	3.30
	20.42	27.65	20.50	2.40		27.80	19.95
							2.40

CAPE TOWN - BELLVILLE VIA MTV				MALMESBURY - KRAAIFONTEIN			
KRAAIFONTEIN				2.00	MALMESBURY		
FISANTKRAAL		8.00		2.00	ABBOTSDALE	5.00	1.00
MELLISH		4.00		1.00	KALBASKRAAL	11.00	1.00
MIKPUNT		5.00		1.00	WINTERVOGEL	8.00	1.00
KLIPHEUWEL		5.00		1.00	KLIPHEUWEL	9.00	1.00
WINTERVOGEL		10.00		1.00	MIKPUNT	4.00	2.00
KALBASKRAAL		10.00		1.00	MELLISH	7.00	1.00
ABBOTSDALE		12.00		1.00	FISANTKRAAL	6.00	1.00
MALMESBURY		8.00		1.00	KRAAIFONTEIN	12.00	1.00
	0	62.00		9.00		62.00	9.00



Table F.4: Official Metrorail running times for Central Lines [99]

## CAPE METRORAIL: TRAIN RUNNING TIMES

STATIONS	KILOMETRE DISTANCE	ALL STATION TRAINS	EXPRESS TRAINS	DWELL TIMES	STATIONS	ALL STATION TRAINS	EXPRESS TRAINS	DWELL TIMES	
CAPE TOWN					KAPTEINSKLIP				
ESPLANADE	2.02	3.15	2.45	0.30	M' PLAIN	3.00	2.00	0.30	
YSTERPLAAT	2.94	4.45	3.15	0.30	LENTEGEUR	2.30	1.30	0.30	
MUTUAL	4.41	5.45	4.45	1.00	PHILIPPI	4.00	2.45	0.30	
LANGA	2.65	4.00	3.3	1.00	NYANGA	4.00	3.00	0.30	
WOODSTOCK	1.97	3.00	2.30	0.15	HEIDEVELD	3.00	2.15	0.30	
SALT RIVER	1.75	2.30	1.30	0.30	NETREG	2.30	1.30	0.30	
KOEBERG RD	1.31	1.45	1.15	0.15	BONTHEUWEL	2.30	1.45	0.30	
MAITLAND	0.8	1.30	0.45	0.30	LANGA	3.00	2.00	1.00	
N'DABENI	1.34	2.30	1.45	0.30	PINELANDS	5.15	4.45	0.30	
PINELANDS	1.41	1.45	1.00	0.30	N'DABENI	2.00	1.00	0.30	
LANGA	4.7	5.15	4.30	1.00	MAITLAND	2.30	1.45	0.30	
BONTHEUWEL	1.94	3.00	2.30	1.00	KOEBERG RD	1.30	0.45	0.15	
NETREG	2.08	2.30	1.45	0.30	SALT RIVER	1.45	1.15	0.30	
HEIDEVELD	1.88	2.30	1.30	0.30	WOODSTOCK	3.00	2.45	0.30	
NYANGA	2.61	3.00	2.15	0.30	CAPE TOWN	3.15	3.45		
PHILIPPI	2.99	4.00	3.00	0.30	MUTUAL	3.45	3.00	1.00	
LENTEGEUR	3.81	3.45	2.45	1.00	YSTERPLAAT	5.00	4.00	0.30	
M' PLAIN	1.91	2.30	1.30	0.30	ESPLANADE	4.45	3.00	0.30	
KAPTEINSKLIP	2.94	2.30	2.30		CAPE TOWN	3.30	3.30		
TOT. VIA ESP	32.18	39.70	29.60	6.10	TOT. VIA ESP	40.10	28.95	4.70	
TOT. VIA SRX	33.44	39.60	28.20	6.00	TOT. VIA SRX	42.25	30.05	6.35	
LANGA - KHAYELITSHA					KHAYELITSHA - LANGA				
LANGA					KHAYELITSHA				
BONTHEUWEL	1.94	3.00	2.30	1.00	NONKQUBELA	3.00	2.15	1.00	
NETREG	2.08	3.30	2.45	0.30	NOLUNGILE	2.30	1.45	1.00	
HEIDEVELD	1.88	2.30	1.30	0.30	MANDALAY	2.45	1.45	1.00	
NYANGA	2.61	3.00	2.15	0.30	STOCK ROAD	1.75	1.30	1.00	
PHILIPPI	2.99	4.00	3.00	0.30	PHILIPPI	1.79	1.30	0.30	
STOCK ROAD	1.79	2.15	2.00	0.30	NYANGA	4.00	3.00	0.30	
MANDALAY	1.754	2.00	1.30	1.00	HEIDEVELD	3.00	2.15	0.30	
NOLUNGILE	1.97	2.45	1.45	1.00	NETREG	2.30	1.45	0.30	
NONKQUBELA	2.45	2.30	1.30	1.00	BONTHEUWEL	3.30	2.45	1.00	
KHAYELITSHA	2.45	3.45	3.00		LANGA	3.00	2.45		
	21.914	27.95	20.25	5.50		26.89	19.15	6.20	
LANGA - BELLVILLE VIA SAREPTA					BELLVILLE - LANGA VIA SAREPTA				
LANGA					BELLVILLE				
BONTHEUWEL	1.94	3.00	2.30	1.00	SAREPTA	6.30	6.15	0.30	
LAVISTOWN	3.12	3.30	2.45	0.30	PENTECH	2.30	2.00	0.30	
BELHAR	2.39	3.00	2.00	0.30	UNIBELL	2.15	1.30	0.30	
UNIBELL	1.83	2.15	1.30	0.30	BELHAR	2.15	1.30	0.30	
PENTECH	1.63	2.15	1.30	0.30	LAVISTOWN	2.45	2.00	0.30	
SAREPTA	1.95	2.30	2.15	0.30	BONTHEUWEL	3.15	2.30	1.00	
BELLVILLE	4.43	6.15	6.00		LANGA	3.00	2.30		
	17.29	22.05	17.50	2.50		21.50	17.35	2.50	

Table F.5: Official SARCC version of running times for Southern Lines [99]

Distances in kilometres and running times of Electric Motor coach sets  
Running times reflect tested passenger trains stopping at all stations.

Distance Kilometres	Cape Town - Simon's Town - Cape Town					
	Point to point	From Cape Town	Stations Down	Running times, point to point	Stations Up	Running times, point to point
	Km	Km		Minutes		Minutes
		0.00	<b>CAPE TOWN</b>		<b>SIMON'S TOWN</b>	
1.97	1.97	1.97	Woodstock	3.05	Glencairn	4.50
1.75	3.72	3.72	<b>SALT RIVER</b>	3.30	Sunny Cove	4.35
1.46	5.18	5.18	Observatory	2.50	<b>FISH HOEK</b>	2.35
1.00	6.18	6.18	Mowbray	2.05	Kalk Bay	4.50
0.89	7.07	7.07	Rosebank	2.05	St James	2.05
0.83	7.90	7.90	Rondebosch	1.50	<b>MUIZENBERG</b>	2.35
1.42	9.32	9.32	Newlands	2.35	False Bay	1.50
0.84	10.16	10.16	Claremont	2.00	Lakeside	2.35
0.85	11.01	11.01	Harfield Road	1.50	Steenberg	2.20
0.78	11.79	11.79	Kenilworth	1.50	Retreat	2.00
1.09	12.88	12.88	<b>WYNBERG</b>	2.20	Heathfield	3.30
1.05	13.93	13.93	Wittebome	2.05	Diep River	2.05
0.90	14.83	14.83	Plumstead	2.00	Steurhof	1.35
0.76	15.59	15.59	Steurhof	1.50	Plumstead	1.50
0.76	16.35	16.35	Diep River	1.50	Wittebome	1.50
1.18	17.53	17.53	Heathfield	2.45	<b>WYNBERG</b>	2.15
1.57	19.10	19.10	Retreat	2.45	Kenilworth	2.05
1.87	20.97	20.97	Steenberg	2.35	Harfield Road	1.50
1.31	22.28	22.28	Lakeside	2.20	Claremont	2.00
1.68	23.96	23.96	False Bay	2.35	Nuweland	1.50
0.82	24.78	24.78	<b>MUIZENBERG</b>	1.50	Rondebosch	2.20
1.41	26.19	26.19	St James	2.35	Rosebank	1.50
1.09	27.28	27.28	Kalk Bay	2.05	Mowbray	2.05
2.40	29.68	29.68	<b>FISH HOEK</b>	5.05	Observatory	1.50
1.11	30.79	30.79	Sunny Cove	2.35	<b>SALT RIVER</b>	3.15
2.55	33.34	33.34	Glencairn	5.05	Woodstock	2.35
2.71	36.05	36.05	<b>SIMON'S TOWN</b>	4.00	<b>CAPE TOWN</b>	3.15
			<b>OBSERVATORY</b>		<b>MAITLAND</b>	
2.62			<b>MAITLAND</b>	5.00	<b>OBSERVATORY</b>	5.00
Distance Kilometres	Cape Town - Retreat (Cape Flats)					
	Point to point	From Cape Town	Stations Down	Running times, point to point	Stations Up	Running times, point to point
	Km	Km		Minutes		Minutes
		0.00	<b>CAPE TOWN</b>		<b>RETREAT</b>	
1.97	1.97	1.97	Woodstock	3.20	Heathfield	3.00
1.75	3.72	3.72	<b>SALT RIVER</b>	3.00	Southfield	3.50
1.31	5.03	5.03	Koeberg Road	2.05	Ottery	3.20
0.8	5.83	5.83	<b>MAITLAND</b>	2.30	Wetton	2.20
1.34	7.17	7.17	Ndabeni	2.50	Lansdowne	2.35
1.41	8.58	8.58	Pinelands	2.10	Crawford	2.20
1.91	10.49	10.49	Hazendal	2.50	Athlone	2.30
1.08	11.57	11.57	Athlone	2.20	Hazendal	2.05
1.53	13.10	13.10	Crawford	2.20	Pinelands	3.00
1.27	14.37	14.37	Lansdowne	2.20	Ndabeni	2.20
1.63	16.00	16.00	Wetton	2.35	<b>MAITLAND</b>	3.15
1.39	17.39	17.39	Ottery	2.20	Koeberg Road	2.05
2.53	19.92	19.92	Southfield	3.20	<b>SALT RIVER</b>	2.30
2.3	22.22	22.22	Heathfield	4.30	Woodstock	3.35
1.57	23.79	23.79	<b>RETREAT</b>	1.45	<b>CAPE TOWN</b>	3.15

Table F.6: Official SARCC version of running times for Northern Lines (1 of 2) [99]

Distances in kilometres and running times of Electric Motor coach sets  
Running times reflect tested passenger trains stopping at all stations.

Distance Kilometres	Cape Town - Mutual - Monte Vista - Bellville - Wellington					
	Point to point Km	From Cape Town Km	Stations Down	Running times, point to point Minutes	Stations Up	Running times, point to point Minutes
		0.00	<b>CAPE TOWN</b>		<b>WELLINGTON</b>	
2.02	2.02		Esplanade	3.30	Mbekweni	5.30
1.11	3.13		<i>Bay Junction</i>	2.00	Dal Josafat	4.45
0.86	3.99		Paardeneiland	1.00	Huguenot	3.45
0.97	4.96		Ysterplaat	2.00	Paarl	4.30
1.25	6.21		<i>Kensington</i>	1.00	Klapmuts	9.45
2.52	8.73		Woltemade	3.45	Muldersvlei	6.30
1.97	1.97		Woodstock	3.00	<b>KRAAIFONTEIN</b>	9.00
1.75	3.72		<b>SALT RIVER</b>	3.30	Eikenfontein	2.45
1.31	5.03		Koeberg Rd	2.00	Brackenfell	4.15
0.80	5.83		Maitland	2.30	Stikland	4.30
1.92	7.75		Woltemade	2.45	<b>BELLVILLE</b>	4.30
0.64	8.39		Mutual	1.45	Tygerberg	3.45
1.68	10.07		Thornton	2.30	Parow	2.30
1.49	11.56		Goodwood	2.15	Elsies River	2.30
1.08	12.64		Vasco	2.00	Vasco	1.45
0.99	13.63		Elsies River	2.15	Goodwood	2.00
1.58	15.21		Parow	2.45	Thornton	2.15
1.46	16.67		Tygerberg	2.15	Mutual	2.30
2.42	19.09		<b>BELLVILLE</b>	4.00	Woltemade	1.30
2.82	21.91		Stikland	4.00	Maitland	3.00
3.83	25.74		Brackenfell	4.00	Koeberg Rd	2.00
3.47	29.21		Eikenfontein	4.30	<b>SALT RIVER</b>	2.15
1.67	30.88		<b>KRAAIFONTEIN</b>	2.45	Woodstock	3.00
10.21	41.09		Muldersvlei	9.45	<b>CAPE TOWN</b>	3.15
5.80	46.89		Klapmuts	5.45	Woltemade	
10.69	57.58		Paarl	8.45	<i>Kensington</i>	3.45
4.24	61.82		Huguenot	5.00	Ysterplaat	2.30
2.53	64.35		Dal Josafat	3.15	Paardeneiland	2.00
3.58	67.93		Mbekweni	4.00	<i>Bay Junction</i>	1.00
4.53	72.46		<b>WELLINGTON</b>	4.45	Esplanade	2.00
<i>Ex CPT</i>	6.21		<i>Kensington</i>		<b>CAPE TOWN</b>	3.45
0.86	7.07		Kentemade	2.30	<b>BELLVILLE</b>	
2.65	9.72		<i>Windermere</i>	3.00	Oosterzee	3.15
1.03	10.75		Akasia Park	2.00	Avondale	2.45
1.91	12.66		Monte Vista	3.00	De Grendel	2.15
2.90	15.56		De Grendel	3.30	Monte Vista	3.15
1.43	16.99		Avondale	2.15	Akasia Park	2.45
1.32	18.31		Oosterzee	2.15	<i>Windermere</i>	2.00
2.17	20.48		<b>BELLVILLE</b>	2.45	Kentemade	2.30
					<i>Kensington</i>	1.00
			<b>MAITLAND</b>		<b>KENSINGTON</b>	
4.44			<b>KENSINGTON</b>	5.00	<b>MAITLAND</b>	5.00

Table F.7: Official SARCC version of running times for Northern Lines (2 of 2) [99]

Distance Kilometres	<b>Bellville - Eerste River - Muldersvlei</b>				
Point to point	From Cape Town	Stations Down	Running times, point to point	Stations Up	Running times, point to point
Km	Km		Minutes		Minutes
	0.00	<b>BELLVILLE</b>		<b>MULDERSVLEI</b>	
2.87	2.87	<i>Kasselsvlei Junction</i>	3.00	Koelenhof	4.45
2.96	5.83	Kuils River	3.30	Du Toit	5.45
4.08	9.91	Blackheath	4.45	Stellenbosch	2.45
3.00	12.91	Melton Rose	4.00	Vlottenburg	5.15
2.00	14.91	<b>EERSTE RIVER</b>	3.00	Lynedoch	3.45
5.36	20.27	Lynedoch	5.45	<b>EERSTE RIVER</b>	5.45
3.40	23.67	Vlottenburg	4.00	Melton Rose	2.30
5.27	28.94	Stellenbosch	5.45	Blackheath	4.15
1.77	30.71	Du Toit	2.45	Kuils River	4.30
6.47	37.18	Koelenhof	6.15	<i>Kasselsvlei Junction</i>	3.30
5.11	42.29	<b>MULDERSVLEI</b>	5.15	<b>BELLVILLE</b>	4.15

Distance Kilometres	<b>Eerste River - Strand</b>				
Point to point	From Cape Town	Stations Down	Running times, point to point	Stations Up	Running times, point to point
Km	Km		Minutes		Minutes
	0.00	<b>EERSTE RIVER</b>		<b>STRAND</b>	
3.31	3.31	Faure	4.30	Van der Stel	5.00
5.54	8.85	Firgrove	6.00	Somerset West	3.15
5.52	14.37	Somerset West	5.45	Firgrove	5.45
1.78	16.15	Van der Stel	2.45	Faure	5.30
3.48	19.63	<b>STRAND</b>	4.45	<b>EERSTE RIVER</b>	4.30

Distance Kilometres	<b>Wellington - Worcester</b>				
Point to point	From Cape Town	Stations Down	Running times, point to point	Stations Up	Running times, point to point
Km	Km		Minutes		Minutes
	0.00	<b>WELLINGTON</b>		<b>WORCESTER</b>	
8.20	8.20	Malan	6.30	Chavonnes	
8.61	16.81	Soetendal	7.00	Goudini Rd	
9.62	26.43	Hermon	8.15	Botha	
7.68	34.11	Voelvrei	8.45	Bree River	
6.99	41.10	Gouda	6.45	Romans River	
8.63	49.73	Tulbaghweg	9.00	Wolseley	
6.28	56.01	Artois	11.00	Artois	7.00
4.84	60.85	Wolseley	6.45	Tulbaghweg	10.45
		Romans River		Gouda	8.45
		Bree River		Voelvrei	6.30
		Botha		Hermon	9.30
		Goudini Rd		Soetendal	9.15
		Chavonnes		Malan	8.15
		<b>WORCESTER</b>		<b>WELLINGTON</b>	8.00

Table F.8: Official SARCC version of running times for Central Lines [99]

Distances in kilometres and running times of Electric Motor coach sets  
Running times reflect tested passenger trains stopping at all stations.

Distance Kilometres	Cape Town - Langa - Kapteinsklip - Khayelitsha					
	Point to point Km	From Cape Town Km	Stations Down	Running times, point to point Minutes	Stations Up	Running times, point to point Minutes
	0.00		<b>CAPE TOWN</b>			
2.02	2.02		Esplanade	3.30	<b>KHAYELITSHA</b>	
1.11	3.13		<i>Bay Junction</i>	2.00	Nonkqubela	3.30
0.86	3.99		Paardeneiland	1.00	Nolungile	3.00
0.97	4.96		Ysterplaat	2.00	Mandalay	3.00
1.25	5.24		<i>Kensington</i>	1.30	Stock Road	2.00
3.16	8.40		Mutual	4.45	<b>PHILIPPI</b>	2.15
2.65	11.05		<b>LANGA</b>	5.00	<b>BELLVILLE</b>	
1.97	1.97		Woodstock	3.15	<i>Kasselsvlei Junction</i>	4.15
1.75	3.72		Salt River	3.00	Sarepta	2.30
1.31	5.03		Koeberg Road	2.00	Pentech	3.00
0.8	5.83		<b>MAITLAND</b>	2.00	Unibell	2.30
2.56	8.39		Mutual	5.30	Belhar	2.45
2.65	11.04		<b>LANGA</b>	5.00	Lavistown	3.15
5.83	5.83		<b>MAITLAND</b>		Bontheuwel	3.45
1.34	7.17		Ndabeni	3.00	<b>LANGA</b>	3.00
1.41	8.58		Pinelands	2.15	<b>KAPTEINSKLIP</b>	
4.7	13.28		<b>LANGA</b>	6.15	Mitchell's Plain	3.30
			<b>LANGA</b>		Lentegeur	3.00
1.94	1.94		Bontheuwel	3.30	<b>PHILIPPI</b>	4.30
2.08	4.02		Netreg	3.00	Nyanga	4.30
1.88	5.90		Heideveld	3.00	Heideveld	3.30
2.61	8.51		Nyanga	3.30	Netreg	3.00
2.99	11.50		<b>PHILIPPI</b>	4.30	Bontheuwel	3.00
3.81	15.31		Lentegeur	4.15	<b>LANGA</b>	4.00
1.91	17.22		Mitchell's Plain	3.00	<b>LANGA</b>	
2.94	20.16		<b>KAPTEINSKLIP</b>	2.30	Pinelands	5.45
			<b>LANGA</b>		Ndabeni	2.30
1.94	1.94		Bontheuwel	3.30	<b>MAITLAND</b>	3.00
3.12	5.06		Lavistown	4.00	<b>LANGA</b>	
2.39	7.45		Belhar	3.30	Mutual	4.15
1.83	9.28		Unibell	2.30	<b>MAITLAND</b>	5.30
1.63	10.91		Pentech	2.30	Koeberg Rd	1.45
1.95	12.86		Sarepta	2.45	Salt River	2.15
1.56	14.42		<i>Kasselsvlei Junction</i>	2.30	Woodstock	3.30
2.87	17.29		<b>BELLVILLE</b>	3.45	<b>CAPE TOWN</b>	3.15
			<b>PHILIPPI</b>		<b>LANGA</b>	
1.79	1.79		Stock Road	2.15	Mutual	4.15
1.754	3.544		Mandalay	2.00	<i>Kensington</i>	3.00
2.27	5.81		Nolungile	3.15	Ysterplaat	2.15
1.97	7.78		Nonkqubela	3.00	Paardeneiland	2.00
2.45	10.23		<b>KHAYELITSHA</b>	3.45	<i>Bay Junction</i>	1.00
					Esplanade	2.00
					<b>CAPE TOWN</b>	3.30

Table F.9: Running times from 1973 and amended version of Metrorail running times for Southern Lines

CAPE METRORAIL: TRAIN RUNNING TIMES													
REWORKED FROM: DOCS_CM3-#158294-v1-TRAIN_RUNNING_TIMES.XLS													
STATION	ABBR	KM DIST	EXP	RUN TIME	SAR 73/74	STOP TIME	RUN & STOP	STATION	EXP	RUN TIME	SAR 73/74	STOP TIME	RUN & STOP
KAAPSTAD - SIMONSTAD VIA WYNBERG								SIMONSTAD - KAAPSTAD VIA WYNBERG					
KAAPSTAD	CWN							SIMONSTAD					
WOODSTOCK	WDC	1.97	2.50	2.75	3.00	0.33	3.08	GLENCAIRN	4.50	4.50	3.25	0.33	4.83
SOUTRIVIER	SRX	1.75	2.00	3.00	2.25	0.50	3.50	SUNNY COVE	3.75	4.25	3.75	0.33	4.58
OBSERVATORY	OVY	1.46	1.75	2.50	2.25	0.33	2.83	VISHOEK	1.50	2.25	1.75	0.33	2.58
MOWBRAY	MWY	1.00	1.00	1.75	1.50	0.33	2.08	KALKBAAI	3.50	4.50	4.00	0.33	4.83
ROSEBANK	RSN	0.89	0.75	1.75	1.50	0.33	2.08	ST JAMES	1.25	1.75	1.75	0.33	2.08
RONDEBOSCH	RCH	0.83	0.75	1.50	1.25	0.33	1.83	MUIZENBERG	1.50	2.25	2.00	0.33	2.58
NUWELAND	NDL	1.42	1.25	2.25	2.25	0.33	2.58	VALSBAAI	1.00	1.50	1.50	0.33	1.83
CLAREMONT	CMC	0.84	0.75	1.50	1.25	0.50	2.00	LAKESIDE	1.50	2.25	2.00	0.33	2.58
HARFIELD ROAD	HRD	0.85	0.75	1.50	1.50	0.33	1.83	STEENBERG	1.25	2.00	2.00	0.33	2.33
KENILWORTH	KLW	0.78	1.00	1.50	1.50	0.33	1.83	RETREAT	1.25	2.50	2.75	0.50	3.00
WYNBERG	WYB	1.09	1.00	1.75	2.00	0.58	2.33	HEATHFIELD	2.00	2.00	2.25	0.50	2.50
WITTEBOME	WTE	1.05	1.00	1.75	1.75	0.33	2.08	DIEPRIVIER	1.25	1.75	1.50	0.33	2.08
PLUMSTEAD	PMS	0.90	0.75	1.50	1.50	0.50	2.00	STEURHOF	0.75	1.25	1.25	0.33	1.58
STEURHOF	STH	0.76	0.75	1.50	1.50	0.33	1.83	PLUMSTEAD	0.75	1.50	1.50	0.33	1.83
DIEPRIVIER	DPE	0.76	0.75	1.50	1.00	0.33	1.83	WITTEBOME	1.00	1.50	1.75	0.33	1.83
HEATHFIELD	HEH	1.18	1.50	2.25	1.50	0.50	2.75	WYNBERG	1.00	1.75	2.00	0.50	2.25
RETREAT	RET	1.57	1.50	2.25	2.25	0.50	2.75	KENILWORTH	1.25	1.75	1.75	0.33	2.08
STEENBERG	STX	1.87	1.75	2.25	2.25	0.33	2.58	HARFIELD RD	0.75	1.50	1.50	0.33	1.83
LAKESIDE	LSD	1.31	1.25	2.00	1.75	0.33	2.33	CLAREMONT	0.75	1.50	1.50	0.50	2.00
VALSBAAI	VSB	1.68	1.75	2.25	2.25	0.33	2.58	NUWELAND	0.75	1.50	1.25	0.33	1.83
MUIZENBERG	MZM	0.82	1.00	1.50	1.50	0.33	1.83	RONDEBOSCH	1.25	2.00	2.00	0.33	2.33
ST JAMES	STJ	1.41	1.75	2.25	2.00	0.33	2.58	ROSEBANK	0.75	1.50	1.25	0.33	1.83
KALKBAAI	KAB	1.09	1.25	1.75	1.75	0.33	2.08	MOWBRAY	0.75	1.75	1.50	0.33	2.08
VISHOEK	VSK	2.40	4.25	4.75	4.00	0.33	5.08	OBSERVATORY	0.75	1.50	1.50	0.33	1.83
TOTAL VISHOEK		29.68	32.75	49.25	45.25	8.75	58.00	SOUTRIVIER	1.75	2.25	2.00	0.50	2.75
SUNNY COVE	SYE	1.11	2.00	2.25	1.75	0.33	2.58	WOODSTOCK	2.00	2.25	2.50	0.33	2.58
GLENCAIRN	GCR	2.55	3.75	4.75	3.75	0.33	5.08	KAAPSTAD	3.00	3.75	3.25		3.75
SIMONSTAD	STW	2.71	4.25	4.00	4.00		4.00	TOTAL STW	41.50	58.75	55.00	9.50	68.25
TOTAL SIMONSTAD		36.05	42.75	60.25	54.75	9.75	70.00	TOTAL VSK	31.75	47.75	46.25	8.50	56.25
STATION	ABBR	KM DIST	EXP	RUN TIME	SAR 73/74	STOP TIME	RUN & STOP	STATION	EXP	RUN TIME	SAR 73/74	STOP TIME	RUN & STOP
KAAPSTAD - RETREAT VIA KAAPSE VLAKTE								RETREAT - KAAPSTAD VIA VLAKTE					
KAAPSTAD	CWN							RETREAT					
WOODSTOCK	WDC	1.97	2.50	3.00	3.25	0.33	3.33	HEATHFIELD	1.50	2.50	2.25	0.50	3.00
SOUTRIVIER	SRX	1.75	1.50	2.50	2.25	0.50	3.00	SOUTHFIELD	2.75	3.50	3.00	0.33	3.83
KOEBERGWEG	KOB	1.31	1.25	1.75	1.50	0.33	2.08	OTTERY	2.25	3.00	3.00	0.33	3.33
MAITLAND	MLD	0.80	1.25	2.00	1.50	0.50	2.50	WETTON	1.25	2.00	1.75	0.33	2.33
NDABENI	NBI	1.34	2.00	2.50	2.00	0.33	2.83	LANSDOWNE	1.50	2.25	2.00	0.33	2.58
PINELANDS	PND	1.41	1.25	1.75	2.00	0.42	2.17	CRAWFORD	1.25	2.00	1.75	0.33	2.33
HAZENDAL	HAZ	1.91	1.75	2.50	2.75	0.33	2.83	ATHLONE	1.25	2.00	2.00	0.50	2.50
ATHLONE	ATL	1.08	1.00	2.00	1.50	0.33	2.33	HAZENDAL	1.00	1.75	1.50	0.33	2.08
CRAWFORD	CRF	1.53	1.25	2.00	2.00	0.33	2.33	PINELANDS	1.75	2.50	2.75	0.50	3.00
LANSDOWNE	LNE	1.27	1.25	2.00	1.75	0.33	2.33	NDABENI	1.00	2.00	2.00	0.33	2.33
WETTON	WTN	1.63	1.50	2.25	2.00	0.33	2.58	MAITLAND	1.75	2.75	2.00	0.50	3.25
OTTERY	OTY	1.39	1.25	2.00	1.75	0.33	2.33	KOEBERG RD	1.50	1.75	1.50	0.33	2.08
SOUTHFIELD	SFS	2.53	2.25	3.00	3.00	0.33	3.33	SOUTRIVIER	1.25	2.00	1.50	0.50	2.50
HEATHFIELD	HEH	2.30	3.25	4.00	3.00	0.50	4.50	WOODSTOCK	2.50	3.25	2.25	0.33	3.58
TOTAL HEATHFIELD		22.22	23.25	33.25	30.25	4.75	38.00	KAAPSTAD	2.25	3.25	3.25		3.25
RETREAT	RET	1.57	1.50	1.75	2.25		1.75	TOTAL RET	24.75	36.50	32.50	5.50	42.00
TOTAL RETREAT		23.79	24.75	35.00	32.50	5.25	40.25	TOTAL HEH	23.25	34.00	30.25	5.00	39.00

Table F.10: Running times from 1973 and amended version of Metrorail running times for Northern Lines (1 of 2)

STATION	ABBR	KM DIST	EXP	RUN TIME	SAR 73/74	STOP TIME	RUN & STOP	STATION	EXP	RUN TIME	SAR 73/74	STOP TIME	RUN & STOP
KAAPSTAD - WELLINGTON VIA KRAAIFONTEIN								WELLINGTON - KAAPSTAD VIA KRAAIFONTEIN					
KAAPSTAD	CWN							WELLINGTON					
WOODSTOCK	WDC	1.97	2.75	3.25	3.25	0.50	3.75	MBEKWENI	4.50	5.00	3.50	0.75	5.75
SOUTRIVIER	SRX	1.75	2.25	3.25	2.25	1.00	4.25	DAL JOSAFAT	2.50	4.50	3.50	0.50	5.00
KOEBERGWEG	KOB	1.31	1.25	1.75	1.50	0.50	2.25	HUGUENOT	2.00	3.25	3.50	0.50	3.75
MAITLAND	MLD	0.80	1.25	2.00	1.25	0.50	2.50	PAARL	3.25	4.25	4.00	0.50	4.75
WOLTEMADE	WTM	1.92	2.50	2.50	2.00	0.50	3.00	KLAPMUTS	8.50	9.50	9.50	0.50	10.00
MUTUAL	MTX	0.64	1.00	1.25	1.25	0.75	2.00	MULDERSVLEI	4.50	6.25	5.00	0.50	6.75
THORNTON	THO	1.68	1.50	2.25	2.00	0.50	2.75	KRAAIFONTEIN	8.00	10.00	8.25	1.00	11.00
GOODWOOD	GDX	1.49	1.25	2.00	1.75	0.50	2.50	EIKENFONTEIN	1.25	2.25	2.50	0.75	3.00
VASCO	VSO	1.08	1.50	1.75	1.50	0.50	2.25	BRACKENFELL	2.50	4.00	3.75	0.50	4.50
ELSIESRIVIER	ERH	0.99	1.00	1.75	1.50	0.50	2.25	STIKLAND	3.00	4.25	3.50	0.75	5.00
PAROW	POW	1.58	1.50	2.25	2.00	0.50	2.75	BELLVILLE	2.75	3.50	3.00	1.00	4.50
TYGERBERG	TYG	1.46	1.00	2.00	1.75	0.50	2.50	TYGERBERG	3.00	3.50	3.00	0.75	4.25
BELLVILLE	BLE	2.42	3.00	3.25	3.50	1.00	4.25	PAROW	1.25	2.00	1.75	0.50	2.50
STIKLAND	SKD	2.82	3.25	3.75	3.00	0.75	4.50	ELSIES RIVER	1.25	2.00	2.00	0.75	2.75
BRACKENFELL	BKL	3.83	2.75	3.75	3.50	0.75	4.50	VASCO	1.00	1.50	1.50	0.50	2.00
EIKENFONTEIN	EIK	3.47	2.75	4.00	2.50	0.75	4.75	GOODWOOD	1.50	1.75	1.50	0.50	2.25
KRAAIFONTEIN	KAI	1.67	1.25	2.25	2.25	1.00	3.25	THORNTON	1.25	2.00	1.75	0.50	2.50
MULDERSVLEI	MUV	10.21	8.50	10.00	9.00	0.75	10.75	MUTUAL	1.25	2.00	2.00	0.75	2.75
KLAPMUTS	KLS	5.80	4.50	5.50	4.75	0.50	6.00	WOLTEMADE	1.25	1.25	1.00	0.50	1.75
PAARL	PAA	10.69	8.00	8.50	8.50	0.50	9.00	MAITLAND	1.75	2.50	2.50	0.75	3.25
HUGUENOT	HNT	4.24	3.00	4.00	3.75	0.50	4.50	KOEBERG RD	1.25	1.75	1.25	0.50	2.25
DAL JOSAFAT	DJT	2.53	2.00	3.00	2.50	0.50	3.50	SALT RIVER	1.25	1.75	1.50	1.00	2.75
MBEKWENI	MKW	3.58	2.75	3.50	3.50	0.50	4.00	WOODSTOCK	2.50	2.75	2.25	0.50	3.25
WELLINGTON	WEG	4.53	4.00	4.50	3.50		4.50	CAPE TOWN	3.25	3.75	3.25		3.75
<b>TOTAL WELLINGTON</b>		<b>72.46</b>	<b>64.50</b>	<b>82.00</b>	<b>72.25</b>	<b>14.25</b>	<b>96.25</b>	<b>TOTAL</b>	<b>64.50</b>	<b>85.25</b>	<b>75.25</b>	<b>14.75</b>	<b>100.00</b>
KAAPSTAD - STRAND VIA SOUTRIVIER								STRAND - KAAPSTAD VIA SOUTRIVIER					
KAAPSTAD	CWN							STRAND					
WOODSTOCK	WDC	1.97	2.75	3.25	3.25	0.50	3.75	VAN DER STEL	4.50	5.00	4.00	0.50	5.50
SOUTRIVIER	SRX	1.75	2.25	3.25	2.25	1.00	4.25	SOMERSET-WES	2.00	3.00	2.75	0.50	3.50
KOEBERGWEG	KOB	1.31	1.25	1.75	1.50	0.50	2.25	FIRGROVE	4.25	5.25	6.00	0.50	5.75
MAITLAND	MLD	0.80	1.25	2.00	1.25	0.50	2.50	FAURE	4.25	5.25	5.25	0.50	5.75
WOLTEMADE	WTM	1.92	2.50	2.50	2.00	0.50	3.00	EERSTE RIVER	3.25	4.50	3.50	1.00	5.50
MUTUAL	MTX	0.64	1.00	1.25	1.25	0.75	2.00	MELTONROSE	1.50	2.50	n/a	0.75	3.25
THORNTON	THO	1.68	1.50	2.25	2.00	0.50	2.75	BLACKHEATH	2.50	4.00	4.75	0.75	4.75
GOODWOOD	GDX	1.49	1.25	2.00	1.75	0.50	2.50	KUILS RIVER	3.00	4.50	4.00	0.50	5.00
VASCO	VSO	1.08	1.50	1.75	1.50	0.50	2.25	BELLVILLE	7.25	6.00	5.25	1.00	7.00
ELSIESRIVIER	ERH	0.99	1.00	1.75	1.50	0.50	2.25	TYGERBERG	3.00	3.50	3.00	0.75	4.25
PAROW	POW	1.58	1.50	2.25	2.00	0.50	2.75	PAROW	1.25	2.00	1.75	0.50	2.50
TYGERBERG	TYG	1.46	1.00	2.00	1.75	0.50	2.50	ELSIES RIVER	1.25	2.00	2.00	0.75	2.75
BELLVILLE	BLE	2.42	3.00	3.25	3.50	1.00	4.25	VASCO	1.00	1.50	1.50	0.50	2.00
KUILSRIVIER	KSV	5.83	6.00	6.25	5.50	0.50	6.75	GOODWOOD	1.50	1.75	1.50	0.50	2.25
BLACKHEATH	BKH	4.08	3.50	4.25	4.00	0.50	4.75	THORNTON	1.25	2.00	1.75	0.50	2.50
MELTON ROSE	MET	3.28	2.25	3.50	n/a	0.50	4.00	MUTUAL	1.25	2.00	2.00	0.75	2.75
EERSTERIVIER	EER	1.60	1.50	2.50	4.50	1.00	3.50	WOLTEMADE	1.25	1.25	1.00	0.50	1.75
<b>TOTAL EERSTERIVIER</b>		<b>33.88</b>	<b>35.00</b>	<b>45.75</b>	<b>39.50</b>	<b>9.25</b>	<b>55.00</b>	MAITLAND	1.75	2.50	2.50	0.75	3.25
FAURE	FAU	3.31	3.50	4.25	3.50	0.75	5.00	KOEBERG RD	1.25	1.75	1.25	0.50	2.25
FIRGROVE	FGV	5.54	5.00	5.50	5.25	0.75	6.25	SALT RIVER	1.25	1.75	1.50	1.00	2.75
SOMERSET-WES	SSW	5.52	4.25	5.25	6.00	0.75	6.00	WOODSTOCK	2.50	2.75	2.25	0.50	3.25
VAN DER STEL	VSL	1.78	2.00	2.50	2.75	0.50	3.00	CAPE TOWN	3.25	3.75	3.25		3.75
STRAND	STD	3.48	4.50	4.75	4.00		4.75	<b>TOTAL STRAND</b>	<b>54.25</b>	<b>68.50</b>	<b>60.75</b>	<b>13.50</b>	<b>82.00</b>
<b>TOTAL STRAND</b>		<b>53.51</b>	<b>54.25</b>	<b>68.00</b>	<b>61.00</b>	<b>13.00</b>	<b>81.00</b>	<b>TOTAL EER</b>	<b>36.00</b>	<b>45.50</b>	<b>39.25</b>	<b>10.50</b>	<b>56.00</b>

Table F.11: Running times from 1973 and amended version of Metrorail running times for Northern Lines (2 of 2)

KAAPSTAD - MULDERSVLEI VIA STELLENBOSCH								MULDERSVLEI - KAAPSTAD VIA SHC					
KAAPSTAD	CWN							MULDERSVLEI					
WOODSTOCK	WDC	1.97	2.75	3.25	3.25	0.50	3.75	KOELENHOF	4.00	4.50	5.00	0.50	5.00
SOUTRIVIER	SRX	1.75	2.25	3.25	2.25	1.00	4.25	DU TOIT	4.75	5.50	6.00	0.50	6.00
KOEBERGWEG	KOB	1.31	1.25	1.75	1.50	0.50	2.25	STELLENBOSCH	1.50	2.50	2.25	0.50	3.00
MAITLAND	MLD	0.80	1.25	2.00	1.25	0.50	2.50	VLOTTENBURG	4.00	5.00	5.00	0.50	5.50
WOLTEMADE	WTM	1.92	2.50	2.50	2.00	0.50	3.00	LYNEDOCH	2.75	3.50	3.50	0.50	4.00
MUTUAL	MTX	0.64	1.00	1.25	1.25	0.75	2.00	EERSTE RIVER	4.75	5.50	5.25	1.00	6.50
THORNTON	THO	1.68	1.50	2.25	2.00	0.50	2.75	MELTONROSE	1.50	2.50	n/a	0.75	3.25
GOODWOOD	GDX	1.49	1.25	2.00	1.75	0.50	2.50	BLACKHEATH	2.50	4.00	4.75	0.75	4.75
VASCO	VSO	1.08	1.50	1.75	1.50	0.50	2.25	KUILS RIVER	3.00	4.50	4.00	0.50	5.00
ELSIESRIVIER	ERH	0.99	1.00	1.75	1.50	0.50	2.25	BELLVILLE	7.25	6.00	5.25	1.00	7.00
PAROW	POW	1.58	1.50	2.25	2.00	0.50	2.75	TYGERBERG	3.00	3.50	3.00	0.75	4.25
TYGERBERG	TYG	1.46	1.00	2.00	1.75	0.50	2.50	PAROW	1.25	2.00	1.75	0.50	2.50
BELLVILLE	BLE	2.42	3.00	3.75	3.50	0.50	4.25	ELSIES RIVER	1.25	2.00	2.00	0.75	2.75
KUILSRIVIER	KSV	5.83	6.00	6.25	5.50	0.50	6.75	VASCO	1.00	1.50	1.50	0.50	2.00
BLACKHEATH	BKH	4.08	3.50	4.05	4.00	0.50	4.55	GOODWOOD	1.50	1.75	1.50	0.50	2.25
MELTON ROSE	MET	3.28	2.25	3.70	n/a	0.50	4.20	THORNTON	1.25	2.00	1.75	0.50	2.50
EERSTERIVIER	EER	1.60	1.50	2.50	4.50	1.00	3.50	MUTUAL	1.25	2.00	2.00	0.75	2.75
LYNEDOCH	LDH	5.36	5.00	5.50	5.25	0.50	6.00	WOLTEMADE	1.25	1.25	1.00	0.50	1.75
VLOTTENBURG	VOB	3.40	3.00	3.75	3.50	0.50	4.25	MAITLAND	1.75	2.50	2.50	0.75	3.25
STELLENBOSCH	SHC	5.27	4.50	5.50	5.25	0.50	6.00	KOEBERG RD	1.25	1.75	1.25	0.50	2.25
DU TOIT	DUT	1.77	1.75	2.50	2.25	0.50	3.00	SALT RIVER	1.25	1.75	1.50	1.00	2.75
KOELENHOF	KHF	6.47	4.75	6.25	6.25	0.25	6.50	WOODSTOCK	2.50	2.75	2.25	0.50	3.25
MULDERSVLEI	MUV	5.11	4.75	5.83	5.25		5.83	CAPE TOWN	3.25	3.75	3.25		3.75
<b>TOTAL MULDERSVLEI</b>		<b>61.26</b>	<b>58.75</b>	<b>75.58</b>	<b>67.25</b>	<b>12.00</b>	<b>87.58</b>	<b>TOTAL</b>	<b>57.75</b>	<b>72.00</b>	<b>66.25</b>	<b>14.00</b>	<b>86.00</b>
KAAPSTAD - BELLVILLE VIA MONTE VISTA								BELLVILLE - KAAPSTAD VIA MONTE VISTA					
KAAPSTAD	CWN							BELLVILLE					
ESPLANADE	EPD	2.02	3.00	3.25		0.50	3.75	OOSTERZEE	2.50	3.00		0.50	3.50
YSTERPLAAT	YPT	2.94	3.50	4.75		0.75	5.50	AVONDALE	1.75	2.00		0.50	2.50
KENTEMADE	KED	2.09	2.50	3.25		0.50	3.75	DE GRENDEL	1.25	2.00		0.50	2.50
CENTURY CITY	CEN	1.85		2.00		0.50	2.50	MONTE VISTA	2.00	3.00		0.50	3.50
AKASIAPARK	AKA	1.84	4.00	2.25		0.50	2.75	AKASIAPARK	1.50	2.50		0.50	3.00
MONTE VISTA	MNV	1.91	1.50	2.50		0.50	3.00	CENTURY CITY		2.00		0.50	2.50
DE GRENDEL	DEG	2.90	2.25	3.25		0.50	3.75	KENTEMADE	3.50	2.25		0.50	2.75
AVONDALE	AVD	1.43	1.25	2.00		0.50	2.50	YSTERPLAAT	2.00	3.25		0.50	3.75
OOSTERZEE	OOZ	1.32	1.25	2.00		0.50	2.50	ESPLANADE	3.25	4.75		0.50	5.25
BELLVILLE	BLE	2.10	2.25	3.00			3.00	CAPE TOWN	3.50	3.75			3.75
<b>TOTAL BELLVILLE</b>		<b>20.39</b>	<b>21.50</b>	<b>28.25</b>		<b>4.75</b>	<b>33.00</b>	<b>TOTAL</b>	<b>21.25</b>	<b>28.50</b>		<b>4.50</b>	<b>33.00</b>



Table F.12: Running times from 1973 and amended version of Metrorail running times for Central Lines

STATION	ABBR	KM DIST	EXP	RUN TIME	SAR 73/74	STOP TIME	RUN & STOP	STATION	EXP	RUN TIME	SAR 73/74	STOP TIME	RUN & STOP
KAAPSTAD - KAPTEINSKLIP VIA SOUTRIVIER								KAPTEINSKLIP - KAAPSTAD VIA SOUTRIVIER					
KAAPSTAD	CWN							KAPTEINSKLIP					
WOODSTOCK	WDC	1.97	2.50	3.00	3.25	0.25	3.25	M'PLAIN	2.00	3.00	3.00	0.50	3.50
SOUTRIVIER	SRX	1.75	1.50	2.50	2.25	0.50	3.00	LENTEGEUR	1.50	2.50	2.50	0.50	3.00
KOEBERGWEG	KOB	1.31	1.25	1.75	1.50	0.25	2.00	PHILIPPI	2.75	4.00	4.00	0.50	4.50
MAITLAND	MLD	0.80	0.75	1.50	1.50	0.50	2.00	NYANGA	3.00	4.00	4.00	0.50	4.50
NDABENI	NBI	1.34	1.75	2.50	2.00	0.50	3.00	HEIDEVELD	2.25	3.00	2.75	0.50	3.50
PINELANDS	PND	1.41	1.00	1.75	2.00	0.50	2.25	NETREG	1.50	2.50	2.00	0.50	3.00
LANGA	LAG	4.70	4.50	5.25	5.50	1.00	6.25	BONTHEUWEL	1.75	2.50	2.25	0.50	3.00
BONTHEUWEL	BTL	1.94	2.50	3.00	2.50	1.00	4.00	LANGA	2.00	3.00	2.50	1.00	4.00
NETREG	NTG	2.08	1.75	2.50	2.25	0.50	3.00	PINELANDS	4.75	5.25	5.50	0.50	5.75
HEIDEVELD	HED	1.88	1.50	2.50	2.00	0.50	3.00	N'DABENI	1.00	2.00	2.00	0.50	2.50
NYANGA	NAG	2.61	2.25	3.00	2.75	0.50	3.50	MAITLAND	1.75	2.50	2.00	0.50	3.00
PHILIPPI	PPI	4.01	3.00	4.00	4.00	0.50	4.50	KOEBERG RD	0.75	1.50	1.50	0.25	1.75
LENTEGEUR	LEN	3.82	2.75	3.75	3.75	1.00	4.75	SALT RIVER	1.25	1.75	1.50	0.50	2.25
MITCHELLS PLAIN	MTP	1.91	1.50	2.50	2.50	0.50	3.00	WOODSTOCK	2.75	3.00	2.25	0.50	3.50
KAPTEINSKLIP	KTE	1.93	2.50	2.50	2.50		2.50	CAPE TOWN	3.75	3.25	3.25		3.25
<b>TOTAL KAPTEINSKLIP</b>		<b>33.46</b>	<b>31.00</b>	<b>42.00</b>	<b>40.25</b>	<b>8.00</b>	<b>50.00</b>	<b>TOTAL</b>	<b>32.75</b>	<b>43.75</b>	<b>41.00</b>	<b>7.25</b>	<b>51.00</b>
KAAPSTAD - CHRIS HANI VIA ESPLANADE								CHRIS HANI - KAAPSTAD VIA ESPLANADE					
KAAPSTAD	CWN							CHRIS HANI					
ESPLANADE	EPD	2.02	2.75	3.25	3.50	0.50	3.75	KUYASA		5.00	5.00	0.50	5.50
YSTERPLAAT	YPT	2.94	3.25	4.75	4.50	0.50	5.25	KHAYELITSHA	7.00	3.50	3.50	0.50	4.00
MUTUAL	MTX	3.76	4.75	5.75	4.75	1.00	6.75	NONKQUBELA	2.25	3.00	3.00	1.00	4.00
LANGA	LAG	2.65	3.50	4.00	3.00	1.00	5.00	NOLUNGILE	1.75	2.50	2.50	1.00	3.50
BONTHEUWEL	BTL	1.94	2.50	3.00	2.50	1.00	4.00	MANDALAY	1.75	2.75	2.75	1.00	3.75
NETREG	NTG	2.08	2.75	3.50	2.25	0.50	4.00	STOCK ROAD	1.50	2.00	2.00	1.00	3.00
HEIDEVELD	HED	1.88	1.50	2.50	2.00	0.50	3.00	PHILIPPI	1.50	2.25	2.25	0.50	2.75
NYANGA	NAG	2.61	2.25	3.00	2.75	0.50	3.50	NYANGA	3.00	4.00	4.00	0.50	4.50
PHILIPPI	PPI	4.01	3.00	4.00	4.00	0.50	4.50	HEIDEVELD	2.25	3.00	2.75	0.50	3.50
STOCK ROAD	SKR	1.97	2.00	2.25	2.25	0.50	2.75	NETREG	1.75	2.50	2.00	0.50	3.00
MANDALAY	MCF	1.84	1.50	2.00	2.00	1.00	3.00	BONTHEUWEL	2.75	3.50	2.25	1.00	4.50
NOLUNGILE	NOL	2.27	1.75	2.75	2.75	1.00	3.75	LANGA	2.75	3.00	2.50	1.00	4.00
NONKQUBELA	NOQ	1.98	1.50	2.50	2.50	1.00	3.50	MUTUAL	3.00	3.75	3.00	1.00	4.75
KHAYELITSHA	KYA	2.44	3.00	3.75	3.75	0.50	4.25	YSTERPLAAT	4.00	5.00	4.75	0.50	5.50
<b>TOTAL KHAYELITSHA</b>		<b>34.39</b>	<b>36.00</b>	<b>47.00</b>	<b>42.50</b>	<b>9.50</b>	<b>56.50</b>	ESPLANADE	3.00	4.75	4.25	0.50	5.25
KUYASA	KUY	2.62	n/a	3.50	3.50	0.50	4.00	CAPE TOWN	3.50	3.50	3.50		3.50
CHRIS HANI	CRT	1.31	7.00	3.75	3.75	0.00	3.75	<b>TOTAL CRT</b>	<b>41.75</b>	<b>54.00</b>	<b>50.00</b>	<b>11.00</b>	<b>65.00</b>
<b>TOTAL CHRIS HANI</b>		<b>38.32</b>	<b>43.00</b>	<b>54.25</b>	<b>49.75</b>	<b>10.00</b>	<b>64.25</b>	<b>TOTAL KYA</b>	<b>34.75</b>	<b>45.50</b>	<b>41.50</b>	<b>10.00</b>	<b>55.50</b>
KAAPSTAD - BELLVILLE VIA LAVISTOWN								BELLVILLE - KAAPSTAD VIA LAVISTOWN					
KAAPSTAD	CWN							BELLVILLE					
ESPLANADE	EPD	2.02	2.75	3.25	3.50	0.50	3.75	SAREPTA	6.25	6.50	5.00	0.50	7.00
YSTERPLAAT	YPT	2.94	3.25	4.75	4.50	0.50	5.25	PENTECH	2.00	2.50	2.25	0.50	3.00
MUTUAL	MTX	3.76	4.75	5.75	4.75	1.00	6.75	UNIBELL	1.50	2.25	2.00	0.50	2.75
LANGA	LAG	2.65	3.50	4.00	3.00	1.00	5.00	BELHAR	1.50	2.25	2.00	0.50	2.75
BONTHEUWEL	BTL	1.94	2.50	3.00	2.50	1.00	4.00	LAVISTOWN	2.00	2.75	2.25	0.50	3.25
LAVISTOWN	LSN	3.12	2.75	3.50	3.25	0.50	4.00	BONTHEUWEL	2.50	3.25	3.25	1.00	4.25
BELHAR	BOH	2.39	2.00	3.00	2.25	0.50	3.50	LANGA	2.50	3.00	2.50	1.00	4.00
UNIBELL	UBL	1.83	1.50	2.25	2.00	0.50	2.75	MUTUAL	3.00	3.75	3.00	1.00	4.75
PENTECH	PEI	1.63	1.50	2.25	2.00	0.50	2.75	YSTERPLAAT	4.00	5.00	4.75	0.50	5.50
SAREPTA	SRP	1.95	2.25	2.50	2.25	0.50	3.00	ESPLANADE	3.00	4.75	4.25	0.50	5.25
BELLVILLE	BLE	4.43	6.00	6.25	5.00		6.25	CAPE TOWN	3.50	3.50	3.50		3.50
<b>TOTAL BELLVILLE</b>		<b>28.66</b>	<b>32.75</b>	<b>40.50</b>	<b>35.00</b>	<b>6.50</b>	<b>47.00</b>	<b>TOTAL</b>	<b>31.75</b>	<b>39.50</b>	<b>34.75</b>	<b>6.50</b>	<b>46.00</b>

# Appendix G

## Removed Workings

The following workings were removed from the WTB before conducting simulations.

### G.1 Diesel Hauled Trains

The following diesel hauled commuter trains were removed from the schedule: 2677, 2630, 5502, 5501

### G.2 Friday Only Empties

The following workings represent empty workings that are only run on Fridays.

**Kapteinsklip to Paardeneiland** 9836

**Philippi to Cape Town** 9744, 9746

**Philippi to Paardeneiland** 9854

### G.3 Yard Movements

The following trains represent yard movements between Cape Town station and the staging yards at Salt River, Cape Town and Paardeneiland. The singular workings between Bellville to Elsiesrivier and Simonstad to Vishoek were also removed. This was regarded as an acceptable simplification of the WTB, mainly

because their short distance and relatively low speed should not have an adverse impact on the general loading of traction energy supply equipment.

**Bellville to Elsiesrivier** 0860

**Bellville Staging Sidings to Cape Town platforms** 0808, 0840, 0802, 0840, 0806, 0846, 0830

**Cape Town platforms to Bellville Staging Sidings** 0835, 0807, 0811, 0813, 0845, 0803

**Cape Town to Paardeneiland** 0863, 9755, 9825, 9739, 9741, 9743, 9745, 9823, 9827, 9903, 9829, 9751, 9117, 9845, 9753, 9757, 9771, 9761, 9831, 9769, 9763, 9835, 9759, 9767, 9115, 9837, 9765, 9847

**Cape Town to Salt River** 0007, 0009, 0011, 0013, 0711, 0713, 0839, 0853, 0843, 0849, 0841, 0847, 0831, 0817, 0889, 0827, 0819, 0829, 0825, 0837, 0809

**Cape Town to Salt River via Esplanade** 0883, 0821, 0823

**Paardeneiland to Cape Town** 0862, 9736, 9730, 9804, 9702, 9754, 9716, 9808, 9704, 9810, 9814, 9706, 9708, 9816, 9818, 9712, 9908, 9714, 9822, 9824, 9718, 9828, 9720

**Salt River to Cape Town** 0010, 0012, 0014, 0016, 0720, 0722, 0814, 0816, 0842, 0818, 0848, 0810, 0820, 0822, 0826, 0828, 0832, 0834

**Salt River to Cape Town via Esplanade** 0824, 0888, 0884, 0836

**Simonstad to Vishoek** 0026

## G.4 Non-withdrawn trains

The simulation results will be compared to energy measurements taken in 2013. The following trains have been reduced, but was kept in the simulations for better comparison to the measurements: 0164, 0172, 0180, 0188, 0145, 0151, 0159, 0167

# Appendix H

## Workings Highlighted During Processing of WTB

The following workings were highlighted during the processing of the WTB as odd or impractical.

### H.1 Cape Flats Line

Too little time is allowed for trains between Heathfield and Retreat. The running time of 1 min 45 s changed to 2 min 15 s, as per SAR timing in Table F.9.

### H.2 Northern Lines

**Paardeneiland** The times calculated for trains that are scheduled to stop at Paardeneiland station is not correct. Alterations were made to the arrival and departure times for trains 2505, 2343, 2835, 2837.

**2804** Train 2804 is scheduled to depart Ysterplaat at 6:42:00, but arrive the next station (Paardeneiland) at 6:40:00. This was changed so that it arrives Paardeneiland at 6:44:00 and departs at 6:44:30.

### H.3 Central Lines

**Distance error** The distance from Cape Town to Mutual via Paardeneiland is wrong on some Metrorail drawings and tables, including the official SARCC

running times [99]. The correct distance is 8,7275 km, as per the small scale drawing [121].

**Empty coaches general** Train sets used for the Central line (to Kapteinsklip and Chris Hani) was originally stabled at the Philippi staging yard. The Paardeneiland running shed was used to service the sets used on this line. The Philippi staging yard has deteriorated to such an extent that no trains are stabled there today. Sets are now stabled at Paardeneiland and Cape Town station. This requires a total of 68 empty coach trains to run every weekday, at between 30 km and 38 km per train. It is unclear how the running times of these trains are determined. Trains are either scheduled very slowly or unrealistically fast. The running times were standardised to the times given in Table H.1. Where these times would cause conflicts with other trains, new times were calculated so that the train runs at 70 km/h and then wait at Philippi and Langa. If no conflict could be foreseen, Langa station was used as the reference time.

**Khayelitsha to Chris Hani** Running time of empty trains for the 3,93 km between Khayelitsha and Chris Hani varies, for no apparent reason. 9709 is allowed 10 minutes, 9713 7 minutes and most other workings 5 minutes. Changed so that all empty trains take 5 minutes between these two stations.

**9733, 9735** The timing of empty coach workings 9733 and 9735 is not good. The origin of the running times is unknown, but it implies that some empty trains run much faster than others. Arrival time for 9733 indicated at Bellville even though it terminates at Chris Hani. Indicated arrival times also clash with that of stopping train 9985. The WTB implies that 9733 will pass 9985 between Bonteheuwel and

Table H.1: Empty coach running times

Departure station	Arrival station	Running time (min)
Kapteinsklip	Langa	20
Langa	Paardeneiland	8
Paardeneiland	Cape Town	6,5
Chris Hani	Philippi	12
Khayelitsha	Philippi	9
Philippi	Langa	11
Langa	Cape Town	13,5

Netreg, this is highly unlikely. The running times for 9733 and 9735 were altered, but 9985 was not changed.

**9801** Train 9801 is allowed 10 minutes less between Bonteheuwel and Mitchells Plain than 9899 and 9819. This means it should travel at 106 km/h. Changed to have the same running times as the other trains.

**9842** An empty coach working, 9842, is allowed only 1 minute between Langa and Salt River. It is unclear where this train really terminates and Langa was used as the terminus.

**9926** The empty coach train 9926 from Kapteinsklip to Salt River yard is instructed to run from Mutual to Salt River via the Maitland link line. Since this is the only train that is instructed to run over this line, it was not modelled. In the simulation the train terminates at Langa.

**Short timing** A number of trains from Kapteinsklip to Cape Town via Salt River is allowed only 1 min 30 s for the 2,08 km from Netreg to Bonteheuwel. The official running time is 2 min 30 s, while the 1973/74 timetable allowed 2 min 15 s. This was addressed by reducing the dwell time at Bonteheuwel from 1 min to 30 s. The following trains were altered in this way: 9526, 9528, 9530, 9534, 9536, 9538, 9540, 9542, 9544, 9546, 9548, 9550, 9552, 9554, 9556, 9560, 9564, 9568.

**9563** Too little time is allowed for 9563 between Pinelands and Langa. It would have to travel at an average speed (including acceleration and deceleration) of 87 km/h in stead of the usual 54 km/h. The old rolling stock is not able to attain this. Stopping time at Pinelands and Langa decreased from 30 s to 15 s each for an average speed of 75 km/h.

**9916** Train 9916 is a semi-express train and does not stop at Nyanga and Netreg. Trains that do stop at Netreg are allowed 6 min between Heideveld and Bonteheuwel, including a 30 s stop at Netreg. Train 9916 is allowed 6 min 30 s between Heideveld and Bonteheuwel. Train 9920, also a semi-express train, is only allowed 4 min 30 s between Heideveld and Bonteheuwel. Although this does not make sense, this timing was not changed.

*APPENDIX H. WORKINGS HIGHLIGHTED DURING PROCESSING OF WTB* 186

**9920** Train 9920 is allowed only 30 s for the 1,84 km between Mandalay and Stock Road. While other trains are allowed 2 min Between Stock Road and Philippi, 1,97 km, this train is allowed 5 minutes. This discrepancy was compensated for by reducing the running time between Stock Road and Philippi and extending the time between Mandalay and Stock Road.

**9934** Too little time is allowed for 9934 between Nonkqubela and Nolungile. Changed to run through Nolungile at 7:39:10.

**9992** Train 9992 is another semi-express train and does not stop at Philippi. Stopping trains are allowed 6 min 30 s between Stock Road and Nyanga, including a 30 s stop at Philippi. Train 9992 is allowed 9 min 30 s between Stock Road and Nyanga. Later investigation also showed a conflict between the path of 9992 and the stopping train 9928. The Marvey diagram shows that the timing of 9928 was changed to eliminate the conflict, but the WTB was not updated. Although this does not make sense, this timing was not changed.

# Appendix I

## Comparison of Traction Energy Consumption

Commuter trains are designed to transport a large number of passengers per unit of their inside area. Consequently, the additional mass of passengers at high loading has a significant effect on the energy use of a train. In order to model the energy consumption of rolling stock accurately, each train's expected loading level should be taken into account.

Detailed data regarding the power demand of rolling stock at different loading levels could not be obtained. As discussed in Section 3.3.1, only one usable current profile could be sought for the present rolling stock. For the future rolling stock, only a limited amount of simulation results, discussed in Section 3.3.2, were made available.

One possibility that was considered was to scale the current values according to the expected loading. Figure I.1 gives a comparison of the traction energy consumption for different classes of commuter rolling stock and load levels. The data represents the total traction energy requirement for a 80 km round trip between Mayfair and Randfontein in Gauteng, South Africa. All data was measured, except for the future rolling stock, for which simulated data has been provided. Notice that there is no discernible link between the loading of a train and its energy use. For example, for the future rolling stock (11M), the total mass at M1 loading is 64 % of the M3 loaded mass, but the net energy use at M1 loading is 75 % of the M3 loaded consumption. Let  $\text{ton} \cdot \text{km}/\text{kWh}$  be a measure of the efficiency of the train, similar to  $\text{km}/\text{l}$  used in combustion-engined cars. For the future rolling stock, the efficiency at M3 loading is  $31,5 \text{ ton} \cdot \text{km}/\text{kWh}$  and at M1 loading



26,8 ton · km/kWh, 85 % of the M3 loaded value. This indicates that the rolling stock becomes more energy efficient as the weight of the train is increased. This can be explained by examining the air, rolling and bearing resistance. Although the data represents trips at relatively low speed and for the same round trip, it seems the influence is large enough to cause this discrepancy.

From this data, the conclusion was made that there is no simple (linear) relationship between the loading of a train and its energy use. It was, therefore, decided that the available data will not be scaled according to loading during this project. A recommendation will be made that the power demand at different loading levels should be determined and used, in accordance with the expected loading of different trains, as simulation input.

### SUBURBAN TRAIN SETS: COMPARISON OF TRACTION ENERGY CONSUMPTION

TEST SECTION: MAYFAIR-RANDFONTEIN-MAYFAIR

NUMBER OF STATIONS 52  
 SECTION LENGTH (km) 80  
 AVG DISTANCE BETWEEN STATIONS (km) 1.54

These energy consumption figures are for traction energy only.

TRAIN PARAMETERS															
TRAINSET	5M2A			6M			7M			8M			11M		
FORMATION	4M-10T			8M-4T			6M-6T			6M-6T			8M-4T		
INSTALLED POWER(MW)	3.52			7.84			6.96			5.88			10.24		
LOADING	M1	M2	M3	M1	M2	M3	M1	M2	M3	M1	M2	M3	M1	M2	M3
MASS (ton)	557	751	819	511	716	794	467	686	772	479	687	765	484	677	755
% OF CRUSH MASS	68%	92%	100%	64%	90%	100%	61%	89%	100%	63%	90%	100%	64%	90%	100%
RUNNING TIMES (min)	101.3	110.9	110.5	84.2	84.1	84.9	85.4	86	87.1	84	84.5	85	85.1	85.5	86.8
ENERGY															
CONSUMED (kWh)	3 299	3 524	3 957	2 610	4 258	4 436	2 591	3 538	4 316	3 012	3 826	4 137	2 536	3 358	3 568
% OF CRUSH ENERGY	83%	89%	100%	59%	96%	100%	60%	82%	100%	73%	92%	100%	71%	94%	100%
REGENERATED (kWh)	0	0	0	875	1 473	1 551	1 027	1 442	1 678	868	1 194	1 320	1 094	1 534	1 648
% OF CRUSH ENERGY				56%	95%	100%	61%	86%	100%	66%	90%	100%	66%	93%	100%
NET (kWh)	3 299	3 524	3 957	1 735	2 784	2 886	1 564	2 096	2 639	2 144	2 632	2 817	1 442	1 824	1 920
% OF CRUSH ENERGY	83%	89%	100%	60%	96%	100%	59%	79%	100%	76%	93%	100%	75%	95%	100%
REGEN. PERCENTAGE	0%	0%	0%	34%	35%	35%	40%	41%	39%	29%	31%	32%	43%	46%	46%
Wh/(ton.km)	74.04	58.67	60.41	42.46	48.61	45.41	41.84	38.17	42.73	55.97	47.90	46.02	37.27	33.69	31.77
ton.km/kWh	13.5	17.0	16.6	23.6	20.6	22.0	23.9	26.2	23.4	17.9	20.9	21.7	26.8	29.7	31.5
% OF CRUSH ton.km/kWh	82%	103%	100%	107%	93%	100%	102%	112%	100%	82%	96%	100%	85%	94%	100%

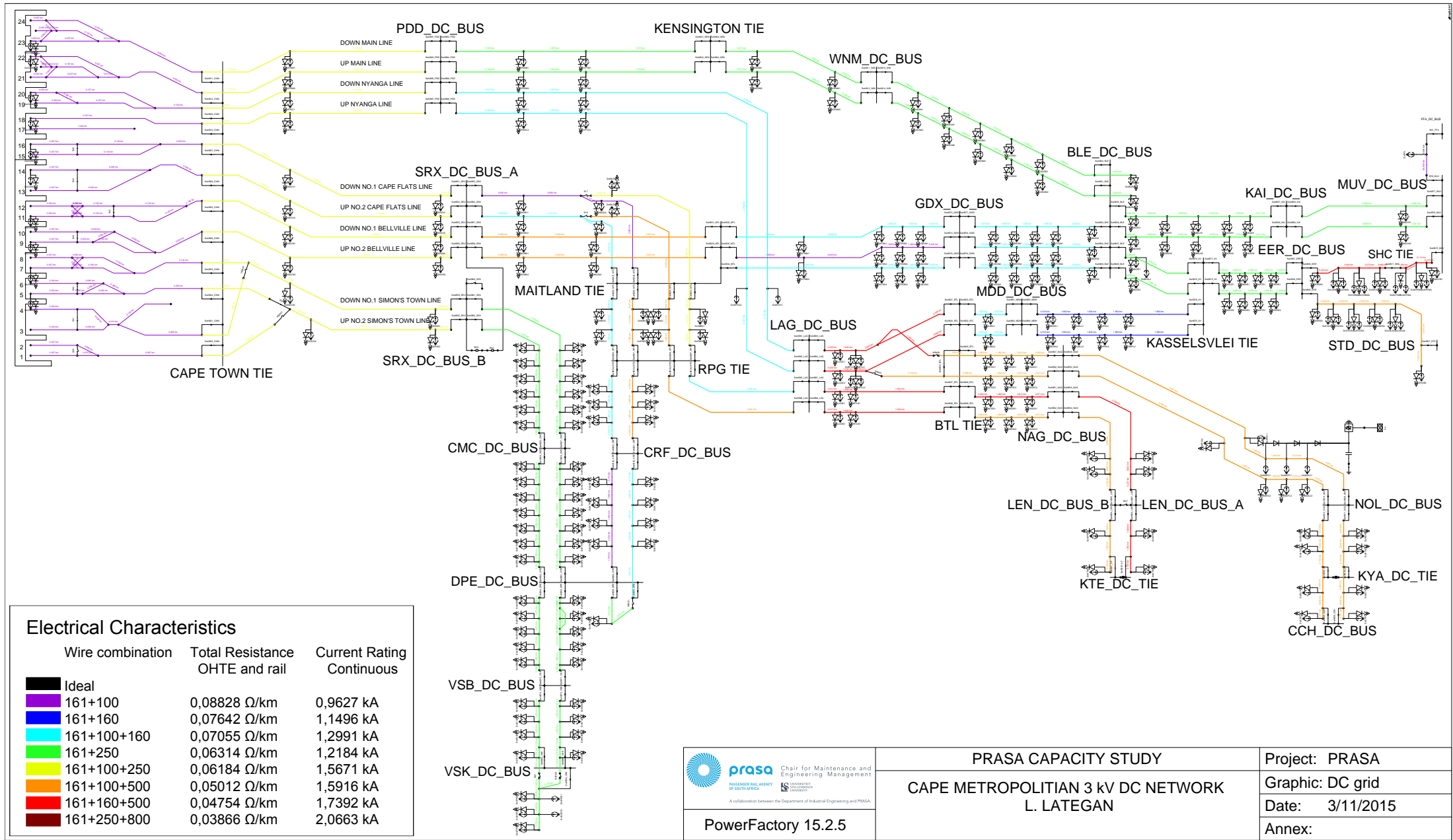
Figure I.1: Comparison of traction energy consumption for different classes of commuter rolling stock and load levels [90; 80]

# Appendix J

## Simulated DC Network Model

A diagram of the DC network, in its normal state [103] and as it is modelled in PowerFactory, is shown on the following page. The layout is based on the diagram in Appendix A.

The colours represent the wire combination that was modelled for each section. The small items are the current sources placed at each station platform and a diode which limit the maximum overhead line voltage to 3,75 kV. These represent the rheostatic braking of the new trains.



**Electrical Characteristics**

Wire combination	Total Resistance OHTE and rail	Current Rating Continuous
■ Ideal		
■ 161+100	0,08828 Ω/km	0,9627 kA
■ 161+160	0,07642 Ω/km	1,1496 kA
■ 161+100+160	0,07055 Ω/km	1,2991 kA
■ 161+250	0,06314 Ω/km	1,2184 kA
■ 161+100+250	0,06184 Ω/km	1,5671 kA
■ 161+100+500	0,05012 Ω/km	1,5916 kA
■ 161+160+500	0,04754 Ω/km	1,7392 kA
■ 161+250+800	0,03866 Ω/km	2,0663 kA



PowerFactory 15.2.5

PRASA CAPACITY STUDY  
CAPE METROPOLITAN 3 kV DC NETWORK  
L. LATEGAN

Project: PRASA  
Graphic: DC grid  
Date: 3/11/2015  
Annex:

# Appendix K

## Detailed Results

The following sections contain some of the processed results from the the Old and New (<sup>m</sup>) scenarios that were investigated.

The complete results can be found at the following URL:

[https://www.dropbox.com/sh/4hexfgrdzjtt6pv/AAAHVKA-SAkJQjMO1Yyq1\\_9ua?dl=0](https://www.dropbox.com/sh/4hexfgrdzjtt6pv/AAAHVKA-SAkJQjMO1Yyq1_9ua?dl=0)

Password: resultSet2016

### K.1 Old

The results are presented in the following order:

1. External Power Feeds (supply points)
2. Transformers
3. 33 kV Transmission-lines

11M with REGEN 3 kV External Power Feed	Total Active Power in MW						Total Energy kWh
	1 sec	5 min		30 min		Continuous	2:00 to 23:00
	Max	Min	Max	Min	Max	Average	Delivered
Xnet Reostate	0.000	0.000	0.000	0.000	0.000	0.000	0
Xnet Tafelbaai Feed-in	44.722	1.924	34.491	1.924	33.055	16.332	342 985
XnetCCH 66kV FROM MUNICIPAL SUPPLY	0.440	0.440	0.440	0.440	0.440	0.440	9 240
XnetEER ESKOM 33kV FEED	6.463	0.049	3.163	0.049	2.553	1.129	23 716
XnetKAI ESKOM 66kV FEED	4.147	0.005	2.109	0.005	1.592	0.741	15 562
XnetLEN C.C.C SUPPLY 11.66kV A	4.061	0.005	2.407	0.005	1.845	0.778	16 341
XnetLEN C.C.C SUPPLY 11.66kV B	5.331	0.905	3.030	0.905	2.757	1.664	34 945
XnetMDD 40MVA 132kV ESKOM SUPPLY	18.217	0.680	13.711	0.680	12.784	5.962	125 198
XnetMUV ESKOM 66kV FEED	5.837	0.007	2.860	0.007	2.154	0.961	20 190
XnetNOL 66kV FROM MUNICIPAL SUPPLY	8.294	0.455	5.058	0.455	4.297	2.036	42 760
XnetSTD ESKOM 66kV FEED	3.450	0.004	1.784	0.004	1.215	0.510	10 721
XnetVHK MAIN INCOMING 11kV MUN SUPPLY	3.438	0.229	2.246	0.229	1.838	0.945	19 843
XnetWNM ESKOM ACACIA NO.1 33kV	2.674	0.025	1.784	0.025	1.565	0.815	17 109
XnetWNM ESKOM ACACIA NO.2 33kV	2.685	0.025	1.790	0.025	1.570	0.817	17 151
Total excl Reostate							695 761

5M2A Transformer	Loading (HV) in %						Total Active Power/HV-Side in MW								
	1 sec		1 min		30 min		Continuous	1 sec		1 min		30 min		Continuous	Total Energy Consumed (kWh)
	Max	Min	Max	Min	Max	Average	Max	Min	Max	Min	Max	Average			
Trf BLEA BP-24768	104.24	0.30	84.67	0.30	55.27	24.37	3.378	0.004	2.777	0.004	1.846	0.824	17 305		
Trf BLEB BP-24761	106.67	0.30	86.40	0.30	56.16	24.67	3.458	0.004	2.835	0.004	1.876	0.834	17 524		
Trf CCHA	0.00	0.00	0.00	0.00	0.00	0.00	0.000	0.000	0.000	0.000	0.000	0.000	0		
Trf CMCA BP-20769	78.96	0.30	64.24	0.30	45.25	18.96	2.616	0.004	2.146	0.004	1.528	0.645	13 542		
Trf CMCB BP-20763	79.50	0.30	64.63	0.30	45.48	19.04	2.634	0.004	2.159	0.004	1.536	0.647	13 597		
Trf CRFA BP-24767	86.52	0.30	71.17	0.30	52.55	22.27	2.869	0.004	2.379	0.004	1.774	0.759	15 942		
Trf CRFB BP-21696	90.16	0.30	73.81	0.30	54.18	22.80	2.991	0.004	2.468	0.004	1.830	0.777	16 325		
Trf DPEA AEG-81/13390	81.63	0.30	67.20	0.30	39.11	17.95	2.540	0.004	2.113	0.004	1.254	0.580	12 189		
Trf DPEB AEG-81/13361	80.59	0.30	66.43	0.30	38.76	17.82	2.508	0.004	2.088	0.004	1.243	0.576	12 099		
Trf EERB BP-24760	196.37	0.30	154.97	0.30	74.36	31.85	6.418	0.004	5.114	0.004	2.508	1.084	22 771		
Trf GWDA BP-28698	115.72	0.30	99.39	0.30	70.79	31.70	3.798	0.004	3.287	0.004	2.373	1.075	22 583		
Trf GWDB BP-24769	118.16	0.30	101.08	0.30	71.51	31.80	3.880	0.004	3.345	0.004	2.397	1.079	22 655		
Trf KAIA ASEA-27869	90.16	0.30	73.09	0.30	33.31	15.38	4.147	0.005	3.403	0.005	1.592	0.741	15 562		
Trf LAGA AEG-81/13393	90.54	0.30	79.24	0.30	58.93	24.49	2.778	0.003	2.450	0.003	1.854	0.785	16 488		
Trf LAGB AEG-81/13362	89.92	0.30	78.74	0.30	58.61	24.39	2.758	0.003	2.435	0.003	1.844	0.782	16 419		
Trf LENA AEG-27644	87.60	0.30	70.69	0.30	38.64	16.14	4.061	0.005	3.313	0.005	1.845	0.778	16 341		
Trf LENB AEG-27644	95.92	0.30	75.21	0.30	38.83	15.84	4.431	0.005	3.518	0.005	1.857	0.764	16 045		
Trf MDDA AEG-81/13394	111.21	0.30	89.29	0.30	59.10	24.36	3.535	0.004	2.861	0.004	1.915	0.795	16 700		
Trf Mddb TUSCO521095	75.23	0.87	62.92	0.87	45.42	23.29	3.215	0.037	2.708	0.037	1.976	1.023	21 481		
Trf MUVA BP-24781	86.59	0.30	73.42	0.30	31.37	13.97	2.921	0.004	2.487	0.004	1.078	0.481	10 099		
Trf MUVB BP-28697	86.44	0.30	73.30	0.30	31.33	13.95	2.916	0.004	2.483	0.004	1.076	0.480	10 090		
Trf NAGA AEG-81/13392	120.04	0.30	104.27	0.30	69.70	28.73	3.680	0.003	3.226	0.003	2.199	0.924	19 396		
Trf NAGB AEG-81/13364	134.68	0.30	115.81	0.30	75.81	30.61	4.137	0.003	3.589	0.003	2.393	0.984	20 670		
Trf NOLA GEC-P303/6	179.36	0.30	149.17	0.30	82.79	33.35	7.844	0.005	6.656	0.005	3.847	1.586	33 310		
Trf PDDA AEG-EL95476	137.64	0.30	116.80	0.30	87.35	34.62	4.336	0.004	3.705	0.004	2.799	1.123	23 593		
Trf PDDB AEG-81/13360	137.63	0.30	116.79	0.30	87.34	34.62	4.335	0.004	3.705	0.004	2.799	1.123	23 592		
Trf SRXA TUSCO-521096	139.59	0.97	124.30	0.97	93.49	46.08	6.357	0.046	5.717	0.046	4.381	2.201	46 217		
Trf SRXB ASEA-27467	100.71	0.81	89.36	0.81	68.99	33.66	4.698	0.037	4.200	0.037	3.280	1.622	34 065		
Trf STDA AEG-81/20065	107.66	0.30	83.81	0.30	37.04	15.53	3.450	0.004	2.707	0.004	1.215	0.510	10 721		
Trf VSBA BP-24762	79.80	0.30	60.75	0.30	40.16	17.80	2.603	0.004	2.007	0.004	1.345	0.602	12 637		
Trf VSKA HS	98.83	0.30	79.98	0.30	48.30	21.41	3.213	0.004	2.628	0.004	1.613	0.720	15 118		
Trf WNMA ASEA-27645	56.46	0.59	48.21	0.59	32.52	16.81	2.674	0.025	2.296	0.025	1.565	0.815	17 109		
Trf WNMB ASEA-27646	56.69	0.59	48.39	0.59	32.61	16.85	2.685	0.025	2.304	0.025	1.570	0.817	17 151		
<b>Total</b>													<b>599 337</b>		

5M2A 33kV Transmission Line	Loading in %						Total Losses kWh 2:00 to 23:00
	1 sec	1 min		5 min		Continuous	
	Max	Min	Max	Min	Max	Average	
Ln33-B1_TM-WTM	37.94	4.69	31.56	4.69	24.50	12.37	124.849
Ln33-B1_WTM-BLE	37.98	4.68	31.60	4.68	24.54	12.38	365.319
Ln33-B2_TM-GWD	37.37	0.46	32.03	0.46	25.01	10.43	231.744
Ln33-B2_GDX-BLE	0.10	0.10	0.10	0.10	0.10	0.10	0.003
Ln33-M1_TM-MLD	0.09	0.09	0.09	0.09	0.09	0.09	0.003
Ln33-M1_MLD-LAG	0.05	0.05	0.05	0.05	0.05	0.05	0.000
Ln33-M1_LAG-NAG	26.75	2.08	23.64	2.08	19.16	8.73	165.691
Ln33-M1A_NAG-MDD	55.34	2.62	50.62	2.62	40.79	17.33	752.056
Ln33-M2_TM-WTM	0.05	0.05	0.05	0.05	0.05	0.05	0.000
Ln33-M2_WTM-MDD	0.18	0.18	0.18	0.18	0.18	0.18	0.015
Ln33-MDD-BLE(proposed)	0.00	0.00	0.00	0.00	0.00	0.00	0.000
Ln33-V1_TM-SRX	59.79	1.37	51.72	1.37	42.92	18.82	38.668
Ln33-V1_SRX-CMC	54.58	1.31	44.55	1.31	36.21	15.39	416.144
Ln33-V1_CMC-DPE	33.24	1.27	27.95	1.27	21.49	9.41	141.524
Ln33-V1_DPE-VSB	12.83	0.23	9.78	0.23	7.61	3.02	18.919
Ln33-V2_TM-SRX	44.00	1.53	39.80	1.53	32.87	15.45	24.695
Ln33-V2_SRX-MLD	28.26	0.54	23.17	0.54	17.90	7.50	41.166
Ln33-V2_MLD-CRF	28.29	0.51	23.19	0.51	17.93	7.51	104.772
Ln33-V2_CRF-DPE	0.31	0.31	0.31	0.31	0.31	0.31	0.098
Ln33-V2_DPE-VSB	0.24	0.23	0.24	0.23	0.24	0.23	0.057
<b>Total</b>							<b>2425.723</b>



## **K.2 New (m)**

The results are presented in the following order:

1. External Power Feeds (supply points)
2. Transformers
3. 33 kV Transmission-lines
4. Legend to the station codes
5. Current and Power Sources

11M 3 kV Pregen	Total Active Power in MW						Total Energy kWh
	1 sec	5 min		30 min		Continuous	2:00 to 23:00
	Max	Min	Max	Min	Max	Average	Delivered
Xnet Reostate	-21.742	-1.225	0.000	-0.552	0.000	-0.274	-5 763
Xnet Tafelbaai Feed-in	68.299	1.923	32.446	1.924	30.552	15.256	320 363
XnetCCH 66kV FROM MUNICIPAL SUPPLY	0.440	0.440	0.440	0.440	0.440	0.440	9 240
XnetEER ESKOM 33kV FEED	17.118	0.049	4.340	0.049	3.660	1.632	34 270
XnetKAI ESKOM 66kV FEED	11.873	0.005	3.350	0.005	2.308	1.001	21 027
XnetLEN C.C.C SUPPLY 11.66kV A	9.227	0.005	2.466	0.005	1.924	0.822	17 263
XnetLEN C.C.C SUPPLY 11.66kV B	27.304	0.905	3.220	0.905	2.866	1.733	36 394
XnetMDD 40MVA 132kV ESKOM SUPPLY	30.832	0.680	14.164	0.680	13.203	6.190	129 983
XnetMUV ESKOM 66kV FEED	16.718	0.007	4.689	0.007	3.501	1.508	31 661
XnetNOL 66kV FROM MUNICIPAL SUPPLY	14.709	0.455	5.451	0.455	4.425	2.127	44 676
XnetSTD ESKOM 66kV FEED	12.141	0.004	2.696	0.004	1.845	0.727	15 267
XnetVHK MAIN INCOMING 11kV MUN SUPPLY	5.396	0.229	1.608	0.229	1.422	0.785	16 484
XnetWNM ESKOM ACACIA NO.1 33kV	5.694	0.025	1.886	0.025	1.562	0.822	17 263
XnetWNM ESKOM ACACIA NO.2 33kV	5.731	0.025	1.893	0.025	1.567	0.826	17 340
Total excl Reostate							711 231.89

11M 3 kV Pregon	Loading (HV) in %						Total Active Power/HV-Side in MW						
	1 sec	1 min		30 min		Continuous	1 sec	1 min		30 min		Continuous	Total Energy Consumed (kWh)
	Max	Min	Max	Min	Max	Average	Max	Min	Max	Min	Max	Average	
Trf BLEA BP-24768	249.17	0.30	111.08	0.30	65.96	29.99	7.356	0.004	3.551	0.004	2.163	0.999	20 974
Trf BLEB BP-24761	260.32	0.30	114.03	0.30	67.31	30.48	7.698	0.004	3.646	0.004	2.207	1.015	21 317
Trf CCHA	0.00	0.00	0.00	0.00	0.00	0.00	0.000	0.000	0.000	0.000	0.000	0.000	0
Trf CMCA BP-20769	157.55	0.30	52.66	0.30	32.92	14.34	5.015	0.004	1.769	0.004	1.114	0.487	10 223
Trf CMCB BP-20763	159.30	0.30	52.97	0.30	33.07	14.40	5.072	0.004	1.780	0.004	1.120	0.489	10 265
Trf CRFA BP-24767	127.60	0.30	67.49	0.30	45.92	19.57	4.139	0.004	2.249	0.004	1.550	0.666	13 989
Trf CRFB BP-21696	134.67	0.30	70.13	0.30	47.33	20.05	4.373	0.004	2.337	0.004	1.599	0.683	14 335
Trf DPEA AEG-81/13390	132.46	0.30	54.09	0.30	29.96	13.75	4.623	0.004	1.704	0.004	0.961	0.443	9 301
Trf DPEB AEG-81/13361	130.18	0.30	53.49	0.30	29.60	13.52	4.557	0.004	1.685	0.004	0.950	0.435	9 144
Trf EERB BP-24760	553.97	0.30	228.54	0.30	109.63	47.48	17.073	0.004	7.324	0.004	3.615	1.587	33 325
Trf GWDA BP-28698	263.58	0.30	120.51	0.30	72.98	33.40	8.102	0.004	3.933	0.004	2.422	1.122	23 571
Trf GWDB BP-24769	278.58	0.30	123.40	0.30	74.10	33.68	8.585	0.004	4.030	0.004	2.460	1.132	23 764
Trf KAIA ASEA-27869	305.36	0.30	134.46	0.30	49.94	21.26	11.873	0.005	5.850	0.005	2.308	1.001	21 027
Trf LAGA AEG-81/13393	177.36	0.30	84.18	0.30	57.59	23.87	5.055	0.003	2.574	0.003	1.802	0.759	15 944
Trf LAGB AEG-81/13362	175.50	0.30	83.60	0.30	57.26	23.71	5.000	0.003	2.556	0.003	1.792	0.754	15 834
Trf LENA AEG-27644	215.87	0.30	84.26	0.30	40.86	17.22	9.227	0.005	3.838	0.005	1.924	0.822	17 263
Trf LENB AEG-27644	250.90	0.30	93.33	0.30	41.64	17.45	10.582	0.005	4.289	0.005	1.966	0.833	17 487
Trf MDDA AEG-81/13394	237.10	0.30	114.26	0.30	65.66	27.44	7.233	0.004	3.610	0.004	2.110	0.889	18 668
Trf Mddb TUSCO521095	140.82	0.66	76.35	0.87	48.69	24.34	5.788	0.026	3.247	0.037	2.104	1.063	22 326
Trf MUVA BP-24781	258.85	0.30	132.61	0.30	51.72	22.14	8.375	0.004	4.389	0.004	1.752	0.754	15 841
Trf MUVB BP-28697	257.89	0.30	132.26	0.30	51.63	22.11	8.343	0.004	4.377	0.004	1.749	0.753	15 820
Trf NAGA AEG-81/13392	244.82	0.30	121.19	0.30	73.17	31.00	6.925	0.003	3.667	0.003	2.288	0.985	20 686
Trf NAGB AEG-81/13364	296.69	0.30	137.95	0.30	80.41	33.46	8.433	0.003	4.182	0.003	2.517	1.064	22 334
Trf NOLA GEC-P303/6	374.25	0.30	179.25	0.30	87.55	36.00	14.259	0.005	7.721	0.005	3.975	1.677	35 226
Trf PDDA AEG-EL95476	231.33	0.30	127.08	0.30	80.71	32.71	7.072	0.004	3.999	0.004	2.582	1.059	22 238
Trf PDDB AEG-81/13360	231.31	0.30	127.07	0.30	80.71	32.71	7.071	0.004	3.999	0.004	2.582	1.059	22 237
Trf SRXA TUSCO-521096	211.49	0.74	128.83	0.97	84.77	41.69	9.144	0.033	5.885	0.045	3.965	1.985	41 679
Trf SRXB ASEA-27467	154.98	0.64	79.62	0.81	58.30	27.78	6.963	0.028	3.753	0.037	2.777	1.339	28 113
Trf STDA AEG-81/20065	412.52	0.30	176.26	0.30	57.52	22.45	12.141	0.004	5.438	0.004	1.845	0.727	15 267
Trf VSBA BP-24762	151.15	0.30	51.18	0.30	30.46	14.08	4.805	0.004	1.701	0.004	1.017	0.473	9 940
Trf VSKA HS	165.30	0.30	55.30	0.30	35.82	16.69	5.171	0.004	1.836	0.004	1.197	0.560	11 760
Trf WNMA ASEA-27645	126.04	0.49	59.78	0.58	32.58	17.04	5.694	0.019	2.807	0.025	1.562	0.822	17 263
Trf WNMB ASEA-27646	126.82	0.49	60.04	0.58	32.69	17.12	5.731	0.019	2.820	0.025	1.567	0.826	17 340
<b>Total</b>													<b>614 500.599</b>

11M 3 kV Pregen 33kV Transmission Line	Max. Loading in %						Total Losses kWh 2:00 to 23:00
	1 sec	1 min		5 min		Continuous	
	Max	Min	Max	Min	Max	Average	
Ln33-B1_TM-WTM	84.48	4.69	40.37	4.69	29.44	14.16	196.137
Ln33-B1_WTM-BLE	84.55	4.68	40.42	4.68	29.48	14.18	573.850
Ln33-B2_TM-GWD	86.14	0.46	38.60	0.46	26.56	10.99	336.260
Ln33-B2_GDX-BLE	0.10	0.10	0.10	0.10	0.10	0.10	0.003
Ln33-M1_TM-MLD	0.00	0.00	0.00	0.00	0.00	0.00	0.000
Ln33-M1_MLD-LAG	0.00	0.00	0.00	0.00	0.00	0.00	0.000
Ln33-M1_LAG-NAG	50.36	2.08	24.87	2.08	19.13	8.55	182.299
Ln33-M1A_NAG-MDD	105.32	2.62	57.51	2.62	41.40	17.84	929.062
Ln33-M2_TM-WTM	0.05	0.05	0.05	0.05	0.05	0.05	0.000
Ln33-M2_WTM-MDD	0.21	0.21	0.21	0.21	0.21	0.21	0.035
Ln33-MDD-BLE(proposed)	0.00	0.00	0.00	0.00	0.00	0.00	0.000
Ln33-V1_TM-SRX	95.16	1.35	42.97	1.36	34.20	15.01	28.633
Ln33-V1_SRX-CMC	95.67	1.31	36.75	1.31	27.98	12.04	314.807
Ln33-V1_CMC-DPE	50.53	1.27	24.53	1.27	17.15	7.52	114.320
Ln33-V1_DPE-VSB	24.12	0.23	8.24	0.23	5.68	2.42	17.871
Ln33-V2_TM-SRX	71.01	1.50	41.59	1.53	30.38	13.95	22.859
Ln33-V2_SRX-MLD	41.79	0.54	21.88	0.54	16.38	6.65	38.346
Ln33-V2_MLD-CRF	41.83	0.51	21.90	0.51	16.40	6.65	97.581
Ln33-V2_CRF-DPE	0.31	0.31	0.31	0.31	0.31	0.31	0.098
Ln33-V2_DPE-VSB	0.24	0.23	0.24	0.23	0.23	0.23	0.056
<b>Total</b>							<b>2852.217</b>

LINE	DESCRIPTION
CHRIS HANI	KAAPSTAD - CHRIS HANI via ESPLANADE and MUTUAL
EERSTERIVIER	BELLVILLE - EERSTERIVIER
HOOFLYN	BELLVILLE - MULDESVLEI via KRAAIFONTEIN
KAPTEINSKLIP	MAITLAND - KAPTEINSKLIP via PHILIPPI and LANGA
LAVISTOWN	BONTEHEUWEL - BELLVILLE via LAVISTOWN
MONTE VISTA	KAAPSTAD - BELLVILLE via MONTE VISTA
NOORD	KAAPSTAD - BELLVILLE via SOUTRIVIER and GOODWOOD
STELLENBOSCH	EERSTERIVIER - MULDESVLEI
STRAND	EERSTERIVIER - STRAND
SUID	KAAPSTAD - SIMONSTAD via WYNBERG
VLAKTE	KAAPSTAD - HEATHFIELD via ATHLONE

Legend	STATION	LINE	DIRECTION
AKAM1	AKASIAPARK	MONTE VISTA	DOWN
AKAM2	AKASIAPARK	MONTE VISTA	UP
ATLV1	ATHLONE	VLAKTE	DOWN
ATLV2	ATHLONE	VLAKTE	UP
AVDM1	AVONDALE	MONTE VISTA	DOWN
AVDM2	AVONDALE	MONTE VISTA	UP
BKHE1	BLACKHEATH	EERSTERIVIER	DOWN
BKHE2	BLACKHEATH	EERSTERIVIER	UP
BKLH1	BRACKENFELL	HOOFLYN	DOWN
BKLH2	BRACKENFELL	HOOFLYN	UP
BLEE1	BELLVILLE	EERSTERIVIER	DOWN
BLEL2	BELLVILLE	LAVISTOWN	UP
BLEE2	BELLVILLE	EERSTERIVIER	UP
BLEH1	BELLVILLE	HOOFLYN	DOWN
BLEH2	BELLVILLE	HOOFLYN	UP
BLEM1	BELLVILLE	MONTE VISTA	DOWN
BLEM2	BELLVILLE	MONTE VISTA	UP
BLEN1	BELLVILLE	NORTH	DOWN
BLEN2	BELLVILLE	NORTH	UP
BLEN3	BELLVILLE	NORTH	3rd Road
BOHL1	BELHAR	LAVISTOWN	DOWN
BOHL2	BELHAR	LAVISTOWN	UP
BTLC1	BONTHEUWEL	CHRIS HANI	DOWN
BTLL1	BONTHEUWEL	LAVISTOWN	DOWN
BTLC2	BONTHEUWEL	CHRIS HANI	UP
BTLL2	BONTHEUWEL	LAVISTOWN	UP
BTLK1	BONTHEUWEL	KAPTEINSKLIP	DOWN
BTLK2	BONTHEUWEL	KAPTEINSKLIP	UP
CENM1	CENTURY CITY	MONTE VISTA	DOWN
CENM2	CENTURY CITY	MONTE VISTA	UP
CMCS1	CLAREMONT	SUBURBAN	DOWN
CMCS2	CLAREMONT	SUBURBAN	UP
CRFV1	CRAWFORD	VLAKTE	DOWN
CRFV2	CRAWFORD	VLAKTE	UP
CRTC1	CHRIS HANI	CHRIS HANI	DOWN
CRTC2	CHRIS HANI	CHRIS HANI	UP

Legend	STATION	LINE	DIRECTION
CWNC1	KAAPSTAD B	CHRIS HANI	DOWN
CWNC2	KAAPSTAD B	CHRIS HANI	UP
CWNM1	KAAPSTAD B	MONTE VISTA	DOWN
CWNM2	KAAPSTAD B	MONTE VISTA	UP
CWNN1	KAAPSTAD B	NORTH	DOWN
CWNN2	KAAPSTAD B	NORTH	UP
CWNS1	KAAPSTAD B	SUBURBAN	DOWN
CWNS2	KAAPSTAD B	SUBURBAN	UP
CWNV1	KAAPSTAD B	VLAKTE	DOWN
CWNV2	KAAPSTAD B	VLAKTE	UP
DEGM1	DE GREDEL	MONTE VISTA	DOWN
DEGM2	DE GREDEL	MONTE VISTA	UP
DPES1	DIEPRIVIER	SUBURBAN	DOWN
DPES2	DIEPRIVIER	SUBURBAN	UP
DUTMA	DU TOIT	MULDERSVLEI	DOWN
DUTMO	DU TOIT	MULDERSVLEI	UP
EERE1	EERSTERIVIER	EERSTERIVIER	DOWN
EERE2	EERSTERIVIER	EERSTERIVIER	UP
EERSD	EERSTERIVIER	STRAND	
EERSH	EERSTERIVIER	STELLENBOSCH	
EIKH1	EIKENFONTEIN	HOOFLYN	DOWN
EIKH2	EIKENFONTEIN	HOOFLYN	UP
EPDC1	ESPLANADE	CHRIS HANI	DOWN
EPDC2	ESPLANADE	CHRIS HANI	UP
EPDM1	ESPLANADE	MONTE VISTA	DOWN
EPDM2	ESPLANADE	MONTE VISTA	UP
ERHN1	ELSIESRIVIER	NORTH	DOWN
ERHN2	ELSIESRIVIER	NORTH	UP
ERHN3	ELSIESRIVIER	NORTH	3rd Road
FAUSA	FAURE	STRAND	DOWN
FAUSO	FAURE	STRAND	UP
FGVSA	FIRGROVE	STRAND	DOWN
FGVSO	FIRGROVE	STRAND	UP
GCRS1	GLENCAIRN	SUBURBAN	DOWN
GCRS2	GLENCAIRN	SUBURBAN	UP
GDXN1	GOODWOOD	NORTH	DOWN
GDXN2	GOODWOOD	NORTH	UP
GDXN3	GOODWOOD	NORTH	3rd Road
HAZV1	HAZENDAL	VLAKTE	DOWN
HAZV2	HAZENDAL	VLAKTE	UP
HEDC1	HEIDEVELD	CHRIS HANI	DOWN
HEDC2	HEIDEVELD	CHRIS HANI	UP
HEDK1	HEIDEVELD	KAPTEINSKLIP	DOWN
HEDK2	HEIDEVELD	KAPTEINSKLIP	UP
HEHS1	HEATHFIELD	SUBURBAN	DOWN
HEHS2	HEATHFIELD	SUBURBAN	UP
HEHV2	HEATHFIELD	VLAKTE	
HRDS1	HARFIELD ROAD	SUBURBAN	DOWN
HRDS2	HARFIELD ROAD	SUBURBAN	UP

<b>Legend</b>	<b>STATION</b>	<b>LINE</b>	<b>DIRECTION</b>
KABS1	KALKBAAI	SUBURBAN	DOWN
KABS2	KALKBAAI	SUBURBAN	UP
KAIH1	KRAAIFONTEIN	HOOFLYN	DOWN
KAIH2	KRAAIFONTEIN	HOOFLYN	UP
KEDM1	KENTEMADE	MONTE VISTA	DOWN
KEDM2	KENTEMADE	MONTE VISTA	UP
KHFMA	KOELENHOF	STELLENBOSCH	DOWN
KHFMO	KOELENHOF	STELLENBOSCH	UP
KLWS1	KENILWORTH	SUBURBAN	DOWN
KLWS2	KENILWORTH	SUBURBAN	UP
KOBN1	KOEBERGWEG	NORTH	DOWN
KOBN2	KOEBERGWEG	NORTH	UP
KOBV1	KOEBERGWEG	VLAKTE	DOWN
KOBV2	KOEBERGWEG	VLAKTE	UP
KSVE1	KUILSRIVIER	EERSTERIVIER	DOWN
KSVE2	KUILSRIVIER	EERSTERIVIER	UP
KTEK1	KAPTEINSKLIP	KAPTEINSKLIP	DOWN
KTEK2	KAPTEINSKLIP	KAPTEINSKLIP	UP
KUYC1	KUYASA	CHRIS HANI	DOWN
KUYC2	KUYASA	CHRIS HANI	UP
KYAC1	KHAYELITSHA	CHRIS HANI	DOWN
KYAC2	KHAYELITSHA	CHRIS HANI	UP
LAGC1	LANGA	CHRIS HANI	DOWN
LAGC2	LANGA	CHRIS HANI	UP
LAGK1	LANGA	KAPTEINSKLIP	DOWN
LAGK2	LANGA	KAPTEINSKLIP	UP
LDHMA	LYNEDOCH	STELLENBOSCH	DOWN
LDHMO	LYNEDOCH	STELLENBOSCH	UP
LENK1	LENTEGEUR	KAPTEINSKLIP	DOWN
LENK2	LENTEGEUR	KAPTEINSKLIP	UP
LNEV1	LANSDOWNE	VLAKTE	DOWN
LNEV2	LANSDOWNE	VLAKTE	UP
LSDS1	LAKESIDE	SUBURBAN	DOWN
LSDS2	LAKESIDE	SUBURBAN	UP
LSNL1	LAVISTOWN	LAVISTOWN	DOWN
LSNL2	LAVISTOWN	LAVISTOWN	UP
MCFC1	MANDALAY	CHRIS HANI	DOWN
MCFC2	MANDALAY	CHRIS HANI	UP
METE1	MELTON ROSE	EERSTERIVIER	DOWN
METE2	MELTON ROSE	EERSTERIVIER	UP
MLDK1	MAITLAND	KAPTEINSKLIP	DOWN
MLDK2	MAITLAND	KAPTEINSKLIP	UP
MLDN1	MAITLAND	NORTH	DOWN
MLDN2	MAITLAND	NORTH	UP
MLDV1	MAITLAND	VLAKTE	DOWN
MLDV2	MAITLAND	VLAKTE	UP
MNVM1	MONTE VISTA	MONTE VISTA	DOWN
MNVM2	MONTE VISTA	MONTE VISTA	UP
MTPK1	MITCHELLS PLAIN	KAPTEINSKLIP	DOWN

<b>Legend</b>	<b>STATION</b>	<b>LINE</b>	<b>DIRECTION</b>
MTPK2	MITCHELLS PLAIN	KAPTEINSKLIP	UP
MTXC1	MUTUAL	CHRIS HANI	DOWN
MTXC2	MUTUAL	CHRIS HANI	UP
MTXN1	MUTUAL	NORTH	DOWN
MTXN2	MUTUAL	NORTH	UP
MTXN3	MUTUAL	NORTH	3rd Road
MUVH1	MULDERSVLEI	HOOFLYN	DOWN
MUVH2	MULDERSVLEI	HOOFLYN	UP
MUVSH	MULDERSVLEI	STELLENBOSCH	
MWYS1	MOWBRAY	SUBURBAN	DOWN
MWYS2	MOWBRAY	SUBURBAN	UP
MZMS1	MUIZENBERG	SUBURBAN	DOWN
MZMS2	MUIZENBERG	SUBURBAN	UP
NAGC1	NYANGA	CHRIS HANI	DOWN
NAGC2	NYANGA	CHRIS HANI	UP
NAGK1	NYANGA	KAPTEINSKLIP	DOWN
NAGK2	NYANGA	KAPTEINSKLIP	UP
NBIK1	NDABENI	KAPTEINSKLIP	DOWN
NBIK2	NDABENI	KAPTEINSKLIP	UP
NBIV1	NDABENI	VLAKTE	DOWN
NBIV2	NDABENI	VLAKTE	UP
NDLS1	NUWELAND	SUBURBAN	DOWN
NDLS2	NUWELAND	SUBURBAN	UP
NOLC1	NOLUNGILE	CHRIS HANI	DOWN
NOLC2	NOLUNGILE	CHRIS HANI	UP
NOQC1	NONKQUBELA	CHRIS HANI	DOWN
NOQC2	NONKQUBELA	CHRIS HANI	UP
NTGC1	NETREG	CHRIS HANI	DOWN
NTGC2	NETREG	CHRIS HANI	UP
NTGK1	NETREG	KAPTEINSKLIP	DOWN
NTGK2	NETREG	KAPTEINSKLIP	UP
OOZM1	OOSTERZEE	MONTE VISTA	DOWN
OOZM2	OOSTERZEE	MONTE VISTA	UP
OTYV1	OTTERY	VLAKTE	DOWN
OTYV2	OTTERY	VLAKTE	UP
OVYS1	OBSERVATORY	SUBURBAN	DOWN
OVYS2	OBSERVATORY	SUBURBAN	UP
PDDC1	PAARDENEILAND	CHRIS HANI	DOWN
PDDC2	PAARDENEILAND	CHRIS HANI	UP
PDDM1	PAARDENEILAND	MONTE VISTA	DOWN
PDDM2	PAARDENEILAND	MONTE VISTA	UP
PEIL1	PENTECH	LAVISTOWN	DOWN
PEIL2	PENTECH	LAVISTOWN	UP
PMSS1	PLUMSTEAD	SUBURBAN	DOWN
PMSS2	PLUMSTEAD	SUBURBAN	UP
PNDK1	PINELANDS	KAPTEINSKLIP	DOWN
PNDK2	PINELANDS	KAPTEINSKLIP	UP
PNDV1	PINELANDS	VLAKTE	DOWN
PNDV2	PINELANDS	VLAKTE	UP



<b>Legend</b>	<b>STATION</b>	<b>LINE</b>	<b>DIRECTION</b>
POWN1	PAROW	NORTH	DOWN
POWN2	PAROW	NORTH	UP
POWN3	PAROW	NORTH	3rd Road
PPIC1	PHILIPPI	CHRIS HANI	DOWN
PPIC2	PHILIPPI	CHRIS HANI	UP
PPIK1	PHILIPPI	KAPTEINSKLIP	DOWN
PPIK2	PHILIPPI	KAPTEINSKLIP	UP
RCHS1	RONDEBOSCH	SUBURBAN	DOWN
RCHS2	RONDEBOSCH	SUBURBAN	UP
RETS1	RETREAT	SUBURBAN	DOWN
RETS2	RETREAT	SUBURBAN	UP
RSNS1	ROSEBANK	SUBURBAN	DOWN
RSNS2	ROSEBANK	SUBURBAN	UP
SFSV1	SOUTHFIELD	VLAKTE	DOWN
SFSV2	SOUTHFIELD	VLAKTE	UP
SHCMA	STELLENBOSCH	STELLENBOSCH	DOWN
SHCMO	STELLENBOSCH	STELLENBOSCH	UP
SKDH1	STIKLAND	HOOFLYN	DOWN
SKDH2	STIKLAND	HOOFLYN	UP
SKRC1	STOCK ROAD	CHRIS HANI	DOWN
SKRC2	STOCK ROAD	CHRIS HANI	UP
SRPL1	SAREPTA	LAVISTOWN	DOWN
SRPL2	SAREPTA	LAVISTOWN	UP
SRXN1	SOUTRIVIER	NORTH	DOWN
SRXN2	SOUTRIVIER	NORTH	UP
SRXS1	SOUTRIVIER	SUBURBAN	DOWN
SRXS2	SOUTRIVIER	SUBURBAN	UP
SRXV1	SOUTRIVIER	VLAKTE	DOWN
SRXV2	SOUTRIVIER	VLAKTE	UP
SSWSA	SOMERSET WEST	STRAND	DOWN
SSWSO	SOMERSET WEST	STRAND	UP
STDSO	STRAND	STRAND	
STHS1	STEURHOF	SUBURBAN	DOWN
STHS2	STEURHOF	SUBURBAN	UP
STJS1	ST JAMES	SUBURBAN	DOWN
STJS2	ST JAMES	SUBURBAN	UP
STWS2	SIMONSTAD	SUBURBAN	UP
STXS1	STEENBERG	SUBURBAN	DOWN
STXS2	STEENBERG	SUBURBAN	UP
SYES1	SUNNY COVE	SUBURBAN	DOWN
SYES2	SUNNY COVE	SUBURBAN	UP
THON1	THORNTON	NORTH	DOWN
THON2	THORNTON	NORTH	UP
THON3	THORNTON	NORTH	3rd Road
TYGN1	TYGERBERG	NORTH	DOWN
TYGN2	TYGERBERG	NORTH	UP
TYGN3	TYGERBERG	NORTH	3rd Road
UBLL1	UNIBELL	LAVISTOWN	DOWN
UBLL2	UNIBELL	LAVISTOWN	UP

<b>Legend</b>	<b>STATION</b>	<b>LINE</b>	<b>DIRECTION</b>
VOBMA	VLOTTENBURG	STELLENBOSCH	DOWN
VOBMO	VLOTTENBURG	STELLENBOSCH	UP
VSBS1	VALSBAAI	SUBURBAN	DOWN
VSBS2	VALSBAAI	SUBURBAN	UP
VSKS1	VISHOEK	SUBURBAN	DOWN
VSKS2	VISHOEK	SUBURBAN	UP
VLSA	VAN DER STEL	STRAND	DOWN
VLSO	VAN DER STEL	STRAND	UP
VSON1	VASCO	NORTH	DOWN
VSON2	VASCO	NORTH	UP
VSON3	VASCO	NORTH	3rd Road
WDCN1	WOODSTOCK	NORTH	DOWN
WDCN2	WOODSTOCK	NORTH	UP
WDCS1	WOODSTOCK	SUBURBAN	DOWN
WDCS2	WOODSTOCK	SUBURBAN	UP
WDCV1	WOODSTOCK	VLAKTE	DOWN
WDCV2	WOODSTOCK	VLAKTE	UP
WTES1	WITTEBOME	SUBURBAN	DOWN
WTES2	WITTEBOME	SUBURBAN	UP
WTMN1	WOLTEMADE	NORTH	DOWN
WTMN2	WOLTEMADE	NORTH	UP
WTNV1	WETTON	VLAKTE	DOWN
WTNV2	WETTON	VLAKTE	UP
WYBS1	WYNBERG	SUBURBAN	DOWN
WYBS2	WYNBERG	SUBURBAN	UP
YPTC1	YSTERPLAAT	CHRIS HANI	DOWN
YPTC2	YSTERPLAAT	CHRIS HANI	UP
YPTM1	YSTERPLAAT	MONTE VISTA	DOWN
YPTM2	YSTERPLAAT	MONTE VISTA	UP

11M 3 kV Place	Theoretical Energy (kWh)			Simulated Energy (kWh)			% Difference			Simulated DC Line voltage				Energy Dissipated	% Energy dissipated	Total time spent (s)		
	Used	Generated	Net Used	Used	Generated	Net Used				Min(kV)	U<2.7kV	U<3kV	Max(kV)			Used	Generated	Dissipated
	Legend																	
AKAM1	1 542	475	1 067	1 573	476	1 098	2%	0%	3%	2.617	17	700	3.744	0	0.00%	8 302	1 094	0
AKAM2	2 059	443	1 616	2 061	443	1 619	0%	0%	0%	2.631	31	951	3.750	1	0.13%	8 054	1 288	3
ATLV1	1 257	174	1 083	1 288	174	1 114	2%	0%	3%	2.838	0	537	3.747	0	0.00%	8 081	1 000	0
ATLV2	963	371	591	989	369	620	3%	-1%	5%	2.835	0	582	3.750	0	0.02%	7 020	1 090	1
AVDM1	1 216	330	886	1 205	330	875	-1%	0%	-1%	2.309	149	2 511	3.745	0	0.00%	6 974	919	0
AVDM2	1 465	165	1 300	1 445	164	1 280	-1%	0%	-2%	2.374	210	2 745	3.744	0	0.00%	8 552	815	0
BKHE1	5 451	1 256	4 196	5 047	1 262	3 785	-7%	0%	-10%	1.965	1 194	6 947	3.751	89	7.05%	19 519	1 626	204
BKHE2	5 408	811	4 596	4 989	813	4 175	-8%	0%	-9%	1.456	1 358	7 030	3.752	35	4.28%	20 414	1 343	85
BKLH1	6 027	1 634	4 394	5 591	1 642	3 950	-7%	0%	-10%	1.725	1 508	6 822	3.750	197	12.00%	21 552	1 815	323
BKLH2	6 432	1 233	5 200	5 977	1 239	4 738	-7%	1%	-9%	1.670	1 455	6 620	3.750	68	5.48%	23 719	1 719	166
BLEE1	5 262	17	5 245	5 318	17	5 301	1%	0%	1%	2.555	31	3 549	3.746	0	0.00%	17 652	769	0
BLEL2	1 714	3	1 711	1 746	3	1 743	2%	-1%	2%							8 520	253	
BLEE2	3 772	1 479	2 293	3 930	1 478	2 453	4%	0%	7%	2.630	10	3 239	3.750	18	1.22%	21 978	1 191	23
BLEH1	3 323	18	3 305	3 347	18	3 329	1%	0%	1%	2.583	15	3 863	3.750	0	0.00%	11 057	663	0
BLEH2	1 503	990	512	1 568	990	578	4%	0%	13%	2.660	5	3 495	3.750	13	1.35%	10 646	876	22
BLEM1	462	284	178	482	283	198	4%	0%	11%	2.649	3	3 037	3.750	0	0.00%	5 738	455	6
BLEM2	1 175	9	1 167	1 188	9	1 179	1%	0%	1%	2.649	3	3 109	3.750	0	0.05%	5 772	455	6
BLN1	1 861	1 165	696	1 948	1 164	784	5%	0%	13%	2.649	3	3 017	3.750	1	0.10%	13 863	1 129	11
BLN2	4 045	24	4 021	4 144	24	4 120	2%	0%	2%	2.649	3	3 017	3.750	1	4.85%	15 054	900	11
BLN3	391	11	380	399	11	388	2%	0%	2%	2.649	3	3 017	3.750	1	10.31%	2 735	20	11
BOHL1	1 889	428	1 461	1 913	428	1 484	1%	0%	2%	2.725	0	701	3.750	0	0.08%	6 264	768	2
BOHL2	2 561	541	2 020	2 563	541	2 023	0%	0%	0%	2.776	0	1 047	3.750	3	0.56%	5 762	943	9
BTL1	4 624	733	3 891	4 680	733	3 948	1%	0%	1%							19 163	1 393	
BTL1	1 751	15	1 736	1 740	15	1 724	-1%	-1%	-1%	2.595	26	4 156	3.750	1	0.13%	4 344	384	5
BTL2	4 516	926	3 590	4 572	926	3 646	1%	0%	2%							17 798	1 621	
BTL2	539	331	208	559	331	228	4%	0%	10%	2.622	21	4 008	3.750	10	0.79%	4 122	318	24
BTLK1	3 873	502	3 370	3 897	502	3 395	1%	0%	1%	2.643	7	3 740	3.750	4	0.77%	14 856	1 190	8
BTLK2	3 265	1 281	1 985	3 324	1 279	2 044	2%	0%	3%	2.597	8	3 690	3.750	8	0.61%	14 269	1 315	18
CENM1	1 657	702	955	1 720	703	1 018	4%	0%	7%	2.826	0	197	3.750	0	0.06%	7 127	1 304	5
CENM2	1 754	740	1 014	1 824	740	1 084	4%	0%	7%	2.865	0	206	3.745	0	0.00%	7 461	1 360	0
CMCS1	1 269	313	955	1 327	313	1 014	5%	0%	6%	2.878	0	73	3.748	0	0.00%	9 349	1 424	0
CMCS2	1 288	310	978	1 351	310	1 041	5%	0%	6%	2.871	0	65	3.748	0	0.00%	9 596	1 431	0
CRFV1	1 045	379	665	1 093	379	714	5%	0%	7%	2.946	0	59	3.747	0	0.00%	8 019	1 080	0
CRFV2	1 233	231	1 002	1 281	231	1 051	4%	0%	5%	2.931	0	77	3.747	0	0.00%	7 566	1 051	0
CRTC1	922	265	657	931	267	664	1%	0%	1%	1.477	3 367	13 919	3.752	17	6.28%	9 437	372	49
CRTC2	3 700	0	1 780	1 637	0	1 636	-8%	0%	-8%	1.408	3 380	13 933	3.750	0	0.06%	11 936	123	0
CWNC1	3 014	9	3 005	3 079	9	3 069	2%	0%	2%	2.549	13	1 795	3.749	0	0.00%	13 990	600	0
CWNC2	1 893	483	1 410	1 983	483	1 500	5%	0%	6%	2.600	6	1 678	3.750	13	2.68%	16 548	692	21
CWNN1	1 155	5	1 151	1 179	5	1 175	2%	0%	2%	2.553	9	1 688	3.749	0	0.00%	7 280	359	0
CWNN2	616	173	442	646	173	473	5%	0%	7%	2.600	7	1 642	3.749	0	0.00%	8 272	368	0
CWNN3	3 187	17	3 170	3 213	17	3 197	1%	0%	1%	2.456	34	1 993	3.749	0	0.00%	13 478	836	0
CWNN4	1 783	506	1 277	1 867	506	1 361	5%	0%	7%	2.597	6	1 738	3.750	6	1.24%	16 327	717	12
CWNS1	1 635	17	1 619	1 659	17	1 642	1%	0%	1%	2.600	11	1 900	3.749	0	0.00%	9 163	845	0
CWNS2	732	215	517	768	215	553	5%	0%	7%	2.595	6	1 675	3.749	0	0.00%	13 381	604	0
CWNV1	2 911	17	2 895	2 912	17	2 896	0%	0%	0%	2.438	38	2 083	3.749	0	0.00%	13 158	864	0
CWNV2	1 217	490	727	1 272	490	782	4%	0%	8%	2.600	7	1 732	3.750	3	0.64%	13 726	824	7
DEGM1	1 635	538	1 097	1 601	539	1 062	-2%	0%	-3%	2.150	209	2 058	3.750	0	0.02%	9 317	1 094	1
DEGM2	2 192	366	1 826	2 089	366	1 723	-5%	0%	-6%	2.192	278	2 323	3.744	0	0.00%	9 190	1 202	0
DPES1	1 208	201	1 007	1 274	201	1 073	5%	0%	7%	2.871	0	199	3.750	1	0.58%	11 858	1 075	4
DPES2	1 441	481	960	1 500	481	1 020	4%	0%	6%	2.838	0	223	3.748	0	0.00%	8 990	1 701	0
DUTMA	1 938	228	1 710	1 654	230	1 424	-15%	1%	-17%	1.527	2 058	5 465	3.750	226	28.81%	6 645	510	269
DUTMO	1 456	549	908	1 345	553	793	-8%	1%	-13%							5 769	518	
EERE1	770	550	220	805	552	253	5%	0%	15%	2.654	20	4 542	3.750	26	4.66%	6 278	602	57
EERE2	2 023	17	2 006	2 005	17	1 988	-1%	0%	-1%	2.530	71	4 601	3.746	0	0.00%	6 299	564	0
EERSD	1 912	294	1 618	1 951	294	1 657	2%	0%	2%	2.650	16	4 175	3.751	12	4.05%	9 116	507	61
EERSH	2 131	356	1 774	2 164	358	1 806	2%	0%	2%	2.650	16	4 175	3.751	12	3.33%	8 474	513	61
EIKH1	4 436	1 159	3 277	4 290	1 164	3 126	-3%	0%	-5%	1.845	963	5 340	3.751	94	8.07%	17 300	1 677	189
EIKH2	5 003	898	4 105	4 765	901	3 865	-5%	0%	-6%	2.018	1 115	5 093	3.750	37	4.12%	18 157	1 632	111
EPDC1	4 322	487	3 836	4 464	486	3 978	3%	0%	4%	2.727	0	1 164	3.749	0	0.00%	24 607	646	0
EPDC2	4 734	544	4 190	4 889	543	4 346	3%	0%	4%	2.696	1	1 174	3.750	0	0.00%	26 884	1 189	4
EPDM1	1 565	206	1 359	1 626	205	1 421	4%	0%	5%	2.728	0	833	3.749	0	0.00%	14 680	420	0
EPDM2	1 558	207	1 351	1 624	207	1 417	4%	0%	5%	2.742	0	833	3.749	0	0.00%	14 807	692	0
ERHN1	4 418	739	3 679	4 357	739	3 618	-1%	0%	-2%	2.419	183	4 274	3.750	2	0.25%	16 043	1 898	7
ERHN2	4 263	1 708	2 554	4 182	1 709	2 473	-2%	0%	-3%	2.519	182	4 321	3.750	30	1.74%	12 973	2 402	50
ERHN3	339	21	318	342	21	322	1%	0%	1%	2.608	12	1 508	3.746	0	0.00%	1 928	17	0
FAUSA	2 549	277	2 272	2 456	278	2 177	-4%	1%	-4%							10 493	589	
FAUSO	2 135	527	1 607	2 122	528	1 595	-1%	0%	-1%	2.213	769	4 690	3.750	129	16.04%	10 331	609	220
FGVSA	2 894	509	2 385	2 702	516	2 186	-7%	1%	-8%							11 255	719	
FGVSO	2 968	647	2 321	2 749	650	2 099	-7%	0%	-10%	1.815	1 145	3 751	3.751	473	40.57%	10 718	743	608
GCRS1	978	80	898	993	80	912	1%	1%	2%	2.476	189	1 126	3.750	3	1.62%	11 302	480	27
GCRS2	874	91	782	896	92	804	3%	0%	3%							10 833	437	
GDXN1	3 865	1 295	2 570	3 940	1 292	2 648	2%	0%	3%	2.754	0	2 254	3.750	15	1.13%	14 770	2 065	17
GDXN2	4 628	907	3 720	4 664	906	3 758	1%	0%	1%	2.626	10	2 756	3.750	12	1.33%	14 382	2 071	20
GDXN3	358	63	295	369	63	306	3%	0%	4%	2.757	0	1 532	3.746	0	0.00%	1 957	61	0
HAZV1	943	338	605	980	337	643	4%	0%	6%	2.821</								

11M 3 kV Place	Theoretical Energy (kWh)			Simulated Energy (kWh)			% Difference			Simulated DC Line voltage				Energy Dissipated	% Energy dissipated	Total time spent (s)		
	Used	Generated	Net Used	Used	Generated	Net Used				Min(kV)	U<2.7kV	U<3kV	Max(kV)			Used	Generated	Dissipated
KABS1	1 498	296	1 202	1 566	296	1 270	5%	0%	6%	2.815	0	605	3.750	1	0.34%	18 884	1 017	6
KABS2	1 675	181	1 494	1 737	181	1 557	4%	0%	4%	2.783	0	752	3.750	1	0.40%	17 685	1 077	5
KAIH1	5 224	948	4 275	5 236	950	4 286	0%	0%	0%	2.225	330	4 054	3.751	72	7.57%	21 111	1 266	141
KAIH2	5 837	915	4 922	5 862	919	4 943	0%	0%	0%	2.227	303	4 021	3.750	63	6.85%	22 097	1 231	97
KEDM1	2 025	293	1 732	2 070	293	1 778	2%	0%	3%	2.727	0	320	3.746	0	0.00%	9 326	1 129	0
KEDM2	1 451	495	956	1 515	495	1 020	4%	0%	7%	2.834	0	280	3.746	0	0.00%	10 319	1 027	0
KHFMA	2 254	495	1 758	2 166	500	1 666	-4%	1%	-5%	2.053	1 125	3 071	3.750	306	29.12%	9 044	567	347
KHFMO	2 303	550	1 753	2 148	553	1 596	-7%	0%	-9%							7 239	630	
KLWS1	1 415	267	1 149	1 473	267	1 207	4%	0%	5%	2.820	0	206	3.748	0	0.00%	10 240	1 435	0
KLWS2	1 191	361	830	1 246	361	885	5%	0%	7%	2.891	0	165	3.740	0	0.00%	10 536	1 430	0
KOBN1	2 643	1 398	1 245	2 726	1 397	1 329	3%	0%	7%	2.658	2	3 004	3.750	7	0.47%	14 712	1 666	13
KOBN2	4 589	493	4 096	4 625	493	4 132	1%	0%	1%	2.626	5	3 259	3.750	2	0.48%	13 573	1 862	8
KOBV1	2 477	1 162	1 314	2 514	1 159	1 355	2%	0%	3%	2.620	13	3 039	3.750	1	0.05%	14 310	1 935	1
KOBV2	3 220	462	2 758	3 240	461	2 779	1%	0%	1%	2.597	8	3 184	3.750	6	1.36%	13 154	1 710	9
KSVE1	6 907	1 122	5 785	6 634	1 124	5 509	-4%	0%	-5%	2.066	1 048	6 992	3.751	10	0.85%	26 989	1 547	38
KSVE2	7 106	1 040	6 066	6 745	1 042	5 703	-5%	0%	-6%	1.503	1 181	7 178	3.750	19	1.81%	25 796	1 400	41
KTEK1	949	925	23	985	927	58	4%	0%	152%	2.241	262	2 522	3.751	70	7.58%	6 644	828	146
KTEK2	2 486	11	2 474	2 412	12	2 400	-3%	0%	-3%	2.204	307	2 542	3.750	0	0.00%	8 352	456	0
KUYC1	2 580	598	1 981	2 563	602	1 960	-1%	1%	-1%	1.581	3 307	13 711	3.750	47	7.77%	18 833	902	101
KUYC2	3 668	50	3 618	3 410	50	3 360	-7%	0%	-7%	1.565	3 314	13 768	3.750	2	3.28%	20 589	617	58
KYAC1	4 052	759	3 294	3 863	760	3 103	-5%	0%	-6%	1.727	2 983	12 532	3.751	84	10.98%	18 902	1 210	176
KYAC2	5 170	648	4 522	4 659	649	4 010	-10%	0%	-11%	1.707	2 978	12 514	3.750	69	10.57%	15 754	1 368	160
LAGC1	5 987	726	5 262	6 172	725	5 447	3%	0%	4%	2.679	1	3 073	3.749	0	0.00%	28 054	1 352	0
LAGC2	7 068	1 132	5 936	7 207	1 131	6 076	2%	0%	2%	2.643	2	3 216	3.750	44	3.87%	25 193	1 803	40
LAGK1	4 044	1 418	2 627	4 170	1 416	2 754	3%	0%	5%	2.673	1	2 816	3.750	25	1.77%	18 034	1 357	28
LAGK2	4 455	494	3 961	4 562	492	4 070	2%	0%	3%	2.694	1	2 851	3.749	0	0.00%	18 918	1 108	0
LDHMA	1 844	381	1 463	1 725	384	1 341	-6%	1%	-8%	1.921	1 447	5 867	3.752	118	15.44%	7 243	528	196
LDHMO	1 775	377	1 398	1 634	378	1 256	-8%	0%	-10%							6 603	507	
LENK1	4 401	739	3 662	4 499	741	3 758	2%	0%	3%	2.593	15	1 783	3.751	45	6.02%	19 598	1 210	102
LENK2	4 705	660	4 044	4 768	662	4 107	1%	0%	2%	2.533	32	1 793	3.751	22	3.30%	18 263	1 251	80
LNEV1	1 190	228	962	1 234	227	1 007	4%	0%	5%	2.876	0	142	3.747	0	0.00%	8 667	1 000	0
LNEV2	1 024	292	733	1 064	291	772	4%	0%	5%	2.920	0	120	3.750	0	0.00%	8 152	975	1
LSDS1	1 713	365	1 347	1 748	365	1 383	2%	0%	3%	2.764	0	1 078	3.750	1	0.18%	11 440	1 485	3
LSDS2	1 498	444	1 053	1 537	444	1 093	3%	0%	4%	2.745	0	1 053	3.750	1	0.14%	11 385	1 392	6
LSNL1	2 105	525	1 580	2 127	525	1 602	1%	0%	1%	2.683	2	1 556	3.748	0	0.00%	7 992	744	0
LSNL2	1 910	1 009	902	1 938	1 009	929	1%	0%	3%	2.711	0	1 564	3.750	0	0.04%	7 293	870	2
MCFC1	4 154	1 361	2 792	3 889	1 365	2 524	-6%	0%	-10%	1.975	2 011	10 738	3.751	128	9.39%	14 034	1 522	241
MCFC2	4 731	783	3 948	4 317	784	3 533	-9%	0%	-10%	2.029	2 199	10 558	3.751	26	3.36%	13 523	1 558	81
METE1	3 396	1 115	2 282	3 364	1 117	2 246	-1%	0%	-2%	2.423	523	5 692	3.750	83	7.40%	15 133	1 412	181
METE2	4 070	528	3 542	3 915	529	3 386	-4%	0%	-4%	1.955	781	5 715	3.750	16	3.03%	16 081	1 167	42
MLDK1	1 431	7	1 424	1 429	7	1 422	0%	0%	0%	2.558	19	3 644	3.747	0	0.00%	5 912	387	0
MLDK2	571	248	323	593	248	345	4%	0%	7%	2.646	3	3 443	3.747	0	0.00%	5 113	351	0
MLDN1	4 861	277	4 585	4 937	276	4 661	2%	0%	2%	2.610	6	3 432	3.750	0	0.02%	18 043	1 595	1
MLDN2	3 189	1 324	1 865	3 289	1 322	1 967	3%	0%	5%	2.662	3	3 392	3.750	22	1.69%	16 816	1 783	28
MLDV1	1 243	385	857	1 281	384	897	3%	0%	5%	2.670	3	3 272	3.747	0	0.00%	12 481	962	0
MLDV2	1 829	117	1 712	1 860	116	1 744	2%	0%	2%	2.630	5	3 405	3.748	0	0.00%	11 632	976	0
MNVM1	1 978	384	1 594	1 950	384	1 565	-1%	0%	-2%	2.336	121	1 322	3.750	1	0.16%	10 277	1 120	4
MNVM2	1 842	693	1 149	1 838	695	1 143	0%	0%	0%	2.330	147	1 608	3.751	4	0.65%	10 128	1 242	19
MTPK1	3 565	747	2 818	3 526	749	2 777	-1%	0%	-1%	2.356	236	2 305	3.750	26	3.46%	13 261	1 445	71
MTPK2	3 345	441	2 904	3 356	442	2 913	0%	0%	0%	2.408	164	2 281	3.750	2	0.46%	14 854	1 026	12
MTXC1	7 701	1 561	6 140	7 820	1 561	6 258	2%	0%	2%	2.540	113	3 315	3.750	14	0.88%	33 234	1 665	22
MTXC2	8 360	1 293	7 066	8 395	1 293	7 102	0%	0%	1%	2.274	271	3 262	3.750	1	0.06%	32 877	1 541	3
MTXN1	4 449	630	3 819	4 321	630	3 691	-3%	0%	-3%	2.428	289	4 615	3.750	3	0.46%	13 552	1 908	6
MTXN2	3 313	1 865	1 448	3 249	1 865	1 383	-2%	0%	-4%	2.402	371	5 385	3.750	47	2.53%	11 988	2 189	59
MTXN3	373	90	283	357	90	267	-4%	0%	-6%	2.473	35	2 224	3.746	0	0.00%	1 331	93	0
MUVH1	5 840	742	5 098	6 081	748	5 333	4%	1%	5%	2.820	0	643	3.750	72	9.67%	23 097	918	131
MUVH2	6 052	617	5 434	6 308	622	5 686	4%	1%	5%	2.787	0	629	3.750	50	8.02%	24 520	882	112
MUVSH	2 192	374	1 818	2 267	376	1 891	3%	0%	4%	2.878	0	713	3.750	65	17.28%	7 493	575	102
MWYS1	1 193	299	894	1 244	299	946	4%	0%	6%	2.849	0	255	3.749	0	0.00%	11 314	1 280	0
MWYS2	1 616	236	1 380	1 655	236	1 418	2%	0%	3%	2.800	0	659	3.750	0	0.00%	10 590	1 495	0
MZMS1	1 307	259	1 048	1 357	259	1 098	4%	0%	5%	2.866	0	524	3.750	0	0.02%	10 175	1 210	1
MZMS2	1 118	295	823	1 168	295	873	4%	0%	6%	2.821	0	468	3.750	3	1.07%	10 094	1 190	15
NAGC1	5 721	701	5 020	5 849	699	5 149	2%	0%	3%	2.612	25	3 941	3.750	1	0.08%	24 657	1 224	4
NAGC2	4 713	1 140	3 573	4 854	1 143	3 711	3%	0%	4%	2.660	7	3 764	3.750	8	0.74%	22 528	1 190	16
NAGK1	5 551	674	4 878	5 608	672	4 935	1%	0%	1%	2.566	36	3 779	3.750	1	0.22%	20 765	1 325	3
NAGK2	4 475	1 761	2 714	4 619	1 760	2 859	3%	0%	5%	2.622	7	3 721	3.752	15	0.87%	21 215	1 366	38
NBIK1	3 064	349	2 715	3 068	348	2 720	0%	0%	0%	2.656	5	3 582	3.746	0	0.00%	9 559	1 161	0
NBIK2	1 795	568	1 227	1 841	568	1 273	3%	0%	4%	2.660	2	3 281	3.746	0	0.00%	9 022	897	0
NBIV1	1 402	162	1 240	1 431	161	1 270	2%	-1%	2%	2.631	3	3 197	3.746	0	0.00%	8 613	1 040	0
NBIV2	820	283	537	849	283	566	4%	0%	5%	2.664	2	3 205	3.746	0	0.00%	9 477	819	0
NDLS1	1 428	364	1 064	1 487	364	1 124	4%	0%	6%	2.868	0	194	3.748	0	0.00%	11 980	1 488	0
NDLS2	1 738	316	1 422	1 796	316	1 480	3%	0%	4%	2.804	0	286	3.748	0	0.00%	11 281	1 561	0
NOLC1	4 013	821	3 192	3 900	823	3 077	-3%	0%	-4%	2.041	1 625	10 383	3.750	35	4.30%	15 391		

11M 3 kV Place	Theoretical Energy (kWh)			Simulated Energy (kWh)			% Difference			Simulated DC Line voltage				Energy Dissipated	% Energy dissipated	Total time spent (s)		
	Used	Generated	Net Used	Used	Generated	Net Used	Min(kV)	U<2.7kV	U<3kV	Max(kV)	Used	Generated	Dissipated					
PDDC1	3 004	70	2 934	3 164	70	3 093	5%	0%	5%	2.836	0	552	3.750	2	3.00%	21 574	679	8
PDDC2	2 854	509	2 345	3 006	509	2 497	5%	0%	6%	2.860	0	339	3.750	1	0.25%	20 008	992	5
PDDM1	1 015	60	955	1 064	60	1 004	5%	0%	5%	2.892	0	258	3.748	0	0.00%	10 675	557	0
PDDM2	957	10	947	1 010	10	1 000	6%	0%	6%	2.897	0	255	3.748	0	0.00%	10 822	371	0
PEIL1	1 779	143	1 636	1 680	144	1 536	-6%	0%	-6%	2.203	293	2 747	3.750	0	0.33%	7 128	577	2
PEIL2	1 506	445	1 061	1 425	446	978	-5%	0%	-8%	2.130	438	2 847	3.750	1	0.29%	5 635	690	4
PMSS1	1 105	357	749	1 148	357	792	4%	0%	6%	2.823	0	436	3.749	0	0.00%	9 224	1 342	0
PMSS2	1 360	217	1 143	1 401	217	1 184	3%	0%	4%	2.795	0	495	3.748	0	0.00%	9 560	1 348	0
PNDK1	5 003	1 024	3 979	4 981	1 023	3 958	0%	0%	-1%	2.604	5	3 370	3.750	3	0.32%	14 126	1 601	11
PNDK2	3 419	869	2 550	3 485	869	2 616	2%	0%	3%	2.629	3	2 808	3.747	0	0.00%	15 004	1 209	0
PNDV1	1 322	470	852	1 345	469	876	2%	0%	3%	2.694	1	2 545	3.747	0	0.00%	8 426	1 280	0
PNDV2	1 197	337	859	1 221	337	884	2%	0%	3%	2.698	1	2 600	3.747	0	0.00%	8 580	1 092	0
POWN1	4 975	1 181	3 794	4 790	1 182	3 608	-4%	0%	-5%	2.272	583	4 971	3.750	3	0.28%	16 972	2 198	11
POWN2	5 353	1 385	3 969	5 085	1 384	3 701	-5%	0%	-7%	2.326	713	5 066	3.750	44	3.16%	15 166	2 477	49
POWN3	354	1	353	363	1	362	3%	0%	3%	2.731	0	1 885	3.745	0	0.00%	2 260	17	0
PPIC1	6 843	1 253	5 590	6 438	1 255	5 184	-6%	0%	-7%	2.003	1 777	8 750	3.751	34	2.69%	19 271	2 042	55
PPIC2	6 018	2 206	3 812	5 653	2 208	3 445	-6%	0%	-10%	2.096	1 662	8 518	3.751	189	8.54%	17 353	2 050	265
PPIK1	5 448	1 260	4 188	5 504	1 262	4 241	1%	0%	1%	2.378	176	2 669	3.751	86	6.77%	23 981	1 376	115
PPIK2	6 574	1 103	5 471	6 508	1 104	5 404	-1%	0%	-1%	2.382	337	2 969	3.750	20	1.79%	21 882	1 622	44
RCHS1	1 554	304	1 249	1 604	304	1 300	3%	0%	4%	2.825	0	378	3.748	0	0.00%	12 016	1 417	0
RCHS2	1 361	485	876	1 411	485	926	4%	0%	6%	2.840	0	479	3.748	0	0.00%	11 341	1 625	0
RETS1	2 233	595	1 637	2 267	595	1 671	2%	0%	2%	2.730	0	1 121	3.750	0	0.03%	14 561	1 949	1
RETS2	2 479	478	2 000	2 518	479	2 039	2%	0%	2%	2.718	0	1 253	3.750	0	0.01%	14 653	1 864	1
RSNS1	1 215	217	997	1 261	217	1 044	4%	0%	5%	2.836	0	338	3.749	0	0.00%	10 408	1 289	0
RSNS2	1 170	301	869	1 214	300	913	4%	0%	5%	2.847	0	583	3.749	0	0.00%	10 785	1 300	0
SFSV1	1 332	427	905	1 388	427	961	4%	0%	6%	2.834	0	408	3.747	0	0.00%	15 004	1 034	0
SFSV2	1 694	230	1 464	1 723	230	1 493	2%	0%	2%	2.642	3	638	3.747	0	0.00%	13 065	1 093	0
SHCMA	1 423	370	1 052	1 295	375	921	-9%	1%	-13%	1.478	2 119	5 992	3.750	106	18.01%	6 255	480	188
SHCMO	1 651	213	1 437	1 379	215	1 164	-16%	1%	-19%	1.478	2 119	5 992	3.750	106	18.01%	5 418	462	188
SKDH1	6 343	847	5 496	5 967	848	5 118	-6%	0%	-7%	2.106	1 193	6 227	3.750	3	0.40%	21 089	1 654	19
SKDH2	5 543	1 242	4 301	5 376	1 247	4 128	-3%	0%	-4%	1.909	919	6 103	3.750	11	0.85%	22 453	1 637	40
SKRC1	4 634	2 714	1 920	4 168	2 720	1 449	-10%	0%	-25%	1.988	2 151	10 205	3.752	583	21.43%	10 977	2 267	616
SKRC2	4 628	1 558	3 070	4 189	1 559	2 630	-9%	0%	-14%	2.040	2 225	10 001	3.752	123	7.92%	10 486	2 237	295
SRPL1	2 131	453	1 678	2 121	454	1 667	0%	0%	-1%	2.303	250	4 163	3.750	0	0.07%	11 472	648	2
SRPL2	2 362	275	2 087	2 301	275	2 026	-3%	0%	-3%	2.004	328	4 185	3.744	0	0.00%	11 438	644	0
SRXN1	5 282	573	4 709	5 367	573	4 794	2%	0%	2%	2.658	3	2 613	3.748	0	0.00%	19 442	1 795	0
SRXN2	4 217	1 466	2 751	4 317	1 465	2 852	2%	0%	4%	2.686	2	2 481	3.750	25	1.71%	17 733	2 134	34
SRXS1	1 738	262	1 476	1 832	262	1 570	5%	0%	6%	2.865	0	224	3.749	0	0.00%	18 526	1 300	0
SRXS2	2 224	382	1 841	2 312	382	1 930	4%	0%	5%	2.840	0	269	3.749	0	0.00%	14 966	1 755	0
SRXV1	4 170	857	3 313	4 260	855	3 405	2%	0%	3%	2.711	0	2 561	3.750	2	0.25%	16 873	2 234	5
SRXV2	3 249	975	2 273	3 337	974	2 363	3%	0%	4%	2.721	0	2 451	3.750	5	0.48%	17 630	1 836	13
SSWSA	1 806	578	1 228	1 784	583	1 200	-1%	1%	-2%	2.296	813	2 310	3.751	383	48.02%	7 692	620	664
SSWSO	2 376	213	2 163	2 249	214	2 035	-5%	1%	-6%	2.176	168	1 603	3.751	135	54.65%	7 922	605	407
STDSD	1 800	242	1 558	1 792	246	1 546	0%	2%	-1%	2.176	168	1 603	3.751	135	54.65%	10 033	430	407
STHS1	1 053	202	851	1 098	202	896	4%	0%	5%	2.830	0	299	3.750	0	0.01%	9 257	1 116	2
STHS2	1 062	390	672	1 109	390	719	4%	0%	7%	2.848	0	317	3.748	0	0.00%	8 378	1 386	0
STJS1	1 356	312	1 043	1 394	313	1 081	3%	0%	4%	2.785	0	702	3.750	1	0.35%	10 890	1 320	9
STJS2	1 335	289	1 046	1 372	289	1 083	3%	0%	4%	2.734	0	785	3.750	2	0.57%	10 840	1 194	12
STWS2	886	134	752	887	135	751	0%	1%	0%	2.205	289	1 221	3.751	13	9.50%	10 674	495	92
STXS1	1 578	592	986	1 612	593	1 019	2%	0%	3%	2.735	0	1 339	3.748	0	0.00%	11 277	1 595	0
STXS2	1 723	343	1 379	1 751	344	1 408	2%	0%	2%	2.741	0	1 361	3.750	0	0.04%	12 186	1 414	1
SYES1	683	77	606	717	77	640	5%	0%	6%	2.738	0	708	3.750	2	1.45%	9 000	408	17
SYES2	628	92	536	659	92	567	5%	0%	6%	2.738	0	708	3.750	2	1.45%	7 912	437	17
THON1	4 940	1 320	3 620	4 868	1 320	3 549	-1%	0%	-2%	2.467	166	3 799	3.750	2	0.12%	16 787	2 292	8
THON2	5 856	1 391	4 465	5 567	1 392	4 175	-5%	0%	-6%	2.433	722	4 743	3.750	22	1.57%	15 003	2 533	32
THON3	359	6	353	370	6	363	3%	0%	3%	2.653	6	1 650	3.746	0	0.00%	2 438	114	0
TYGN1	5 508	1 302	4 206	5 415	1 302	4 112	-2%	0%	-2%	2.429	394	4 837	3.750	4	0.30%	21 449	2 005	16
TYGN2	5 619	1 058	4 562	5 526	1 057	4 469	-2%	0%	-2%	2.454	450	4 919	3.750	13	1.27%	21 987	2 077	29
TYGN3	494	0	494	507	0	507	3%	0%	3%	2.734	0	2 323	3.745	0	0.00%	3 700	20	0
UBLL1	1 215	504	711	1 229	504	725	1%	0%	2%	2.508	91	1 776	3.750	2	0.47%	6 768	601	11
UBLL2	1 689	359	1 330	1 603	359	1 244	-5%	0%	-6%	2.345	295	1 986	3.750	2	0.52%	5 282	713	6
VOBMA	1 892	365	1 527	1 682	370	1 312	-11%	1%	-14%	1.564	1 831	6 445	3.750	160	20.01%	7 276	525	265
VOBMO	1 774	425	1 349	1 559	428	1 131	-12%	1%	-16%	1.564	1 831	6 445	3.750	160	20.01%	6 146	532	265
VSBS1	1 189	468	721	1 246	468	777	5%	0%	8%	2.861	0	423	3.750	0	0.03%	9 955	1 430	2
VSBS2	1 547	253	1 294	1 603	253	1 350	4%	0%	4%	2.869	0	448	3.750	0	0.04%	10 013	1 289	1
VSKS1	1 102	144	958	1 167	144	1 023	6%	0%	7%	2.828	0	320	3.750	0	0.31%	16 820	635	4
VSKS2	1 335	75	1 261	1 402	75	1 327	5%	0%	5%	2.804	0	346	3.750	0	0.00%	15 830	622	0
VLSA	1 469	252	1 217	1 491	255	1 235	1%	2%	1%	2.520	198	1 831	3.751	212	46.96%	7 403	462	569
VLSO	1 348	194	1 154	1 395	196	1 200	4%	1%	4%	2.520	198	1 831	3.751	212	46.96%	7 980	423	569
VSON1	3 178	846	2 331	3 237	846	2 391	2%	0%	3%	2.551	9	2 975	3.750	6	0.71%	13 816	1 748	13
VSON2	3 564	1 141	2 423	3 610	1 141	2 468	1%	0%	2%	2.674	3	3 138	3.750	22	1.94%	12 279	2 018	38
VSON3	263	2	262	272	2	270	3%	0%	3%	2.774	0	1 475	3.746	0	0.00%	1 575	28	0
WDCN1	4 435	713	3 722	4 575	712	3 863	3%	0%	4%	2.638	8	2 348	3.750	2	0.32%	25 481	1 384	5
WDCN2	4 428	864																

11M 3 kV Place	Theoretical Energy (kWh)			Simulated Energy (kWh)			% Difference			Simulated DC Line voltage				Energy Dissipated	% Energy dissipated	Total time spent (s)		
	Used	Generated	Net Used	Used	Generated	Net Used				Min(kV)	U<2.7kV	U<3kV	Max(kV)			Used	Generated	Dissipated
YPTC1	7 591	593	6 999	7 642	593	7 049	1%	0%	1%	2.613	48	1 653	3.750	41	6.97%	26 674	1 533	43
YPTC2	5 833	1 022	4 810	6 024	1 022	5 002	3%	0%	4%	2.640	5	1 196	3.750	1	0.14%	28 279	1 198	10
YPTM1	1 263	335	928	1 310	335	975	4%	0%	5%	2.818	0	267	3.748	0	0.00%	8 936	892	0
YPTM2	1 321	260	1 061	1 371	260	1 111	4%	0%	5%	2.807	0	261	3.748	0	0.00%	10 225	458	0
<b>Total</b>	<b>705 200</b>	<b>144 597</b>	<b>560 603</b>	<b>703 566</b>	<b>144 711</b>	<b>558 855</b>	<b>0%</b>	<b>0%</b>	<b>0%</b>	<b>75 414</b>	<b>721 610</b>			<b>5 763</b>	<b>4%</b>	<b>297 253</b>	<b>10 411</b>	

# Bibliography

- [1] Randewijk, P.-J.: Prasa electrical bursary advert, October 2013. PDF file, received via e-mail. (Cited on page 1.)
- [2] Wikipedia: Metrorail Western Cape — Wikipedia, The Free Encyclopedia. 2016. [Online; accessed 3-August-2016]. Available at: [https://en.wikipedia.org/w/index.php?title=Metrorail\\_Western\\_Cape&oldid=732835588](https://en.wikipedia.org/w/index.php?title=Metrorail_Western_Cape&oldid=732835588) (Cited on page 2.)
- [3] Eskom: Salt river power station. 2016. [Online; accessed 20-December-2015]. Available at: <http://www.eskom.co.za/sites/heritage/Pages/SaltRiver.aspx> (Cited on page 2.)
- [4] Pivnic, L.: Photo journal, volume 2 no 13. ISSN 1028169X. (Cited on page 2.)
- [5] de Rijke, C.: Uzi van Freddy, 2012. Write-up of energy saving measures on the Dutch Railways, in Dutch. Available at: <http://www.feijenoordsemeesters.nl/UZI%20van%20Freddy.htm> (Cited on page 5.)
- [6] Slats, F.: ECO driving @ NS, 2012. PDF slideshow, available on request. (Cited on pages 5 and 6.)
- [7] Slats, F. and Poncin, C.: DAS - Driver Advisory System, 2014. Presented at the UIC Energy Efficiency Days 2014 in Antwerpen. Available at: [http://www.energy-efficiency-days.org/IMG/pdf/eco\\_driving\\_and\\_das.pdf](http://www.energy-efficiency-days.org/IMG/pdf/eco_driving_and_das.pdf) (Cited on pages 7 and 8.)
- [8] Luijt, R.: Van Statisch advies — UZI naar dynamisch advies — DAS: minder energieverbruik, meer punctualiteit en minder spreiding in de uitvoering, 2014. Presented at the “Eerste workshop — Dotteren Groene Golf”. Available at: <http://www.duurzaamspoor.nl/wp-content/uploads/2014/01/20140123-sheets-workshop-groene%20golf-22-jan-2014.pdf> (Cited on page 7.)

- [9] Toshiba Corporation: Greener Driving System. 2014. Pamphlet. Available at: [http://www.toshiba.co.jp/sis/railwaysystem/en/products/catalog/pdf/greener\\_driving\\_system.pdf](http://www.toshiba.co.jp/sis/railwaysystem/en/products/catalog/pdf/greener_driving_system.pdf) (Cited on page 9.)
- [10] G., F.R.: Regenerative equipment for railway rolling stock. *Power Engineering Journal*, pp. 105–113, May 1991. (Cited on page 9.)
- [11] Pecharromás, R.R., López-López, A., Cucala, A.P. and Fernández-Cardador, A.: Riding the rails to DC power efficiency. *IEEE Electrification Magazine*, vol. 2, no. 3, pp. 32–38, September 2014. (Cited on pages 9, 10, 11, 12, 15, 17, and 18.)
- [12] Wikipedia: Railway electrification system — Wikipedia, The Free Encyclopedia. 2016. [Online; accessed 10-September-2016]. Available at: [https://en.wikipedia.org/w/index.php?title=Railway\\_electrification\\_system&oldid=734198149](https://en.wikipedia.org/w/index.php?title=Railway_electrification_system&oldid=734198149) (Cited on page 11.)
- [13] EN50388: *EN50388: Railway Applications — Power supply and rolling stock Technical criteria for the coordination between power supply (substation) and rolling stock to achieve interoperability*. CENELEC: European Committee for Electrotechnical Standardization, Brussels, Belgium, 2012. (Cited on page 11.)
- [14] EN50163: *EN50163: Railway Applications — Supply voltages of traction systems*. CENELEC: European Committee for Electrotechnical Standardization, Brussels, Belgium, 2004. (Cited on page 11.)
- [15] Barrero, R.: *Energy Recovery Technologies in Public Transport*. PhD, Electrical Engineering and Energy Technology, Vrije Universiteit Brussel, Brussels, Belgium, November 2012. Promoter: Prof. Dr. Ir. Joeri Van Mierlo. (Cited on pages 13, 16, 17, 18, 19, 20, 27, and 28.)
- [16] Devaux, F.-O. and Tackoen, X.: Wp2b energy recovery, guidelines for braking energy recovery systems in urban rail networks — deliverable 2. September 2014. Publication of “Ticket to Kyoto” project. Available at: [http://www.tickettokyoto.eu/sites/default/files/downloads/T2K\\_WP2B\\_Energy%20Recovery\\_Final%20Report\\_2.pdf](http://www.tickettokyoto.eu/sites/default/files/downloads/T2K_WP2B_Energy%20Recovery_Final%20Report_2.pdf) (Cited on pages 13, 26, 27, and 33.)
- [17] Bonne, H.: *Spoorwegtechniek*, 2012. Class notes (in Dutch). (Cited on pages 14 and 15.)



- [18] Zo Investeer Ik: Slim schakelen, 2009. YouTube video on paralleling posts used by ProRail (in Dutch). Available at: <http://www.youtube.com/watch?v=B1oI10eUWqw> (Cited on page 15.)
- [19] Caputo, L.: *Control of Energy Storage Devices for Rail Vehicles*. Master's thesis, Department of Automatic Control, Lund University, Sweden, Lund, Sweden, October 2000. Document Number: ISRN LUTFD2/TFRT--5647--SE". (Cited on pages 15 and 17.)
- [20] AlstomECOPACK: Citadis ecopack, full on-board autonomy for trams. Product Sheet. Available at: <http://www.alstom.com/Global/Transport/Resources/Documents/brochure2014/Citadis%20Ecopack%20-%20Product%20Sheet%20-%20EN.pdf?epslanguage=en-GB>, [2016, September 17], 2016. Version: TCITADIS ECOPACK/EN/09.2016. (Cited on page 15.)
- [21] Chen, H., Cong, T.N., Yang, W., Tan, C., Li, Y. and Ding, Y.: Progress in electrical energy storage system: A critical review. *Progress in Natural Science*, vol. 19, no. 3, pp. 291–312, 2009. (Cited on page 16.)
- [22] Bolund, B., Bernhoff, H. and Leijon, M.: Flywheel energy and power storage systems. *Renewable and Sustainable Energy Reviews*, vol. 11, no. 2, pp. 235–258, 2007. (Cited on page 16.)
- [23] Vazquez, S., Lukic, S.M., Galvan, E., Franquelo, L. and Carrasco, J.M.: Energy Storage Systems for Transport and Grid Applications. *IEEE Transactions on Industrial Electronics*, vol. 57, no. 12, pp. 3881–3895, December 2010. (Cited on page 17.)
- [24] Suzuki, T.: DC power-supply system with inverting substations for traction systems using regenerative brakes. *IEE Proc. B*, vol. 129, no. 1, pp. 18–26, January 1982. (Cited on page 17.)
- [25] Cornic, D.: Efficient recovery of braking energy through a reversible dc substation. In: *Electrical Systems for Aircraft, Railway and Ship Propulsion*, pp. 1–9. Oct 2010. ISSN 2165-9400. (Cited on page 17.)
- [26] González-Gil, A., Palacin, R., Batty, P. and Powell, J.P.: Energy-efficient urban rail systems: strategies for an optimal management of regenerative braking energy. In: *Transport Research Arena*. Paris, 2014. Available at: [http://www.traconference.eu/papers/pdfs/TRA\\_2014\\_Fpaper\\_19902.pdf](http://www.traconference.eu/papers/pdfs/TRA_2014_Fpaper_19902.pdf) (Cited on pages 18 and 27.)

- [27] ABB: ENVILINE™ ERS — Energy Recuperation System for DC rail transportation. Brochure. Available at: [http://www05.abb.com/global/scot/scot221.nsf/veritydisplay/087767be06c87bdfc1257b59004d9651/\\$file/enviline\\_ers\\_en.pdf](http://www05.abb.com/global/scot/scot221.nsf/veritydisplay/087767be06c87bdfc1257b59004d9651/$file/enviline_ers_en.pdf), [2014, November 11], 2013. Version: 4116PL858-W1-en. Edition 05.2013. (Cited on pages 23 and 24.)
- [28] Railway Gazette: Łódź launches tram energy recovery system. Available at: <http://www.railwaygazette.com/news/business/single-view/view/lodz-launches-tram-energy-recovery-system.html>, [2014, November 11], 2013. (Cited on page 24.)
- [29] AEG Power Solutions: Thyrobox RI — Rail traction power recuperation. Product sheet. Available at: [http://www.aegps.com/fileadmin/user\\_upload/MEDIA\\_PDFs\\_JPEGs/EES/Industrial\\_Power\\_Supply\\_Systems/Thyrobox\\_RI/FLY\\_Thyrobox\\_RI\\_EN.pdf](http://www.aegps.com/fileadmin/user_upload/MEDIA_PDFs_JPEGs/EES/Industrial_Power_Supply_Systems/Thyrobox_RI/FLY_Thyrobox_RI_EN.pdf), [2014, November 11], 2013. Version: AEGPS - Thyrobox RI - EN - 12/2013 V2. (Cited on page 24.)
- [30] AEG TransCom: Halfjaarlijks evaluatierapport 2013. Available at: <http://www.tranzcom.be/Repository/PDF/Halfjaarlijksevaluatierapport2013.pdf>, [2014, November 14], 2013. In Dutch. (Cited on page 24.)
- [31] AEG TransCom: Remenergie recuperatie systeem - metro brussel. Available at: <http://www.aegtranzcom.com/nl/news>, [2014, November 14], 2012. In Dutch. (Cited on page 24.)
- [32] Barrero, R.: Braking energy recovery comet & nova. Available at: <https://prezi.com/nycy2vrp-vwc/braking-energy-recovery-comet-nova/>, [2014, November 14], 2014. Prezi presentation. (Cited on pages 24 and 27.)
- [33] ALSTOM: Hesop, All-in-One Energy & Cost Saver. Product Sheet. Available at: <http://www.alstom.com/Global/Transport/Resources/Documents/brochure2014/HESOP%20-%20Product%20sheet%20-%20EN%20-%20LD.pdf?epslanguage=en-GB>, [2016, September 24], 2016. Version: Hesop/EN/09.2016. (Cited on pages 24 and 25.)
- [34] HESOP: All-in-one energy & cost saver, 2014. “HESOP - Standard customer PPT”. Available from: HANDSCHIN Matthias, received via e-mail. (Cited on page 25.)
- [35] Maurin, F. and Gajan, B.: Personal Interview, July 18 2014. Paris, France. (Cited on page 26.)

- [36] Loizaga, F.: Ingeber system for kinetic energy recovery in railway systems, February 2014. PDF presentation, available on request. (Cited on page 26.)
- [37] Ingeteam Traction: Ingeber, energy recovery systems for railway systems. Available at: [http://www.ingeteam.com/Portals/0/Catalogo/Sector/Documento/SSE\\_17\\_Archivo\\_ingeber.pdf](http://www.ingeteam.com/Portals/0/Catalogo/Sector/Documento/SSE_17_Archivo_ingeber.pdf), [2014, November 17]. (Cited on page 26.)
- [38] Siemens AG: Sitras tci – thyristor controlled inverter for dc traction power supply. Product sheet. Available at: <https://w3.usa.siemens.com/mobility/us/Documents/en/rail-solutions/railway-electrification/dc-traction-power-supply/sitras-tci-en.pdf>, [2014, November 11], 2010. Version: 1.1.0 No. A6Z08110420199. (Cited on pages 26 and 27.)
- [39] Siemens Mobility and Logistics Media Service: Siemens-equipped driverless underground metro line in singapore starts operations. Available at: <http://www.siemens.com/press/pool/de/materials/infrastructure-cities/mobility-logistics/newsletter/2014/2014-02-11-mobility-logistics-news-e.pdf>, [2014, November 17], February 2014. (Cited on page 27.)
- [40] Siemens AG: Increasing energy efficiency: Optimized traction power supply in mass transit systems. Available at: <https://w3.usa.siemens.com/mobility/us/Documents/en/rail-solutions/railway-electrification/dc-traction-power-supply/increasing-energy-efficiency-en.pdf>, [2014, November 17], . (Cited on page 27.)
- [41] González-Gil, A., Palacin, R. and Batty, P.: Sustainable urban rail systems: strategies and technologies for optimal management of regenerative braking energy. *Energy conversion and management*, vol. 75, pp. 374–388, 2013. (Cited on page 27.)
- [42] Meinert, M., Rechenberg, K., Hein, G. and Schmieder, A.: Energy efficient solutions for the complete railway system. In: *Proceedings of the 8th World Congress on Railway Research*. 2008. (Cited on page 27.)
- [43] Tzeng, Y.S., Wu, R.-N. and Chen, N.: Electric network solutions of DC transit systems with inverting substations. *IEEE Transactions on Vehicular Technology*, vol. 47, no. 4, pp. 1405–1412, Nov 1998. (Cited on page 29.)

- [44] PowerFactory: DIgSILENT PowerFactory 2016. Brochure. Available at: <http://www.digsilent.de/index.php/downloads.html>, [2016, September 25], 2016. (Cited on pages 29 and 30.)
- [45] De Gussemé, K.: Simulation of the 3kv network, September 2008. PowerPoint presentation, available on request. (Cited on pages 31 and 32.)
- [46] De Gussemé, K.: Personal Interview, August 21 2014. Brussels, Belgium. (Cited on page 33.)
- [47] Romo, A.: Ingeber system for kinetic energy recovery, June 2012. PDF presentation, available on request. (Cited on page 33.)
- [48] Siemens AG: System design with sitras sidytrac. Product sheet. Available at: [http://www.downloads.siemens.com/download-center/Download.aspx?pos=download&fct=getasset&mandator=ic\\_sg&id1=DLA14\\_106](http://www.downloads.siemens.com/download-center/Download.aspx?pos=download&fct=getasset&mandator=ic_sg&id1=DLA14_106), [2014, November 17], 2014. Version 1.2.0 No. A6Z08111122394. (Cited on page 33.)
- [49] Altmann, M.: Personal Interview, September 26 2014. Innotrans, Berlin. (Cited on page 33.)
- [50] Irlam, M.J.: South african electrification. Available at: <http://mikes.railhistory.railfan.net/r025.html>, [2014, November 17], 2010. (Cited on page 34.)
- [51] Paxton, L. and Bourne, D.: *Locomotives of the South African Railways*. 1st edn. Struik, Cape Town, 1985. ISBN 0869772112. P. 125. (Cited on page 34.)
- [52] Brazil, H.: *Electrical Substations*. Edward Arnold and Co, 1928. Chapter: The South African Railways Electrification, page 110. (Cited on page 34.)
- [53] Haler, J. (ed.): *This is SAR&H Railways Handbook*. Thomson Publications S.A., Johannesburg, 1978. (Cited on page 34.)
- [54] Randewijk, P.-J.: *Inverting DC traction substation with active power filtering incorporated*. Master's thesis, Electrical and Electronic Engineering, University of Stellenbosch, Stellenbosch, South Africa, December 1995. (Cited on pages 34, 36, and 37.)
- [55] Scherrer, P., Groves, D. and Swart, E. (eds.): *South African Railways & Harbours & Airways handbook*. Thomson Publications S.A., Johannesburg, 1979. (Cited on page 34.)

- [56] Du Toit, W.J.: *Elektriese Lokomotief*. Spoorwegkollege Esselenpark - Afdeling drywers, Esselenpark, c 1970. In Afrikaans. (Cited on page 34.)
- [57] Wikipedia: South African Class 3E — Wikipedia, The Free Encyclopedia. 2014. [Online; accessed 18-November-2014].  
Available at: [http://en.wikipedia.org/w/index.php?title=South\\_African\\_Class\\_3E&oldid=626693985](http://en.wikipedia.org/w/index.php?title=South_African_Class_3E&oldid=626693985) (Cited on page 34.)
- [58] Wikipedia: South African Class 8E — Wikipedia, The Free Encyclopedia. 2014. [Online; accessed 19-November-2014].  
Available at: [http://en.wikipedia.org/w/index.php?title=South\\_African\\_Class\\_8E&oldid=633127765](http://en.wikipedia.org/w/index.php?title=South_African_Class_8E&oldid=633127765) (Cited on page 34.)
- [59] Wikipedia: South African Class 1E — Wikipedia, The Free Encyclopedia. 2014. [Online; accessed 18-November-2014].  
Available at: [http://en.wikipedia.org/w/index.php?title=South\\_African\\_Class\\_1E&oldid=624544364](http://en.wikipedia.org/w/index.php?title=South_African_Class_1E&oldid=624544364) (Cited on page 34.)
- [60] Wikipedia: South African Class 2E — Wikipedia, The Free Encyclopedia. 2014. [Online; accessed 18-November-2014].  
Available at: [http://en.wikipedia.org/w/index.php?title=South\\_African\\_Class\\_2E&oldid=626020188](http://en.wikipedia.org/w/index.php?title=South_African_Class_2E&oldid=626020188) (Cited on page 34.)
- [61] Wikipedia: South African Class 4E — Wikipedia, The Free Encyclopedia. 2014. [Online; accessed 18-November-2014].  
Available at: [http://en.wikipedia.org/w/index.php?title=South\\_African\\_Class\\_4E&oldid=633797984](http://en.wikipedia.org/w/index.php?title=South_African_Class_4E&oldid=633797984) (Cited on page 34.)
- [62] Wikipedia: South African Class 5E1, Series 1 — Wikipedia, The Free Encyclopedia. 2014. [Online; accessed 18-November-2014].  
Available at: [http://en.wikipedia.org/w/index.php?title=South\\_African\\_Class\\_5E1,\\_Series\\_1&oldid=632729147](http://en.wikipedia.org/w/index.php?title=South_African_Class_5E1,_Series_1&oldid=632729147) (Cited on page 34.)
- [63] Wikipedia: South African Class 5E, Series 1 — Wikipedia, The Free Encyclopedia. 2014. [Online; accessed 18-November-2014].  
Available at: [http://en.wikipedia.org/w/index.php?title=South\\_African\\_Class\\_5E,\\_Series\\_1&oldid=626276799](http://en.wikipedia.org/w/index.php?title=South_African_Class_5E,_Series_1&oldid=626276799) (Cited on page 34.)
- [64] Wikipedia: South African Class 6E — Wikipedia, The Free Encyclopedia. 2014. [Online; accessed 18-November-2014].

- Available at: [http://en.wikipedia.org/w/index.php?title=South\\_African\\_Class\\_6E&oldid=628013153](http://en.wikipedia.org/w/index.php?title=South_African_Class_6E&oldid=628013153) (Cited on page 34.)
- [65] Wikipedia: South African Class 6E1, Series 1 — Wikipedia, The Free Encyclopedia. 2014. [Online; accessed 18-November-2014].  
Available at: [http://en.wikipedia.org/w/index.php?title=South\\_African\\_Class\\_6E1,\\_Series\\_1&oldid=632048663](http://en.wikipedia.org/w/index.php?title=South_African_Class_6E1,_Series_1&oldid=632048663) (Cited on page 34.)
- [66] Wikipedia: South African Class 10E — Wikipedia, The Free Encyclopedia. 2014. [Online; accessed 18-November-2014].  
Available at: [http://en.wikipedia.org/w/index.php?title=South\\_African\\_Class\\_10E&oldid=633154163](http://en.wikipedia.org/w/index.php?title=South_African_Class_10E&oldid=633154163) (Cited on page 34.)
- [67] Wikipedia: South African Class 12E — Wikipedia, The Free Encyclopedia. 2014. [Online; accessed 19-November-2014].  
Available at: [http://en.wikipedia.org/w/index.php?title=South\\_African\\_Class\\_12E&oldid=632756158](http://en.wikipedia.org/w/index.php?title=South_African_Class_12E&oldid=632756158) (Cited on page 34.)
- [68] Wikipedia: South African Class 7E — Wikipedia, The Free Encyclopedia. 2014. [Online; accessed 18-November-2014].  
Available at: [http://en.wikipedia.org/w/index.php?title=South\\_African\\_Class\\_7E&oldid=630581622](http://en.wikipedia.org/w/index.php?title=South_African_Class_7E&oldid=630581622) (Cited on page 34.)
- [69] Wikipedia: South African Class 9E, Series 1 — Wikipedia, The Free Encyclopedia. 2014. [Online; accessed 18-November-2014].  
Available at: [http://en.wikipedia.org/w/index.php?title=South\\_African\\_Class\\_9E,\\_Series\\_1&oldid=630715596](http://en.wikipedia.org/w/index.php?title=South_African_Class_9E,_Series_1&oldid=630715596) (Cited on page 34.)
- [70] Wikipedia: South African Class 11E — Wikipedia, The Free Encyclopedia. 2014. [Online; accessed 18-November-2014].  
Available at: [http://en.wikipedia.org/w/index.php?title=South\\_African\\_Class\\_11E&oldid=633302693](http://en.wikipedia.org/w/index.php?title=South_African_Class_11E&oldid=633302693) (Cited on page 34.)
- [71] Wikipedia: South African Class 14E — Wikipedia, The Free Encyclopedia. 2014. [Online; accessed 19-November-2014].  
Available at: [http://en.wikipedia.org/w/index.php?title=South\\_African\\_Class\\_14E](http://en.wikipedia.org/w/index.php?title=South_African_Class_14E) (Cited on page 34.)
- [72] Wikipedia: South African Class 38-000 — Wikipedia, The Free Encyclopedia. 2014. [Online; accessed 18-November-2014].

- Available at: [http://en.wikipedia.org/w/index.php?title=South\\_African\\_Class\\_38-000](http://en.wikipedia.org/w/index.php?title=South_African_Class_38-000) (Cited on page 34.)
- [73] Middleton, J.N.: *Railways of Southern Africa Locomotive Guide - 2002 (as amended by Combined Amendment List 4, January 2009)*. 2nd edn. Herts, England: Beyer-Garratt Publications, 2002. Pp. 49-51, 57. (Cited on page 35.)
- [74] Wikipedia: South African Class 18E, Series 1 — Wikipedia, The Free Encyclopedia. 2014. [Online; accessed 18-November-2014].  
Available at: [http://en.wikipedia.org/w/index.php?title=South\\_African\\_Class\\_18E,\\_Series\\_1&oldid=624309053](http://en.wikipedia.org/w/index.php?title=South_African_Class_18E,_Series_1&oldid=624309053) (Cited on page 35.)
- [75] Wikipedia: South African Class 15E — Wikipedia, The Free Encyclopedia. 2014. [Online; accessed 18-November-2014].  
Available at: [http://en.wikipedia.org/w/index.php?title=South\\_African\\_Class\\_15E&oldid=624303853](http://en.wikipedia.org/w/index.php?title=South_African_Class_15E&oldid=624303853) (Cited on page 35.)
- [76] Wikipedia: South African Class 19E — Wikipedia, The Free Encyclopedia. 2014. [Online; accessed 18-November-2014].  
Available at: [http://en.wikipedia.org/w/index.php?title=South\\_African\\_Class\\_19E&oldid=624544318](http://en.wikipedia.org/w/index.php?title=South_African_Class_19E&oldid=624544318) (Cited on page 35.)
- [77] Wikipedia: South African Class 20E — Wikipedia, The Free Encyclopedia. 2014. [Online; accessed 18-November-2014].  
Available at: [http://en.wikipedia.org/w/index.php?title=South\\_African\\_Class\\_20E&oldid=624544698](http://en.wikipedia.org/w/index.php?title=South_African_Class_20E&oldid=624544698) (Cited on page 35.)
- [78] Munshi, R.: Transnet applies for electricity licence. Available at: <http://www.bdlive.co.za/business/transport/2014/04/15/transnet-applies-for-electricity-licence>, April 15 2014. (Cited on page 35.)
- [79] Department, E.E.: South african railways class 5m2a suburban stock experimental train set fitted with hitachi thyristor control equipment and knorr-bremse air brakes — interim report, volume 1, May 7 1981. Reference: CEE/LAB 23/2/4/1, Report Number: E LAB 27/81. (Cited on page 35.)
- [80] Vockerodt, L.C.: Suburban trainsets — comparison of energy consumption, July 31 1998. Report, received via e-mail. (Cited on pages 36, 163, and 189.)

- [81] South African Railways: *No. 6: Plaaslike Aanhangsel tot die Treinbedryfsregulasies, Algemene Aanhangsel en Bedryfstydboeke – Afdeling Wes-Kaapland*. Die Staatsdrukker, Pretoria, 1966. In Afrikaans. See Afdeling V, Onderafdeling 4, Klousule 54. (Cited on pages 36, 105, and 108.)
- [82] KZN, M.: Local operating instructions. 2014. Clause 2034.0. (Cited on page 36.)
- [83] van Zyl, G., Leon, A., Koos, F. and Dreyer, C.: 5m2B Train Drivers Training Manual. 2014. Section 11.14.12. (Cited on page 36.)
- [84] Fuchs, H.D.: *Development and Implementation of a 1.5MW Inverter and Active Power Filter System for the Injection of Regenerated Energy in a Spoornet Traction Substation*. Master's thesis, Electrical and Electronic Engineering, University of Stellenbosch, Stellenbosch, South Africa, December 2005. (Cited on page 37.)
- [85] Rosa, T.M.: Traction substation: Maximum power demand, 1995. (Cited on pages 39 and 40.)
- [86] Tamini VTD Energy Transformers: TDS-4639 Technical Data Sheet, 2015. (Cited on page 40.)
- [87] Gibb: Rollingstock - energy aspect, September 2008. Document acquired from Gibb via e-mail. (Cited on page 41.)
- [88] Dreyer, C.: 5M2B Train Drivers Training Manual, 2014. (Cited on page 42.)
- [89] Lategan, L.: 5M2A acceleration. 2012. [Online; accessed 18 November 2014]. Available at: [youtu.be/-xVxCsgzBnQ](https://www.youtube.com/watch?v=xVxCsgzBnQ) (Cited on page 43.)
- [90] Consortium, G.R.T.: Description of traction system - 3KV, note = File name: CDRL #2 4-15 1 Description of Traction System 3kV 66%\_ VersionB.DOCX. (Cited on pages 43, 47, and 189.)
- [91] Vockerodt, L.: Line current and power consumption for new Prasa trains, May 2015. Based on information supplied by Gibela. (Cited on pages 44, 45, 46, 48, 99, and 100.)
- [92] Scrooby, M.: Personal e-mail communication, September 30 2015. (Cited on page 50.)
- [93] Wikipedia: Cape Flats — Wikipedia, The Free Encyclopedia. 2015. [Online; accessed 22-December-2015]. Available at: [https://en.wikipedia.org/w/index.php?title=Cape\\_Flats&oldid=688466052](https://en.wikipedia.org/w/index.php?title=Cape_Flats&oldid=688466052) (Cited on page 87.)



- [94] Wikipedia: Rail transport in South Africa — Wikipedia, The Free Encyclopedia. 2015. [Online; accessed 22-December-2015]. Available at: [https://en.wikipedia.org/w/index.php?title=Rail\\_transport\\_in\\_South\\_Africa&oldid=686639984](https://en.wikipedia.org/w/index.php?title=Rail_transport_in_South_Africa&oldid=686639984) (Cited on page 87.)
- [95] South African Railways: Small scale section. . Drawing CT-110-B.1-B.302. (Cited on page 87.)
- [96] Alstom: Operational Context Description. 2016. [Provided by Alstom]. (Cited on pages 87 and 88.)
- [97] South African Railways: Small scale section. . Drawing CT-189-B.1-B.300. (Cited on page 91.)
- [98] South African Railways: Small scale section. . Drawing CT-101-B.1-B.311. (Cited on page 91.)
- [99] Metrorail, C.: DOCS\_CM3-#158294-v1-TRAIN\_RUNNING\_TIMES.xls, 2001. (Cited on pages 91, 169, 170, 171, 172, 173, 174, 175, 176, and 184.)
- [100] Dc sub. DOS computer program containing substation parameters. (Cited on page 105.)
- [101] Metrorail: Cape suburban 33 kV distribution, 2013. Drawing CEM-PEB-033, last revision 28/02/2013. (Cited on pages 105 and 108.)
- [102] Prasa: none specified. 2000. Supplied by Johan van Wyk as “Western Cape Map.pdf”, shows coding of sections. Last revision 05/10/2000. (Cited on page 105.)
- [103] Metrorail: Emergency control book, 2014. Drawing CEM-TTA-1, last revision 18/06/2014. (Cited on pages 105, 131, and 190.)
- [104] Zazworka, A.: Rail and overhead wire resistances. 09 1983. Drawing CEE-TA-111, last revision T2/83/85. (Cited on pages 105, 131, and 132.)
- [105] Buckle, C.: Rail and overhead wire resistances. 09 2012. Drawing CEE-TA-0111 AMD 5. (Cited on pages 105, 131, and 132.)
- [106] Erlank, S.: Personal Interview, February 19 2015. Salt River ERS, Cape Town. (Cited on page 105.)
- [107] Van der Merwe, P.: Personal Interview, February 19 2015. Koebergweg School of Rail, Cape Town. (Cited on page 105.)

- [108] Van Wyk, J.: Personal Interview, March 21 2015. Salt River ERS, Cape Town. (Cited on page 105.)
- [109] Xolile, D.: E-mail communication, July 17 2015. Transnet Engineering Technician. (Cited on page 105.)
- [110] Reid, B.: Brief report: Metering study outcomes. 10 2013. Report by Royal Haskoning DHV, Revision 0. (Cited on pages 105, 127, 137, 138, and 139.)
- [111] Batt, M.: Personal Interviews, 2015. Gibb Offices, Cape Town. (Cited on page 105.)
- [112] *Technical Reference Documentation: External Grid (ElmXnet)*. DIgSILENT GmbH, 2014. (Cited on page 107.)
- [113] *DIgSILENT Power Factory 15: User Manual, organization = DIgSILENT GmbH, year = 2015, month = jul.* (Cited on page 112.)
- [114] *Technical Reference Documentation: Rectifier / Inverter (ElmRec, ElmRecmono, TypRec)*. DIgSILENT GmbH, 2014. (Cited on pages 112, 113, and 114.)
- [115] *Traction Substations Technical Assistant Handbook*, apr 1993. File Referene: SI(W)2/4/4/3/EP.001, Section 5.1.1.4. (Cited on page 115.)
- [116] Dixon, J.: Chapter 12 three-phase controlled rectifiers. (Cited on pages 118, 119, 120, 121, 122, 124, and 125.)
- [117] Rashid, M.: *Power Electronics Handbook*. Academic Press, 2001. (Cited on page 125.)
- [118] Metrorail: 11 kv signal supply cape peninsula, 2014. Drawing CEM-PEB-24, last revision 09/04/2014. (Cited on page 127.)
- [119] *Technical Reference Documentation: PWM Converter (ElmVscmono)*. DIgSILENT GmbH, 2015. (Cited on page 133.)
- [120] Gibela: Trainset diagram. Drawing. (Cited on page 161.)
- [121] South African Railways: Small scale section. . Drawing CT-109-B.1-B.303. (Cited on page 184.)